Reconstruction and safety assessment of the Hengelo Brinefield phase 1 area

Calis, R. (Randy)

8/7/2018

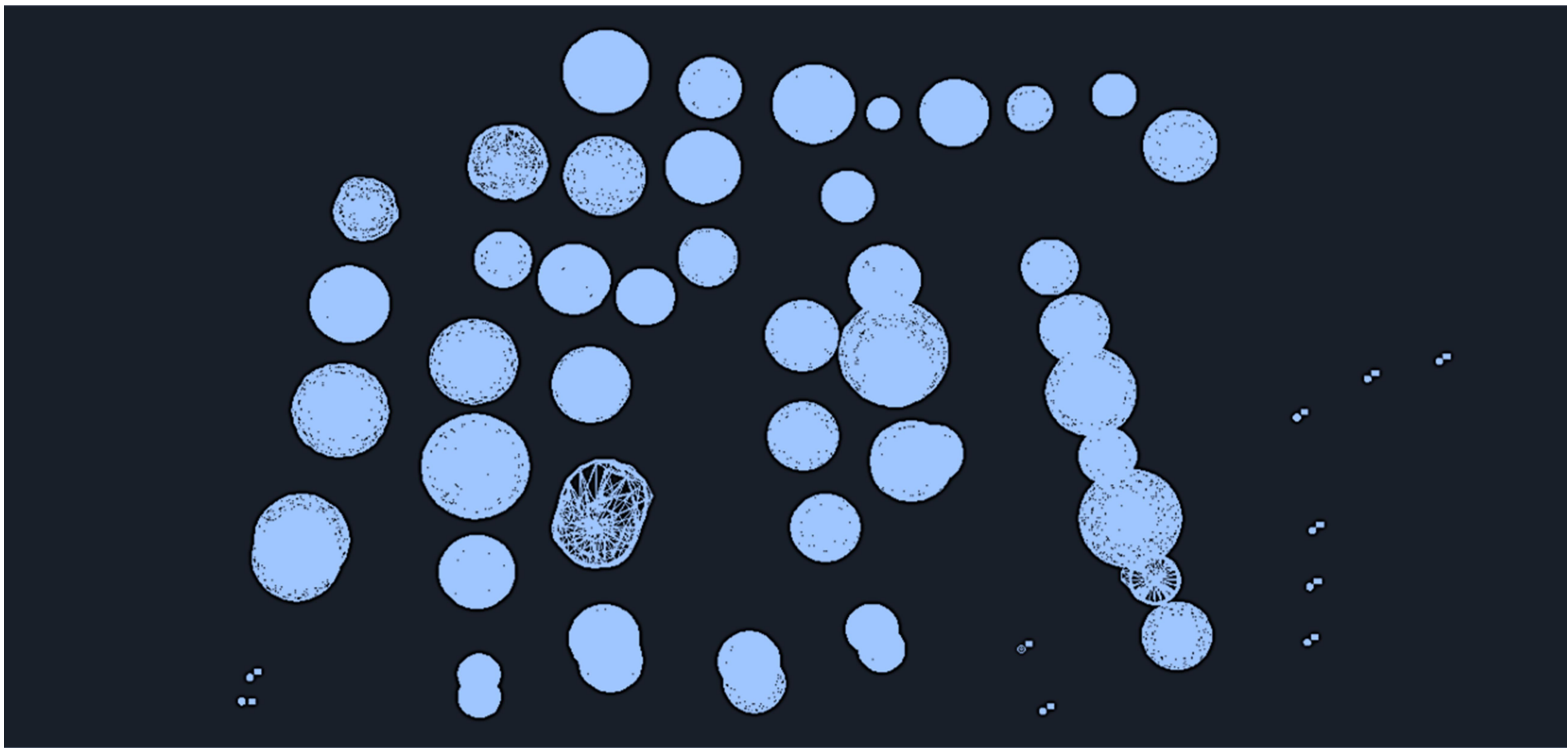

TU Delft Delft University of Technology

AkzoNobel Tomorrow's Answers Today

Reconstruction and safety assessment of the Hengelo Brinefield phase 1 area

By

Randy Calis

Master of Science

In Geosciences and Engineering

At Delft University of Technology

Randy Calis

Student number: 1548476

Thesis committee:

• Dr. M.W.N. Buxton	supervisor, TUDelft.
• D.Sc. M. Rinne	co-supervisor, Aalto University.
• Dr. B.G. Lottermoser	co-supervisor, RWTH Aachen.
• MSc. A.M. den Hartogh	counsellor/ daily supervisor, AkzoNobel Specialty Chemicals

Postal address: Department of Geosciences & Engineering
Delft University of Technology
P.O. Box 5028
The Netherlands

Telephone: (31)152781328 (Service desk)

TU Delft

i. Abstract

Since 1918 AkzoNobel produces salt by means of solution mining from the bedded Triassic Röt Evaporite deposit in the eastern part of the Netherlands. In this technique water is pumped into the rock salt layer through a well and dissolves the halite in situ. Subsequently the brine is pumped to the purification plant at surface level where the NaCl is extracted from the brine after several impurities have been removed.

Near the city of Hengelo, the Hengelo Brine field has been exploited by AkzoNobel since 1933 and based on the technological progress during the years it can be divided into five phases:

1. 1933-1958, 53 wells, 42 caverns
2. 1959-1975, 226 wells, 94 caverns
3. 1976-2005, 213 wells, 72 caverns
4. 2006-2013, 37 wells, 36 caverns
5. 2014-present day, 31 wells, 31 caverns

The area corresponding to the first phase comprises 42 caverns which have been developed from 50 production wells. The production wells have been drilled between 1933 and 1958 and during later stages 3 appraisal wells have been drilled.

Present-day AkzoNobel pursues stable caverns at the end of their production life. This is achieved by leaving a sufficient thickness of salt in the roof above the cavity. The result is a ductile boundary between the void and the overburden material. The directly overlain anhydrite layer is much stiffer and shows brittle behavior. When this anhydrite layer is not supported by a sufficient amount of rock salt underneath it can potentially collapse. This roof failure occurs when the span of the exposed anhydrite is large enough. The fragments of the collapsed roof layer will deposit on the bottom of the cavern leaving the next roof layer exposed. With each roof layer collapsing the cavern top and bottom attain a new depth. This process is called cavern migration, which continues until the cavern reaches a status where the roof layer is stable either by sufficient support or strength.

Most of the 42 caverns of the phase 1 area have migrated and in five cases this led to significant surface subsidence. Currently AkzoNobel prepares abandonment of the last open wells in the phase 1 area. In order to proof long term safety after closure, the caverns have been examined, simulated, reconstructed, and modelled. By analyzing the available data and scrutinizing a few caverns where extensive migration did occur, the cavern migration behavior and its influential parameters were identified. This report clarifies how the caverns have been reconstructed and how the maximum migration potential is determined with the model.

The phase 1 area comprises the oldest part of the Hengelo Brine field. The wells were drilled between 1933 and 1958. During this phase some of the wells were positioned close to each other, intentionally allowing interconnections. The motive was to complete these wells as doublets, while the rest were setup as single completion caverns. Despite these intentions, the leaching during this phase was performed in a less restrained manner than what is acceptable today. The majority of the caverns in the phase 1 area have established unintentional connections and were completed as series of caverns. Due to this lack of control overmining occurred at some of the caverns and as a

result most of the caverns have migrated upwards through the overburden and some induced significant subsidence at the surface.

As the amount of data and especially measurements of these phase 1 caverns is scarce, the caverns needed to be reconstructed to enable a comprehensive analysis. In order to reconstruct the cavern development and final dimensions, the caverns have been simulated based on their historical production and on interpretations of the geology and logbooks. After cross-correlating the dimensions with the available data, the dimensions are used in an analytical model. Considering multiple influential parameters the post-production 'residual' volume and dimensions of the caverns are deduced. Thereafter the maximum potential migration is determined using a migration model.

ii. Acknowledgements

During this thesis research I have obtained extensive knowledge regarding solution mining and the cavern migration behavior. In all of the stages several individuals have been helpful to me.

First of all I would like to thank Marinus den Hartogh for all his help, advice, support and guidance. From the beginning till the end he was my daily supervisor at AkzoNobel and has always been available. Furthermore Marinus has provided me with all the available data and documents.

I would like to thank Mike Buxton, my supervisor from TUDelft, for his advice, feedback and guidance during this thesis.

Furthermore I would like to thank the Mining Development & Compliance department of AkzoNobel specialty chemicals. All the members have always been helpful and willing to answer questions. During the Monthly Mining Meetings additional input and feedback have been helpful. A special thanks to Ronald van Steveninck for the dinners and informal discussions, Henk Leusink for answering all my questions, Johan Oosterloo for helping out with constructing the simulated cavern map, Bas Wagenvoord for answering questions and informal discussions as shared office partners and Winny van der Zee for all the support.

Delft,

August 7th, 2018 R. Calis

Contents

i. Abstract 2

ii. Acknowledgements 4

1. Introduction 9

1.1 Introduction to AkzoNobel specialty chemicals. 9

1.1.1 AkzoNobel 9

1.1.2 Company history 9

1.1.3 Mining history 9

1.1.4 Solution mining 10

1.1.5 Expansion phenomena 10

1.2 Introduction to the Hengelo Brine Field 11

1.3 Motivation 13

1.4 Research questions 14

1.5 Aim and objectives 15

1.6 Hypotheses. 15

1.7 Thesis outline 16

1.8 Scope and limitations 16

1.9 Approach 18

1.10 Database 19

1.10.1 Wells 19

1.10.2 Geology 20

1.10.3 Production 20

1.10.4 Research 20

1.10.5 Results from this research 21

2. Project background 22

2.1. The socio-economic importance of salt 22

2.2 Solution mining of salt 22

2.3 Hengelo Leaching Technique 23

2.4 Geology 24

2.4.1 Regional Geology 24

2.4.2 Triassic 25

2.4.3 Jurassic and Cretaceous 27

2.4.4 Tertiary and Quarternary 28

2.4.5 Structural setting (based on Geowulf, 2005) 28

2.4.6 Salt thickness and evaporite cyclicity 29

2.4.7 Lithostratigraphy of the Röt Evaporite 30

2.5. Cavern migration 31
2.5.1 Cavern migration background 31
2.5.2 Extinction of migration 32
3. Development and exploitation of the phase 1 area. 33
3.1 Drilling technology 33
3.2. Production methodology 35
3.2.1 Introduction 35
3.2.2 Cavern development 35
3.2.3 Morning glory 36
3.2.4 Hydraulic connections 38
3.3 production numbers 39
3.3.1 Production of the caverns as single cavern 39
3.3.2 Production of the caverns as series 39
3.3.3 Statistical analysis interpretation 41
4. Reconstruction of the caverns 47
4.1 Simulations 48
4.2 Insoluble content 50
4.3 Simulation results and correlations with sonar measurements 53
4.3.1 Cavern 15 53
4.3.2 Cavern 37 54
4.3.3 Cavern 49 56
4.3.4 Cavern 50 58
4.3.5 Doublet 33-34 59
4.4 synthesis 61
5. Cavern migration behavior for the phase I caverns 63
5.1 Subsidence and migration categories. 65
5.2 Correlation between production history and surface subsidence 66
5.3 Migration model parameters 69
5.4 Isolating and correlating the parameters 73
5.4.1 Cavern 15 73
5.4.2 Analytical explanation of the decreasing diameter modelling. 77
5.4.3 Cavern 7 79
5.4.4 Cavern 37 80
5.5 summarized explanation of the model 81
5.6 Evaluation of the migration model 82
5.6.1 Introduction 82

5.6.2. cross-correlation of the migration behavior with seismic data 83
5.6.2.1 Introduction to seismic survey 83
6. Results of the modelled migration and safety assessment 90
6.1 Cavern 1 92
6.2 Cavern 2 93
6.3 Cavern 3 93
6.4 Cavern 4 94
6.5 Cavern 5 94
6.6 Cavern 6 95
6.7 Cavern 7 95
6.8 Cavern 8 95
6.9 Cavern 9 96
6.10 Cavern 10 96
6.11 Cavern 11 98
6.12 Cavern 12 99
6.13 Cavern 13 99
6.14 Cavern 14 99
6.15 Cavern 15 100
6.16 Cavern 16 100
6.17 Cavern 17 101
6.18 Cavern 18-24 101
6.19 Cavern 19-20 102
6.20 Cavern 21 103
6.21 Cavern 22 103
6.22 Cavern 23 104
6.23 Doublet 25-26 104
6.24 Cavern 27 104
6.25 Cavern 28 105
6.26 Cavern 29 105
6.27 Doublet 30-31 106
6.28 Cavern 32 107
6.29 Doublet 33-34 107
6.30 Doublet 35-36 107
6.31 Cavern 37 108
6.32 Cavern 38 109
6.33 Cavern 39 109

6.34 Doublet 40-41 109
6.34 Doublet 42-43 110
6.35 Cavern 44 110
6.36 Cavern 45 110
6.37 Cavern 46 111
6.38 Cavern 47 111
6.39 Cavern 48 111
6.40 Cavern 49 111
6.41 Cavern 50 112
7. Additional correlations 113
7.1 Additional data regarding the insoluble content 113
7.2 Additional data regarding the decreasing diameter 114
7.3 Additional data regarding the slurry 117
8. Evaluation & Discussion 119
8.1 Discussion about the decreasing diameter 120
8.2 sensitivity analysis 124
8.3 Evaluation & discussion on the reconstructed production and simulated caverns. 127
9. Conclusions 129
9.1 Answers to the research questions 129
10. Recommendations 132
10.1 recommendations regarding the production 132
10.2 recommendations regarding the simulations 132
10.3 recommendations regarding the migration model 132
12. Reference list 134
13. Bibliography 136
Appendix A 138
Appendix B 139
Appendix C 142
Appendix C2 143
Appendix C3 144
Appendix D 147
Appendix E 150
Appendix E3: Figures of the simulated caverns. 155
Appendix F 193

1. Introduction

1.1 Introduction to AkzoNobel specialty chemicals.

1.1.1 AkzoNobel

AkzoNobel is a leading global paints and coatings company and major producer of specialty chemicals (AkzoNobel.com). In 2017 the company had revenue of 2.377 billion euros and in June 2018 AkzoNobel had a market value of $ 22.4 billion. During 2017 the company decided to split up into two components: performance coatings & decorative paints and specialty chemicals. The specialty chemicals branch produces a large variety of products; amongst this is the range of salt-chlorine products that are being produced from salt. This range can be categorized into the following market components: food, retail (road salt), pharmaceutical, agricultural, industrial and water treatment. Well-known brand names under which the products from AkzoNobel are sold are: Jozo, KNZ, Sanal, Suprasel, Broxo and Broxomatic.

1.1.2 Company history

The ancestry of AkzoNobel can be traced back to 1777 in Denmark and the oldest Dutch roots can be tracked to 1792. The company is a consortium of several merged enterprises and in 1969 this led to the name Akzo which is an abbreviation for 'Algemene Kunstzijde Unie en Koninklijke Zout Organon'.

The salt producing component, depicted by the 'Z' in the name abbreviation Akzo, originates from the 'Koninklijke Nederlandse Zoutindustrie' (KNZ) and is celebrating its 100's anniversary in 2018. In 1994 Akzo took over Nobel industries and the company was named AkzoNobel.

1.1.3 Mining history

As early as in 1886 rock salt was coincidentally encountered in the subsurface near Hengelo during the drilling of a water well at the 'Twickel' estate (Visser et al., 1987). The well was drilled into an artesian aquifer at approximately 450 meters depth. During the completion of the well the fresh water became saline and indicated the presence of rock salt in the underground. Soon J.P. Vis, an owner of a salt purification plant in the western part of Holland became interested in the potential.

At the same time the German Geological Survey stated that hard coal could potentially occur at viable depths in the province of Limburg (Southern Netherlands). The Dutch government keenly responded by adopting a law that solely allowed the Dutch state to conduct the exploration of hard coal, lignite, rock salt and potash. The law came active in 1903 for a duration of six years and applied to the eastern parts of the Netherlands. In 1908 however the application area was extended to the entire country for a period of 15 years (Visser et al., 1987).

In 1903 the state established the 'Rijks Opsporings Dienst' (state institution for mineral exploration). The 'ROD' consulted a group of geologists and salt producers and started to drill some appraisal wells in 1903. In 1909 rock salt belonging to the Zechstein group was found. This was at such an extensive depth (approximately 1000m) that the search for shallower salt continued as the water

well clearly indicated a less deep occurrence. In 1911 rock salt belonging to the Röt Evaporate member was detected at a much more favorable depth of approximately 350m.

After completing a feasibility study a concession was officially applied for. In the first instance the Dutch government rejected due to the fear of segregation of the salt market. After WWI ended the dependency of importing salt from other countries (especially the high import taxes on German salt) was the main reason to grant the concession. In 1918 the 'KNZ' was found by J.P. Vis, A.A. Kolff and L.F.D. van der Minne in collaboration with the Dutch state (source: AkzoNobel archive).

1.1.4 Solution mining

In the exploitation agreement it was stated that the goals of the entity were to mine salt and establish facilities to purify the salt and fabricate chemical products from salt. The chosen method of extraction was solution mining. Solution mining as a technique for salt exploitation was presumably applied for the first time in Szechuan, China (Kurlansky, 2003). Even though there was no fundamental knowledge or experience with solution mining in the Netherlands at that time, the method was the most viable one. The following circumstances led to that conclusion:

- The Röt-salt in eastern Netherlands was the most shallow and therefore easiest accessible salt known at the time.
- The geological setting of the Röt-salt was elementary compared to the complex structures that were encountered in the Zechstein-salt.
- The thickness of the salt layer was assessed as insufficient for underground mining.
- The considerably high content of interbedded impurities such as clays and anhydrite are very poorly soluble compared to the rock salt.
- The content of mineralogical impurities such as K and Mg salts is very low.
- The development of an underground mine would consume an ample amount of time.
- Imported rock salt was generally already being dissolved for purification.

1.1.5 Expansion phenomena

The first production wells were drilled in the neighborhood of Boekelo and were part of the Buurse concession. The production restricted to a maximum of 30000 tons per year and the brine was to be sold directly to separate salt works intrinsically. Directly at the same time as the first well was being drilled (12/8/1918), the construction of AkzoNobel's own salt purifying plant in Hengelo commenced as well (Harteveld, 1961). Already in September 1919 the first brine coming from Boekelo was transported through the 2500m pipeline to the plant. In pursuance of obtaining a higher efficiency in the purification process, the first series of vacuum vessels was installed in 1926.

The main reason to relocate the purification plant- and later the base of the entire company- to Hengelo was due to governmental project of the 'Twente-Rijnkanaal'. This channel had as purpose to connect the larger cities in the East of the Netherlands to the Rhine. Relocating the whole company from Boekelo to Hengelo meant that a new concession area around the site needed to be filed accordingly. In 1933 'KNZ' obtained the concession area called Twente-Rijn. The drilling of the wells in this area began in 1933 already and the construction works of expanding the plant were carried out coextensively. Production increased to 200000 tons annually by 1940, with the Boekelo

field still running. By 1955 the production reached 585000 ton per year while the Boekelo field was closed off in 1952 (Roordink, 1993). In 1957 a new plant- and accessory field- in Delfzijl in the province of Groningen was commissioned and this field started with an annual production of 350000 tons. In 1960 the annual production in Hengelo was 750000 tons and approximately 40 production wells were being exploited. In 1963 a third production site was set up in Mariager, Denmark. Nowadays the refinery in Hengelo produces approximately 2.6Mton of salt per year (Marinus Den Hartogh, personal communication, 2018).

1.2 Introduction to the Hengelo Brine Field

As mentioned in 1.1.5 the base of AkzoNobel relocated to Hengelo and the exploitation of the new Hengelo field started in 1933. The original concession area is called 'Twente-Rijn' which clearly illustrates the ambition of the company and moreover that of the government in that time. Twente is the name of the local region that comprises the most eastern half of the province of Overijssel. The channel that the government dug in order to connect the big cities in this area to River Rhine lends its name directly to the connection. The channel was named 'Twente-Rijn kanaal' –nowadays just Twente-kanaal- even though the channel does not actually reach the Rhine itself but a side branch namely the River Ijssel (figure 1.1).

Figure 1.1 Map with the geographical position of the Twente-Kanaal (red line) (source: Kadaster.nl)

The original concession covered an area of 4745 hectares (figure 1.2) and was extended with de 'Uitbreiding Twente-Rijn',' Helmerzijde' and 'Oude Maten' areas. In addition AkzoNobel nowadays also holds the concession areas: Weerselo and Isidorushoeve as future mining areas. The scope of this study only focusses on the Northern part of the original Twente-Rijn concession area.

Figure 1.2 Map with concession areas (source: AkzoNobel archive)

1.3 Motivation

The Hengelo Brine Field can be divided into 5 chronological phases (Den Hartogh, 2017):

1. From 1933 to 1958, 53 wells, 42 caverns
2. From 1959 to 1975, 226 wells, 94 caverns
3. From 1976 to 2005, 213 wells, 72 caverns
4. From 2006 to 2013, 37 wells, 36 caverns
5. From 2014 to present day, 31 wells , 31 caverns

The phases are distinguished based on adaptions in drilling and production technique that resulted in major changes in the mode of operation in the field. Based on the locations of the wells this does result in a map consisting of complex shaped zones that correspond to the phases.

During phase 1 a total of 50 production wells have been drilled initially, later 3 appraisal wells were drilled in this area additionally. From the initial 50 production wells, 42 caverns have been developed. Eight of these caverns were developed as doublets, where the wells were positioned close to each other. The other 34 caverns were produced as Single Completion Caverns.

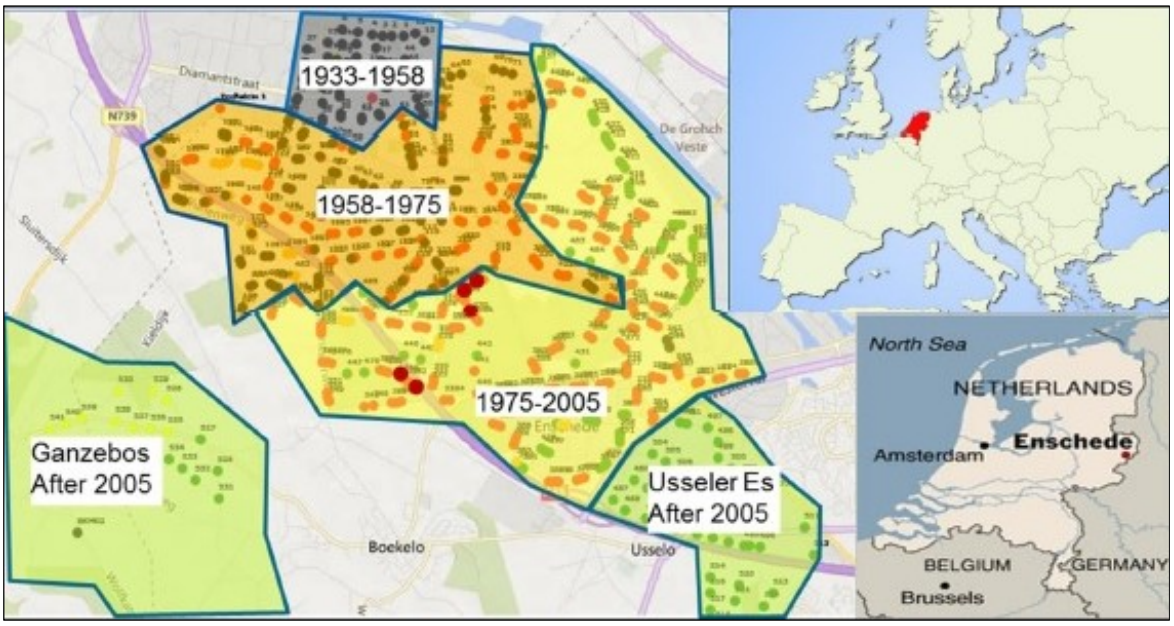

Figure 1.3 overview map of Twente-Rijn concession area with the phases indicated (source: AkzoNobel archive)

As mentioned earlier the production technique and methodology was improved over the years. Solid examples of these improvements are the roof protection method called 'oil blanketing', Sonar measurements for controlled cavern development and the installation of the micro-seismic monitoring system that registers collapsing cavern roof fragments. The drilling technique has improved substantially as well, starting with the introduction of the rotary drilling rig in 1959 (AkzoNobel archive). Unfortunately some less successful methods used as well. The most evident one was the double set of large scale experiments of hydraulic fracturing in the early 60's (Wassmann, 1980b). The aim was to obtain fast hydraulic connections between wells in order to develop systems of caverns such as the doublets or triplets. Later this was refined to the triple well

cavern development which was named the Multiple Cavern Completion technique that was implemented during phase 2 and 3. Ultimately the introduction of the Good Salt Mining practice in 2005 led to the decision to adopt a modern and controlled version of the 'old' Single Completion Cavern technique. This technique is currently being applied and is depicted by phase 4 and phase 5.

Despite the entire technological advance none of the new adaptions were present during the phase 1 production era and the production method and technique can be described as the most basic form. Due to the lack of measuring techniques, the caverns were leached out in a more or less uncontrolled manner. The caverns reached the top of the salt quite rapidly and spread out radially. In addition the caverns became interconnected because of this substantial radial growth underneath the anhydrite roof layer. Most of the phase 1 caverns have started to migrate through the overburden and some induced severe surface subsidence (personal communication with Marinus den Hartogh, 2018).

Currently only 2 of the 53 wells of phase 1 are still open; the rest have been abandoned. A substantial amount has been abandoned in the early 60's and a lot in the early 80's. AkzoNobel is planning to abandon these last 2 wells in 2018. With this the entire phase 1 are can finally be closed. Still for a reliable assessment of the long term safety and stability of the area a reconstruction addressing the following components is needed:

1. Geology
2. Drilling technology
3. Production methodology
4. Return stream processing
5. Cavern migration history
6. Remaining subsidence risk

A lot of old, segregated data regarding the geology, production history and workovers is available. Additionally data regarding the cavern migration is available for 3 caverns and for 5 caverns sonar measurements are available. Yet no clear overview on the phase 1 area has been made so far. The aim of this thesis is to create a reconstruction of the phase 1 area, integrating the loose data into a comprehensive overview of the entire history and the remaining potential risks.

1.4 Research questions

The main research question is defined as:

How does the measured amount of cavern migration and subsidence in the phase 1 area of the Hengelo Brine Field relate to the production history and what does this mean for the long term safety of the area?

The aim of this project is to assess the long term safety of the phase 1 area by investigating the relation between the production history and cavern migration and surface subsidence. The complete historic development and post-production behavior of the caverns need to be reconstructed. The following sub-questions have been formulated to meet the objectives of this study:

1. How have the phase 1 salt reserves formed in terms of geology and how are they accessed in terms of drilling technology and production configuration?
2. How are the phase 1 salt reserves extracted in the initial setup in terms of inflow / outflow and cavern shape prior to any connection?
3. How are the phase 1 caverns operated after connections with other caverns have been established in terms of inflow / outflow, return stream processing and final cavern shape?
4. How did the vertical position of the caverns develop during and after production in terms of migration in the main Röt Evaporite and through the overburden and surface subsidence?
5. What is the current and most likely future state of the caverns in terms of the production and migration relationship and the long term safety assessment?

1.5 Aim and objectives

The aim of this project is outlined in 1.3 and 1.4 already and in order to achieve this aim the following 5 objectives have been defined to tackle the problems related to the aim:

1. Reconstruction of the production per well by integrating data regarding geology and drilling
2. Reconstruction of the shape of the caverns before connection with other caverns by integrating production data with reconstruction of the production method.
3. Reconstruction of the most likely final shapes of the caverns by using production data, data regarding connection between caverns and data regarding return stream processing
4. Reconstruction of the cavern migration history by using well intervention data and the reconstruction of the final cavern shape.
5. Assessment of the measured subsidence in relation to the final shape and the migration history.

1.6 Hypotheses.

During the research of this thesis work a model is developed that approaches the cavern's behavior during their production life and moreover the migration behavior afterwards. All the available data have been scrutinized, assessed and implemented accordingly in contemplation of being able to reconstruct the unknown from the known.

Firstly the parameters that influence the migration process have been identified. After the identifications the parameters have been narrowed down to certain ranges of likely values based on the caverns with available data regarding the migration (for 3 caverns the extinction depth of the migration is known). Based on the parameters that influence the migration process a model has been constructed that is fitted to 3 known cases. Subsequently the model has been cross-correlated to multiple caverns from outside of the scope in order to isolate and determine the normal values of certain parameters more accurately. Additionally the migration behavior has been cross-correlated with available data from a seismic survey and three reported subsidence bowls at surface level above specific caverns.

The following hypotheses will be tested in this thesis:

- The dimensions of the caverns can be simulated with adequate precision.

- Based on the cavern dimensions an equivalent geometrical shape can be described with the corresponding diameter and volume.
- The equivalent geometrical shape can be used to model the maximum potential migration height from the top of the salt upwards.
- The identified influential parameters that are considered and limited to a range of potential values are representing the migration behavior adequately.
- The end result is the comprehensive reconstruction of the phase I area.

1.7 Thesis outline

The outline of the thesis will follow the chronology of the research and is as follows:

- Chapter 2 comprises the relevant background information of this project. Amongst this are: an introduction to solution mining, the geology and the concept of cavern migration.
- Chapter 3 comprises the factual development of the phase I caverns. Amongst this are: The drilling and production technology and methodology, the production numbers for the single cavern production phase and the most likely production numbers for the final caverns.
- Chapter 4 comprises the reconstruction of the caverns. Amongst this are: The simulations that are based on the production, the logbook interpretations and geology.
- Chapter 5 comprises the reconstruction of observed migration behavior. Amongst this are: analysis of migration behavior, identifying influential parameters, constructing a migration model, correlating the model with known data and explaining the model.
- Chapter 6 comprises the reconstructed migration potential, current state and predictions for all the phase 1 caverns. This is done by running the migration model for all caverns and discussing the results
- Chapter 7 comprises additional correlation material. This comprises data that can be used for additional correlation as it is representative while it does not belong to the phase I data.
- Chapter 8 comprises the evaluation of this research.
- Chapter 9 comprises the conclusions. In this chapter the answers to the research questions can be found as well.
- Chapter 10 comprises the recommendations.

1.8 Scope and limitations

Included in this research are:

- Production for the single completion phase of the cavern
- Production for the caverns within the series phase
- Reconstruction of the cavern volumes from the production
- Reconstruction of the cavern dimensions by simulations
- Identification of influential parameters on the residual cavern volume compared to the produced volume
- Identification of influential parameters on cavern migration
- Determining what values the parameters can attain

- Construction of a migration model
- Correlation of the migration model and its parameters
- Analysis and evaluation of the migration model
- Reconstruction of known subsidence cases and migration behavior
- Reconstruction of the most likely maximum migration potential and current and future status.
- Safety assessment purely in terms of migration

Important assumptions are:

- The production in tonnage can be converted into cavern volume using the standard AkzoNobel parameters (appendix C2) and this applies to under saturated brine and additional saturation of brine as well. The reason is that the equivalent volume corresponding to the maximum saturation of brine (i.e. 312kg of salt per m^3) can always be used. The leached out volume will be the same if the brine concentration is lower and more fluid is pumped around.
- If no information is available regarding the production setup when caverns were connected, the production may be divided equally over all the active wells.
- The tonnages that have been derived by mass balancing with the flow rate and brine concentration are accurate.
- The casing is well cemented and leaching cannot progress upwards much faster due to leakages.
- The rock layers in between the rock salt layers and roof anhydrite are so poorly soluble compared to the rock salt that they can be considered as insoluble
- The same applies to the so-called: 'insoluble content' to a certain extent. It is assumed that approximately 1vol% does come up with the brine.
- The insoluble rock layers can be considered as roof protection blankets for the time they remain in place.
- When no salt roof is left in place, the insoluble rock layers and all overburden strata will eventually fail.
- Both the compaction and consolidation can be approached as instantaneous behavior and both have been caught in one overall factor.
- The phase II bulking factor already accounts for the potential consolidation of the debris column and is therefore considered as instantaneous as well.
- The compaction of the debris column is partly comprised in the phase II bulking factor and potentially some more can occur, resulting in small subsidence potentials.

Excluded from this research are:

- Extensive analysis of leaching coefficients
- Cavern development for unsaturated brine extraction and for additional brine saturation
- Research on the cementing of the casings and what the effects on the leaching behavior are if the cemented casing did not seal of the salt layer at the shoe.
- Investigating the mechanical strength of the insoluble rock layers and overburden strata.

- Comprehensive research on the compaction and consolidation behavior of the insoluble content, slurry and failed roof material in the cavern.
- The compaction behavior of the debris column in terms of the maximum potential, duration and the corresponding subsidence potential.
- Exact subsidence predictions.

1.9 Approach

First the production methodology and production numbers have been reconstructed. With digitalizing the valuable information regarding the repair works and production methodology a new database arose that could easily be correlated with the geology. The digital database regarding the production numbers and methodology form the basis for the simulations.

Subsequently the limitations and influential parameters for the simulations have been identified as well. Simultaneously the identification of the parameters affecting the cavern migration was progressing; especially from cross-correlating the well –known cavern migration cases with the interpreted data from the logbooks and the reconstructed cavern dimensions from the simulations. After this the simulations have been carried out as accurately as possible.

The construction of the migration model commenced after the simulations. With fitting the model to the known cases and several cross-correlations, the model was finalized. After the model was finalized the model was ultimately used in order to reconstruct the migration for all caverns. In figures 1.4 and 1.5 the approach is summarized into two overviews. The first one comprises the reconstruction of the cavern dimensions and residual volume; this can be considered as all cavern behavior prior to migration. The second figure comprises the approach for the migration behavior.

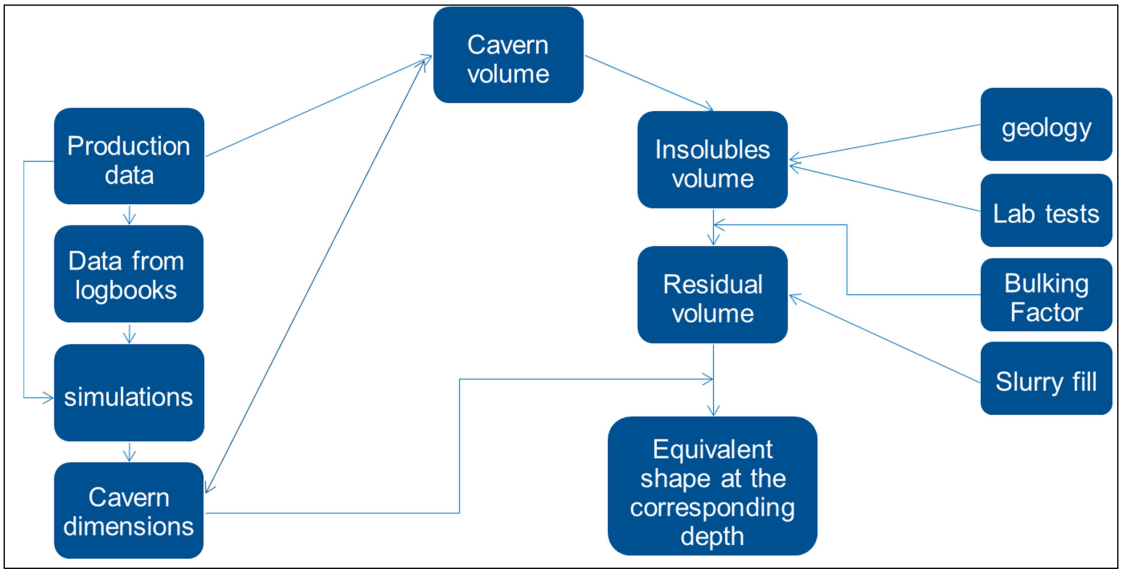

Figure 1.4 schematic overview of the reconstruction approach part 1

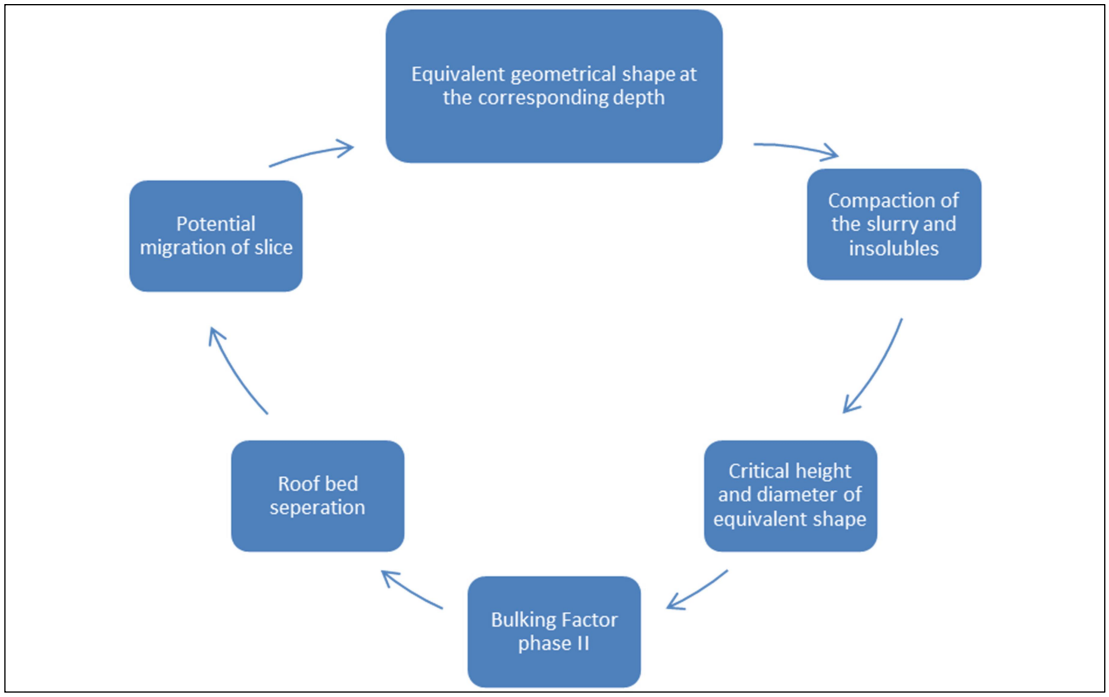

Figure 1.5 schematic overview of the reconstruction approach part 2

Additionally it should be noted that in figure 1.5 that the approach is actually shown as a closed loop. Moreover it can be seen that the migration potential is stated as: 'potential migration of slice'. This indicates that the model has been repeatedly run. In fact the model was indeed incrementally implemented in for one scenario which required iterations. This will be explained thoroughly in chapter 5.

1.10 Database

1.10.1 Wells

In 1.3 it is stated that there is a lot of data about the phase 1 of the Hengelo Brine Field available. First of all for each well there is a scanned version of the original, hand-written logbook. Additionally the hard-copy original scrapbook is still in the archive for most of the wells. The log and scrapbooks contain valuable information about: how the borehole was drilled, how the casing was cemented, at what depth the casing and tubing were originally, what production method was used, and from workovers the new casing and tubing depths, and again production method.

Nowadays most information can be accessed through the BPB-database. This stands for BoorPutten Beheer (=Management of wells). This database contains information of each individual well; amongst this are the location at surface, total depth, casing and tubing depths, production numbers etc. For the caverns where sonar measurements have been conducted, these are displayed in BPB as well. This is actually one of the most visual features of the database.

Unfortunately only at 4 caverns in the phase I area sonar measurements have been performed. At cavern 15 multiple sonar measurements over an interval of several years and from caverns 37, 33-34, 49 and 50 only one single sonar measurement is available. Moreover the BPB database has been

setup during the late 90's and therefore no production data has been included in the database concerning the phase 1 wells.

Furthermore a section with the lithological description of each well was available on NLOG[1]. The website also contained a lot of well intervention measurement data such as: Gamma Ray and Casing Collar Locater logs. Unfortunately for the phase 1 there are no logs for each well and the logs that have been made are often only CCL or CCL and GR. Another probe that was often used in the well interventions from the 1960's onwards is the 'bottom probe'. This does not result in a plot or a log, but gives direct information about the bottom depth of the cavern at that time and was always written down in the logbook.

1.10.2 Geology

An extensive geological study on the 'Hengelo Solution Mining Area' has been delivered by Geowulf in 2010. Within this study the HBF has been dissected into 2 areas and on both areas a comprehensive report has been composed. The reports contain all the lithological sections of all the boreholes and derived from this are: lithostratigraphy, chronostratigraphy and thickness maps for all the layers. Moreover the geological setting, facies and tectonic phase have been correlated with the lithostratigraphy. Finally faults that have been recognized have been mapped as well.

1.10.3 Production

The production numbers were closely tracked for the phase 1 well. The salt tonnage that was derived from the brine volume and concentration that came from a cavern was written down each month. Monthly and yearly overviews from 1936 to the mid 90's are still available in the archive. Unfortunately there are no numbers available from 1933, 1934 and 1935.

Additionally there are also binders that contain the amount of water that was pumped into the caverns and sometimes the numbers of the return streams are stated as well. Sadly only in 3 cases the volume of this return stream has been written down. For at least 22 more wells there are distinct hints that return stream has been pumped back into the cavern, though no numbers of the volume are available.

The production binders state the annual production- and for most years the monthly- per well until the caverns became interconnected. After the caverns became interconnected to each-other the production for the series was written down. Only 5 of the total 42 caverns have established no connection to any other cavern.

1.10.4 Research

Throughout the years AkzoNobel has established a sizeable archive of reports that have been published either internally or publicly. Some of the reports are describing studies that AkzoNobel

[1] Public Dutch website containing a database about exploration and exploitation in the Netherlands and North Sea continental shelf, hosted by the Dutch government

employees conducted themselves, and the majority of the reports are on studies that external companies or consultants or students have carried out in command of AkzoNobel.

The studies comprise the complete geology (1.10.2), multiple studies on surface subsidence, in situ geotechnical phenomena of the caverns and overburden, backfill, cavern stabilization, well intervention reports, bulking of collapsing roof layers and a seismic survey.

A lot of the reports containing research or information on topics related to this study have been read and found helpful.

1.10.5 Results from this research

During the course of this research the caverns of the phase 1 area have been reconstructed, this resulted in a comprehensive database.

Firstly a production overview has been made containing the production of all caverns and total.

A summarized overview in the form of an excel sheet for each cavern containing the lithology, casing and tubing depths after each repair work and production methodology. Later on this overview was complemented with a tab containing the annual production numbers of the specific well and all the vital data for the simulations.

The results of the simulations have been stored and form their own database containing the simulation files and pdf illustrations of all caverns.

Finally each cavern has its own excel sheet containing the modelled maximum potential migration.

2. Project background

2.1. The socio-economic importance of salt

Sodium Chloride is indispensable for the survival of mankind and several other living organisms (Kurlansky, 2003). The history of the world from the perspective of salt is simple: animals have cuts paths in search for salt licks, men followed with trails and settlements near the salt licks, trails became roads and settlements grew (Time magazine, 1982). Human dietary has changed substantially over the years, especially when comparing the current to the most ancient normal consumptions. Meat was the main source of nourishment and was rich in salt, nowadays salt has to be added to a large variety of nutrients as a supplement. Furthermore salt became more and more important for conserving food - without salt the extensive exploring trips to discover new continents would not have been possible. Therefore the demand salt in its mineralogical form increased as mankind grew. While civilization spread across the globe, salt became one of the primary trading commodities and salt trading routes traversed all over the world. According to Kurlansky (2003) several wars have been fought over salt and the production and trading of salt has been fundamental for the rise of peoples.

The Romans were the first ones to name the mineral sal, after the cousin of salus, the goddess of health. The so-called salubrious crystals were not only adequate for preserving food, it was a good antiseptic as well hence the name. In fact it was of such importance to the Romans that the word salary is a derivation of their 'solarium argentum' which was a soldier's reimbursement that consisted party of salt. Finally the importance of salt to humans can be deduced from the numerous symbolic and ceremonial uses and expressions that are known.

2.2 Solution mining of salt

The oldest salt production can be traced back to China approximately 6000BC (Kurlansky, 2003). The technique that was applied was the so-called: drag-and-gather technique where floating salt crystals were collected. The salt crystals were formed by the evaporation of the lake in the summer. The first records about salt production date from 800BC and originate in China as well. The books describe how 1000 years prior to that moment salt production by boiling seawater in clay pots. From written documents it can be derived that already in 3000BC salt was being produced in the Sichuan province in China. Firstly this was done by the former techniques such as described above, however at some point it became apparent that the brine in the natural ponds came from the underground and travelled upwards. In 252BC the governor of Sichuan, Li Bing, ordered the first recorded brine well to be dug. With the wells becoming deeper and deeper, bamboo sticks were used for fluid transport. Although the Chinese lifted these sticks up and discharged the brine –that was hold in place by a kind of valve- it was essentially the first form of solution mining as only the brine was brought up. After several centuries of developing whole transportation networks made of bamboo on surface and improving the production method as well, the very same Sichuan Chinese invented the renowned technique of percussion drilling around 1050AD. An iron chisel was attached to a 2,5m long rod and was dropped through a larger bamboo guidance tube. At the end the rod was attached to a lever which allowed the driller to lift the rod and let it drop consecutively. Throughout the centuries that followed both the drilling and solution mining equipment evolved.

Nowadays solution mining is generally performed by drilling a well to the base of the salt layer or the desired depth inside a dome. A casing is cemented to the desired depth, which usually depends on the structure of the salt as well. Yet the cemented casing normally does not reach the depth of the entire borehole. Subsequently tubing of smaller diameter is hung inside the casing, almost reaching the base of the salt. Now by injecting water through one of the pipes and extracting the salt enriched water –brine- through the other the salt can be mined from the underground. At the surface the brine is heated in kettles – nowadays vacuum vessels – evaporating the water from the brine. At the end of the evaporating process the salt contains less than 2% of water. At the purification plant in Hengelo the process is much more complex, than what was just outlined. Prior the evaporation cycle the vast majority of impurities is removed by different separation techniques.

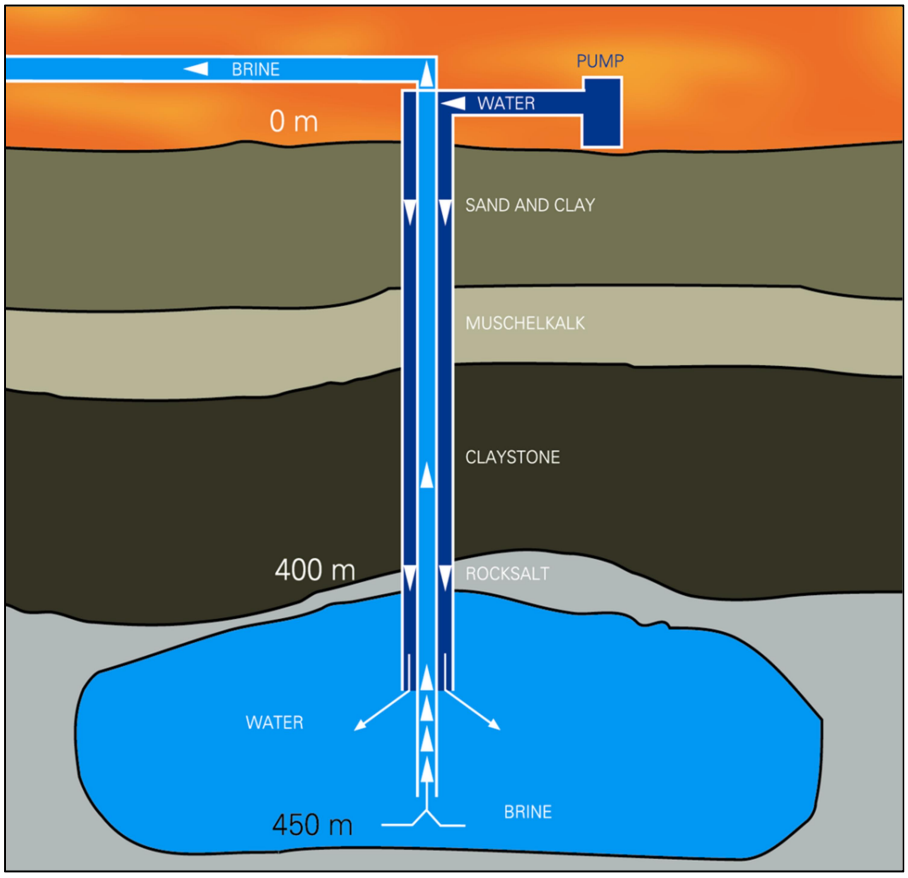

Figure 2.1 schematic overview of the concept of solution mining (source: AkzoNobel archive)

2.3 Hengelo Leaching Technique

During the in 1.3 outlined phases of the Hengelo Brine Field AkzoNobel attained a lot of experience. As a result of all this experience the company has their own leaching technique – Hengelo Uitloog Techniek (HUT, 2018). The technique was already setup during phase 3 and therefore the technique was initially describing the MCC caverns with 3 boreholes. As mentioned the decision to go back to SCC caverns based on the Good Salt Mining Practice preluded phase 4 and phase 5. Needless to say the HUT versions that have been composed afterwards all describe the methodology of safely developing and completing a SCC cavern.

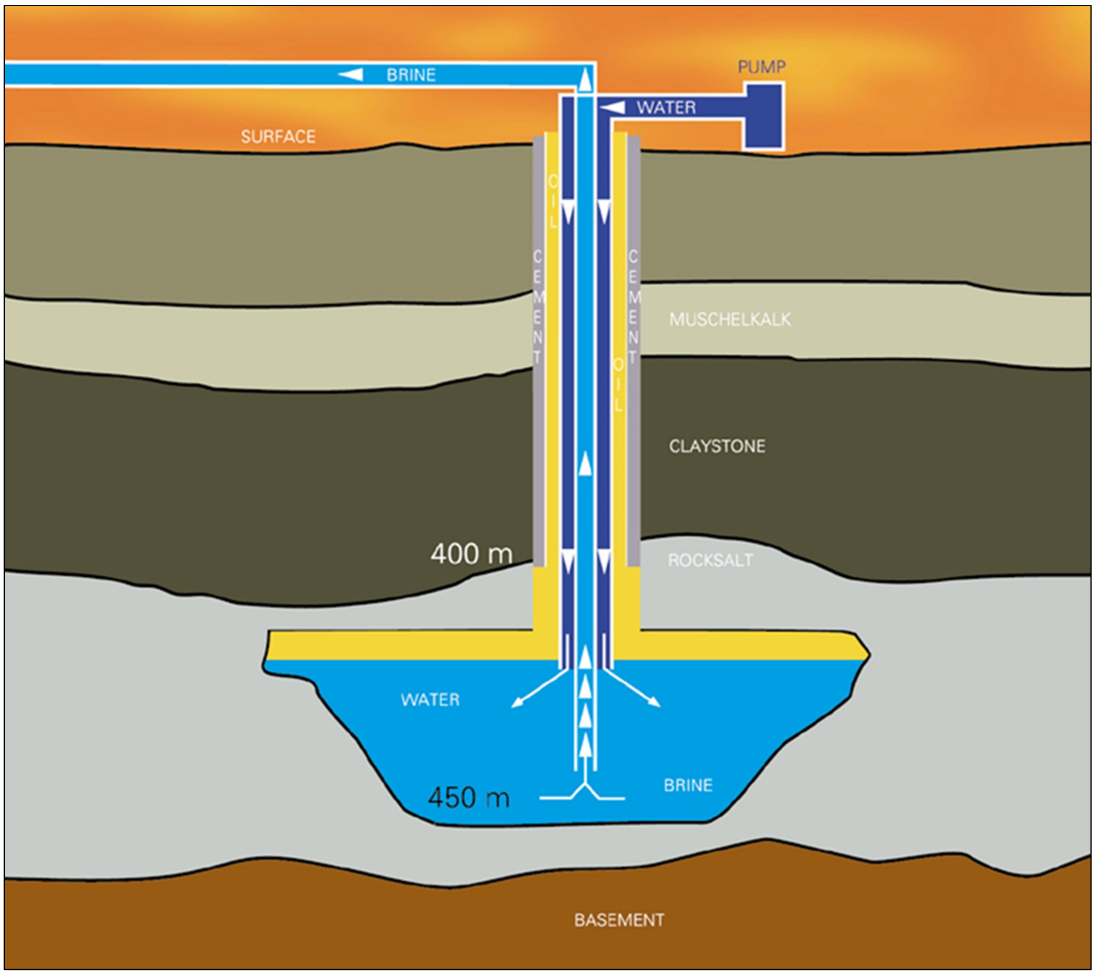

Figure 2.2 schematic overview of a SCC system with oil blanketing (source: AkzoNobel archive)

2.4 Geology

2.4.1 Regional Geology

The oldest deposits that have been identified in boreholes in de vicinity of the Hengelo Brine Field belong to the Limburg Group – late Carboniferous- and mainly consist out of sandstones with interbedded claystones. These carboniferous deposits are located at approximately 1000m depth and are unconformably overlain by the conglomerates and sandstones of the upper Rotliegend Group from the early Permian (Van Lange, 1994).

The area of the Hengelo Brine Field is located within the much larger confines of the famous Southern Permian Basin. As the name suggests this basin was the result of extensive rifting during the Permian although the origin of the subsidence of the basin can actually be traced back to the carboniferous (van Wees et al., 2000). The rifting was the extensional tectonics of the supercontinent Pangea that was disintegrating, which continued throughout the Triassic (Ziegler, 1990). As a result of this tectonic rifting the basin became filled with a large inland sea in the late

Permian – 272 to 252 Ma. This sea was the Zechstein Sea and as a result of evaporation due to the warm and arid climate this left a thick – 600 to 1600m- evaporite deposit all over the basin. Not only salts but carbonates and anhydrites precipitated as well during the evaporation completing the Zechstein group.

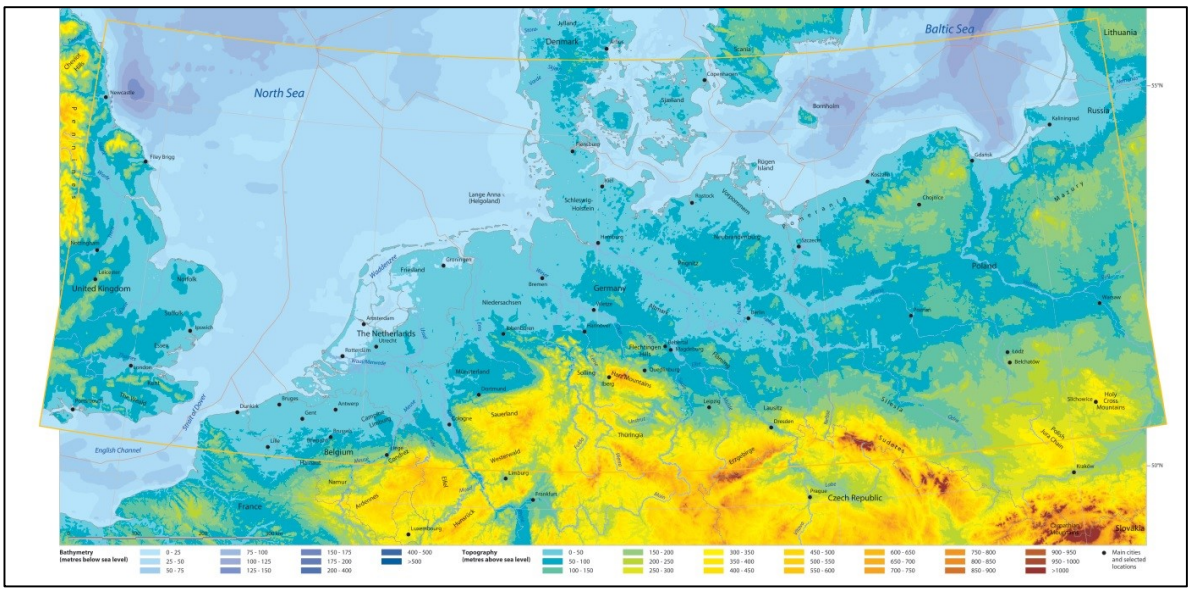

Figure 2.3 present day bathymetry map of the Southern Permian Basin (source: Doornenbal & Stevenson, 2012)

As mentioned in 1.1.3 this Zechstein salt was found in one of the exploration wells in 1909, however it is also already stated that the rock salt, that is being mined in Hengelo is from the Röt Evaporite member. This member finds its origin in the early Triassic and is part of the lower Bundsandstein, which is overlying the Hardegsen unconformity during a phase of coastal plain to coastal sebkha facies (Geowulf, 2005).

2.4.2 Triassic

At the end of the Permian the cyclic deposition of the Zechstein deposits was terminated due to the withdrawal of the sea (Ziegler, 1990). A complex rifting system within the basin was formed and clastic sediments from southern sources found their way into the basin, resulting in the sand-and-claystones of the Solling Formation from the lower Bunter Group. Correspondingly to this complex rifting system the central eastern part of the Netherlands started subsiding even further, this is known as the Central Netherlands Basin (see figure 2.4).

In the early Triassic this basin was exposed to another era of cyclic deposits primarily caused by tectonics and bound by unconformities (Geluk, 2005). The deposits in this basin that are associated with that era belong to the Röt Formation, which is part of the lower Bunter Group from the Germanic Triassic Group. At the location of the HBF this Röt Formation can be subdivided into the main Röt Evaporite Member and the upper Röt Claystone Member. The main Röt Evaporite Member contains halite alternated with anhydrite layers; the upper claystone member is dominated by clay-and-siltstones (Geluk, 2005).

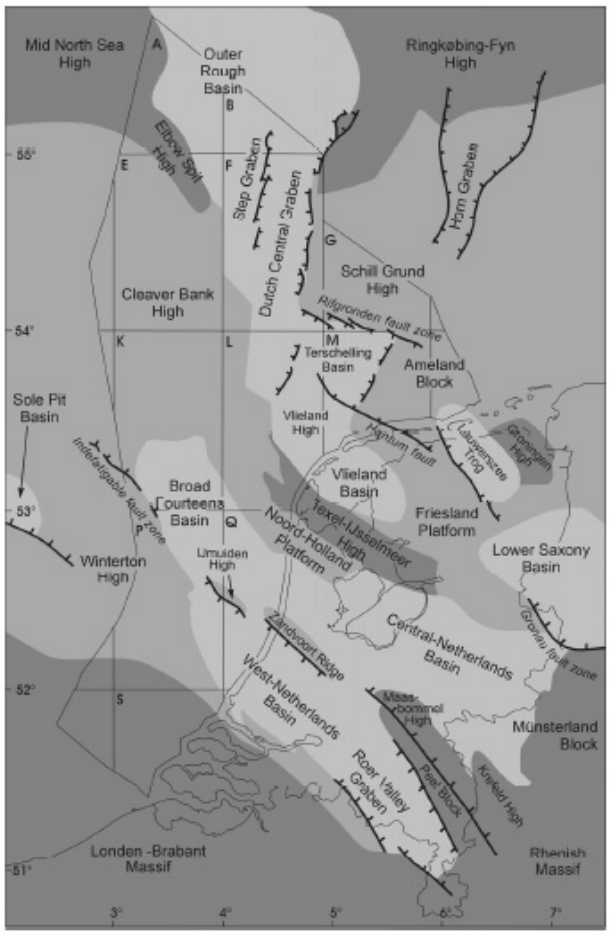

Figure 2.4 map of the Central Netherlands Basin (source: Geluk, 2005)

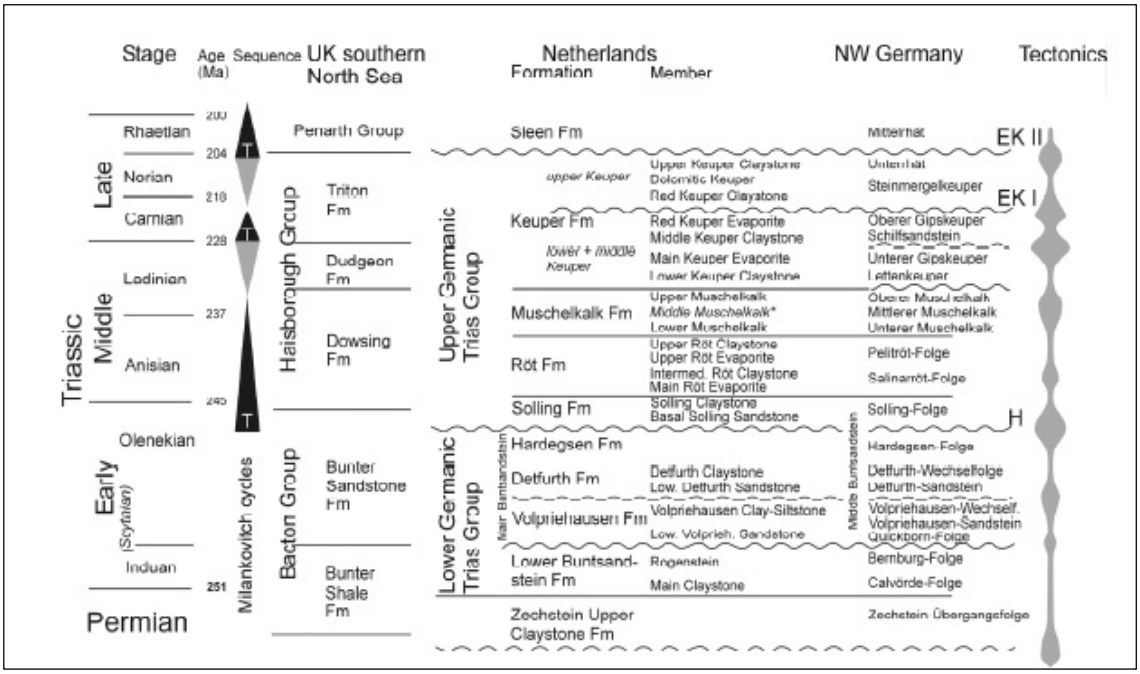

Figure 2.5 stratigraphical overview of the Triassic (source: Geluk, 2005)

The upper Röt Claystone Member which is part of the upper Germanic Triassic Group is overlain by the Muschelkalk Formation from the same group. The Muschelkalk was accommodated by transgression that led to the deposition of limestone, dolomite and thinly bedded calcareous claystone (Van Lange, 1994). This formation is partly eroded and wedges out the Northeast of the HBF area. The Muschelkalk is therefore not always present at each well location.

2.4.3 Jurassic and Cretaceous

At the location of the HBF the Triassic is unconformably overlain by the Tertiary, which itself is concordant followed by the Quarternary. Originally the chronological conforming Keuper Formation – upper Triassic - was deposited on top of the Muschelkalk. Yet during the early kimmerian phase the Keuper was completely eroded (Geowulf, 2005). During this phase the above cited partly erosion of the Muschelkalk occurred as well.

Chronostratigraphy		Lithostratigraphy Mid - Eastern Netherlands regional codes			Formation/Member	facies	tectonic phase
		N			North Sea Supergp.	marine	
Quaternary	Pleistocene	NU					
Tertiary	Pliocene		NUOT		Oosterhout Fm.		
	Miocene		NUBA	NUBAS	Upper Breda Sand Mb.		
				NUBAC	Lower Breda Clay Mb.		Savian
	Oligocene	NM	NMRF		Rupel Fm.		Pyrenean
	Eocene	NL	NLFF	NLFFB	Asse Clay Mb.		
				NLFFM	Brussels Marl Mb.		
				NLFFS	Brussels Sand Mb.		
				NLFFY	Ieper Clay Mb.		
				NLFFT	Basal Dongen Tuff Mb.		
	Paleocene		NLLF		Landen Fm.		Laramide
Cretaceous	Upper Cret.	CK	CKGR		Ommelanden Chalk Fm.		Sub-Hercynian
			CKTX		Texel Chalk Fm.		
		KN	KNGL	KNGLU	Upper Holland Marl Mb.		
				KNGLM	Middle Holland Shale Mb.		
				KNGLL	Lower Holland Marl Mb.		
	Lower Cret.		KNNC		Vlieland Claystone Fm.		
			KNNS		Vlieland Sandstone Fm.	marine coastal	
		SK			Niedersachsen Gp.		
			SKCF		Coevorden Fm.	lagoonal	
Jurassic	Malm		SKWF		Weiteveen Fm.		Late Kimmerian
		AT	ATBR		Brabant Fm.		
	Dogger		ATWD		Werkendam Fm.		Mid Kimmerian
	Lias		ATPO		Posidonia Shale Fm.		
			ATAL		Aalburg Shale Fm.		
Triassic	Keuper		ATRT		Sleen Shale Fm.	lagoonal	
		RN	RNKP	RNKPU	Keuper Fm.		Early Kimmerian
				RNKPD	Dolomitic Keuper Mb.		
				RNKPR	Red Keuper Claystone Mb.		
				RNKPE	Red Keuper Evaporite Mb.		
				RNKPM	Mid Keuper Claystone Mb.		
				RNKPS	Main Keuper Evaporite Mb.		
				RNKPL	L. Keuper Claystone Mb.		
	Muschelkalk		RNMU		Muschelkalk Fm.	coastal	
				RNMUE	Muschelkalk Evaporite Mb.		
				RNMUL	Lower Muschelkalk Mb.		
	Buntsandst.		RNRO	RNROU	Upper Röt Claystone Mb.	coastal plain	
				RNRO2	Upper Röt Evaporite Mb.	coastal sebkha	
				RNROM	Intermediate Röt Clayst. Mb.	coastal plain	
				RNRO1	Main Röt Evaporite Mb.	coastal sebkha	
			RNSO	RNSOU	U. Solling Claystone Mb.	coastal plain	
				RNSOS	Solling Sandstone Mb.		
							local hiatus

Figure 2.6 summarized regional stratigraphy (source: Geowulf, 2012)

After the early Kimmerian phase, sedimentation succeeded during the Jurassic with the deposition of the Altena Group. Though this depositional phase was terminated by the Mid Kimmerian tectonic phase, where the Altena group was severely eroded – in best cases only leaving the basis of the Altena.

Yet this was not the last deposition–erosion cycle. After the Mid Kimmerian phase ended a flat topography was subjected to the deposition of the Niedersachsen Group – Lower Cretaceous. This depositional phase continued with the Rijnland and Chalk Groups, when it ultimately ceased by the Sub-Hercynian tectonic phase. This tectonic phase had a compressional setting which re-activated the older Kimmerian extensional structures with a reversed off-set (Geowulf, 2005). The effects can be traced to the Röt Claystone. The Sub-Hercynian phase was directly followed by another erosional phase that completely erased the Chalk, and Rijnland Groups, and most of the Niedersachsen Group.

2.4.4 Tertiary and Quarternary

After the drastic erosional phases of the Jurassic and Cretaceous ended, sedimentation picked up in the early Tertiary and continued to the mid Eocene – Quarternary. Clastic sands and clays followed each other and left an approximately 100m thick package of unconsolidated soil. This is consecutively overlain by the approximately 30m thick upper quarternary sands, clays and gravels.

2.4.5 Structural setting (based on Geowulf, 2005)

The HBF area has been exposed to multiple phases of tectonic activity. Geowulf (2005) subdivided the Twente-Rijn area into 3 areas, which have their own tectonic characteristics (figure 2.7).

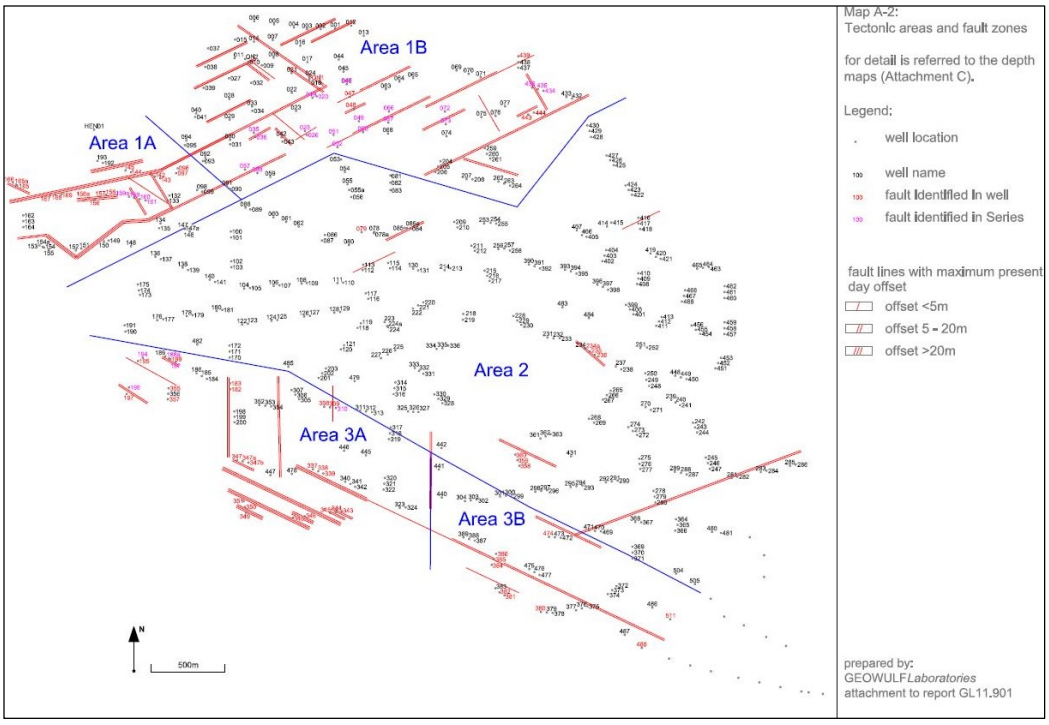

Figure 2.7 sub-areas defined by Geowulf (source: Geowulf, 2005)

As the scope of this study only comprise the boreholes of the phase 1 area – that are completely located within the area 1B outlined by Geowulf – only sub area 1B will be further discussed here.

A complex system of Kimmerian and Sub-Hercynian faults is identified. The tectonics of the early Kimmerian phase had very little effects on this area as it was smothered by the 'ductile' salt of the Röt Evaporite. Therefore the faults related to this phase are only visible in the Solling Fm underneath the Röt – the structural mapping is based on the borehole data, that almost all have the Solling Fm as end point. The mid and late Kimmerian phase show much more distinct phenomena in the area as the complete Jurassic and Cretaceous deposits are absent. During the Kimmerian phase the tectonic setting was extensive, which resulted in various extensional faults. The faults that are associated with the mid and late Kimmerian have a WNW – ESE strike and mostly have off-sets towards the SSW. On behalf of these numerous faults that are associated to each other, fault systems and blocks have been defined. Contrary to the early Kimmerian faults the mid and late Kimmerian faults do continue through the salt of the Röt Fm. At or between several boreholes they have been identified in the Muschelkalk.

In contrast to the earlier extensive regimes the Sub-Hercynian phase had a compressional tectonic setting and most faults from the Sub-Hercynian phase have been identified as re-activated and inverted Kimmerian faults. During this phase some new faults have formed as well.

During the Tertiary further faulting occurred, though most of these faults are interpreted as re-activated Kimmerian and sometimes Sub-Hercynian faults.

2.4.6 Salt thickness and evaporite cyclicity

Geowulf (2005) explains that the alternations in the thickness of the salt deposit can primarily be related to the tectonics. The extensional rifting of Pangea during the Permian that created the Central Netherlands Basin led to Horst-Graben-like structures locally. The area of Twente-Rijn is located at the graben-like structure and was confined by higher located Horst-like areas. The conditions were outstanding for the deposition of evaporites within the depressed and confined structure.

The cyclicity of evaporates is mainly caused by the alternating composition of the seawater. The seawater within the basin is replenished from time to time with fresh seawater, while the water in the basin becomes more concentrated due to evaporation. When the evaporation has greatly exceeded the new inflow for a longer time the water ultimately becomes oversaturated and present minerals start to crystalize. The order of individual facies that allow the crystallization and precipitation of the minerals depend on the solubility and ion concentration of the specific minerals in the seawater (Jeremic, 1994). Again the tectonics have an impact on this as well as the facies change during shoreline trans-and-regression.

Under normal coastal – according to Geowulf the Röt Fm has been deposited under coastal facies-conditions the order of precipitation is: Aragonite/Calcite, gypsum, Halite and subsequently the K-and-Mg-salts. In the Röt evaporites in Hengelo the K-and-Mg-salts are dispersed through the Halite. Halite does form the most distinct layer and could be up to 100m thick, although the thickness does not exceed 61m in the phase 1 area. According to Van Lange (1994) 100m of the Röt Evaporite in

Hengelo would contain 75m of Halite, 23m of Anhydrite and 1m of Calcite – again the K-and-Mg-salts are dispersed. This indicates that the evaporite cycles were not completed prior to the start of a new one.

In order to precipitate an evaporite deposit of this extensive thickness, large quantities of the minerals needed to be present. Under normal marine conditions this sea would have been several Kilometers deep to accommodate this. This was not the case at al. The thick evaporite deposit can yet be explained by the barred basin model which correlates to the tectonic induced confined graben-like structure. The barred basin model describes how a confined basin is cut-off from a larger sea by a barrier that can be overcome by increasing sea levels (Jeremic, 1994). Correspondingly the water in the basin gets replenished with fresh seawater from time to time, altering the concentration. In contemplation of the thick Halite layers with the dispersed K-and-Mg-salts through the halite, this helps to explain why the evaporation cycles in this region are not complete.

2.4.7 Lithostratigraphy of the Röt Evaporite

The Röt Evaporite Member locally consists out of four - sometimes three or two- layers of Halite. AkzoNobel has named these rock salt layers salt A, B, C, D from bottom to top. Between the different salt layers are the inter-bedded anhydrite layers. The names of these are: intermediate bench AB, BC, CD. Beneath the basis of the salt is the Solling claystone Member and the salt is capped by a thick anhydrite layer which is overlain by anhydritic shaly mudstones that already belong to the Röt claystone Member.

In the phase 1 area salt A and salt C are the most dominant layers and the thicknesses can reach 30 and 20m respectively. The insoluble rock layers often are approximately 1m thick and salt B is diversely interpreted. Often salt B is a layer of about 4m thickness; however at some wells it has been interpreted as 15 or even more than 20m thick (appendix A1.). An extraordinary fact that cannot be ignored is that in virtually all those cases salt C and salt D are not present. Likewise it can be observed that salt D is only present in the stratigraphic descriptions of 12 of the 50 wells, where in all those cases salt C is relatively thin. Additionally the salt layers have occasionally been described as rough and foul with local thin anhydrite layers interspersed through the salt. This further proves that the cycles were not completely finished before new a cycle started due to the influx of new seawater.

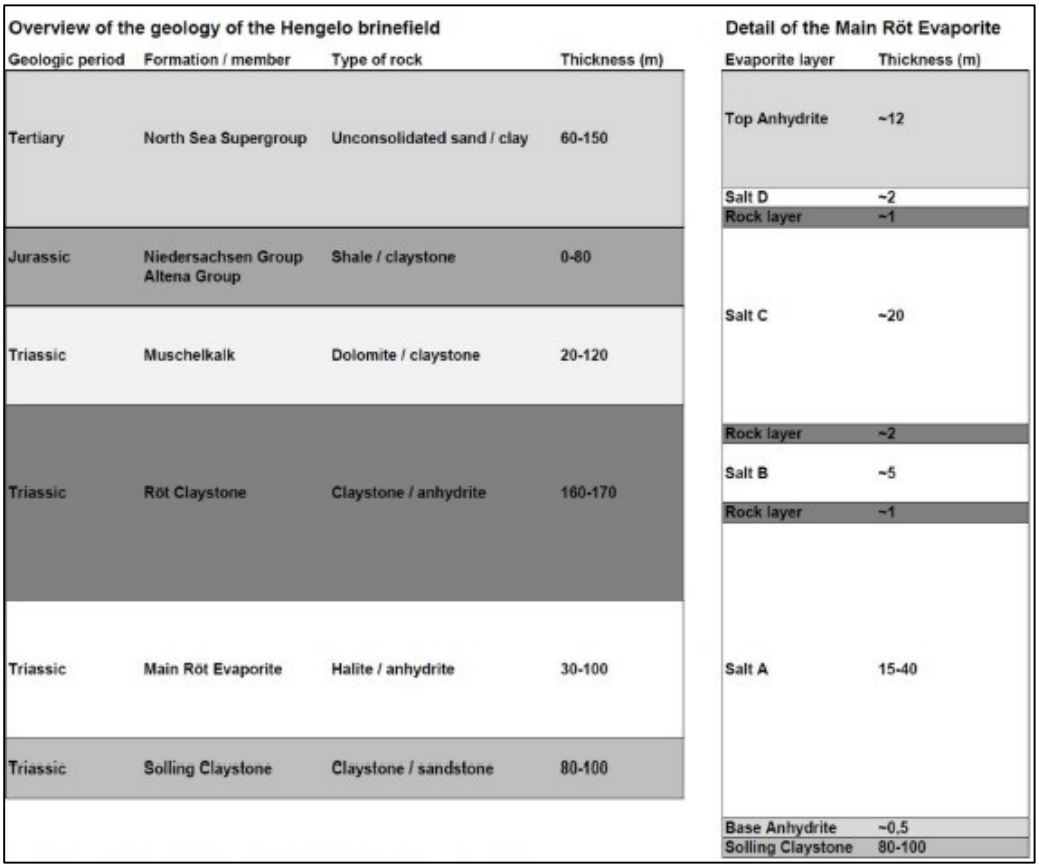

Overview of the geology of the Hengelo brinefield

Geologic period	Formation / member	Type of rock	Thickness (m)
Tertiary	North Sea Supergroup	Unconsolidated sand / clay	60-150
Jurassic	Niedersachsen Group Altena Group	Shale / claystone	0-80
Triassic	Muschelkalk	Dolomite / claystone	20-120
Triassic	Röt Claystone	Claystone / anhydrite	160-170
Triassic	Main Röt Evaporite	Halite / anhydrite	30-100
Triassic	Solling Claystone	Claystone / sandstone	80-100

Detail of the Main Röt Evaporite

Evaporite layer	Thickness (m)
Top Anhydrite	~12
Salt D	~2
Rock layer	~1
Salt C	~20
Rock layer	~2
Salt B	~5
Rock layer	~1
Salt A	15-40
Base Anhydrite	~0,5
Solling Claystone	80-100

Figure 2.8 overview of the regional geology and typical composition of the main Röt Evaporite (source: AkzoNobel)

2.5. Cavern migration

2.5.1 Cavern migration background

In chapter 1 it is outlined that due to a lack of control the caverns from the phase 1 area have migrated upwards and that some have caused severe surface subsidence. Cavern migration is the non-technical term for upward movement of the void. The mechanics behind are simple:

- As a result of a (too) large unsupported cavity span, to which the overlying roof stratum is exposed, mechanical failure of the roof occurs.
- The collapsed roof layers fall onto the cavern bottom. Due to the mechanical breaking during the collapse and the further disintegration of the roof layers upon impact at the cavern bottom, the roof layer is loosened.
- The increase of the volume that the failed roof layer will take at the cavern bottom is larger than the original in situ volume that the layer had. The volume increase can be described with the so-called Bulking Factor (loosening factor).
- Since the direct roof layer above the cavern has collapsed the new cavern top is at the depth of the top of the roof layer that has broken off. The cavern bottom has moved as well and as described has decreased in depth even more due to the bulking effect.

- This process of cavern top and bottom upward movement due to the roof failure is called cavern migration
- The cavern migration continuous until extinction occurs
- Migration extinction can be caused by the following phenomena:
    - Volume; The cavity volume decreases during the migration on behalf of the bulking effect of the collapsed roof strata; at some point the volume reaches the limit of zero. At zero cubic meters of cavity volume, the new direct roof layers is not unsupported any more.
    - Geological; the migrated cavern reaches a more competent rock at a geological boundary (discordant or concordant or by fault offset). The new roof stratum is stable under the in situ conditions (stress, unsupported span, depth).

2.5.2 Extinction of migration

In case the migration is extinguished by the volume decrease, Bekendam (1996) describes that under a constant cavern diameter – and therefore surface area- the extinction depth can be derived from the original cavity height and the bulking factor. In chapter 5 a new mathematical derivation of this phenomenon is depicted.

Nonetheless in case the cavern diameter is not constant during migration, this extinction will remain a result of volume decrease. Therefore the geometry of the cavern initially and during migration is vital. When the diameter is indeed not constant during migration, there is another possible phenomenon that can cause the extinction. This is under the circumstance that the cavern diameter decreases during the migration. As the diameter cannot become negative the limit is zero – likewise to the volume limit- which results in a geometrical extinction criterion. In this case the initial cavern diameter and volume and the angle under which the diameter decreases all have influence on the migration progress –next to the bulking factor. In order to determine the maximum potential migration 'slices' of a truncated cone can be described and modelled accordingly. Still the bulking needs to be applied to each 'slice' that has migrated, therefore iterations between the decreasing surface area and the height of the 'new' slice in the roof strata are needed. In chapter 5 the mathematical derivation can be found.

3. Development and exploitation of the phase 1 area.

The boundaries between the extraction phases of the Hengelo Brine Field are technologic based rather than geographic. In the phase 1 area the wells have all been drilled with a percussion drill between 1933 and 1959.

Figure 3.1 photograph of the percussion drill

3.1 Drilling technology

The percussion drill was a robust machine built on a kind of locomotive carriage (see figure 3.1).The machine primarily consists of a large, spring suspended, lever. Attached to the beam of the lever is the haulage and transmission of the drill string. The drill string consists out of steel rods that can be attached via screw connections with a drill bit at the end. In this specific case the drill bit was often a flat chisel. Under the propulsion of a steam – and later diesel- engine a crank and connection rod convert the rotary motion into a reciprocating motion. The reciprocating motion is forcing the drill string with the chisel downwards and upwards. At each impact with the rock strata the chisel is able to break of little chips of rock. After each blow the chisel had to be rotate slightly by hand in order to create a circular hole.

During phase 1 the wells were drilled in the following chronological order:

1. A wooden derrick was constructed at the location (figure3.2). The derricks were about 20m high and were initially equipped with a hoisting crane. After drilling and production preparation activities had been completed the hoisting crane was removed and only the wooden structure would remain. Nowadays only a few of these old wooden derricks are left as cultural heritage.

2. A 12'' – later a 10.5''- stove pipe was 'pulsed' into the quaternary soils – usually till 30 to 40 meters depth.
3. The soil inside the stove pipe was removed by either an auger or by flushing.
4. The loco mobile was positioned and the percussion drilling commenced with a 244mm (9.6'') chisel till the base of the Tertiary was reached at approximately 130m depth. The cuttings were transported upwards by means of a drilling fluid. The drilling fluid was mainly water in the beginning and brine at greater depths.
5. A paraffin coated 9'' conductor pipe built in with its shoe placed on the 'hard' Triassic rock; this helped the hole from collapsing during the rest of the drilling.
6. Drilling continued with a 210mm (8.3'') chisel until the hole collapsed. This was generally somewhere between 250 and 300m depth.
7. A 7.5'' casing was built in and through this casing the drilling carried on with a 174mm (6.8'') chisel until the top of the salt – or anhydrite- was reached.
8. Now the rotary motion was not converted into the reciprocating motion at the percussion drill anymore. Instead the rotary motion was directly transferred onto the drill string, where a hollow 'crown' was attached instead of a chisel. The whole Röt Evaporite was generally cored this way. The coring drill bit was generally made from tungsten carbide and had an outer diameter of 106mm (4.2'').
9. The 106mm hole was reamed by the 174mm chisel to the base of the salt.
10. After this the chisel was followed by a 216mm reamer, that folded out its knives about 1m deeper than the shoe of the 7.5'' was located at, leaving a 1m ridge for the casing to stand on.
11. The 7.5'' casing that stands on this ridge was lifted up one meter and the ridge was also reamed, enabling the further lowering of the casing. Subsequently the casing was built in to the desired initial production depth. This was generally 5 to 10m from the base of salt A.
12. The 7.5'' casing was cemented. In the first years this was done by depositing the cement through the annular space between the 9'' conductor and the 7.5'' casing. As they did find out that the cement did occasionally not reach the bottom of the hole at all, they altered the cementing technique. During the new technique the shoe of the 7.5'' was plugged with a wooden plug and perforated directly above the plug. The cement was pumped into the casing and was pushed down with another wooden plug that was placed at the well head after enough volume of cement was pumped down. The second plug was thrusted down, pushing all the cement through the perforations into the space between the borehole and casing and cementing the hole upwards.
13. The plugs were drilled out with the 174mm chisel.
14. The 4'' production tubing was built in to the desired initial production depth. This was generally 50cm above the base of salt A.

After establishing connections to the on land pipelines for the water inflow and brine outflow, the well was ready for production.

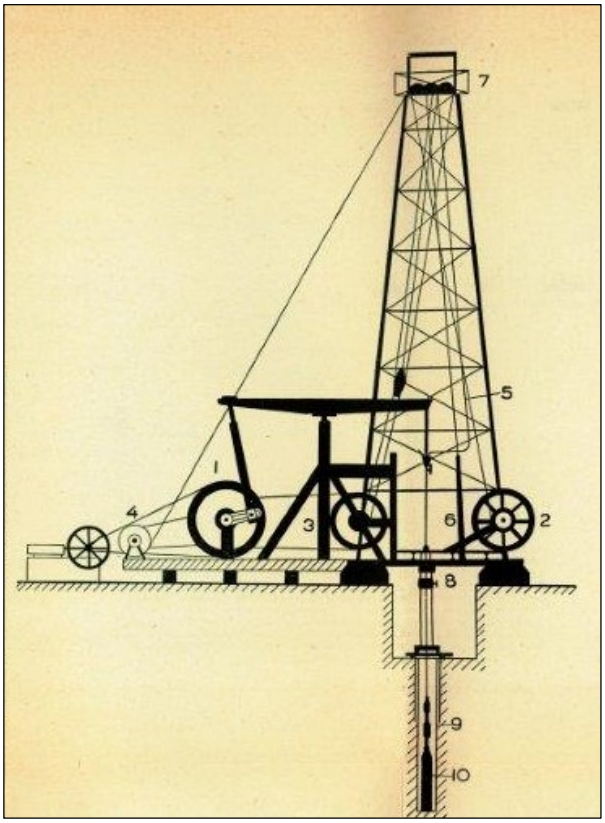

Figure 3.2 illustration of the derrick setup with the percussion drill implemented (source: AkzoNobel archive)

3.2. Production methodology

3.2.1 Introduction

As mentioned in chapter 1 the caverns at the Hengelo Brine Field were designed as so-called 'Single Completion Caverns'. By definition the aim is to completely develop these caverns as single caverns without any hydraulic connections to other caverns. The salt deposit is accessed by one well which forms the center of the cavern and the leaching out of the salt proceeds radially away from this well. Since the connection between the cavern and the surface is limited to this single well, both the fresh injection water and the saturated production brine have to flow through this well. There are two production methods for developing single completion caverns. Injecting the fresh water through the annular space between the casing and the tubing is called 'TOP' injection or reversed circulation. Injecting the fresh water through the tubing is called 'Bottom' injection or direct circulation.

3.2.2 Cavern development

When producing by means of top injection, the water, which is injected between the casing and tubing, enters the cavity in the most upper part. While dissolving the salt the water evolves into saturated brine. Since brine is denser than fresh water it moves towards the bottom of the cavern. As a result of the continuous inflow of fresh water at the top, the brine at the bottom is forced to

rise to the surface through the tubing. When the brine is becoming more and more concentrated, it will be able to dissolve less salt upon moving downwards in the cavern. This subsequently results in fully saturated brine that cannot dissolve any more salt. In addition the fresh water at the top will dissolve in a radial motion away from the well, resulting in a continuously growing flow pathway. The cavern will develop accordingly as little or no dissolving takes place at the bottom emerging into a 'morning glory' shape.

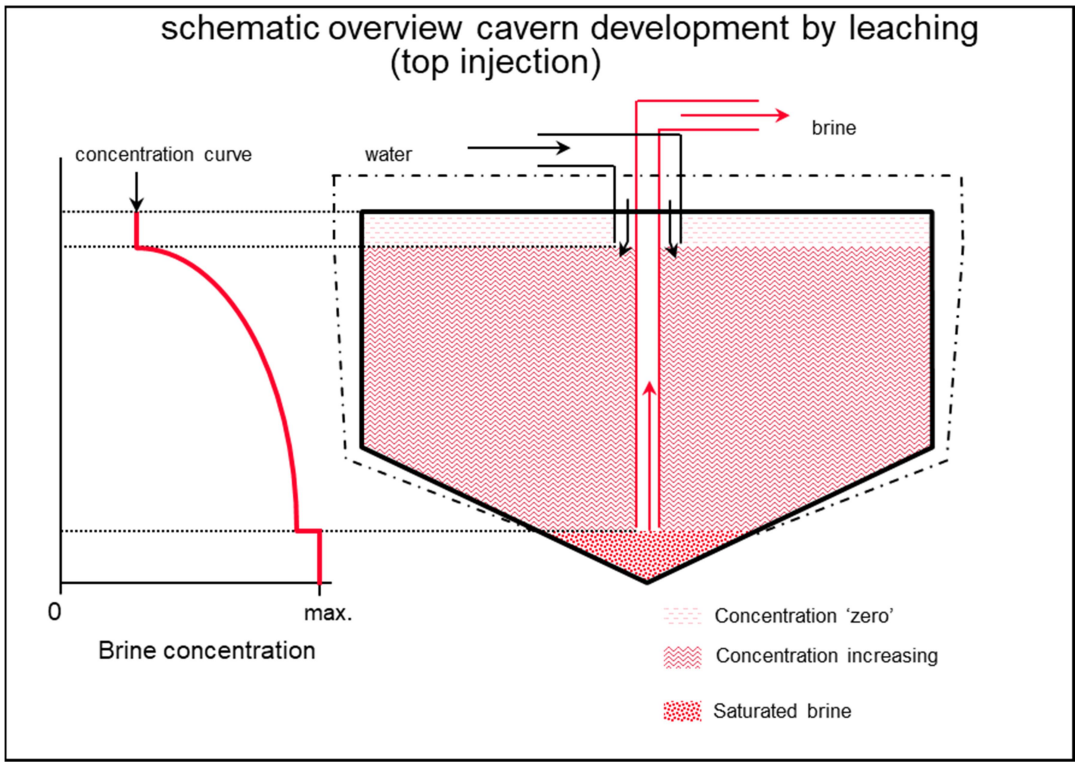

Figure 3.3 schematic overview of the cavern development by leaching (source: HUT 2018)

3.2.3 Morning glory

The 'morning glory' shape– wide at the top and narrow at the bottom- describes the shape of the cavern that is leached out by a single completion well. Durrie and Jessen (1964a and b) have described this shape and its phenomena without using the term 'morning glory'. In 1972 Von Schonfeldt states: '' the term morning-glory shaped was used by Dr. Frank Jessen to describe the characteristic cavern shape which resembles that of the morning glory blossom''.

In figure 3.3 it can be derived that the brine concentration inside a cavern increases from the top to the bottom of the cavern. This is especially in case of low production rates (Durrie & Jessen, 1964a). As a result the salt in the lower region of the cavern will not dissolve. The cavern geometry is therefore dominated by the concentration curve.

As described in 3.2.2, with the TOP injection methodology the cavern develops radially outwards, directly underneath the roof. Again nowadays the roof is protected by a fluid insulant blanket, yet during phase 1 all the salt directly underneath the first insoluble layer was leached out. With the

Bottom injection methodology the geometry of the cavern is initially reversed and can be described as a 'pear' shape. Upon continued production this converges into a 'barrel' shape and ultimately the 'morning glory' shape as well.

The difference between the two methods is the rate of decay of the cavern condition (Jeremic, 1994). With Top injection the cavern roof is exposed more quickly than with Bottom injection. According to Jeremic (1994) this means that the with the Top injection method the roof is more prone to caving. Based on interpretations of the logbooks this only has an effect on how quickly it will start caving and not on if it will cave.

Before the gradual implementation of sonar measurements at AkzoNobel during the 1960's, it was not known with a high degree of certainty what shapes and dimensions the caverns had in those days. Primarily based on the old field at Boekelo, and adapted with new data from the Hengelo Brine Field, AkzoNobel assumed that the caverns had the 'morning glory' shape.

Likewise almost all previous reports that concern the 'old' caverns in the Hengelo Brine Field assume that the leaching always took place via Top injection. According to Wassmann & Brouwer (1987) was the only used technique from 1933 to 1947. Examining the old logbooks of the wells within the scope of this study led to conclusion that this was not the case for the majority of the caverns. In total 6 of the 42 have only been produced with Top injection (figure 3.4) while 11 have been produced with only Bottom injection and the remaining 25 where completed using both production methods. In most of these 25 diversified caverns the pumping direction was switched multiple times.

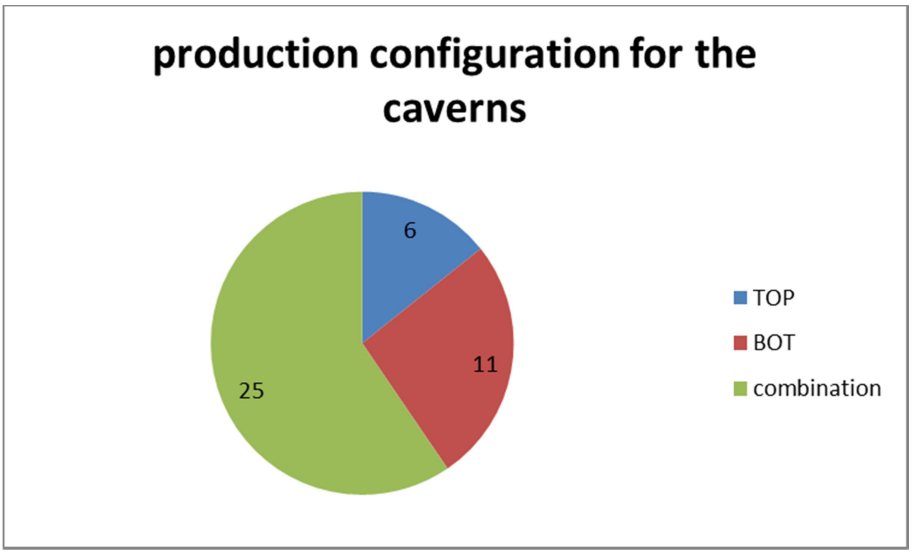

Figure 3.4 Production setup for the single completion production phase

As the production technology improved, reports that describe more recent caverns do distinguish other shapes. In Bekendam (1996) & Oranjewoud (2005) three different possible shapes are described (appendix B1). Both state that only shape 1 ('morning glory') and shape 2 ('inverted cone with cylinder of equal diameter on top') are possible amongst the phase 1 caverns and that most of them should have shape 1 as a result of 'over' mining during, and directly after the second world war. In the Oranjewoud reconstruction the upper part is approached by a cylinder that has a height of 10m and can reach a quite large diameter. The lower part is approached by an inverted cone with

a diameter of 50m. This 10m height of the upper part – which depicts the morning glory pinching out of the caverns-, seems a bit exaggerated and is actually not in line with the 'morning glory' theory.

Upon reconstructing the cavern volumes that Oranjewoud uses, it became clear that they make use of the volumes from Van Lange (1994). Van Lange published a table with the cavern volume in his appendix. The table however is never introduced and neither the source nor the conversion calculations from tonnage to volume are present. Recalculations of the tonnages from the volumes in the original Van Lange data made it possible to retrieve the source of his production numbers. This was not that easy as for the first 32 wells – with the exception of the doublets- as Van Lange calculated the volume based on the tonnage the wells produced prior to any connection and the remainder was based on the average contribution to the total of the series to which the wells belong. This means that the first 32 wells have been under estimated and that the last 18 wells have been smoothed out – some over and some under estimated. In addition some of the wells that belong to a doublet and well 37 as well have been greatly over estimated as they were allocated with the total tonnage of the series that they belong to. In conclusion: the Van Lange volumes are not always based on the correct numbers and most realistic assumptions.

3.2.4 Hydraulic connections

While it is easy to conclude that the volumes from Van Lange are less representative, it is understandable that he had trouble with determining the production numbers. In chapter 1 it is already outlined that the majority of the phase 1 caverns have established hydraulic connections with other caverns. In fact some have made multiple connections making that specific position a 'T-junction' between the wells – for example well 4 (see figure 3.5). The production continued and was written down per series as AkzoNobel, at the time, also did not know how to tell which cavern contributed what amount.

The following series are described by AkzoNobel:

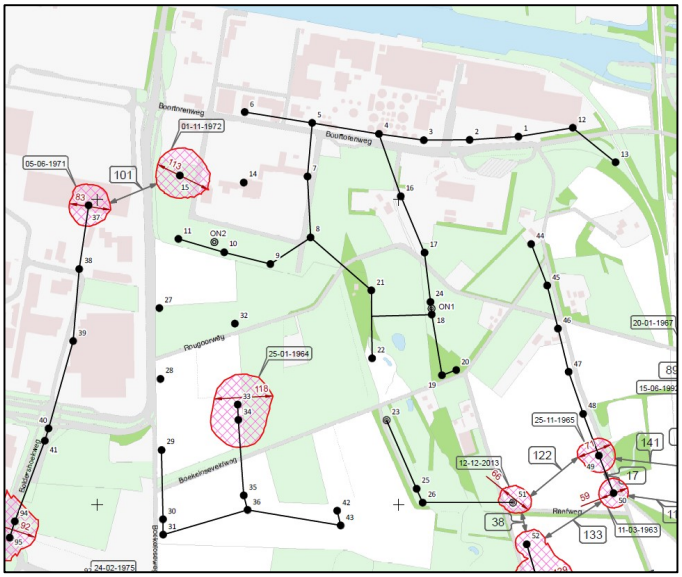

Figure 3.5 map of wells and connections (source: AkzoNobel archive)

	Wells
series 1	1,2,3,4,5,6,7,8,9,10,11,12,13, 16,17,18,19,20,21,22,24
series 2	23,25,26
series 3	29,30,31,33,34,35,36,42,43
series 4	37,38,39,40,41
series 5	44,45,46,47,48,49,50

Table 3.1 overview of the series

As outlined in chapter 1 sometimes the wells of phase 1 were placed close to each other for the sake of creating fast intentional connections. These wells clearly were not designed as SCC's but rather as doublets. In contemplation of allocating the tonnages to the right specific caverns these doublets are considered as one cavern instead of two (after agreement with Marinus den Hartogh, personal communication 2018).

The following wells have been identified as doublets:

- 18-24
- 19-20
- 25-26
- 30-31
- 33-34
- 35-36
- 40-41
- 42-43

3.3 production numbers

3.3.1 Production of the caverns as single cavern

The production of the caverns before any hydraulic connection was made – again with the doublets considered as one cavern- could easily be deduced from the old production binders from the AkzoNobel archive. Yet some pondering was unavoidable as the binders did sometimes contain typos and other ambiguities. In addition the implementation of the doublets as one instead of two caverns needed to be executed and the production of this doublet with other wells traced. This resulted in some additional production that is also considered as so-called single cavern production.

In addition to the production numbers, the annual productive days and production methodology per cavern have been traced. This info is derived from the logbooks (appendix B3, B4, B5).

An important note is: all the reported tonnages in this document represent metric tonnes.

3.3.2 Production of the caverns as series

Additionally the logbooks sporadically contained information on how the pumping configuration was after the caverns were connected. For example sometimes it was mentioned that water was pumped into one cavity and brine was extracted at the other. Wassmann (1980b) explains that if two caverns are connected and the water is pumped into one and the brine is extracted at the other, the majority of about 90% of the leaching will take place at the well where the water is injected. With respect to this and sporadic information from the logbooks it was possible to allocate the tonnages of the series in the early stages of the series. If too many caverns joined the series and if there was no information on the production setup, the remaining tonnages have been divided equally amongst the active members of the series. This last part did in fact require some interpretation as well. From the logbooks the date at which each well was abandoned could be retrieved, and sometimes it is even mentioned how long the cavern was taken out of production

already before abandonment. In addition the map with the connections enables the observations that some caverns cannot have contributed to the production of the series after a specific date. Therefore the word active is vital in the equal dividing sentence.

cavern	single production [ton]	final production [ton]
1	101119	182111
2	241240	269425
3	63895	92080
4	344445	365177
5	110555	139973
6	322890	342653
7	129360	158778
8	174080	209593
9	120500	160425
10	249885	284846
11	172120	193974
12	123750	141944
13	221840	237768
14	176610	176610
15	413919	413919
16	79370	87097
17	195700	261305
18-24	215690	296148
19-20	342640	385670
21	72570	153598
22	119320	200348
23	220515	252118
25-26	266380	297983
27	187602	187602
28	272118	272118
29	233865	331373
30-31	321720	404984
32	154420	154420
33-34	410783	410783
35-36	457750	529984
37	125892	142570
38	278467	313327
39	150556	264446
40-41	300933	414823
42-43	274515	343731
44	45315	65046
45	127535	147266
46	191432	201605
47	82854	110082
48	148548	186463
49	138886	159728
50	188362	223842

Table 3.2 total production in tons for the single and final production per cavern

In addition to the previous stated methodology series 1 can be broken down into sub parts. Series 1 consists out of wells 1,2,3,4,5,6,7,8,9,10,11,12,13,16,17,18,19,20,21,22,24. This is a complicated series that should be spitted into 3 sub parts.

In 1946 cavern 2 and 3 became connected and one year later cavern 1 became connected to cavern 2 as well. This is the start of series 1a and in 1951 cavern 4 and cavern 12 joined the series. Subsequently cavern 13 became connected to the series in 1952.

In 1951 caverns 8 and 9 became connected, which is the start of series 1b. In 1952 cavern 10 joined the series and caverns 5 and 7 became connected to each other, joining series 1b one year later. In 1954 cavern 11 joined series 1b as well.

Since the production at caverns 2,3,4,12 and 13 stopped per January 1955 and the production total of series 1b did not increase after January 1954 it can be assumed that no production occurred at these caverns after 1953.

Series 1b is expanded by cavern 6 in 1954 and series 1a and 1b merged together in 1955 as cavern 5 and cavern 4 became connected. Yet this connection came after the caverns of 1b had stopped producing. From the production point of view it can therefore be stated that only series 1b continuous and that series 1a - even though connected to 1b- has stopped.

Series 1c started developing around the same time as well as in 1955 cavern 17 joined doublet 18-24 and cavern 21 and 22 became connected. One year later 17, 18-24, 19-20, 21 and 22 were all connected. Series 1c is finally joined by cavern 16 in 1957.

In 1958 cavern 16 established a hydraulic connection to cavern 4. With this the complete series 1 became complete. Yet due to series 1a not contributing to the production after 1953 it can be said that sub series 1b and 1c probably still produced their own tonnages for the rest of 1958 and 1959 as the connecting cavern (cavern 4) was out of production for years. Additionally the connection (indicated by the line in figure 3.5) between cavern 8 and cavern 21 cannot be found in either the logbooks or the overview of connected wells from AkzoNobel. It is very likely that either this connection is not present or that this connection developed after production had ended.

Series 2, 3, 4 and five are much smaller and less complicated and all the wells joined incrementally. The production for these series can therefore be divided over all the active caverns that belong to the series.

3.3.3 Statistical analysis interpretation

In table 3.3 the total tonnages of all the wells of phase 1 are summarized. The total over all the caverns sums up to 10167733 tons. In the end this correlates to a 0.12% surplus compared to the total from the original AkzoNobel overview. In the table the corrected delta depicts a correction on the surplus due to the production after the overview list of AkzoNobel was published. The list was published in 1972 and series 4 kept producing until 1980. Therefore the production of the last 8 years is not accounted for in the overview. This unaccounted production is 33432 tons. The corrected total of the AkzoNobel overview will be 10155452 tons instead of 10122020 tons; however the offset will remain 0.12% surplus.

	Total of this report [tons]	original total AkzoNobel overview [tons]	Delta [tons]	Corrected delta [tons]	offset in [%]
series 1	4.162.911	4.163.494	-583	-583	-0,01
series 2	550.100	544.560	5.540	5.540	1,02
series 3	2.020.855	2.020.865	-10	-10	0,00
series 4	1.135.167	1.097.165	38.002	4.570	0,42
series 5	1.094.031	1.091.267	2.764	2.764	0,25
singles	1.204.669	1.204.669	0	0	0,00
total	**10.167.733**	**10.122.020**	**45.713**	**12.281**	**0,12**

Table 3.3 overview of production total per series

The total tonnage of the phase 1 wells until the moment of connection (e.g. the single production total of all the wells) sum up to 6462905 tons. Compared to the original AkzoNobel overview of 6455374 tons this translates to a 0.12% surplus. Here it should be noted that these numbers correlate to the single production of the wells as the original AkzoNobel overview has listed them. This means that the production of the doublets, after the two wells of the doublet have established connection, is not accounted for. The production total of the single caverns, with the doublets considered as one cavern, sums up to 8587986 tons. This translates to 84.6% of the end total and therefore it means that 15.6% of the end total comes from the production within series.

In figure 3.6 the distribution of the total production per cavern is illustrated. On the left-hand side the caverns that have no connections at all depicted with 100% production from Single Cavern Completion.

What immediately draws the attention is that doublet 33-34 also has 100% single contribution, while this doublet is connected to doublet 35-36 according to AkzoNobel. This can be explained by the moment the connection established (31-3-1965), which was half a year after the production of doublet 33-34 had stopped. The production binders indicate that doublet 35-36 also stopped producing after the start of 1965. Though the single production for 35-36 was extensive (457750 tons in roughly 6.5 years, while the production at 33-34 was 410783 tons in roughly 10 years) and the doublet readily established connections to the series 29, 30-31 in 1961 and to 42-43 in 1962. Therefore it can be assumed that it was doublet 35-36 that grew extensively. Additionally the production at cavern 33-34 during 1964 was only 8597 tons (while the average annual production was 37343 tons) as the production laid still during considerable production works. The average annual production of doublet 35-36 is 65350 tons (highest of all phase I wells).

From well 46 to well 8 the contribution of the production within series accounts for 5 to 20%. After this the range from 20 to 30% is still acceptable and concerns wells 7 to 3. The last wells – 22, 39, 1, and 21- all have a more than 40% - and 21 even more than 50% - this is a striking amount and a large question mark considering the reliability is justified.

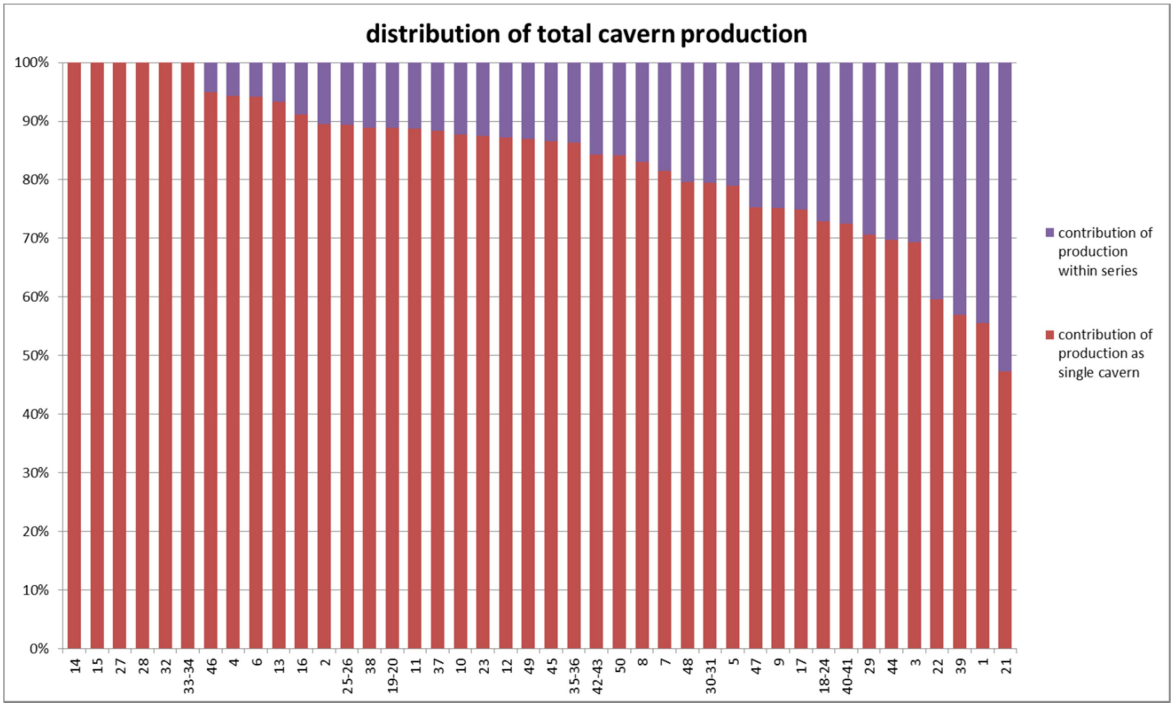

Figure 3.6 production distributions per cavern

Figures 3.7 and 3.8 show the histograms belonging to the single production and total production. In the single production histograms it can be derived that the mean and median lie at 204.000 and 188.000 tons respectively. On the right-hand side the caverns that have already produced more than 300.000 tons stand out:

- 40-41 with 300933 tons
- 30-31 with 321720 tons
- 6 with 322890 tons
- 4 with 344445 tons
- 33-34 with 410783 tons
- 15 with 413919 tons
- 35-36 with 457750 tons

The non-doublets (e.g. 6, 4 and 15) have a high production and again this is with a very high certainty as this comprises only the single production. Assuming that the tonnage calculations, and moreover the measurements of the brine concentration and flow rate from AkzoNobel back in those days were quite accurate; the allocation of the tonnages to the caverns is precise.

The histogram of the total production shows that the histogram is drawn to the right a bit more in total compared to the single production histogram. This is the direct result of the additional production during the series phase. The distribution is more scattered and has a larger spread. This can primarily be explained by the different additional amounts of production that the series phase account for. The mean and median from this histogram are respectively 216717 and 241659 tons. Looking at the right-hand side again, the following caverns stand out:

- 33-34 with 410783 tons
- 15 with 413919 tons
- 40-41 with 414823 tons
- 35-36 with 529984 tons

What is important to remember here is that cavern 15 and doublet 33-34 have no contribution in the series phase, as they did not have any connection (cavern 15) or the connection was made posterior to the production life of the cavern (doublet 33-34). Therefore these remarkable large production numbers can still be stated with a high certainty.

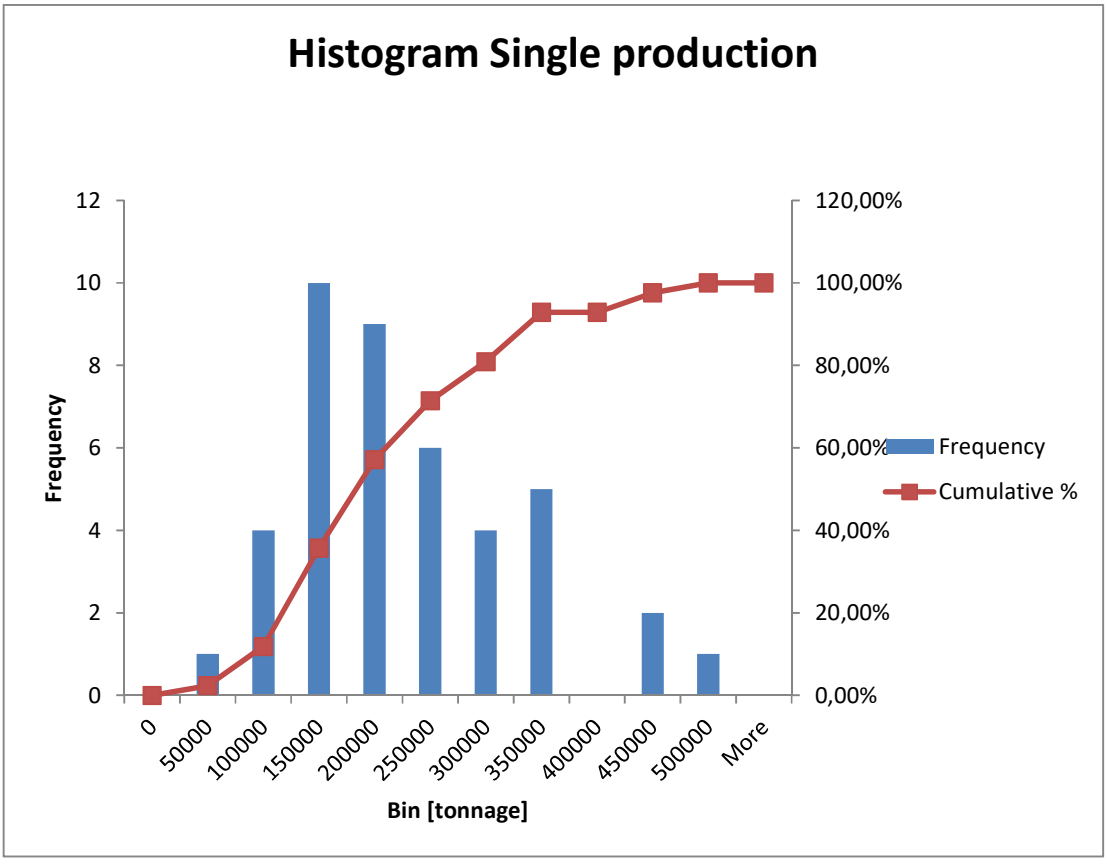

Figure 3.7 histogram of single production phase

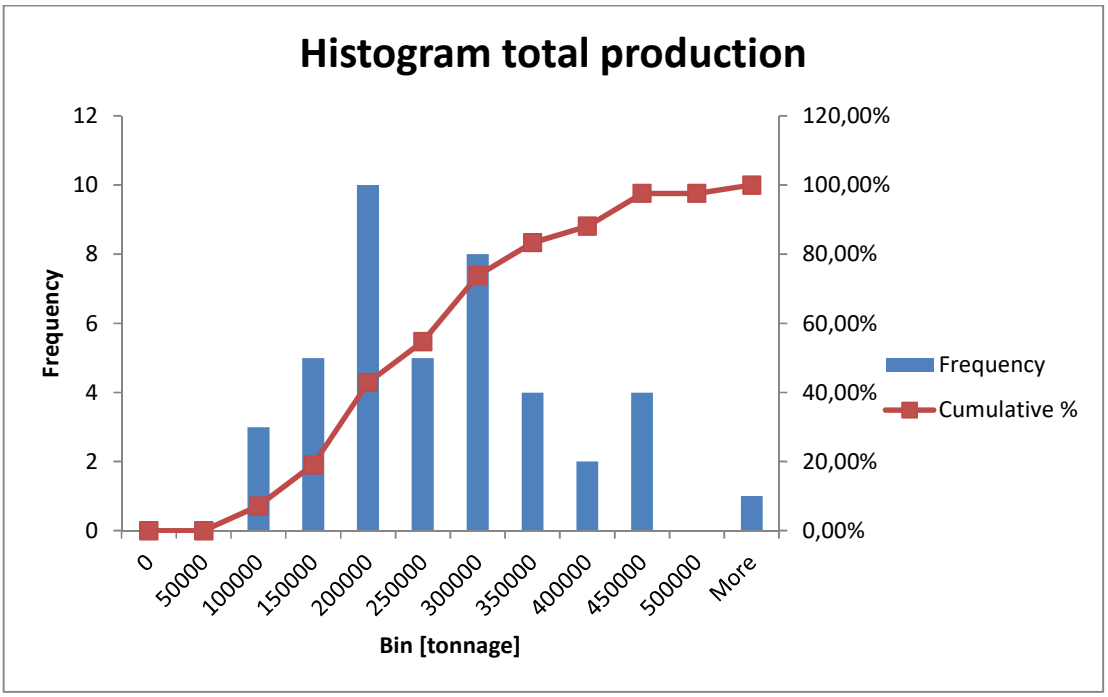

Figure 3.8 histogram of the final 'total' production phase

In figure 3.9 the sensitivity for the total production is shown. This does illustrate a highly exaggerated and dramatic range in some cases as the maximum production (purple bars) is very large. Some explanation is required in order to place this chart into the right perspective:

- The minimum – in red- represents the Single production per cavern.
- The most realistic – in green- represents the total production per cavern, with contribution of the caverns within the series phase allocated according to my method. Again based on the old logbooks as far as this was possible and equally divided when this was not possible and/or when too many caverns joined the series.
- The maximum – in purple- represents the absolute maximum that a cavern can potentially have produced. This maximum consists out of the total production of the series until this specific cavern was taken out of production.

As mentioned in 3.3.2 the closed off wells are assumed to not contribute to production any more. However the likelihood that one of the caverns, belonging to a series, accounts for all the production after the connections have occurred is low. Moreover it depicts a distorted picture as the contribution to production of all the other wells, within the same series, during the series phase would be zero in that case. In other words: in the unlikely case that one of the wells within a series has produced this maximum, all the others of that series have produced the minimum until this specific well was taken out of production. With all that being outlined the graph does show how sensitive the data is. Especially for wells 17, 21 and 22, where the maximum exceeds double the amount of the minimum depict an undesirable spread.

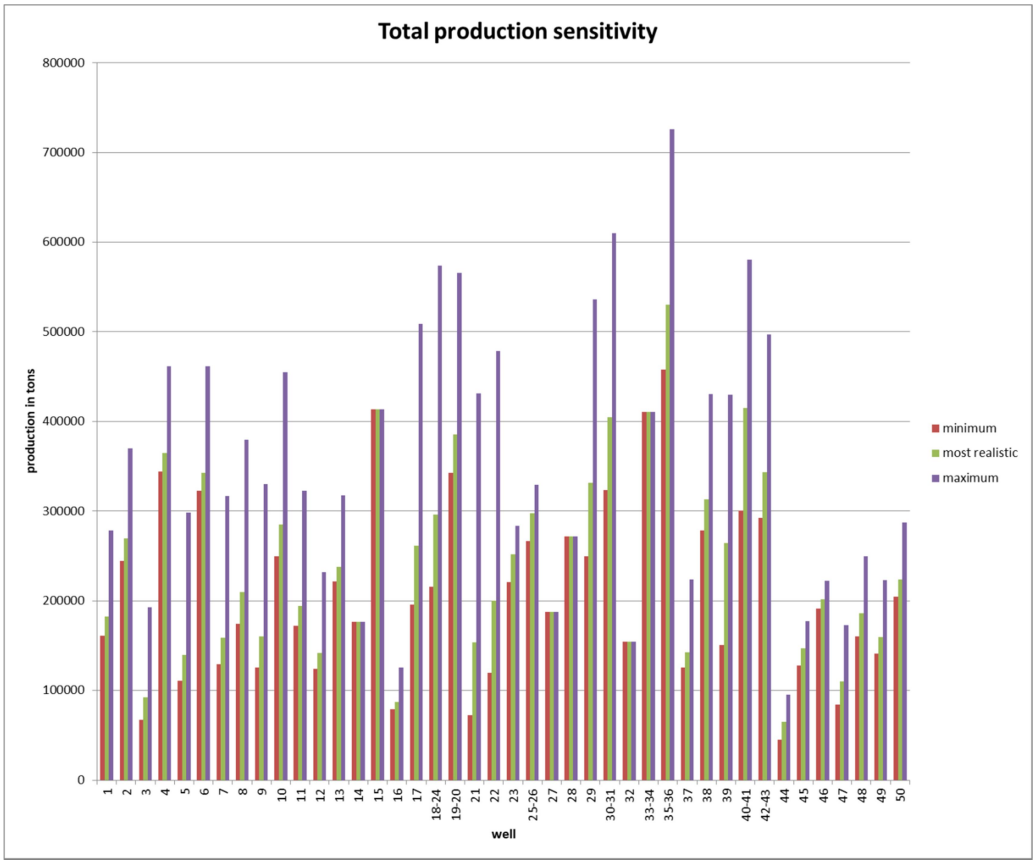

Figure 3.9 bar chart with the sensitivity for the total production

4. Reconstruction of the caverns

Chapter 3 showed that the volumes that Oranjewoud (2005) used came from Van Lange (1994) and that these volumes are not based on the best assumptions. Moreover the shapes that they used were based on the assumption that the caverns only produced with the Top injection methodology, which was not the case for most of the wells. As a result the diameters at the top of the salt are at some caverns over estimated and at some under-estimated. During the reconstruction they clearly tried to make sure that the uppermost diameters of the caverns overlap at the places where connections between caverns are known (Appendix C1). This seems quite logical and it correlates well with the known hydraulic connections. However at the locations where sonar measurements have been made, and connections had already been made with other caverns, were not detected. During the more recent phases of the Hengelo Brine Field it actually often occurred that the hydraulic connections between caverns were detected by pressure monitoring, but the sonar measurements showed no such connections.

Within the scope of this study a good example is cavern 37. The sonar measurement was made in 1971 and the cavern was known to be connected to cavern 38 already in 1967. Yet the connection is not visible in the sonar and moreover the maximum cavern diameter is 84m at the top of the cavern, while the distance to cavern 38 is almost 127m. This proves that the 10m thickness of the upper cylinder of the type 1 shape that Oranjewoud (2005) applied cannot have been true. The 10m thick cylinder would have been very distinctly detectible in the sonar measurement. In fact this does correlate more with the 'morning glory' shape, where very thin pinch-outs underneath the salt roof extended far enough to establish connections. These thin upper parts of the 'morning glory' would indeed not be detectable in sonar measurements due to their thin and elongated shape – the sonar waves would not reflect back to the tool in a clean manner if they come back to the tool at all.

Another remarkable artefact is that cavern 1 has an abnormally small diameter. After examining the volume and tonnages from Van Lange (1994) again, the cause had a quite innocent root. The volume that he outlined corresponds to 10119 tons of produced salt and in fact this number was published on the 1972 AkzoNobel overview of production of single caverns. However upon retrieving the yearly production numbers, from the old production binders, the total sums up to 101119 tons. Therefore a relatively small mistake such as a typo can have large consequences when nobody notices.

The new insights on the production method and volumes afford plenty of motivation to make new reconstructions of the caverns. In order to reconstruct the caverns shape and dimensions a simulation-software called WinUbro has been used.

4.1 Simulations

In order to simulate and reconstruct the cavern development as precisely as possible the simulations needed to be performed in phases. Multiple influential parameters - and what kind of effect they have on the simulations – have been identified. This resulted in the following setup where parameters derived from logbooks – some direct and some are interpretations are used:

- Flow rate [m^3/h]
    - Assumption 1: Inflow = outflow.

        ** This is in the ideal case. Normally the inflow always exceeds the outflow by a little as the cavern grows in size.*

    - Assumption 2: The outflow contains fully saturated brine (e.g. 312 kg of salt per m^3).

        ** This is idealized as well. During the production history of the caverns a lot of times the brine concentration was lower. When the concentration was considered to be too low by AkzoNobel, the brine would be pumped into another cavern for additional saturation. In case of brine with lesser salt concentrations it would mean that more water was pumped around and that the inflow and outflow was even higher. Therefore the inflow and outflow that are used in the simulations represent the equivalent fully saturated brine flows. The cavern volume would in fact not be larger as a result of long periods of under saturated brine production.*

    - Outflow rate [m^3/h] calculated from produced tons per year and productive days per year:

$$\frac{\left(\frac{tonnage}{0.312}\right)}{(amount\ of\ productive\ days*24)} = outflow\ rate\ [\frac{m^3}{h}] \quad (4.1)$$

- Depths of the casing and tubing (injection and production depths)
    - Data from old logbooks
    - Especially repair works are important indications
    - All depths from the logbooks and simulations are in m-MV (meters below surface level) in the drill hole database (BPB) the depths are depicted in m-NAP (Amsterdam water level). The differences in depth are generally about 20m for most of the phase I caverns as the topography is approximately 20m above the NAP level.

- Production method
    - Either Top or Bottom injection
    - Often written down in the logbooks
    - Sometimes no info is found for a long period of time
    - Assumption: only if a switch of the injection method is mentioned in the logbook – and if the new method continues for at least one month- the production methodology is changed in the simulation.

        **Sometimes there are indications that the pumping direction was switched at some point without it being written down in the logbook. In addition sometimes during tests the direction was switched several times in just a few days.*

- Duration of each phase
    - Alterations in casing and/or tubing depths – again from repair works- result in a boundary between phases.
    - Assumption: the casing and tubing depths maintain their former depths until the logbook indicates otherwise.

        ** Sometimes the workover crew found out that the depths were not the same as in the previous reported situation anymore. It is however impossible to tell when exactly the change in depth occurred if nothing is mentioned during that time.*

    - Alterations in the production method also results in a boundary between phases.
    - The last possible boundary between phases is production limit due to the dissolution angle and the position of the intermediate bench (blanket)
    - Assumption: limiting dissolution angle of 15° (figure 4.1)

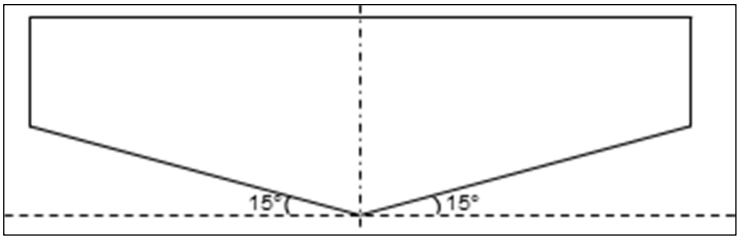

Figure 4.1 illustration of limiting dissolution angle for simulations

- Blanket
    - Assumption: each insoluble rock layer (anhydrite) prevents the leaching of the salt in the upwards direction for a certain amount of time and is therefore used as a blanket during the simulation. At some point this anhydrite layer is exposed underneath (undermined) to a span that is so large that it cannot bear the overlying strata anymore and it fails. The salt that is directly above is more ductile and stays in position.
    - The moment of collapse is based on my interpretations of the repair works that are mentioned in the logbooks
    - After a insoluble rock layer has failed, the leaching continues under the next 'blanket'
    - Eventually the leaching continues to the most upper stage with the top anhydrite as the final 'blanket'
    - Assumption: anhydrite = insoluble

        ** compared to the solution rate of NaCl the dissolution of anhydrite is negligible. In the lab analysis of Westendorp (1969a,b,c,)of core sections it can be derived that the contents that he states as insoluble content comprises anhydrite, gypsum and other components. The core samples have been brought into a specific amount of water of 90℃ and are continuously stirred. The brine is removed and the insoluble content is filtered and measured. During the dissolution that continued for one hour only the halite had dissolved.*

    - Again the dissolution angle and produced tonnage can also induce that the blanket has to move up.

** Examples can be listed were the anhydritic, intermediate benches have failed without noticeable effects (e.g. brine concentration did not drop, no differences in casing and tubing depths noticed)*

- Leaching coefficients
  - Based on lab analysis of salt cores (appendix C3)
  - Horizontal leaching rate: 8.7 mm/h
  - Vertical leaching rate: 19 mm/h

- Insoluble content inside the halite
  - Based on lab analysis of salt cores

All of these parameters do affect the geometry and dimensions of the cavity that is being leached out. For caverns 37, 49 and 50 a correlation with the existing sonar measurement was possible for both the geometry and the dimensions. For Cavern 15 the first sonar measurement could only be used for correlating the cavern diameter at the top. Later, during the modelling of the cavern migration behavior, the cavern volume was correlated as well. This will be discussed in chapter 5.

4.2 Insoluble content

In chapter 2 it is described that the evaporation cycles during the deposition of the Röt Formation were not completed due to several moments of new influx of seawater. As a result the thick Halite layer was deposited, with other minerals dispersed through the halite. From the mineral processing point of view all other components than NaCl are considered as impurities.

During the purification process at the processing plant AkzoNobel efficiently removes practically all of the impurities in several steps. It is important to realize that this only comprises the impurities that are present in the brine that is pumped up. In other words the impurities that the purification plant removes have either completely or partly been dissolved. The impurities can actually be divided into a soluble and insoluble group. From a mining point of view both should be considered. Schootstra (2015) and several other authors have described the challenges related to the insoluble content, when calculating the recovery rate.

During the mass balance calculations it can be assumed that the tonnages of salt that is purified are correct and representative. The related brine volume and cavern volume however are more difficult to precisely determine. The impurities that have come up are removed at the plant and can therefore be measured as well. The impurities that are left behind in the cavern create the largest uncertainty however. These impurities are the so-called insoluble content. In fact this name is a bit ambiguous as it only contains components that do dissolve in water – all were deposited as evaporates and originate from seawater. The solubility is just much lower than that of NaCl and therefore the brine becomes saturated with NaCl much quicker, leaving the majority of the other components behind. Therefore the name should actually be undissolved content.

In 1969 lab analysis was performed on cores from 3 different wells (Westendorp, 1969a,b,c). Samples of the cores were homogenized and approximately 100g of each sample was added to 350

ml of pure water. After 10 minutes of stirring at 90°C the fluid was cooled down and filtered. The residue that was caught during the filtration was dried and analyzed. In the Hengelo Uitloog Techniek (2018) the mean value that is referring to this research is depicted as 10%. It states that the percentages variate quite a lot and that 10% as an average is representative, based on well 151. In the original document of Westendorp (1969a) no statistical analysis is present; hence the average is not stated there. The question of where this derived mean value comes from in combination with the total absence of a variance or standard deviation – while it is noted that the spread is large- demanded an own analysis.

The results were nicely published in tables (appendix C3) and digitalizing the tables enabled performing some basic statistical analysis. The average insoluble content turned out to be 6.7% overall for well 151. The cores from this well were from salt A, B and C and therefore the averages for the specific salt layers could be derived as well (table 4.1).

insoluble content	**mean [%]**	**σ [%]**
Salt A	6,3	2,9
Salt B	13,2	6,6
Salt C	5,1	2,9
overall	6,7	3,5

Table 4.1 insoluble content per salt layer in wt% for well 151

For only salt A the mean is 6.3% which is coincidentally in line with the 7.1% that Schootstra (2015) reports. The word coincidentally is specifically used in this case as these two percentages cannot be compared to each other directly. The percentage from the core analysis is given in weight percentage as the undissolved particles, which were retrieved from the filter, were weighted and their fraction towards to original weight –of 100g- was reported. The percentage that Schootstra reports was determined from the volume decrease during multiple sonar measurements. Hence this is volume %.

An important aspect of the insoluble content that Schootstra (2015) determined is that it comprises the material that is left behind after mining. Therefore it is either still intact and in position or it is deposited at the bottom of the cavern. In both cases it can be assumed that the salt, which originally occurred within the frameworks and between the particles of the insoluble content, has been leached out leaving voids. These voids can be considered as porosity. These frameworks of insoluble content can be explained again by the dispersed deposition of the other minerals throughout the halite. Figures 4.2 and 4.3 illustrate quite well what kind of structures the insoluble content can attain.

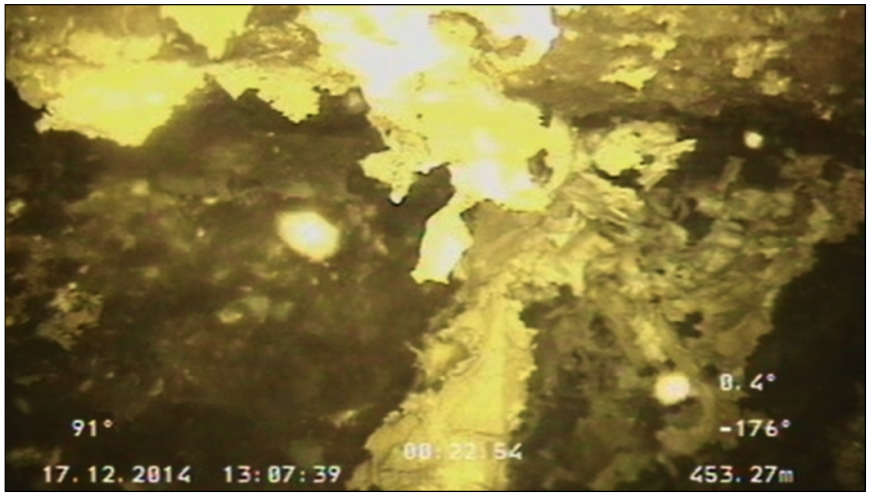

Figure 4.2 downhole photograph of insoluble content (source: AkzoNobel archive)

Figure 4.3 photograph of core section with insoluble content

Westendorp (1969b,c) analyzed cores from boreholes 171 and 182 as well and additionally more recent lab analyses were conducted on cores from boreholes 534 and well Beckum 2 (AkzoNobel internal documentation). Unfortunately all of these only contain cores from salt A. The new analysis stated both the weight and volume percentage of the insoluble content and additionally the leaching rates were reported. The averages and standard deviations, stated in volume % are summarized in table 4.2 and the full tables can be found in appendix C3. The average and standard deviation for are based on wells 171, 182, 151, 534 and well Beckum 2 and have been weighted according to the lengths. Salt B and salt C are only based on 151 as the others did not contain cores from B and C. At none of the locations cores from salt D were analyzed; at wells 151,171,182 this is because salt D was not cored.

insoluble content	mean [vol %]	σ [vol %]
Salt A	2,5	2,4
Salt B	6,3	6,6
Salt C	2,4	2,4

Table 4.2 average and standard deviation for the insoluble content in vol%

Now even with a 35% porosity, that Schootstra (2015) assumes, the mean volume percentage of the insoluble content of salt A is only 3.8%. The characteristics of the return stream slurry, the insoluble content and insoluble rock layers will be further discussed in chapter 7 and 8.

4.3 Simulation results and correlations with sonar measurements

4.3.1 Cavern 15

In total five sonar measurements have been taken inside cavern 15. This provides valuable information regarding the migration behavior of the cavern. In 5.4.1 this will be further discussed. The very first sonar measurement has been taken in 1967 while the cavern did not produce any tonnage after 1961. In fact the cavern had already started migrating and AkzoNobel started filling up the cavern to decrease the migration height and therefore the possible subsidence at the surface. Unfortunately the cavern was extensively filled during the first sonar. Therefore the simulation dimensions cannot fully be correlated with the sonar measurement. Only the diameter at the top of the cavern can be correlated. The shape is not perfectly circular and the equivalent circular diameter can be set at 96m, with a maximum span of 101m (figure 4.4).

The simulated final cavern – 15 did not develop any hydraulic connections to other caverns so therefore the single production phase is the total production phase- can be found in appendix E3; figure15. The diameter at the top of the simulated cavern is 100m, which corresponds quite well to the measured diameter. Furthermore it can be seen in the side view of the sonar measurement that the cavern has started to migrate through the roof anhydrite (black-white striped upper part in figure 4.5). Finally the fill cone of the return-stream slurry fill is very noticeable and in 5.4.1 the angles of the slurry cone are derived. The very last component that can be detected in both the

sonar measurement and the simulated cavern is that the cavern walls in the upper part are straight for several meters and no pinch-outs can be observed in the uppermost part of the cavern. This would suggest that the cavern does not have a 'morning glory' shape and helps to explain why this cavern did not have any hydraulic connections to other caverns.

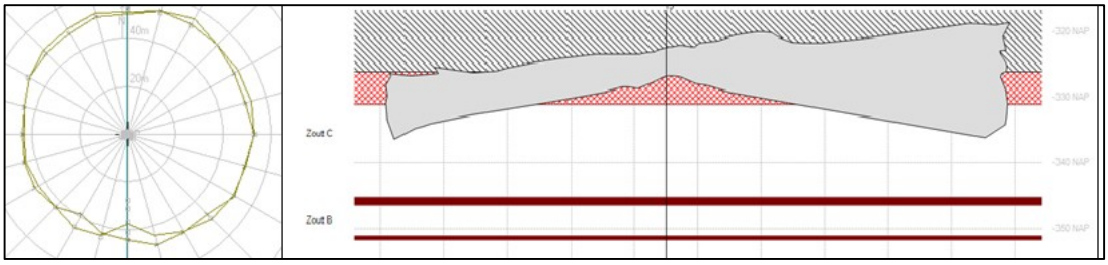

Figure 4.4 top contour (left-hand side) and side view (right-hand side) of first sonar measurement at Cavern 15

4.3.2 Cavern 37

In figure 4.5 the simulated cavern – contour filled in with grey- is overlain by the original sonar measurement – only contour line- from 1971. The diameter at the top corresponds quite well and it can be noticed that one of the two contours is slightly off-center. Upon using the measurement tool in BPB it can be determined that the original sonar measurement is positioned a little bit to the right. The distance to the left-hand boundary is 38.9m and the distance to the right-hand boundary is 43.4m. This sums up to a diameter of 82.3m while the diameter of the simulation is 83m. That the sonar is indeed not a perfect circle in its cross-sectional area can be seen in the planar view depicted in figure 4.6 the max contour that indicates what the maximum diameter of the cavern is indicates a diameter of 84m. This corresponds very well.

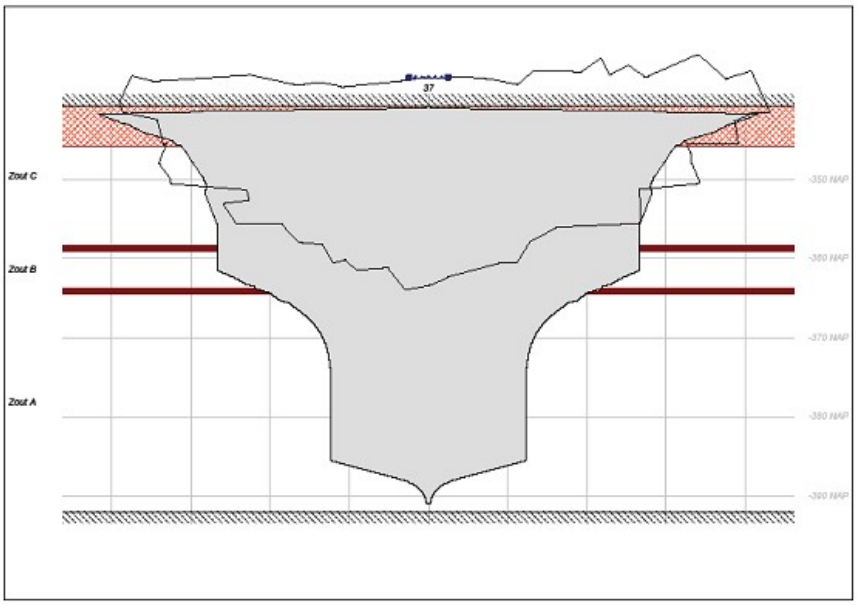

Figure 4.5 side view of sonar and simulation result for cavern 37

It should be noted that the lower part of the cavern is filled with the sump material (i.e. insoluble content and insoluble rock layers). Therefore the original sonar does not show this part. The last two noticeable differences are position of the top and the shape at the upper part. At the time that the sonar measurement was made the cavern had clearly started to migrate already. The contour shows that at least 4m – contour is a bit irregularly shaped- of the anhydrite roof layer has collapsed. This contributes to the filled up lower part as well. The simulation stops directly underneath this roof layer which explains this difference. The shape of the upper part of the simulation does slightly alter from the original sonar, especially looking at the pinch-outs at the sides directly underneath the roof. The simulation seems to under-estimate the cavern extent in salt C. Yet this is a distorted image as the time is not completely synchronized. The sonar measurement was made at 6/5/1971 while the simulation only accounts for the single cavern production (125892 tons). At 29/6/1967 cavern 37 became connected to the series of caverns 38, 38, 40, 41. Consequently the production during the series phase explains this difference. The most likely total production of 142570 tons has been simulated as well and does indeed (figure 4.7) show that the leaching during the series phase broadens the cavern width in salt C.

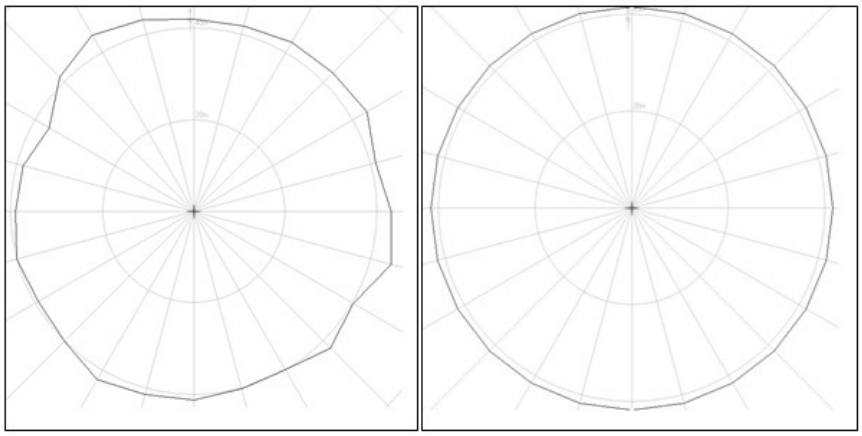

Figure 4.6 top view of sonar (left) and simulation (right) contour for cavern 37

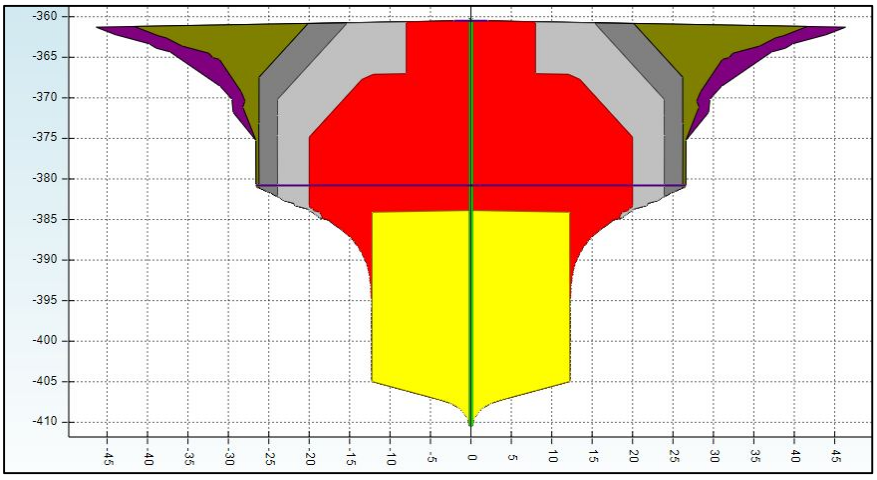

Figure 4.7 side view of simulation result for cavern 37 final production case

4.3.3 Cavern 49

In figure 4.8 the simulated cavern – contour filled with grey- is overlain by the original sonar measurement from 1965. In this case the sonar measurement was taken only two months after the connection between 49 and 50 had been noticed. The production during the series phase had therefore only started for 2 months, which strongly suggests that the production of 49 in this period cannot have been very much.

The sonar measurement is positioned directly underneath the roof while the upper part of salt C has not been mined completely yet in the simulation. Thus it can be concluded that in this case the simulation was a little bit too conservative when it comes to the vertical leaching. The most plausible reason is that the insoluble rock layers have fallen much earlier than assumed and that the leaching indeed progressed upwards much faster. In case of wells 44 to 50 it has often been extremely difficult to interpret at what time the insoluble rock layers have fallen as no repair works indicate so. Indeed for this cavern the casing and tubing were positioned in salt A for a long time and only during the series phase the casing depth was 1m underneath the cavern roof suddenly. This suggests that until that moment either no insoluble rock layer had fallen –which is very unlikely- or the insoluble rock layers had fallen much sooner without causing damages. The phenomena of salt B including insoluble rock layers AB and BC falling at once can be excluded here as that should have caused noticeable damages.

As part of the same phenomena the bottom seems to be a bit high as well; even with taking the deposition of the insoluble rock layers and insoluble content at the bottom into account. Therefore in order to correlate the bottom depth, both the cavern height and the remnant volume should be compared. The cavern height from the original sonar can directly be compared to the cavern height from figure 4.9 where the sump is displayed with the horizontal line at approximately 375m. The remnant volume of the simulation is the cavern volume above this sump line and comes from the simulation; this can be compared with the original sonar volume.

	simulation	Sonar
remnant volume [m^3]	71699	67030
sump volume [m^3]	12435	-

Table 4.3 volumes of cavern 49

The remnant volume from the simulation is approximately 7% larger than that of the sonar. This correlates quite well and does not indicate large inconsistencies. The cavern height that can be measured from the simulation (i.e. the height of the cavity above the sump) is at minimum 25 and at maximum 30 meters – depending on if the bulge at the top counts as roof. This correlates well with the height from the sonar that is 26.9m in the middle and 21.6m at the periphery.

In conclusion the volume and cavern height do correlate and so does the maximum cavern diameter. The only thing that does not correlate is the overall positon of the remnant cavern that should be higher. This can be explained by the timing at which the insoluble rock layers have failed. As explained the general rule that is followed is that the insoluble rock layer holds its place until the logbook –repair works- indicates that it could have failed. Upon additional tries to simulate the right

position, using trial and error, it proved that the right dimensions and position were possible to attain. However in order to achieve this not only the blankets had to move substantially earlier, the casing and tubing depths needed to move up earlier as well; which is actually in line with the potential damages from an insoluble rock layer falling earlier.

Due to the multiple assumptions on the moments of insoluble rock layer failure and casing and tubing damages, that cannot be proven, it is indeed justified to stick to the rule and accept the original simulation. The most important factors (e.g. maximum diameter, remnant volume and geometry) do correlate nicely.

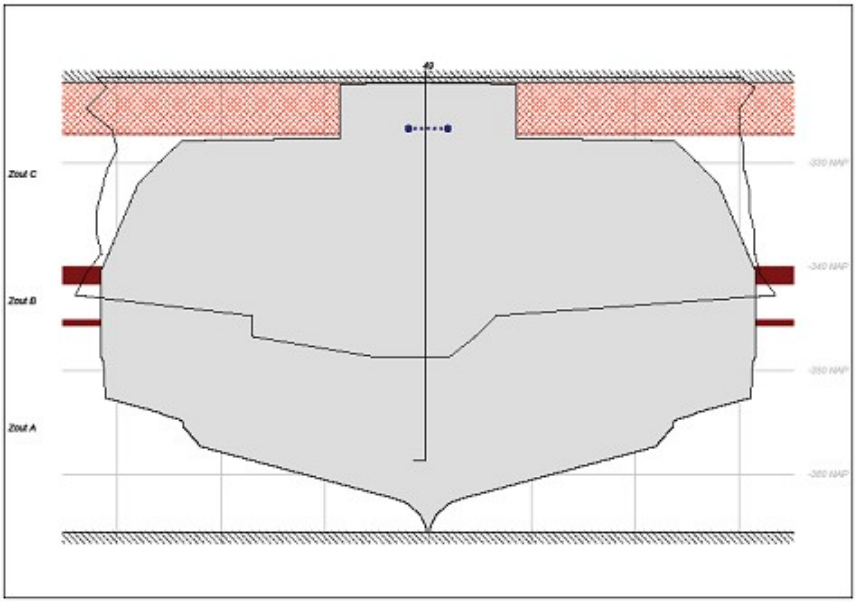

Figure 4.8 side view of simulation result and sonar measurement for cavern 49

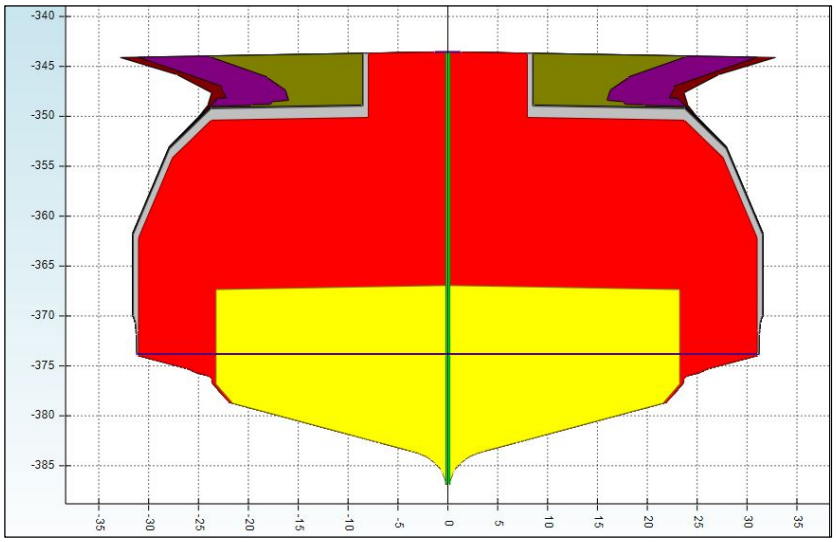

Figure 4.9 side view of simulation result for cavern 49 in case of the final production

4.3.4 Cavern 50

In figure 4.10 the original sonar and two simulations are shown. The first simulation – contour filled with grey- is the simulated cavern until the sonar measurement of 1963. This sonar measurement – capricious smaller contour inside the grey- was made at 11-3-1963. From comparing these shapes and remnant volumes it is clearly visible that the simulation over-estimates the produced tonnages at that time. This can be explained by the likelihood that the cavern stood still in the first few months of 1963, while 25% of the production in 1963 within that snapshot of the simulation has been accounted for. Nevertheless this tonnage will have been produced later during that year anyway. The shape and cavern height correlate perfectly - again the bottom depth of the simulation does not contain the sump material here and should therefore be a little bit higher.

There is an additional phenomena –which can also be seen at 37 and 49- and this is that the sump line of the simulation (figure 4.11 at 361m) is drawn as a perfect horizontal line. In the sonar measurements the bottom of the cavern is so far never perfectly flat. Considering the original bottom shape – which does have a clear angle- it is very logical that the bottom moves up, respecting this angle. WinUbro however cannot implement failing insoluble rock layers and lets the 100% insoluble interlayer behave like a fluid – as can be expected from a sump- and deposits this with a water levelled upper boundary(i.e. the bulked and deposited insoluble content and failed insoluble rock layers).

The last contour that is visible in figure 4.10 is the contour of the simulated cavern with the total single production accounted for. This is a stretched version of the earlier snapshot which correlates if it comes to the shape, however the dimensions and volume can unfortunately not be correlated to the sonar measurement. The reason is that the sonar measurement is made much earlier and therefore does not represent the cavern at the end of its production life.

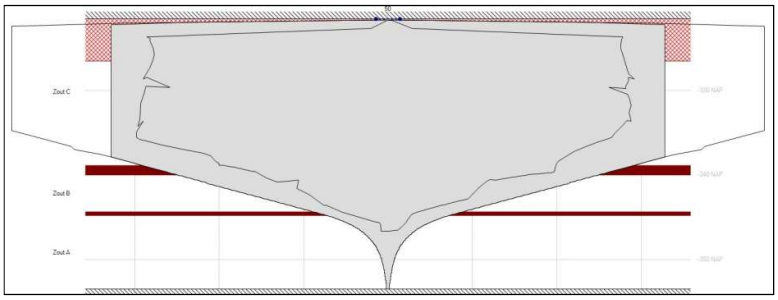

Figure 4.10 side view with simulation result and sonar measurement for cavern 50

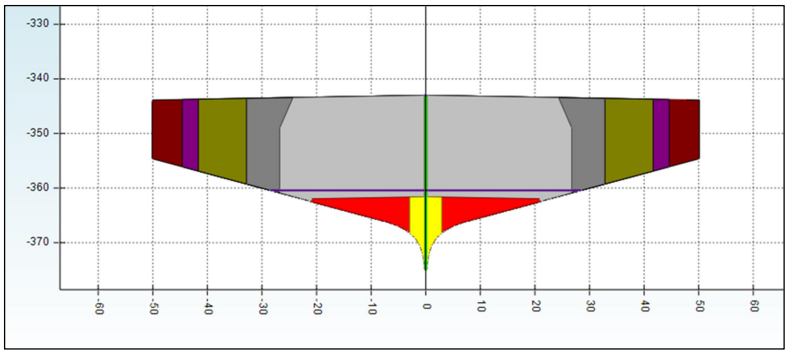

Figure 4.11 side view of the simulation result for cavern 50 in case of final production

4.3.5 Doublet 33-34

As mentioned in chapter 3 the doublets of phase 1 were intentionally positioned close to each other, allowing the hydraulic connections, and have been produced as so-called multiple completion caverns. Due to the choice to consider them as one cavern instead of two during the reconstruction of the production it was most obvious to simulate them as one cavern as well. However in light of additional cross-correlation and the desired development of a new reconstructed cavern map, the caverns were simulated secluded as well. The main reason is that WinUbro cannot implement multiple well locations. This means that WinUbro will always create caverns with a cylindrical shape around the centered well. In the case of the doublets the shape will in reality be an ellipsoid. In contemplation of being able to correlate the simulated doublet as one cavern with the sonar measurement, the surface area at the top of the cavern was compared. Additionally the equivalent circular diameter was derived from this surface area. This equivalent diameter was subsequently compared with the diameter that came from the simulation.

The diameter of the simulated cavern (figure 4.12) – as one cavern- is 128m. The equivalent circular diameter, corresponding to the sonar measurement can be retrieved by describing a circular cross-section with the same surface area.

$$A_{ellipse} = \pi * a * b \quad (4.2)$$

$$A_{equivalent\ cirlce} = A_{ellipse} = \frac{1}{4}\pi D^2 \quad (4.3)$$

$$D_{equivalent\ circle} = \sqrt{\frac{4*A_{ellipse}}{\pi}} \quad (4.4)$$

In equation 4.2 a and b represent the 'small' and 'large' radius belonging to the ellipse. From the original sonar a and b have been derived as 55m and 73m. This corresponds to a surface area of 12527m^2. The sonar measurement however also directly reports the surface area which is 12850m^2. This is slightly larger and can be explained by the fact that the ellipse shape is not perfect (figure 4.14 right-hand side). Nevertheless the equivalent circular diameter can be calculated by applying equation 4.4 to this surface area. The result is 127,9m which correlates perfectly to the simulation.

As outlined in chapter 3 doublet 33-34 did not contribute to any production within the series phase as the cavern became connected to 35-36 half a year after the production at 33-34 had ended. Subsequently the sonar measurement was made in 1964 which was the final production year. During 1964 the production was 8597 tons and in the simulation this is accounted for as well. In case this production occurred after the sonar was made the simulation has produced 2% to much at that moment, which is negligible.

Hence the remnant volume from the simulation can in this case be directly compared with the sonar volume. They are respectively: 210130m^3 and 211339m^3. This translates to a slight over estimate of the simulated volume of 0.6%. Therefore it can be concluded that this correlates perfectly as well.

Figure 4.12 side view of the simulation result of doublet 33-34

As noted the doublets have also been simulated separately. In figure 4.13 the individual caverns 33 and 34 are illustrated in grey and green. The overlying dark green contour represents the original sonar. In this case it should be noted that there is an extensive overlap of caverns 33 and 34 that is actually needs to be corrected for; it cannot be produced twice. As the volume, shape and diameter already perfectly correlated to the equivalent single cavern simulation this is not further pursued – it would have consumed a lot of time as several iterations would have been needed to attain the right volume and shape of the caverns. More importantly is that the extent of the cavern at the top does correlate. Especially in figure 4.14 it can be seen that the ellipsoid is approached by the simulations quite well. This is important for the reconstructed cavern map as it represents the cavern shape much better than the circular one.

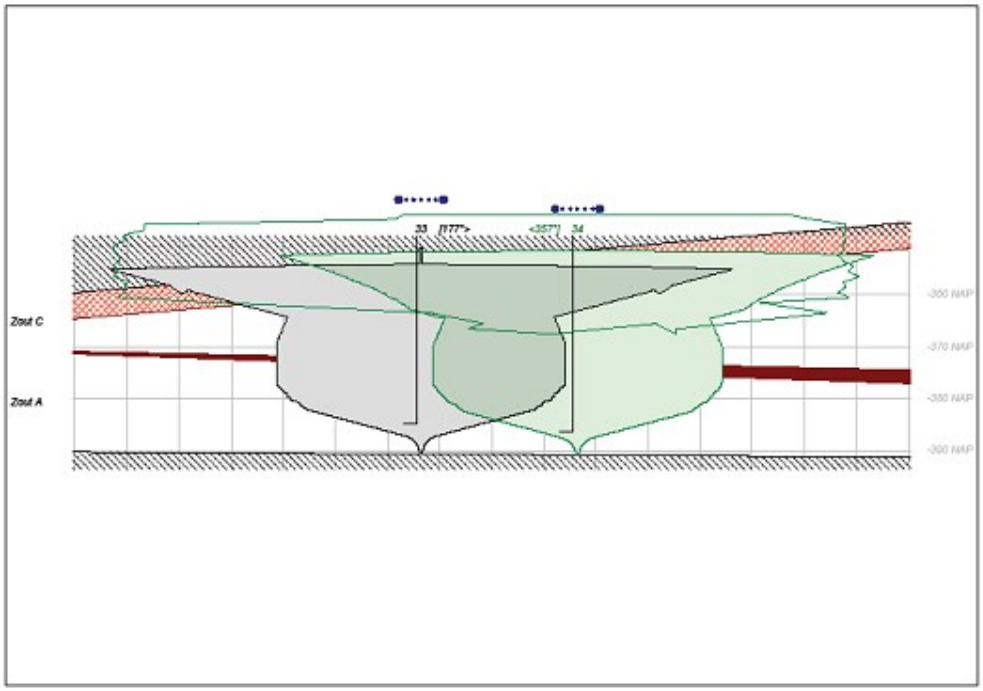

Figure 4.13 side views of sonar measurement and individually simulated caverns 33 and 34

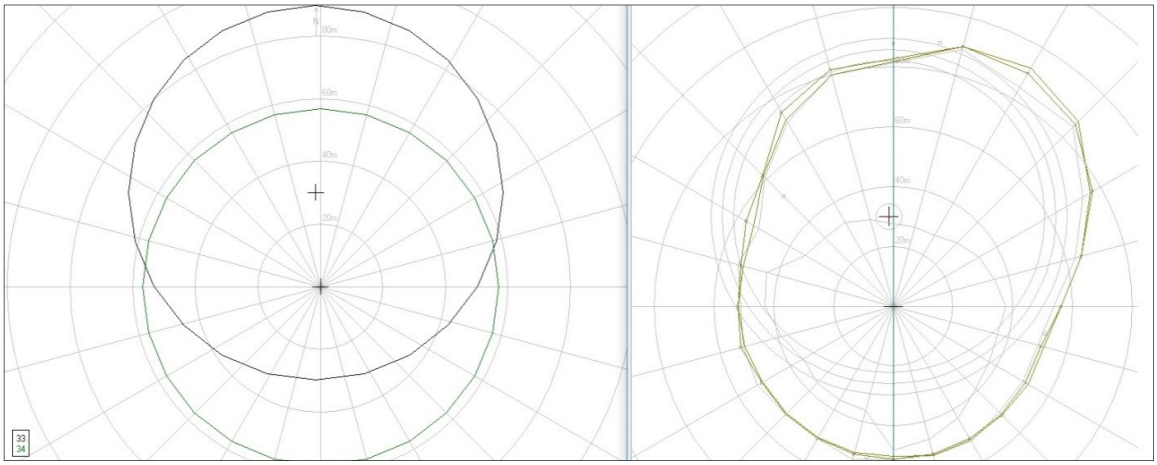

Figure 4.14 top view of individually simulated caverns 33 and 34 (left), and sonar measurement (right)

4.4 synthesis

The simulations correspond very well to the known cavern dimensions and geometries from the sonar measurements. Therefore it can be concluded that the simulations are sufficiently suited to reconstruct the caverns. On top of this the simulations support the theory that the hydraulic connections between the caverns have been established through thin channels or pinch outs at the top of the cavern.

In figure 4.15 the map of the simulated, single production phase, caverns is shown (for caverns 33-34, 37 and 49 the original sonar is implemented instead of the simulated cavern). Apart from all the doublets the vast majority of the caverns do not seem to be connected in this map. While in 3.2.4 five large series are reported. Only caverns 14, 15, 27, 28 and 32 do not have any known hydraulic connections with other caverns.

The sonar measurements do not display any noticeable pathways to other caverns and as figure 4.15 shows the simulations often do not either. During the simulations the so-called thin pinch-outs did occasionally occur. In reality they would probably have been even thinner; which could perhaps have been approached by lowering the dissolution angle in WinUbro and forcing the leaching upwards quickly, ensuring the small pathway without leaching out a large volume with the pinch outs.

These small channels or pathways represented in the so-called pinch outs would indeed not have very large volumes; again otherwise they would clearly be visible in the sonar measurements. Therefore the maximum surface areas – which are generally at the top of the cavern- from the sonar measurements and simulations, are justified and do not have to be considered much larger in contemplation of explaining the hydraulic connections.

Additionally during the cavern migration these thin pinch outs will be filled with broken roof material rather quickly, while the rest of the cavern- that has much larger volume and cavern height- will continue to migrate far more extensively.

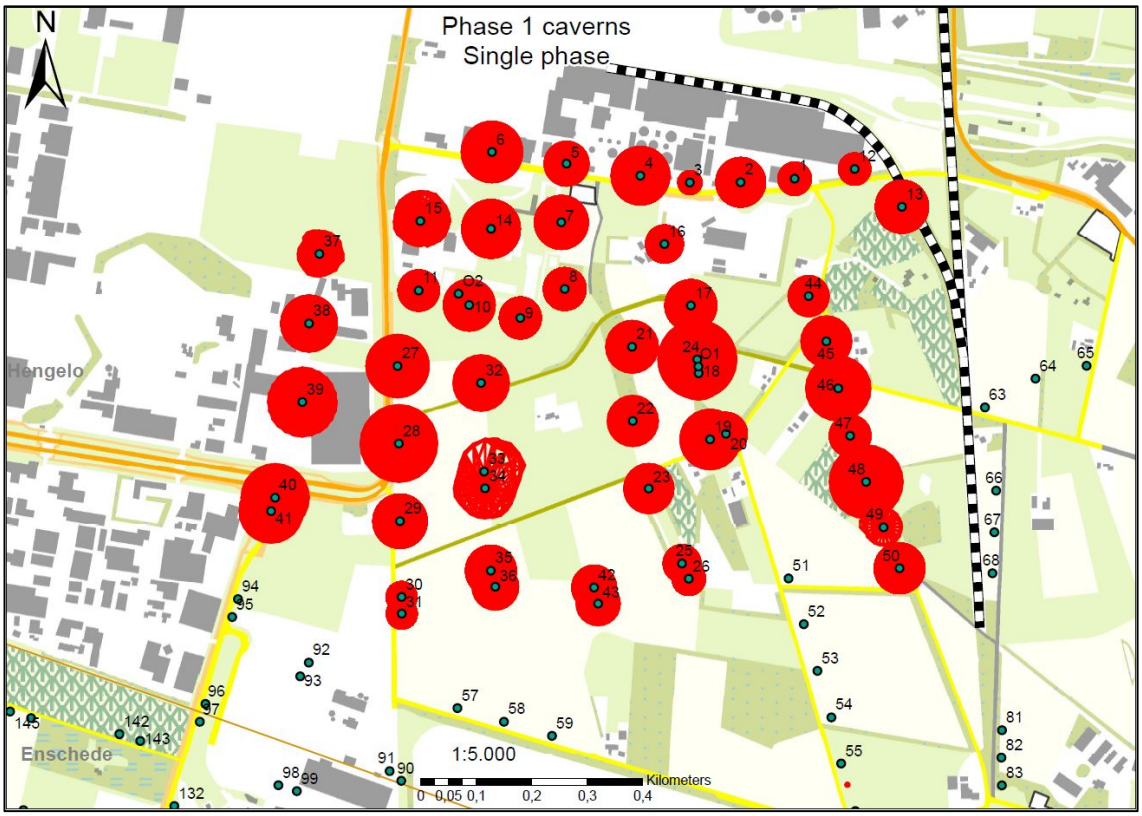

Figure 4.15 map with simulated single production phase caverns of the phase 1 area

Besides the absent visual indications for all the known connections there are a few caverns that draw attention. This concerns a few of the caverns that did not establish any hydraulic connections. First of all cavern 14 and 15 seem large and the gap between them seems small. Both of the simulated caverns have vertical side walls and therefore do not resemble the 'morning glory' shape. In this case it is important to know that at cavern 14 only salt A has been produced. Therefore if cavern 14 did develop pinch-outs they would be underneath insoluble layer AB, while cavern 15 would have grown more extensively underneath the top Anhydrite.

Furthermore cavern 27 and 28 almost touch. In 6.24 it becomes clear that the simulation of cavern 27 is probably not accurate. Potentially only salt A has been produced, or the cavern diameter is smaller. From this map it can also be derived that cavern 28 is probably overestimated in extent by the simulation as the gap to cavern 29 is not that large and it is known that 29 did continue production after the single phase. In fact 29 has a known hydraulic connection to doublet 30-31 which is not what the map suggests. This can mainly be attributed to doublet 30-31 having a too small simulated extent. The simulation does have a remarkable small diameter, which should probably be much larger, explaining that the connection to 29 is possible. On top of this the single phase simulation for cavern 29 shows that the cavern leached out in kind of a 'pear' shape. The maximum diameter is in the middle section of the cavern while the diameter at the top is not large at all. It is more likely that the leaching progressed upwards faster, rather than side wards which would have resulted in either a cylinder shape or 'morning glory'. In both cases the horizontal extent would be smaller.

5. Cavern migration behavior for the phase I caverns

The final pillar of this research – after the reconstructed production and cavern dimensions- is the reconstruction of the cavern migration. In fact it is the most vital part as it comprises the safety assessment of the phase 1 area. The extent of the cavern migration dictates the potential surface subsidence directly. In Bekendam (2009, 2012, 2013) it is extensively outlined that phenomena such as pillar deformation, cavern deformation (non-migration behavior) and debris column compaction could cause subsidence as well. These indirect phenomena can however never cause the severe deformations as the cavern migration itself can cause directly. The order of subsidence that can be attributed to these phenomena is on the scale of centimeters to decimeters. The most severe case that the cavern migration can cause directly is a sinkhole at surface. Reversely outlined a cavern cannot cause any serious surface subsidence if the cavern did not migrate at all. In that case no debris column is present, which means that this cannot induce serious subsidence either. Ultimately no serious subsidence can occur if the caverns and pillars between the caverns are stable. This may sound ideal; this is what AkzoNobel pursues in the newest phases (phase 3-5) of the Hengelo Brine Field. In fact with the implementation of new production methodologies, roof protecting and the several monitoring technologies this has succeeded for all wells drilled after 1976.

However as noted in chapter 1, in phase 1, all of the production and cavern monitoring improvements were not present yet. In fact almost all of the phase 1 caverns migrated and some did cause serious subsidence. One of the most uncompromising cases was the subsidence bowl above doublet 18-24 (figure 5.1). In 5.3 the extent of the depressed landscape will be described. Furthermore the width of the subsidence bowl will be compared to the cavern dimensions that Wassmann and Oranjewoud assumed. The measured subsidence area does provide valuable information concerning the migration behavior and the subsidence behavior caused by the migration.

Figure 5.1 Aerial photograph of the water filled subsidence bowl above 18-24, on the right-hand side the wooden derricks of 19 and 20 present (source: AkzoNobel archive)

If the migrated cavern reaches the base of the Tertiary soils– which means that the residual cavern volume still is not completely reduced to zero by the bulking effect- a through or sinkhole will surely

form (Bekendam, 1996 & Wassmann, 1980a). This is exactly what happened at cavern 70 (sinkhole) and at caverns 4, 18-24, 30-31, 35-36 (troughs). When the cavern migration extinguishes at a greater depth a sinkhole can be out ruled and the potential of subsidence depends on multiple factors. In several internal AkzoNobel documents it can be traced that 40m below the base of the Tertiary is a critical boundary. This boundary is primarily based on the migration process of cavern 15 which stopped migrating at approximately 40m below the Base Tertiary. The migration extinguished. In other cases it was found that severe surface subsidence occurred when the migration exceeded beyond this depth. Therefore the BT+40m boundary describes the safety limit.

In the cases of the serious subsidence bowls it can generally be ruled out that the migrated cavern reached the base Tertiary as this would have resulted in a sinkhole, though migration did surpass the BT+40 limit. In reality the subsidence can be possibly be caused by two phenomena. The first is the compaction of the debris column which is the result of the migrated cavern and is therefore indirectly related to the cavern migration. The second option is by downward deflecting roof layers that have detached from the other strata. This has been described by several authors throughout the years and the potential has been investigated by Bekendam (2009) in the Hengelo field as well.

At cavern 37 it helps to explain the displacement that is clearly present in the gamma ray log of 2003 compared to the log of 1979. In the workover report (Paar, 2003) it is described that from 311,1m to 324.8m depth loose rock was drilled into. Drilling mud losses increased dramatically and the rotary drill often lost contact to the rock. This indicates that this comprises the debris column, which indeed consists of loose failed rock fragments.

The cavity that was still clearly visible in the 1979 GR log is no longer present and no trace of a cavity can be found in the section above (appendix D1). The extinction depth of the cavern is therefore at 311.1m below surface. Above this the new gamma-ray was shifted down from approximately 270m depth till the extinction depth. Bekendam (2009) describes that the shift in the GR log already starts at 210m and that it increases with depth. The fact that this section did not consist out of loose rock yet indicates that the roof layers have not collapsed.

The distinct downward deformation of the strata can be explained by the decreasing cavern height. The cavern height decreases due to the bulking of the failed roof material. If the cavern height – and therefore fall height for the new exposed roof layers- becomes smaller and smaller the fragmentation of the roof layer will be less. On top of this according to the roof bed separation theory the roof layer that becomes detached from the other strata, starts to deflect downwards. If the cavern height is large enough the deflecting layer will at some point collapse. If the height is limited however the downward deflecting layer could reach the migrated cavern bottom in the middle resulting in the support of this deflecting layer. Hence the layer that is now stabilized will not fail anymore. As a result the overlying strata can still deflect downwards a bit as well as the layer in case has created a void at its initial position. In the case of well 37 maximum shift in the GR logs is 2.86m at 308.24m depth. According to Bekendam this corresponds to a downward deflecting layer and means that the extinction depth of the cavern migration is actually 308.24m at the sides. By filling in his equation (equation 5.1) the maximum downward deflection can be calculated.

$$\eta = \frac{3(1-\nu^2)(\gamma_r-\gamma_b)r^4}{16Eh_r^2} \quad (5.1)$$

With (values after Bekendam, 2009):

ν= 0.3
γ_b= 2.4*10^4 N/m^3
γ_r= 1.2*10^4 N/m^3
E=5*10^8 N/m^3
r= the radius of 40m which was the known cavern radius from the sonar measurement.

In this case the maximum deflection is already known and by reversely filling in the equation it can be found that the roof layer had a thickness of 1.9m.

The theory of the downward deflecting roof layers does help to explain the increasingly shifted Gamma Ray curve, while the strata can be considered as not collapsed. On top of this it would help to explain why in some cases the migration does extinguish earlier than expected. It does however not explain the migration behavior of the cavern itself.

5.1 Subsidence and migration categories.

In Bekendam (1996) three phases of surface subsidence have been identified for the Hengelo Brine Field. The phases have been adopted by AkzoNobel and are referred to in numerous documents after 1996. The phases are defined as follows:

Phase I: The subsidence induced by cavern convergence such as salt creep. This comprises the deformation of the cavern while it is still located in the Röt salt. In other words this subsidence is not related to cavern migration. According to Bekendam (1996) the subsidence per cavern at surface is negligible.

Phase II: The subsidence is indirectly caused by the cavern migration. The migration did extinguish before reaching the base of the Tertiary. Therefore the subsidence is caused by the compaction of the debris column and although a serious subsidence bowl can be formed, no hazard of a sinkhole is present.

Phase III: The subsidence is directly caused by the cavern migration. The migration did not extinguish before reaching the Tertiary. The unconsolidated soils of the Tertiary and quaternary drop down into the void with virtually no bulking at all. The migration perpetually continuous to the surface and is therefore not extinguished. The result is in the worst case a sinkhole.

The migration that subsequently is the cause of the 3 possible subsidence phases can therefore also be divided into the corresponding phases:

Phase I migration is in fact no migration as described by the subsidence definition. It does however comprise the convergence of the cavern. Therefore the behavior of the failed insoluble rock layers and insoluble content belong to this phase. The bulking of the failed insoluble rock layers and porosity of the insoluble content needs to be accounted for when determining what volume these

components consume upon deposition at the cavern bottom. The long-term phenomena, which will lead to a volume reduction of these components, are the consolidation and compaction. The consolidation and compaction behavior of slurry is assessed by Drost (2012) and will be discussed in the rest of this chapter and in chapters 7 and 8. The volume decrease of the deposited material caused by the compaction and consolidation will only result in surface subsidence when the cavern has started to migrate. In that case it does contribute to the scale of the phase II subsidence.

Phase II migration can be defined as the cavern migration from the anhydrite roof up to the Tertiary base +40m (figure 5.2). The migration itself does indeed not directly cause the surface subsidence. The secondary effects such as the compaction and consolidation of the complete debris column (so this comprises all the deposited material at the cavern bottom) does induce the subsidence.

Phase III migration can be defined as the migration that did not extinguish before reaching the BT+40 boundary (figure 5.2) and therefore does cause surface deformation directly. If the migration exceeds the Tertiary base + 40m it can be described as phase III migration. The severity of the surface deformation still depends on multiple factors. If the migrated cavern is still not completely filled by failed roof fragments, the migration can exceed the Tertiary base and a sinkhole will definitely form if there is still any remnant volume at the Tertiary base. If the cavern is however filled up by the bulking of roof fragments somewhere during those critical 40m a through is more likely.

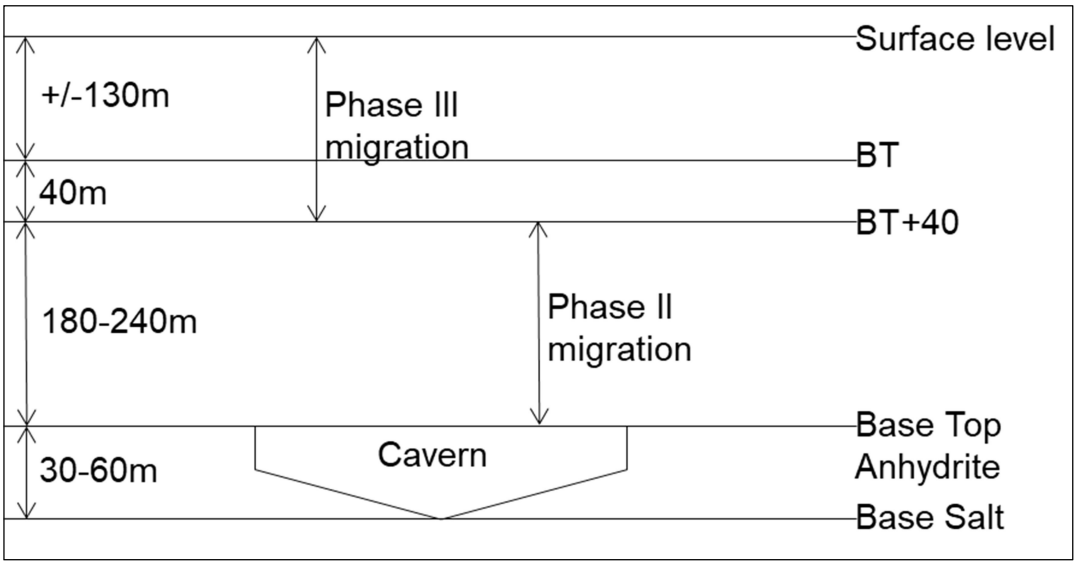

Figure 5.2 Illustration of migration phases

5.2 Correlation between production history and surface subsidence

In 1963 the first severe case of subsidence was observed at the surface (Wassmann, 1980a). The subsidence bowl was about 20m in diameter and had subsided 30cm at the center. This first case of

subsidence was located above caverns 18 and 24(figure 5.3). The area at the surface was closely monitored for several years after the subsidence was firstly identified. Later a maximum area of influence with a diameter of 270m and 1.85m subsidence at the center was documented by AkzoNobel. In his paper Wassmann (1980a) clearly states:

''Nevertheless the small area influenced at the surface with a diameter of only 270m could not be explained in relation to the depth of the original cavity at 340m (angle of draw)''

Undeniably the diameter of the area of influence should have been larger, when following the area of influence and original cavity diameter. In fact, assuming that the angle of draw of 45° is correct, the area of influence can easily be calculated with basic goniometric laws.

For example the diameter that Oranjewoud (2005) determined for doublet 18-24 is 136.6m. If the cavern diameter –and therefore surface area- during the cavern migration remains constant, the diameter would still have been 136.6m when it reached the base of the Tertiary in 1963. Applying the angle of draw of 45°(Wasmann, 1980a), the maximum area of influence should have 136.6 + 2*126.5*tan45 = 389.6m.

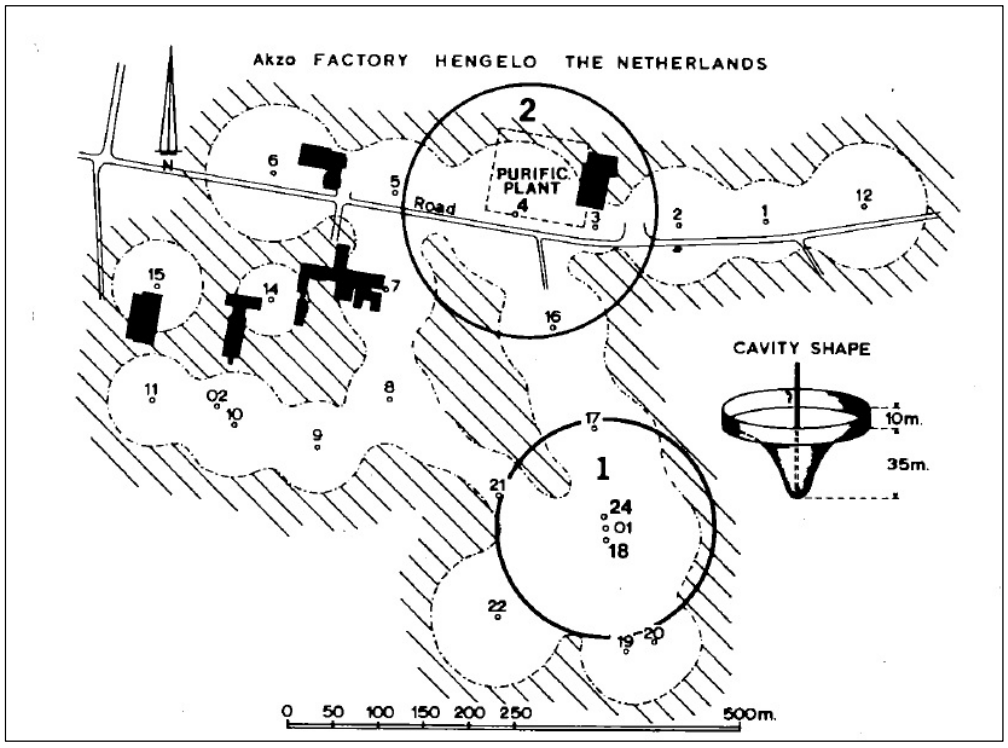

Figure 5.3 map with subsidence bowls of case I and 2 outlined (source: Wassmann, 1980)

Later reports state that the maximum span of the area of influence was 305m, yet this is still much lower than the 389.6m that Wassmann expected.

When analyzing this phenomenon in the reversed order it can be derived that the cavern diameter at the base Tertiary should have been approximately 52m in order to respect the angle of draw. This immediately draws the attention as it would indicate that the diameter would not have remained constant during the migration, but would have decreased. In 5.7 the analysis of the seismic data

indicates the same phenomenon and in sections 5.4 and 5.5 it is explained how this is implemented in the migration model.

The second extensive surface subsidence was monitored in 1973, almost directly above cavern 4 (figure 5.3). In this case the subsidence bowl had an area of influence with a diameter of 270m as well. Ambiguously Wassmann (1980) states that this area of influence is in extreme good correspondence with the 135m depth of the Tertiary and the angle of draw of 45°. Applying the angle of draw of 45° degrees to the 270m diameter, of the area of influence, in the reversed calculation results in a cavern diameter of 0m at the base of the Tertiary.

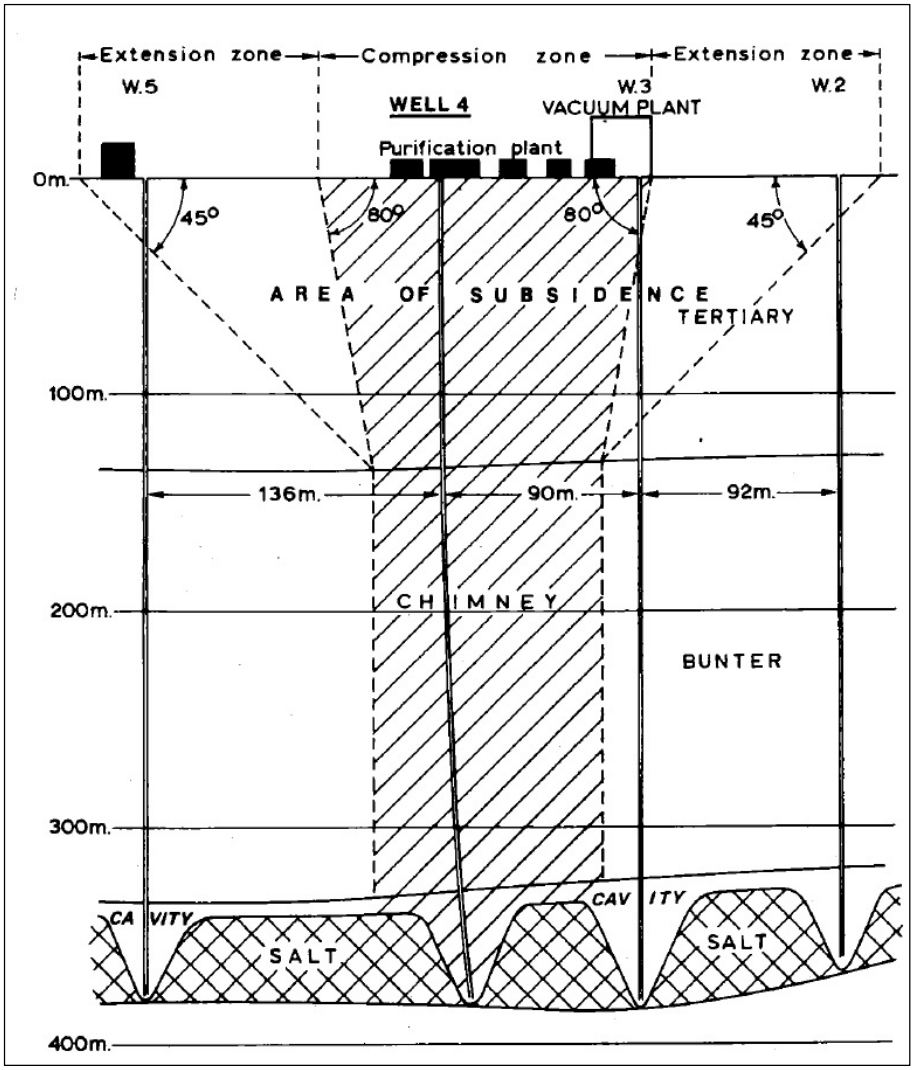

Figure 5.4 schematic overview of the migrated cavern 'chimney' and the angle of draw (source: Wassmann, 1980)

Furthermore he states that the cavern had a volume of 360000m^3 and that therefore the cavity was able to store the whole Triassic cylindrical column. This cavern volume corresponds to a production of 667000 tons. Looking at the production numbers, cavern 4 has a minimum, most likely, and maximum production of respectively 344445 tons, 365177 tons and 461810 tons. As cavern 4 is located at a 'T-crossing' it could be possible that the maximum production is larger than the most

likely final production number determined in 3.3.2. The maximum of 461810 tons is based on the production data and logbook information that wells 1,2,3,4 were taken out of production in the end of 1953. In 1954 they did not produce anymore and in 1960 they were abandoned. The connections to well 5 and well 16 occurred in 1956 and 1958 respectively. In the case that cavern 4 did contribute to the series much longer than the final production, from 3.3.2 that ends in 1954, it could indeed have been much more. The 667000 tons do curiously correspond quite well to the production of wells 1,2,3,4,5,6,7,8,9,10,11 within series added to the minimum of 344445 tons of cavern 4. Based on the old logbooks that actually do contain information about how wells 5 and 7 were operated together with the other wells joining later on. The same can be found for wells 2 and 3 with 1 joining in later and 4 joining much later. Together with the positioning of all these caverns this clearly indicates that cavern 4 can in reality never have produced the total of all these caverns.

In later reports it can be found that after 1980, another few severe subsidence cases were observed. The most striking case was the formation of a sinkhole at well 70 in 1991. Additionally a large subsidence bowl did occur in the vicinity of wells 33 to 36 and less severe subsidence bowls were encountered in the vicinity of well 10 and at the location of doublet 30-31.

In the cases of 4, 30-31, 33 to 36 it can be recognized that the production was extensive and that these already drew attention due to this large production numbers. However other caverns that had similar production numbers did not induce the same serious subsidence (e.g. caverns 6, 15 and doublet 40-41). No conclusive relationship between the production numbers and the subsidence can be drawn from this as it is. More information is needed and in chapter 8 the topic will be further discussed.

5.3 Migration model parameters

From the workover reporting in the logbooks it could be derived that most of the caverns started to migrate quite early. Only at caverns 14, 21 and 42 no damages at casing and/or tubing can be found at depths corresponding to the anhydrite roof layer. While this strongly suggests that the migration did not start yet, it cannot be concluded with certainty that the caverns have not migrated at that point. Potentially some roof layers had already collapsed without causing noticeable damages to the casing and tubing – as sometimes the insoluble rock layers probably do so as well. On top of this, and more importantly, it does not guarantee that the migration will not still start at a later point if it really did not start yet.

In excess of these three specific cases, all the others have certainly started to migrate. Some resulting in subsidence bowls, while most did not induce severe subsidence yet indicating that the migration did indeed extinguish deep enough. Since the migration behavior and moreover the influential parameters had not thoroughly been investigated before, a model has been constructed. The model is based on several parameters that have been identified. In order to validate the model the model was fitted to some caverns where sufficient information was available about the migration. These caverns are 15, 37 and 7. Again at 15 the migration stopped at approximately 40m below the base of the Tertiary and several sonar measurements have been made during the migration of the cavern. At cavern 37 one sonar measurement is available and in 2003 the well was drilled open again allowing logging measurements. At cavern 7 no sonar is available unfortunately;

multiple logging measurements have been taken in 2017 when a new well (7A) was drilled in order to locate the migrated cavern.

After evaluation of the migration the following parameters have been identified:

- Bulking factor

  In the density log taken at well 7A it can be derived that the rock mass density decreased approximately by 12.5% when comparing the intact rock to the debris column. According to Bekendam (2017) this translates to a bulking factor of 1.143 to 1.157 depending on if the local or overall initial density for the Röt Fm was considered. After personal communication with Marinus den Hartogh the bulking factor of 1.15 has been chosen. This bulking factor is already a bit higher than the conservatively chosen bulking factor of 1.11 that AkzoNobel used so far.

  The bulking factor of 1.15 describes the average bulking of the Röt Formation at well 7. The bulking of the anhydrite does most likely differ from the claystones and above this the bulking very likely decreases as the cavern height decreases. For the failing of the insoluble rock layers and the deposition of the insoluble content the bulking is different as well. Additionally this phase I behavior is not necessarily directly associated with surface subsidence. An individual phase I bulking factor is implemented in the model as well. In order to account for the compaction and consolidation an additional factor is introduced as well. In chapter 7 and 8 the bulking and compaction factor for the phase I cavern migration will be further discussed.

- Insoluble content

  This concerns the lesser soluble impurities that are dispersed through the rock salt. The volume the insoluble content will consume when deposited at the bottom of the cavern is vital for determining the maximum potential migration extent. In order to determine this volume not only the insoluble content inside the salt is needed. The porosity or void ratio is vital as well. With the porosity or void ratio the bulking of the insoluble content can be determined. The volume of the bulked material can be determined by applying a bulking factor to the volume of insoluble content that the cavern most likely has. This volume can be derived from the leached out cavern dimensions – from the production and simulations- and the insoluble volume percentage from the lab analysis. The resulting bulked insoluble content, which will precipitate at the bottom of the cavern, lead to a cavern volume reduction upon the migration trajectory. During the later stages of the migration the weight of the debris column will cause further consolidation and compaction of this material at the initial cavern bottom. Again this will be further discussed in chapter 7.

- Insoluble rock layers

  Identical to the insoluble content the anhydrite insoluble rock layers will result in a volume reduction of the leached cavern due to its deposition at the bottom. As the insoluble rock layers can be considered as 100% insoluble, their entire thickness that can be found in the lithological

profile will be accounted for. The benches of insoluble rock layers will in most cases certainly fail at some point as the history of the phase I caverns indicate. With the addition of the cavern dimensions from the simulations, the volume of the intact insoluble rock layers can be calculated. Yet again a bulking factor needs to be applied to determine what volume they will consume at the cavern bottom. As salt A has an average thickness of 18.5m for the phase I caverns. This means that the falling height of the first insoluble rock layer AB is generally at least 10m, even considering the morning glory effect of the caverns. A larger bulking factor than 1.15 would be possible due to the extensive fragmentation of the rock due to large fall height. Equal to the behavior of the insoluble the voids between the bulked insoluble rock layers will be filled during the consolidation and compaction under the weight of the debris column.

- Return stream (slurry fill)

At several of the phase I caverns traces can be found indicating that waste slurry has been pumped into the cavern. In 4.2 it is outlined that some part of this inaccurately named insoluble content does come up together with the brine. During the purification these are extracted from the brine before the salt is being crystalized and retrieved. The resulting waste slurry needs to be disposed of and the caverns form a perfect disposal system. Additionally the slurry helps to stabilize the caverns by reducing the volume of the cavity. The behavior of the return stream slurry can be assumed to be similar to the behavior of the insoluble content as it consists out of the very same material. Drost (2012) analyzed the consolidation and compaction of the return slurry. This will be discussed in chapter 7.

- Cavern dimensions

In chapters 2 and 4 it became clear that the cavern dimensions have a crucial role in the cavern migration. The extinction of the migration is generally the result of the migrated cavern volume reaching zero by the bulking of the failed roof strata. The effect of the cavern geometry has previously not been investigated very thoroughly. During the investigation into the cavern migration and its influential parameters it became clear that the cavern diameter at the top and volume are decisive.

In former studies it became clear that the cavern dimensions were difficult to reconstruct. The cavern heights were often retrieved from the logbook repair work notations; later –from the 1960's- the bottom depth was often measured. These heights were often not accurate however and moreover the reconstructed diameters of the caverns were often largely exaggerated in order to explain the known hydraulic connections. As a result of the inaccurate cavern heights and reconstructed diameters and in combination with the limited knowledge, the prediction of the maximum potential migration has been challenging.

In Bekendam (1996) – and later works as well- the theory of a constant cavern diameter is adopted. As outlined in chapter 2 the cavern volume can be substituted by the cavern height if the surface area of the migrating cavity remains constant. The resulting migration model is currently still being applied by AkzoNobel. In this model the Bulking Factor is set at 1.11 and the

average cavern height is nowadays retrieved from sonar measurements. Yet the cavern heights for the older caverns were indeed often not precisely known as there were no measurements. If the noted repair works in the logbooks indicate the cavern height it is only representative –if it is accurate at all- at the location of the well at the center of the cavern. On account of the positively correlated, reconstructed cavern dimensions that come from the simulations it is however possible to predict the migration more accurately.

- Residual volume

In the above stated it already becomes clear that the cavern volume is great importance for the migration modeling. The volume of the void that is created by the extraction of the leached out salt forms the basis. This volume is directly related to the production and can be calculated by applying the mass balance calculations of appendix C2. Yet this volume cannot directly be used for determining the potential migration. It still needs to be corrected for the insoluble content and insoluble rock layers. The first effect is that the leached cavity becomes larger as the insoluble content is not contributing to the salt tonnage, though it is being extracted partly and deposited at the bottom partly. In both cases – extraction and deposition- it does contemplate that more volume of the Röt salt must have been extracted in order to get the purified tonnage at surface. In accordance to the earlier outlined increase in volume upon deposition at the bottom of the insoluble content and insoluble rock layers, the cavern volume now decreases. After subtracting the in situ volumes of the insoluble content (both) and the insoluble rock layers and adding the bulked volumes of the deposited insoluble content (only the insoluble content that stays in the cavern) and insoluble rock layers, the initial residual cavern volume is reconstructed.
This initial residual cavern volume now can be used to model the potential migration. In light of the volume reduction by the bulking effect the residual cavern volume or migrating cavern volume decreases as the cavern is migrating.

- Compaction and consolidation

As outlined the consolidation and compaction behavior of the insoluble content, insoluble rock layers and of the return stream material (again this is the very same material as the insoluble content, however with completely different grain sizes and distributions) do have a negative impact on the migration. The increase in volume of the bulked deposited material is counter affected by this behavior. Subsequently the residual cavern volume that decreased due to the bulking of these components will increase again. While in reality the compaction and consolidation is time dependent, it is assumed as instantaneous in this migration model. The reason for this is that the maximum potential migration is the targeted outcome. In order to determine the maximum potential migration, the moment of when it can possible occur is of lesser relevance than the extent itself. Additionally if the compaction and consolidation is considered as instantaneous this results in the worst case scenario.

An important note is that the besides the compaction and consolidation of the insoluble rock layers and insoluble content that is accounted for in the model, the compaction and consolidation of the phase II migration is not accounted for. The reason for this is that in my assumption this is accounted for in the phase II bulking factor. This bulking factor – set at 1.15- has been derived from the density log taken at well 7A. The debris column that had a decreased density compared to the initial intact rock mass is located from 288.5m to 338.5m below surface. Directly above this column the lithology is not considered as failed strata, but is deflecting downwards over the trajectory of 38.5m. In 1960 the cavern had already started to migrate and the new roof depth was around 308m below surface. The migration after this continued for 20 more meters while the first 30m already occurred before 1960. Therefore it can be concluded that the time between the measurements in 2017 and the migration trajectory should be sufficient to allow the compaction and consolidation to progress extensively.

Likewise this helps to explain why the bulking factor during the cavern migration is very low compared to the literature values (table 5.1).

Rock type	Bulking factor
Salt	1,5
Limestone	1,6-1,7
Clays	1,25-1,4
Salt	1,5
Shale	1,3-1,5

Table 5.1 Bulking factors for different rock types after Ofoegbu et al (2008) and Blyth and the Freitas (1984)

5.4 Isolating and correlating the parameters

In contemplation of determining the unknown parameters, the parameters that are known to a certain degree have been implemented in the fitting of the model to the cases were the migration was known. The caverns where the extinction depth of the migration is measured are: 7, 15 and 37.

5.4.1 Cavern 15

Firstly the model has been fitted to cavern 15 where the exact volume of return stream slurry has been reported. Additionally several sonar measurements have been made during the migration of the cavern and subsequently the extinction depth of the migration is known as well. In total 634347m^3 of slurry was pumped into this cavern in roughly 9 years after AkzoNobel realized that the cavern had grown excessively due to the large production it delivered. After deriving the volume of the sump material and correlating this with the simulated cavern shape and bottom depth indications of the logbooks, the most likely bottom depth prior to the slurry fill was at 370m below surface in 1959. More importantly from the first sonar measurement the cone of the slurry fill can be observed. The minimum and maximum angles of repose, which can be calculated from the sonar measurement, are 11° and 12.8°. Now the volume of the slurry cone can be calculated using the cavern diameter and the height of the cone. This volume is the volume that the particles of the slurry consume after they have been deposited and sums up to 138913m^3.

The simulated cavern had a volume of 212046m^3 without sump. During the first sonar measurement the cavern volume was 80520m^3, this volume is the residual cavern volume after the slurry cone had been deposited. Therefore the fill volume of the slurry can be retrieved from this. This fill volume is: 212046-80520=131526m^3 which corresponds well to earlier approached volume that the slurry consumes.

Now that the volume the slurry consumes has been determined via two different methods it can be concluded that it has most likely reduced the cavern volume with 131526m^3. It can be traced back that at the time of the sonar 508443m^3 of the in total 634347m^3 had been brought into the cavern. From this total slurry volume and the deposited fill volume it can be derived what the porosity and solids content must have been. Based on the average solids content from p2/p3 (from percentage of solids.xls; internal file from AkzoNobel) of 13.27vol% and standard deviation of 3.39 vol% iterations became possible. After iterating it is deduced that the slurry most likely had a solids content of approximately 16.9vol% and a porosity of 35%. However it became abundantly clear that additional data was vital in order to formulate a reliable assessment.

The analysis from Drost (2012) that can be found in chapter 7 is in this case very helpful. Although the analysis comprises the slurry material that more recent caverns have produced, and the purification process changed slightly during the years, it can be assumed that the slurry characteristics are representative. The average porosity that was encountered in the four samples that Drost analyzed is initially 34.7% and the standard deviation of 0.1%. This correlates perfectly to the 35% that is, assumed in this research, based on literature values. With this porosity a bulking factor of 1/(1-0.347)=1.53 can be derived.

Additionally the solids content needed to still attain the fill volume now needs to be 16.9vol%. 16.9 vol% corresponds to 28wt% (using the slurry density of 1450kg/m^3 and average solids density of 2400kg/m^3). This is slightly higher than the currently applied 15 to 25wt% but very much possible.

During the migration the slurry, deposited insoluble content and failed insoluble rock layers will consolidate and compact. In fact without these phenomena the cavern would not have migrated far. For example cavern 15 with a diameter of 96m and volume of 80520m^3 – which was even less after the last 125904m^3 slurry was brought in the cavern- could have maximally migrated 75m under the assumption that the cavern diameter remains constant during the migration and with the bulking factor of 1.15.

The extinction depth that has been determined at 175.75m below surface tells that the cavern has migrated about 170m from the cavern top at 345.85m below surface. Therefore the first conclusion that can be drawn is that the compaction and consolidation phenomena have resulted in the much further migration of the cavern.

Upon analyzing the Oedometer tests in Drost (2012) it can be derived that the porosity in the end has decreased to an average of 11.14% and standard deviation of 0.95%. This reduction of porosity can be used to determine an overall compaction and consolidation related factor that approaches this decrease in volume. This factor has consecutively been implemented in the model. The maximum decrease in volume as described above here corresponds to the overall compaction and consolidation factor of 0.735.

When applying the overall consolidation and compaction factor of 0.735 the maximum migration can now be 95m, which still does not explain the actual migration. Even when applying an overall factor of 0.66 – which completely undoes the bulking effect - is only 108m. It simply does not fully explain the extent of the migration that has been observed.

After a closer look at the sonar measurements during the migration it became clear that it can be observed that the diameter of the migrating cavern decreases during the migration. In figure 5.5 this can be observed.

It should however be noted that the sonar measurements do contain some inaccuracy and that the shapes of the cavern cannot fully be seen in this illustration. Each sonar measurement has been analyzed and especially the surface area and equivalent diameter of the perfect circle that approaches the shape of the sonar. The diameters that can be derived from the equivalent diameters that approach the sonars have been plotted. In figure 5.6 it is shown that the decrease in diameter can be described as linearly constant. As a result of this the angle from the start of the migration can be determined as well. If the angle is 90° the diameter would remain constant. The angle that can be obtained from the sonars at 15 is approximately 80°.

Upon implementing this decrease in diameter into the migration model it became clear that it has a significant impact. As the surface area of the cavern is not constant anymore during the migration, the maximum migration cannot be obtained directly from the cavern height anymore. As mentioned in 5.3 the volume of the cavern is of great importance and indeed only in the case of a constant diameter the substitution of volume by the cavern height was justified. With the decreasing surface area it becomes more complicated to determine the maximum potential migration. In fact in order to do so several iterations are necessary.

The shape of the debris column can in this case be described by a cone instead of a cylinder. It can be assumed that if the roof layers start to fail it will fill up the residual cavern volume. This is the maximum it can fill at that point. The collapsing of the roof layers that fill up this residual volume however creates a new void –again this is the definition of cavern migration- so now the migrated cavern can be described by the new created void. Therefore slices of the cone can be described that have the volume required to fill up the residual migrated volume each time. The residual migrated volume logically decreases accordingly with the phase II bulking factor.

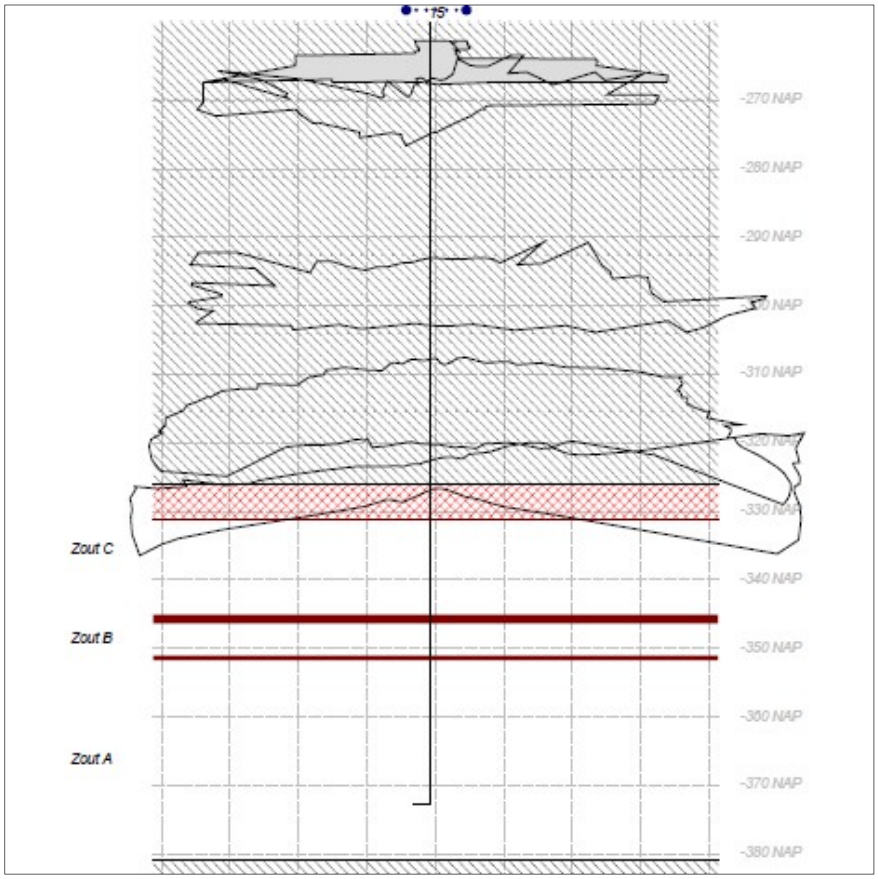

Figure 5.5 overview of side views of sonar measurements taken at well 15 during the migration

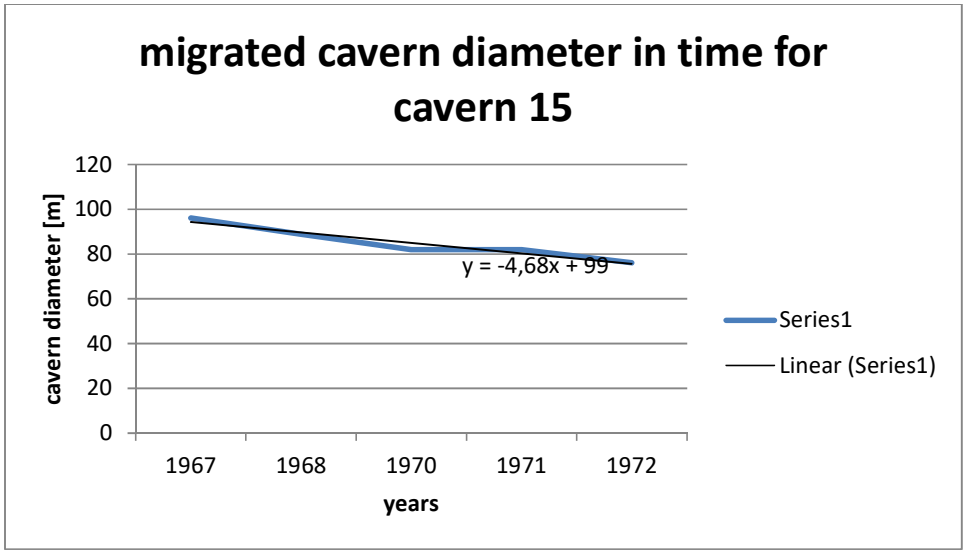

Figure 5.6 graph of the diameters of the migrating cavern (15) derived from the sonar measurements

After implementing the required iterations (see section 5.4.2) the model was able to approach a maximum potential migration that is sufficient to explain the real case. Now in case of the extreme overall compaction and consolidation factor of 0.66 the cavern could have migrated almost 335m. This is much more extensive than the 170m that in reality occurred. Therefore the compaction and consolidation should indeed be less severe. After iterating between this overall factor and the maximum migration it became clear that under the already reported parameters and decreasing diameter the factor should be 0.77. It should however be noted here that both this factor as the bulking factor have uniformly been applied to the insoluble content, slurry and the interbedded insoluble benches.

5.4.2 Analytical explanation of the decreasing diameter modelling.

In 2.5.2 and 5.2 the extinction of the migration is introduced for a constant cavern diameter. In case the diameter – and therefore the surface area- remains constant it can be taken out of the equation, leaving only the cavern height. In figure 5.7 and equations 5.2 to 5.10 the derivation of maximum migration height Δd_t (=extinction depth) is explained.

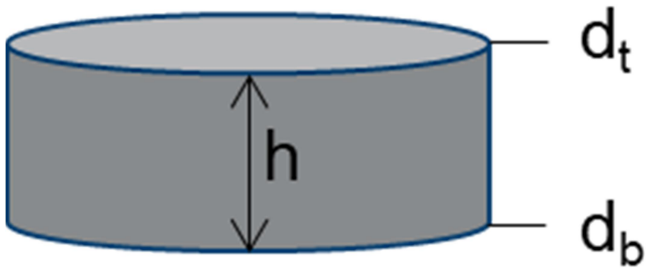

Figure 5.7 schematic overview of a cylinder describing the cavern geometry

With h: Initial cavern height [m]
d_t: depth of the top of the cavern [m below surface]
d_b: depth of the bottom of the cavern [m below surface].
d_b': migrated bottom depth [m below surface]
d_t': migrated top depth [m below surface]
Δd_b: migrating distance of the bottom [m]
Δd_t: migrating distance of the top [m]

By definition: $BF = \frac{V_{broken}}{V_{intact}}$ (5.2)

If the surface area remains constant: $BF = \frac{\Delta d_b}{\Delta d_t}$ (5.3)

Extinction depth is by definition: $d_b' = d_t'$ (5.4)

So: $d_b + \Delta d_b = d_t + \Delta d_t$ (5.5)

$\Delta d_t = \Delta d_b + d_b - d_t$ (5.6)

Substituting $h=d_t-d_b$ into 5.6: $\Delta d_t = h + \Delta d_b$ (5.7)

From 5.3 we can get: $\Delta d_b = BF * \Delta d_t$ (5.8)

Now 5.7 becomes: $\Delta d_t = h + BF * \Delta d_t$ (5.9)

Solving the ODE (5.9) we get: $\Delta d_t = \frac{h}{(BF-1)}; \; for \; BF \neq 1$ (5.10)

As the surface area is not constant in case of the decreasing diameter during the migration the maximum potential migration height or extinction depth is derived in a different manner.

In figure 5.8 the slices of the migrating cone shape are depicted. In order to determine the height of the new slice h_{n+1} that meets the volume requirements in order to fill up the previous slice iteration is necessary. The reason is that the new diameter D_{n+1} also needs to be determined and this diameter is the result of the initial diameter, the angle of 80° and the height of the slice.

In equations 5.11 to 5.19 the derivation of the new slice height expressed in terms of updated residual volume, angle alpha, previous diameter and height can be found.

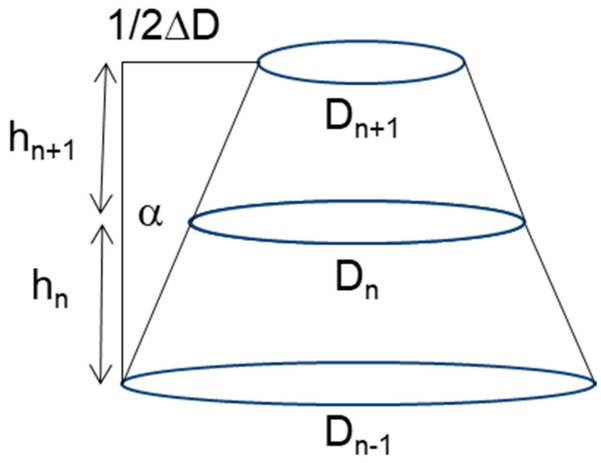

Figure 5.8 schematic overview of the cone slices describing the migrating cavern geometry

With D_{n-1}: Initial cavern diameter at the top of the cavern [m]

D_n: upper diameter of the n^{th} migrated cone slice and lower diameter of the n+1 migrated cone slice [m]

D_{n+1}: upper diameter of the n+1 migrated cone slice and lower diameter of the n+2 migrated cone slice [m]

α: angle under which the diameter decreases while migrating upwards [°]

$$\Delta D = D_n - D_{n+1} \quad (5.11)$$

$$\tan\alpha = \frac{\frac{1}{2}*\Delta D}{h_{n+1}} = \frac{(D_n - D_{n+1})}{2h_{n+1}} \quad (5.12)$$

$$D_n - D_{n+1} = 2 * \tan\alpha * h_{n+1} \quad (5.13)$$

$$D_{n+1} = D_n - 2 * \tan\alpha * h_{n+1} \quad (5.14)$$

$$V_{n+1} = \frac{V_n}{BF} \quad (5.15)$$

$$V_{n+1} = \frac{1}{4}\pi(D_n - 2 * (\tan\alpha) * h_{n+1})^2 * h_{n+1} = \frac{V_n}{BF} \quad (5.16)$$

$$\frac{4\pi * V_n}{BF} = D_n * h_{n+1} - 4D_n * (\tan\alpha) * h_{n+1} + (2\tan\alpha)^2 * h_{n+1}^3 \quad (5.17)$$

$$h_{n+1} * \left(D_n^2 + h_{n+1}((2\tan\alpha)^2 * h_{n+1} - 4D_n * \tan\alpha)\right) - \frac{4\pi * V_n}{BF} = 0 \quad (5.18)$$

$$h_{n+1} = \frac{\frac{4\pi * V_n}{BF}}{\left(D_n^2 + h_{n+1}((2\tan\alpha)^2 * h_{n+1} - 4D_n * \tan\alpha)\right)} \quad (5.19)$$

And at the end the maximum migration height= $\sum_1^N h_n$ (5.20)

With N: the last slice of the cone that is needed to complete the cycle

And h_{n-1}: the initial cavern

The iterations have been performed by hand once and proven to be a monstrous amount of work. Luckily Microsoft excel has the possibility to perform iterative calculations as well. This saved loads of time and after the results checked out to be accurate this was directly implemented into the migration model instead of the analytical equations.

5.4.3 Cavern 7

The drilling of the new research well 7A provided both the extinction depth of the migration and the bulking factor of the debris column. Unfortunately no sonar data is available. The bulking factor which is set on 1.15 represents the effective bulking factor and accounts for the compaction and consolidation of all the failed roof material after a substantial amount of time (there is almost 60 years between the data of well 7A and the readily extensive migration of the cavern in 1960).

The logbook does indicate that it is possible that salt B, including insoluble layer AB and BC, have fallen. This is however not certain. The production is at its minimum 129360 tons and the most likely maximum is 158778 tons. The corresponding leached cavern volumes are 69812m^3 and 137761m^3.

With the decreasing migrating cavern diameter of initially 90m at the top of the salt – from the simulation- the cavern can indeed reach the corresponding extinction depth of 288.5m below surface. If the insoluble content and insoluble rock layers corresponding to the average values and geology at well 7 have been implemented in the model – with the bulking factor and overall compaction / consolidation factor at 1.53 and 0.77 respectively- the maximum extinction depth could have been 285m in case of a constant diameter and 257m in case of the decreasing diameter. This is for the minimum production case and salt B including the insoluble rock layers failing.

In case of the most likely final production the extinction depths are 236m for the decreasing diameter and 277m for the constant diameter.

This would suggest that even in the most positive scenario the migration extinguished 11.5m earlier which can be explained by either less compaction and consolidation or an even higher bulking factor for the insoluble content, or by the downward deflecting roof layers.

The more likely scenario of the decreasing cavern diameter during the migration would however require a certain amount of slurry fill in order to explain the extinction depth. In chapter 6 this will be further discussed and for now it can be concluded that only the bulking factor and the extinction depth are certain here as they have been measured.

5.4.4 Cavern 37

At this cavern the available sonar allowed the correlation of the simulation and the re-opening in 2003 provided additional information regarding the migration. The insoluble contents (volume percentage) are set on 2.5% for Salt A and 2.4% for Salt C and under the assumption that salt B including insoluble rock layers AB and BC have fallen completely resulting in the insoluble content of 100% over that entire range. This phenomenon of salt B including insoluble rock layers falling down has been detected a few times in the more recent phases of the Hengelo brine field by AkzoNobel and in the case of cavern 37 the logbook indicates that at cavern 37 it occurred as well.

> *In 1958 the roof was most likely still insoluble rock layer AB as the previous deformations did occur at 384.27m below surface or even deeper, with the insoluble rock layer located at 383.15m to 383.9m below surface.*
>
> *In 1959 the repair works after a large reported collapse – causing the brine concentration to drop dramatically- tell that the tubing shot through their security clamp. After inserting the casing cutter it became stuck at 370.75m below surface and upon hoisting it back the drill string broke. The casing cutter accompanied by 47 pipes form the drill string was lost in the cavern never to be retrieved again.*
>
> *Sequentially new tubing was installed and in 1962 this tubing broke at 356.91m below surface. The successful milling made the pathway free again.*

What immediately draws the attention is that the events of 1959 and 1962 are at depths that correspond to the middle and top of salt C respectively. With the insoluble rock layer AB still in place in 1958, and no reporting of deformations inside salt B or in the neighborhood of insoluble rock layer BC between those years, it can be deduced that it is very plausible that Salt B including the surrounding insoluble rock layers have collapsed entirely.

The above described phenomenon of salt B including the insoluble rock layers collapsing, does help to explain the position of the bottom in the sonar measurement to a better extend. Moreover it does contribute more to the volume decrease of the total cavern volume towards the residual cavern volume. In the case of cavern 37 where the logbook suggests that no slurry has been pumped into the cavern at all this residual volume was quite problematic. The residual volume can directly be derived from the sonar measurement –has also been used for cross-correlating the simulations and the reconstructed behavior of the insoluble content and insoluble rock layers – is 71800m^3. With this volume, the diameter of 82m and the rest of the parameters at the same values as used for cavern 15 and 7 the maximum potential migration is 232m. In case of a constant diameter the migration is logically much less but still too large with over 90m. The observed real migration was 52m as outlined in this chapter. Therefore it can be concluded that in both cases the observed extinction of the migration cannot be fully explained yet by either the constant or decreasing diameter approach.

The theory of the downward deflecting roof layer as mentioned does help to explain why the migration is terminated earlier. The maximum deflection of 2.86m at the center that has been suggested by Bekendam (2009) would lead to a reduced maximum potential migration of 71.6m instead of 90m. This still does not fully explain the early extinction. From the cavern diameter of 84m and the maximum deflection of 2.86m at the center it can be derived that the detached roof layer deflects under an angle of 4° compared to the horizontal roof. This 'deflection angle' could directly be used to determine the maximum deflection from the cavern diameter. More data and research will be needed to verify this angle.

Another possibility is that the bulking factor of phase II is substantially larger than 1.15. However with the compaction and consolidation that will almost certainly have occurred to some degree here as well, this is still very precarious. Additionally the bulking effect cannot have been larger and the compaction and consolidation not any less considering the insoluble rock layers and insoluble content at the bottom. With the bulking factor at 1.53 and the consolidation and compaction factor at 0.77 the residual volume of the cavern becomes 72640m^3. This corresponds well to the measured volume from the sonar measurement.

With the multiple ambiguous notations that have been encountered during the analysis of the logbooks and the distinct hint of the cavern being used for return stream deposition in an AkzoNobel overview from 2005, it can be concluded that it is likely that slurry has been pumped into this cavern.

This would help to explain why the migration extinguished much earlier than the maximum potential indicates without expanding the bulking effect which is unlikely.

5.5 summarized explanation of the model

The model has been fitted to caverns 15, 37 and 7 where along the way it became possible to isolate some of the influential parameters and determine their typical values. Now that the construction, fitting and correlation of the model is done it can be used in order to estimate the maximum potential migration for all of the phase I caverns.

It should be noted that both scenario's (constant and decreasing diameter) are implemented in the model in order to check what the potential migration in both cases would be. In both cases the residual volume, which either comes from a sonar measurement or the earlier explained derivation from the simulations, is leading for the migration. This means that from this volume and the surface area at the top of the cavern – again either from sonar or simulations- the height of an equivalent geometrical shape can be derived. This equivalent geometrical shape and height approach the real cavern shape and height at the start of the migration. The important assumptions here are:

1. For this modeling of the maximum migration it does not matter if the migration already started during the production life of the cavern. Therefore the model implements the cavern volumes at the end of their production life.
2. The fragments from the collapsing roof layers will fill up the cavern bottom equally. Therefore the inverted cone shape that the caverns have at the bottom will persist for some of the migration and eventually the bottom of the cavern will attain a horizontal line. In other words: again the volume is leading as the whole cavern will be considered as a void that 'needs' to be filled by the overlying strata after it collapsed and bulked.
3. The equivalent geometrical shape is a representative ideal approach of the real cavern.
4. The starting diameter in both cases is the diameter that the cavern attains in the highest located salt layer. Generally this is the diameter at the top of the cavern in salt C. however in some cases the production methodology leads to a pear shape. In those cases the most upper diameter that can be derived is much smaller than the maximum diameter, which is often not that much lower. In these cases it can be assumed that either this upper most salt has in reality been produced – the simulated cavern should be shifted upwards- or that if the salt was indeed not produced it will fail as well. In the latter option this will in reality result in some additional fill at the cavern bottom and therefore a less extensive migration. This is not taken up into the model as the maximum potential migration is approached.
5. The migrated cavern diameter cannot become negative.

With the implementation of the decreasing diameter approach, the migration has a new possibility that causes the extinction. This is when the diameter becomes zero and the volume is not brought back to zero. In this event the migration is therefore not volumetrically extinguished but due to the geometry. This leads to the additional assumption that the tip of the cone – where the diameter becomes zero- is a stable structure and does indeed not converge.

5.6 Evaluation of the migration model

5.6.1 Introduction

Compared to the former model that AkzoNobel used this model is much more complex and detailed. The amount of influential parameters that are implemented in the model is much larger. Additionally the behavior of the processes and parameters has been investigated more detailed resulting in a much more detailed and complex approach to describe and explain the migration behavior. Perhaps the most drastic phenomenon is the decreasing diameter.

Previously in chapter 2 and 3 it became clear that the constant diameter could not explain the extent of the observed subsidence area's at the locations of cavern 4, 18-24 and 35-36. In fact from the

analysis of Wassmann and additionally the migration behavior analysis in this thesis it became clear that a much smaller diameter, compared to the initial cavern diameter, was needed at the BT (or BT+40) to explain why the subsidence bowls were not much larger. In case the angle of draw of 45° needs to be continued to a larger depth – this is when the extinction is indeed between BT+40m and BT- the subsidence bowls would have been even greater. Bekendam describes that in this case the angle of draw in the last parts of the claystone is not 45° but 35°. The diameter of the subsidence bowl would still have been larger compared to the one drawn from the BT directly to the surface with 45° as the depth is also larger (see appendix D2).

5.6.2. cross-correlation of the migration behavior with seismic data

5.6.2.1 Introduction to seismic survey

In 1993 a 3D high resolution seismic survey was conducted in the TWR concession area (see figure 5.9), after a previously performed 2D seismic survey showed encouraging results. The 2D sections did show faults and subsidence structures, though no caverns were visible. The 3D seismic sections show cavities and the faults and subsidence structures were more meticulously visible compared to the 2D ones from the earlier survey. This rationally resulted in a higher degree of confidence in the 3D data than in the 2D data (Meekes & van Vliet, 1994). As multiple reports about the interpretation of the data (HIRES SESOM, 1995; Meekes & van Vliet, 1994; Bekendam, 1996) declared the seismic data to be of excellent quality, it can be assumed that the data is of good quality.

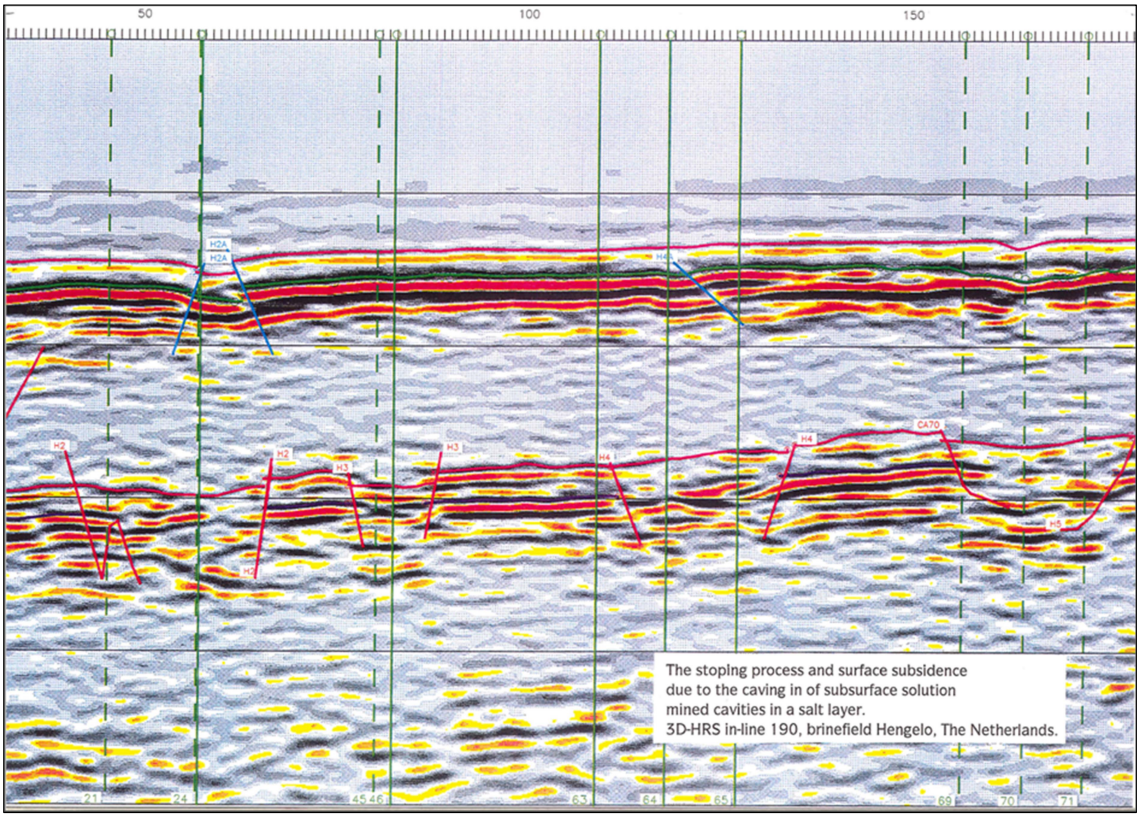

Figure 5.9 colored cross-section of seismic line 190 (source: HIRES SESOM, 1994)

5.6.2.2 Seismic stratigraphically interpretation of the data

According to Meekes & van Vliet (1994) and Bekendam (1996) four seismic-stratigraphic units can be characterized:

1. The upper unit.

   This comprises the section from the surface down to the Base Tertiary Reflector (BTR). The BTR is a very visible reflector as corresponds to the base of the Tertiary formations. Since the soft Tertiary is discordance on top of the hard Triassic layers, it forms a perfect reflector. Within the upper unit another reflector labelled. This is the Continuous Tertiary Reflector (CTR), which is visible in the lower part of the upper unit and corresponds to the first boundary within the Tertiary.

2. The upper middle unit.

   This comprises the section from the BTR to the top of the series of Röt Member reflectors. Within this range the sometimes absent Muschelkalk and upper Röt Claystones are featured. Unfortunately the reflections encountered in this unit often are medium amplitude reflections. These reflections are typically very discontinuous and not consistent over the area, which makes distinguishing subsidence patterns related to the caverns virtually impossible.

3. The lower middle unit.

   As the Röt Member is an extensive layer, this area it holds multiple strong reflectors that also belong to the Röt Member. Often four and sometimes even five or six reflections can be distinguished here. According to Meekes and Wijn (1993) the most upper reflection does not correlate to the top of the salt, it does however correspond with a thick anhydrite layer within the Röt Claystone Member. This anhydrite reflector is labelled as NTAA. The reflector that Meekes (1994) does associate with the top of the salt is the Near Top Salt (NTS) reflector as it is most likely the reflection of the anhydrite layer that is deposited on top of the rock salt layers. This layer could be several meters thick and does illustrate the deformations of the caverns at their top perfectly. The last reflector present in this unit is identified as the base of the salt.

4. The lower unit.

   This contains the lithology from the base of the salt downwards and is associated with the Solling claystone member. In this unit again very discontinuous and inconsistent medium amplitude reflections are present.

5.6.2.3 Structural interpretation of the data

Variable area wiggle trace sections from in-lines (figure 5.10) have been visualized (figures 5.9, 5.11 and 5.12)

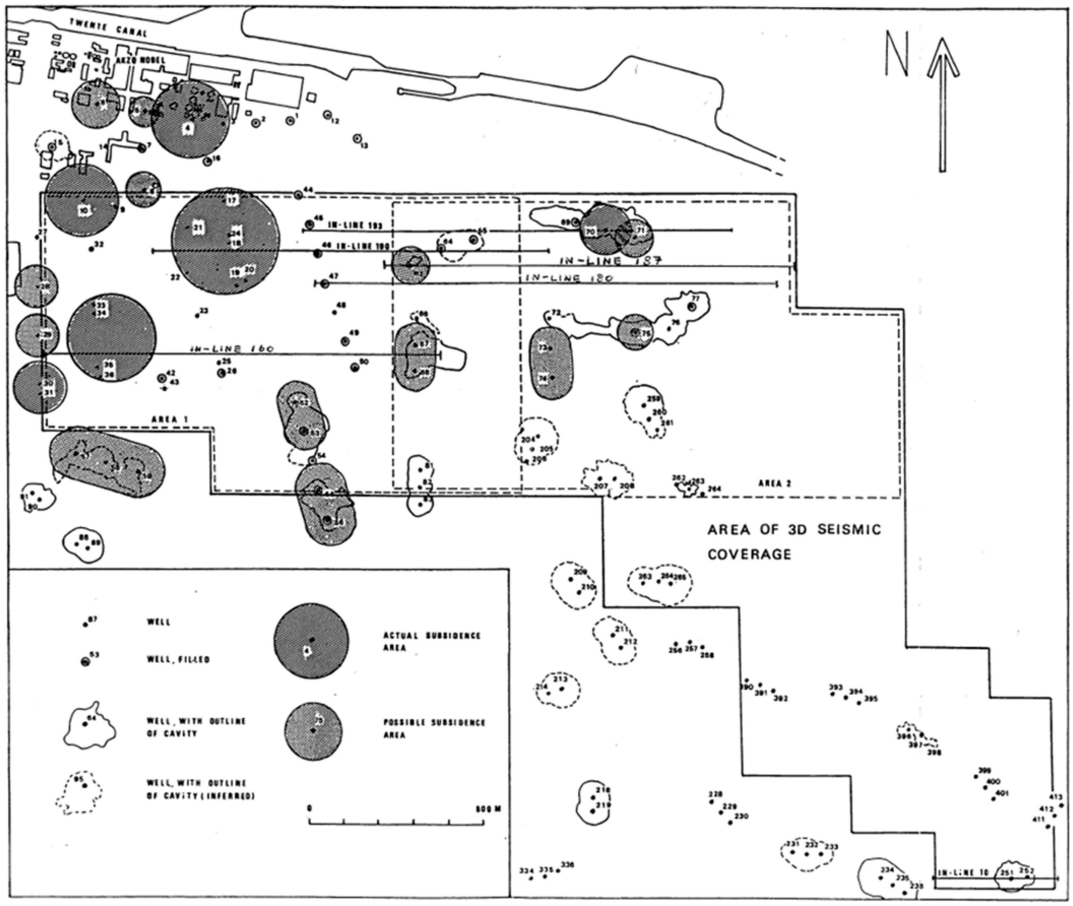

Figure 5.10 map with the locations of the in-line sections of the seismic survey (source: Bekendam & van Vliet, 1995)

In-line section 190

This section line is located in the northwestern part of the seismic survey area and intersects with wells 21 and 18-24 on the western side. As 18-24 has caused an extensive subsidence bowl at the surface it is especially interesting to analyze this section on that location. According to Bekendam (1996) both the surface subsidence area and the cavern related disturbances in the four lower middle unit reflectors, including the NTS reflector, are clearly visible in all the cross-lines in the vicinity of 18-24. At the wiggle trace section of in-line 190 the original cavern is clearly visible in the lower middle unit as well (see figure 5.11). The NTS reflector is disturbed over a cross-sectional diameter of approximately 180 meters. This corresponds directly to the original cavern position and geometry. Inside the confines of this structure the NTS reflector cannot consistently be distinguished, this is corresponding to the roof collapse that definitely occurred. Research well ON-1 and the logbooks of 18 and 24 do indicate that this already started in the late 1950's / early 1960's. Upon examining the upper middle unit reflectors it can be recognized that there is a downward dip,

directly above the original cavern and its position also correlates with the center of the subsidence bowl at the surface. Both the CTR and BTR are depressed over a cross-sectional diameter of approximately 60 meters. Using an angle of draw of 45° from the base of the Tertiary (126.5m below surface) upward to determine the maximum diameter of the subsidence area at the surface, it indicates a width of 313m. Wassmann (1980) describes the subsidence Area 1, located at 18-24, and shows that the measured subsidence bowl has a width of 305m; later Bekendam (2009) analyzed the subsidence and predicted the maximum up to 2050 over an ellipsoid area that is even slightly smaller.

An important aspect that should not be overlooked is that the in-line 190 is in the east –west direction and wells 18-24 are aligned in the north-south direction. The shape of the cavern that is leached by 18-24 can be described by an ellipsoid with the largest cross-section in the north-south and the smallest cross-section in the east-west direction. The seismic data in the cross-lines in the vicinity of 18-24 do indeed confirm that the extent of the cavity induced dip in the BTR is larger than the 60m that can be derived from the east-west 190 in-line. According to Bekendam (2009) this relates to a maximum width of 94 and minimum width of 64m. The widths of the deformations at the NTS reflector, which is associated to the roof of the caverns, are pretty large. This can be attributed to the 'morning glory' development of the caverns when the roof anhydrite is reached and the leaching of the salt continues radially underneath this roof. These 'wings' however do not develop in a considerable thickness, but rather in thin slices (see chapter 3 and 4). Therefore it can be assumed that during the collapse of the roof layers, the height of these 'wings' will be filled up rather quickly, resulting in a smaller diameter that will actually continue to migrate upwards. The real migration diameter of the cavities will thus not be as extensive as the NTS map suggests.

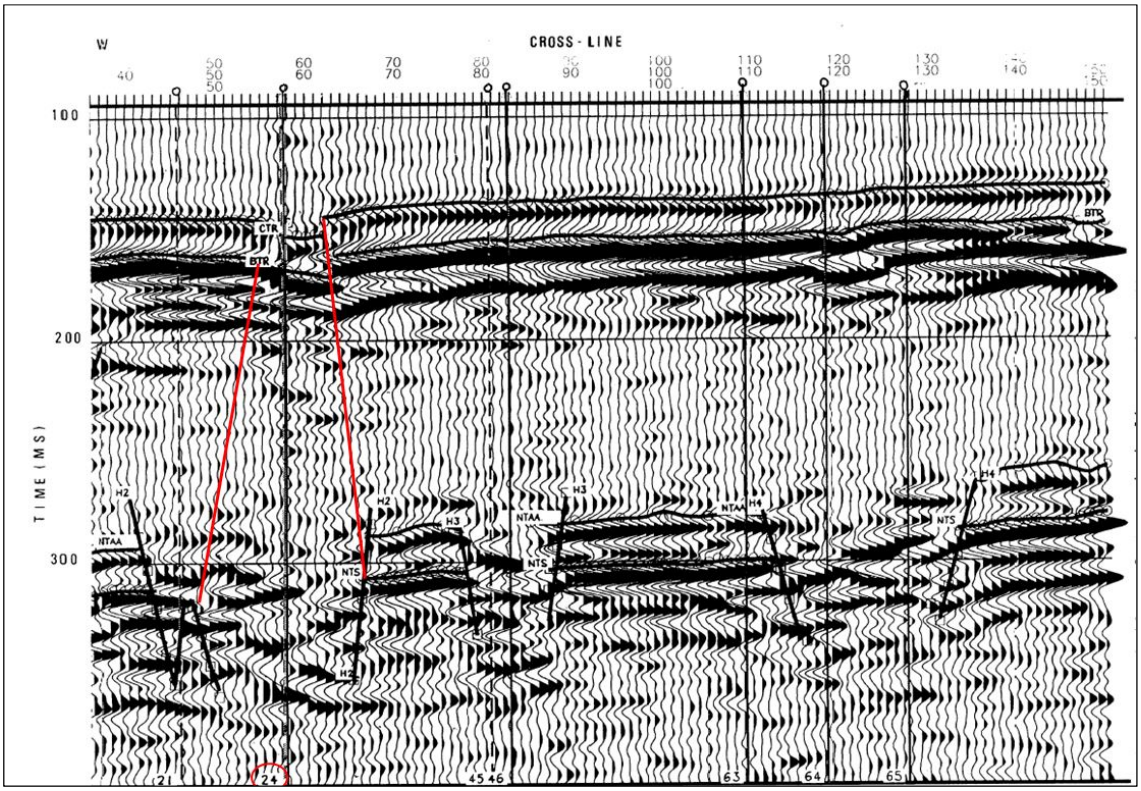

Figure 5.11 cross-section of in-line section 190 (source: HIRES SESOM, 1994)

The dimensions of cavern 18-24 that is simulated and reconstructed translate to a large and small diameter of 110m and 170m respectively. Within the simulations the wings were not really generated, while in reality it can be concluded that they did really develop. Important here is that the cross-section is taken perpendicular to the largest axis of doublet 18-24. Therefore the smaller ellipsoid diameter of the cavern should be compared with the cross section. The smaller diameter of 110m is still much smaller than the 180m that can be retrieved from the cross section. Therefore the seismic data does indeed seem to overestimate the extent of the deformation.

If the diameter of the cross-section would indeed decrease from 180m to 60m between the top of the salt and the Base Tertiary, the angle under which the diameter decreases would be 74°. If the reconstructed small diameter of 110m is taken and the 60m at the BTR deflection is respected the angle under which the diameter decreases would be 83°. If the reconstructed large diameter of 170m is correlated with the 94m at the BTR, the angle under which the diameter decreases would be 79.8°.

So it can be said that even if the caverns extensions at the top of the salt (small and large ellipsoidal diameters) are smaller than the seismic data suggests, they still decrease when migrating upwards. In correspondence to the morning glory theory all of the above stated could be explained. Taking the diameters of 94m and 64m directly as migrating diameters at the top of the salt (so in case they did not decrease during the migration) the extinction depth would be 113m for the bulking factor of 1.15. Since this far beyond the Base Tertiary it can be concluded that a large sinkhole should have resulted. Since this did not happen it can be said that those migrating extensions at the top of the salt are not likely.

With taking 110m and 170m as extents, the migration of the cavity would actually reach the base of the Tertiary with the widths that are indicated in the seismic profiles. In order to generate the initial cavern with these extents tough, it is very likely that production would have been 474858 tons, which corresponds to the total of wells 17,18,19,20,21,22,24.

Directly from the seismic data it can be distinguished that reflector disturbances caused by 18-24 (both in the north-south and east-west) do decrease in width when comparing the NTS and BTR. As mentioned the disturbances at the NTS are partly induced by the thin ‘wings (morning glory)’ of the caverns directly underneath the anhydrite roof, resulted in a distorted image. The somewhat smaller extents, which come from the simulations, seem justified as they do correspond to cavern heights of 15 to 20 meters at the sides (cavern height at the center is about 20 meters).

In-line section 160

This wiggle trace section (left hand side of figure 5.12) intersects cavern 35-36. Furthermore in the middle the section intersects 25-26 and on the right-hand side it intersects 49 and 50. The deformations of the NTS reflector are highly visible again. The BTR and CTR reflectors are however only deformed at the location of doublet 35-36. The extent of the deformation at the top of the salt is about 200 meters. The BTR reflector suggests a depression of approximately 130m width. Again the surface area of a doublet (in this case 35-36) is more ellipsoidal than circular. From looking at the cross-sections and NTS disturbance map (appendix D4) it can be derived that the large diameter of the ellipse is about 200m and the small diameter 190m. The equivalent circular diameter to describe

the cavern would be 194.9m. With this large equivalent diameter the cavern could not have migrated far enough to induce serious surface subsidence. The extent of the deformation seems exaggerated and would in reality probably be less.

In chapter 6 it is outlined that for cavern 35-36 the equivalent circular diameter of 140m has been used. This diameter is based on the simulation and does enable the cavern to migrate extensively. The corresponding large and smaller diameters that correspond to the ellipse are 170m and 115m respectively. The NTS reflector shows a large deformed area, while the cavern was not this large throughout a considerable thickness at all. From this it can be derived that either the seismic profile over estimates the extent of the deformation in inline 160 or that the cavern had extensive pinch-outs underneath the roof that were not simulated.

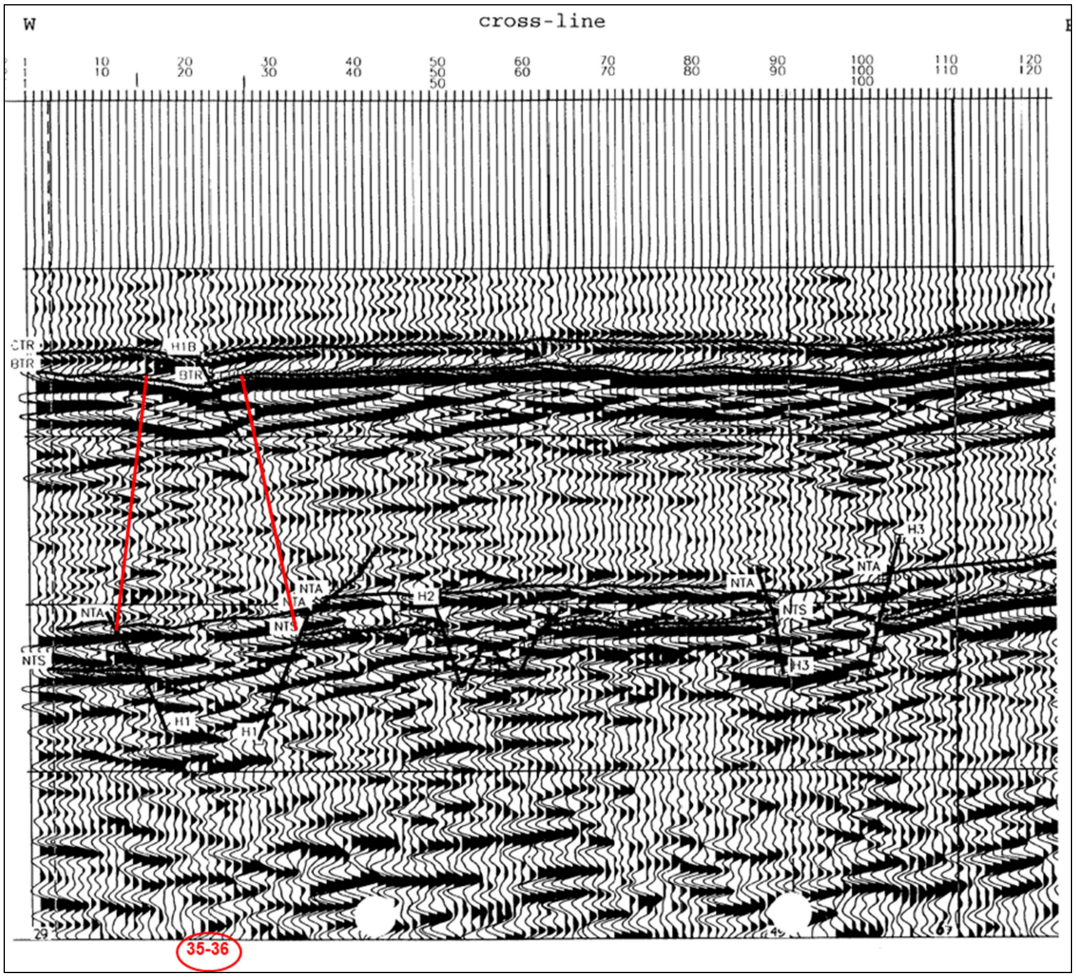

Figure 5.12 cross-section of in-line section 160 (source: HIRES SESOM, 1994)

5.6.2.4 Conclusion on seismic data

The HIRES SESOM confidential report contains seven conclusions about the seismic data. The conclusions mainly indicate that the reflectors have proven to be very useful for identifying the caverns, and migrated caverns. While most of the conclusions are not especially worth mentioning in this report there is one that draws attention. This is conclusion number 5:

'' 5. The horizontal extent of the CTR and BTR deflections was generally less than the area of the NTS disturbances. Thus, if a cavity reaches the base of the Tertiary, it is commonly not over its full initial horizontal extent'' (Directly from: HIRES SESOM, 1997).

This is the same conclusion that can be drawn from the interpretations in this report. Even if the extents of the deformations are exaggerated in the cross-sections it can still be derived that the deformations at the BTR are generally smaller than the deformations at the NTS.

6. Results of the modelled migration and safety assessment.

In chapter 5 the construction of the migration model is comprehensively explained and the parameters are introduced and fitted. With the parameters set on the most likely values all caverns have been modelled to reconstruct the potential cavern migration. This potential migration depicts the maximum migration height that could potentially occur under the most likely circumstances (parameters). In theory the absolute maximum potential could be much higher if the bulking factor is set at a much lower value. At AkzoNobel the bulking factor has previously been set on 1.11 and earlier even lower. Since the lower bulking factor of 1.11 cannot be completely excluded, the migration has been modelled with this bulking factor as well. The standard bulking factor used in this research is 1.15 and for the corresponding bulking factors two possible scenarios for the cavern diameter have been implemented:

Scenario 1: The cavern diameter remains constant during the migration

Scenario 2: The cavern diameter decreases during the migration according to the 80° angle (5.4.1).

The standard setting for the phase I overall compaction and consolidation factor is set at 0.77 (5.4.1). Thus the volume of the fill material in the cavern – insoluble content, insoluble rock layers and possibly slurry- is first multiplied by the phase I bulking factor of 1.53, accounting for some volume increase and porosity (7.3). And subsequently it is multiplied by 0.77 approaching the volume decrease due to the compaction and consolidation. As stated in chapter 5 this is implemented as instantaneous, which is a simplification of reality. However it does represent extensive compaction; which in reality has extensively occurred at all of migrated phase I caverns as the migration started about 60 years ago for the vast majority.

The factor of 0.77 has been fitted to cavern 15 and is slightly higher than the mean value of 0.734 that applies to the decrease in void space under maximum load that was derived from the Oedometer test results of Drost (2012). As 0.77 has been derived from the available data regarding the extensive migration phenomena of cavern 15 it is the best available value. Slightly lower factors could in reality be possible. In order to reconstruct the worst case scenario the very low value of 0.726 had been modelled as well. This factor corresponds to the mean value of the decrease in void space subtracted by two times the standard deviation. The resulting potential cavern migration is in most cases up to a few meters larger. The results have been placed in appendix E4 and E5.

In tables 6.1 and 6.2 the extinction depths in meters below surface are depicted. In both tables the values have been determined with the BF set on 1.15. In table 6.1 the depths for the single production caverns are depicted and in table 6.2 the depths for the final caverns are shown. The tables corresponding to the lower bulking factor, for both the single and final production cases are placed in appendix E2 & E3. Additionally appendix E1 displays a table that contains the most recent roof depths at the time of abandonment and most recently. Often the moment of abandonment is the most recent indication, while sometimes more recent indications are available. The roof depths are vital as they indicate if a cavern started migrating at that specific time.

In tables 6.1 and 6.2 firstly the migrating cavern diameter, the depth of the top of the salt and the BT+40 boundary are present at the left-hand side. Then the direct extinction depths of the migration

are depicted if no slurry fill has been applied. The columns in light grey show what the extinction depths would be if the corresponding volume of slurry had been brought into the cavern. Finally the most right positioned columns contain the slurry volume, the volume of the solids, the leached cavern volume and the slurry fill factor (solids volume to leached cavern volume).

The yellow colored cells indicate that the extinction depth is geometrically induced and therefore not volumetric (see 2.5.2). In the slurry volume column the bold values represent the known slurry volumes that have been retrieved from the AkzoNobel archive.

BF 1,15				Extinction depths [m-MV]							
	[m]	[m-MV]	[m-MV]	single direct		single with fill		[m3]	[m3]	[m3]	[-]
cavern	Dmig	top salt	BT+40	scenario 1	scenario 2	scenario 1	scenario 2	V_slurry needed	V_solids	V_cav_leach	fill factor
1	60	315,8	166,8	175,0	141,8	260,0	200,0	180000	46543	59428	0,78
2	90	319,3	180,3	182,0	58,3	239,3	182,0	280000	72400	245345	0,30
3	40	323,5	170,5	142,6	207,5	195,5	207,5	50000	12929	34483	0,37
4	100	330,0	173,2	174,7	40,0	239,0	153,5	380000	98257	185891	0,53
5	80	333,4	174,4	256,0	118	261,0	197,0	20000	5171	59664	0,09
6	100	336,6	175,3	190,8	46,6	250,0	184,0	350000	90500	174256	0,52
7	90	348,5	172,4	279,3	87,5	300,0	287,8	100000	25857	67346	0,38
8	80	346,8	169,2	223,7	114,8	271,3	181,3	180000	46543	93947	0,50
9	65	350,0	171,4	181,0	176,0			no fill at this cavern			
10	90	354,8	172,3	233,9	64,8			no fill at this cavern			
11	72	356,9	173,8	206,4	153,9			no fill at this cavern			
12	60	307,5	167,9	151,6	133,5	252,6	200,0	240000	62057	66785	0,93
13	95	309,3	166,0	199,0	48,3	230,1	180,0	170000	43957	119721	0,37
14	100	368,9	170,9	286,5	233,1			no fill at this cavern			
15	96	345,9	174,8	87,3	55,9	257,4	175,2	**634347**	164023	223382	0,73
16	68	335,3	171,8	259,6	161,3			no fill at this cavern			
17	92	337,5	167,7	235,6	76,5			no fill at this cavern			
18-24	90	337,0	166,5	220,8	76,0			no fill at this cavern			
19-20	120	332,1	165,6	230,0	156,6			no fill at this cavern			
21	30	327,8	167,0	0,0	0,0			no fill at this cavern			
22	90	357,0	166,4	291,5	260,6			no fill at this cavern			
23	80	357,0	166,4	202,6	96,0	282,0	197,0	300000	77571	119006	0,65
25-26	90	354,3	164,9	206,0	93,3	270,1	177,0	340000	87914	143759	0,61
27	100	375,7	172,0	290,9	230,5			no fill at this cavern			
28	110	383,1	169,9	283,4	191,3			no fill at this cavern			
29	30	375,3	169,8	0,0	288,5			no fill at this cavern			
30-31	72	384,0	169,9	152,2	152,0			no fill at this cavern			
32	90	371,3	171,0	286,0	182,7			no fill at this cavern			
33-34	128	374,9	169,3	261,4	166,6			no fill at this cavern			
35-36	100	372,3	167,9	162,3	82,3			no fill at this cavern			
37	84	360,2	176,0	271,1	98,2	323,7	308,0	140000	36200	71800	0,50
38	100	367,7	173,5	242,4	77,7	276,0	188,0	200000	51714	150282	0,34
39	100	383,4	172,3	191,9	209,4	327,0	262,4	**395640**	102301	81251	1,26
40-41	100	397,7	171,5	262,2	107,7	302,9	182,8	240000	62057	162406	0,38
42-43	110	367,5	166,8	259,3	77,5			no fill at this cavern			
44	60	330,6	165,7	273,9	207,3			no fill at this cavern			
45	84	336,6	164,8	256,1	144,2	258,5	175,9	10000	2586	68827	0,04
46	100	339,6	165,2	254,1	191,5			not needed			
47	80	338,3	165,0	277,7	246,5			not needed			
48	100	338,9	165,9	272,2	245,9			not needed			
49	60	343,5	167,3	169,9	169,5	292,0	254,4	240000	62057	74953	0,83
50	90	342,9	165,6	236,1	81,9	318,2	316,1	**380489**	98383	101654	0,97

Table 6.1 Cavern migration extinction depths [m below surface] for the single production caverns in case of BF 1.15.

BF 1,15				Extinction depths [m-MV]							
	[m]	[m-MV]	[m-MV]	final direct		final with fill		[m3]	[m3]	[m3]	[-]
cavern	Dmig	top salt	BT+40	scenario 1	scenario 2	scenario 1	scenario 2	V_slurry needed	V_solids	V_cav_leach	fill factor
1	80	315,8	166,8	186,0	83,8	246,5	193,7	200000	51714	182111	0,28
2	100	319,3	180,3	197,6	29,3	234,8	181,0	230000	59471	269425	0,22
3	40	323,5	170,5	61,9	178,5	178,0	178,5	110000	28443	49693	0,57
4	110	330,0	173,2	193,8	11,0	233,0	153,3	280000	72400	197078	0,37
5	80	333,4	174,4	235,0	101,4	261,0	197,0	100000	25857	75540	0,34
6	100	336,6	175,3	181,8	46,6	249,5	181,3	400000	103428	184921	0,56
7	90	348,5	172,4	235,7	87,5	300,5	288,0	310000	80157	137761	0,58
8	84	346,8	169,2	212,7	114,8	267,9	177,9	230000	59471	113112	0,53
9	98	350,0	171,4	277,5	241,8			no fill at this cavern			
10	100	354,8	172,3	227,4	64,8			no fill at this cavern			
11	80	356,9	173,8	219,6	124,9			no fill at this cavern			
12	80	307,5	167,9	206,8	75,5	238,5	186,8	120000	31028	76603	0,41
13	100	309,3	166,0	202,0	19,3	229,6	182,5	160000	41371	128318	0,32
14		368,9	170,9								
15		345,9	174,8								
16	68	335,3	171,8	262,9	161,3			no fill at this cavern			
17	104	337,5	167,7	230,0	153,4			no fill at this cavern			
18-24	120	337,0	166,5	319,1	117,2			no fill at this cavern			
19-20	120	332,1	165,6	233,5	181,7			no fill at this cavern			
21	90	327,8	167,0	244,7	160,6			no fill at this cavern			
22	90	357,0	166,4	246,4	96,0			no fill at this cavern			
23	80	357,0	166,4	180,0	96,0	282,0	198,0	380000	98257	136061	0,72
25-26	90	354,3	164,9	194,0	93,3	270,7	182,8	390000	100842	152442	0,66
27		375,7	172,0					no fill at this cavern			
28		383,1	169,9					no fill at this cavern			
29	30	375,3	169,8	0,0	259,5			no fill at this cavern			
30-31	135	384,0	169,9	260,9	152,0			no fill at this cavern			
32		371,3	171,0					no fill at this cavern			
33-34		374,9	169,3					no fill at this cavern			
35-36	140	372,3	167,9	250,0	153,9			no fill at this cavern			
37		360,2	176,0								
38	100	367,7	173,5	226,4	77,7	275,5	183,0	290000	74985	169095	0,44
39	100	383,4	172,3	264,7	93,4	289,4	181,5	**395640**	102301	142715	0,72
40-41	120	397,7	171,5	268,2	49,7	289,3	190,8	180000	46543	223870	0,21
42-43	120	367,5	166,8	260,0	167,7			no fill at this cavern			
44	68	330,6	165,7	271,6	206,6			no fill at this cavern			
45	90	336,6	164,8	255,3	181,7			not needed		68827	0,00
46	100	339,6	165,2	249,4	168,2			not needed		108801	0,00
47	80	338,3	165,0	258,2	170			not needed			
48	100	338,9	165,9	209,4	201,2			not needed			
49	60	343,5	167,3	143,3	169,5	287,0	223,5	290000	74985	86201	0,87
50	102	342,9	165,6	240,0	52,9	308,5	304,2	**380489**	98383	120802	0,81

Table 6.2 Cavern migration extinction depths [m below surface] for the final production caverns in case of BF 1.15.

6.1 Cavern 1

The most recent location of the roof is indicated at 281.8m depth in 1960 (appendix E1). This is 34m above the top anhydrite and although the depth is only indicative it can be concluded that phase II migration certainly has started. The simulation showed that the cavern only had a diameter of 60m in case of the single production and approximately 80m in the final case. In table 6.1 it can be seen that with the bulking factor of 1.15 the migration would only not exceed the BT+40 Boundary in case of a constant diameter. Since both the logbooks as the AkzoNobel well overview of 2005 indicate that return stream has been pumped into this cavern it can be concluded that this has occurred. Yet the volume is not known. If at least 180000 cubic meters of slurry would have been pumped into the single production phase cavern the cavern would be safe for both scenarios (extinction depths 260m and 200m respectively, see table 6.1). This slurry volume corresponds to a fill factor of 0.78 compared to the cavern volume. In case of the final production phase a fill factor of 0.28 is sufficient.

In case of the lower BF of 1.11 it can be seen in appendix E2 and E3 respectively that the cavern is not safe for both scenarios if no slurry is considered. Yet, in both cases a higher slurry fill factor (0.91 for single production and 0.41 for final production) would be sufficient. In all of the above stated

cases it can be noted that for scenario 1 lesser volumes of slurry would be needed as a minimum to make the cavern safe.

Conclusion: under the assumption that the sufficient amount of slurry has been pumped into this cavern, the cavern could not migrate beyond the BT+40 boundary. Since the cavern started migrating before 1960 it can be assumed that the slurry amount was indeed sufficient. Otherwise the subsidence that could have been extensive – worst case even a sinkhole was possible- would have occurred already since 60 years have passed. The cavern can be categorized as safe under the assumption of sufficient slurry fill. Maximum potential subsidence is phase II.

6.2 Cavern 2

At cavern 2 the situation is similar. The most recent roof indication is at 271.8m depth in 1951 (Appendix E1). This is over 40m higher than the base of the top anhydrite so the phase II migration has certainly started at that time. The diameters are 90m for the single cavern and 100m for the approached final cavern. In both the single and final production cases, for scenario 2 a substantial slurry volume is needed in order to declare this cavern safe. In the corresponding tables it can be found that the required slurry fill factors in the cases of cavern 2 are all lower than the required fill factors that cavern 1 needed.

Conclusion: Since the largest potential subsidence at the surface – sinkhole or after this at least a large subsidence bowl- did not occur it can be assumed that the cavern has been filled with return stream slurry sufficiently. This cavern can be categorized as safe under the assumption of slurry fill. Maximum subsidence potential is phase II.

6.3 Cavern 3

Here the production was relatively small and as a result the residual volume is not that large. The diameters of 40m for the single and 50m for the final cavern are very small as well. It can be concluded that the phase II migration started already in 1960 as at that moment the roof was indicated at 35m above the top of the salt (appendix E1). Scenario 2 is safe in all cases. It should however be noted that in most cases this is based on the geometrical extinction and not the volumetric extinction. Still this is the first cavern where the minimum volume of slurry – 50000m^3 in case of BF 1.15 and single production- is needed in order to make scenario 1 safe. The slurry volume of 50000m^3 corresponds to a leached out cavern fill of 37% by the solids (the solids consume 12928m^3). In case of the final production phase the required fill factor is 0.57.

Conclusion: As the decreasing diameter scenario has largely been adopted in this thesis it can be concluded that in those cases the cavern would never migrated to the BT +40 boundary. Additionally there are distinct hints that slurry fill did occur in this cavern and it is likely that the required fill factors have been established. Maximum potential subsidence potential is phase II.

6.4 Cavern 4

At cavern 4 a large subsidence bowl evolved at the surface level. Therefore it can be concluded that the migration did indeed exceed the BT+40 boundary. As a sinkhole did not form it can also be concluded that the migration did not exceed the Tertiary base itself. The logbook and overview do indicate that slurry has been deposited in this cavern and upon analyzing the modelled migration it can be concluded that this helped to suppress the migration. The migration could in almost all cases have led to a sinkhole without any slurry fill. Only for a bulking factor of 1.15 and scenario 1 the migration would have extinguished at 174.7m. It can however be concluded that this scenario did not occur in reality, since no subsidence bowl should have occurred in that case. In chapter 3 it was already outlined that the diameter of the subsidence bowl at surface relates to a very small to virtually no diameter at the BT. Therefore scenario 2 is much more likely and the slurry can now also be explained. In case of scenario 2 with the bulking factor of 1.15 the cavern would have migrated to 153.5m depth if 380000m3 slurry had been pumped into the cavern. This slurry volume translates to a solids fill of 108599m^3 and compared to the leached out cavern volume of 185891m^3 the fill factor was 0.53.

The migration stopped just before reaching the Tertiary base and the diameter would have been about 37m at that point. Due to the compaction of the debris column the formation of the subsidence bowl would now occur. In case of the even larger diameter in case of the series phase the extinction of scenario 2 would be at 153.3m depth and the diameter would still be about 45m at that depth. Now 280000m3 slurry would suffice. This last example has the largest likelihood that this is what happened in reality. The reason that in the case of the series phase considered as well the amount of slurry needed is less compared to the single phase is that the diameter in the single phase is substantially smaller while the volume is not.

Conclusion: Phase III subsidence has already occurred in the form of a subsidence bowl. As a sinkhole did not occur it can be concluded that with this subsidence bowl the worst case has already occurred. Further subsidence will be related to the further compaction of the soil and will not be extensive.

6.5 Cavern 5

The most recent measured roof was at 283.2m depth in 1985 and in 1995 the bottom was measured at 284m. The roof had migrated 49m at least and it can indeed be concluded that phase II migration had commenced. In the notification of the measurement of 1985 it is also mentioned that a cavity is identified from 283.2 to 281m depth. This translates to a migrated cavity height of 2.2m.

If 210000m^3 of slurry – corresponding to a solids-to-void fill factor of 72%- the modeled migrated cavern has a height of 2.2m at 284m depth. This correlates perfectly. The extinction depth would in that case be at 268.8m depth.

Conclusion: The migration has most likely extinguished at 268.8m below surface. Therefore the cavern can be classified as safe and the maximum potential subsidence is phase II.

6.6 Cavern 6

During the most recent indication the roof was already more than 31m higher positioned than the top of the salt in 1951 (Appendix E1). Therefore it can be concluded that Phase II migration has commenced. The cavern did grow in volume when considering the series phase, however during this phase the diameter did not increase compared to the single phase. The reason is the leached out shape from the simulation (can be found in appendix E5; figure 6). If the fill factor would be 52% and 56% for the single and total case respectively, the migration would have ended at 184m and 181.4m depth respectively for scenario 2 and BF 1.15.

Conclusion: This cavern has produced a large tonnage; in fact the production of the single cavern is comparable to the production of cavern 4. In case cavern 4 has been filled with a fill factor of 53%, the migration would have ended at 153.5m depth (so exceeding the BT+40 boundary). This does correlate quite well with the actual subsidence bowl. For cavern 6 a fill factor of 52% would terminate the migration at 181.4m depth. This illustrates the thin line that is caused by a slightly larger volume, while the diameter is the same. It also indicates that indeed the series phase should be considered. In that case the fill factor at cavern 4 is 37%, which would result in the extinction depth of 153.3; which explains the subsidence bowl. For cavern 6 the fill factor would now be 56% in order to let the extinction depth be at 181.3 and therefore making the cavern safe. Based on the fill factor of 72% that was needed to explain the migration of cavern 5 and the known fill factor of 73% at cavern 15 it is likely that AkzoNobel did fill the caverns for indeed approximately 70% to 80%. If indeed a percentage in this range was used for the fill factor, cavern 6 would be extra safe. Since no subsidence bowl occurred at the surface above 6, it can be assumed that the sufficient amount of slurry was brought into the cavern. The maximum subsidence potential is phase II.

6.7 Cavern 7

Cavern 7 is one of the few caverns were the extinction depth of the migration is actually known. In 2017 the construction of well 7A near the old well 7 provided valuable data. The debris column was drilled into at 288m below surface and no cavity was measured. It can therefore be concluded that this is the extinction depth of the migration. The cavern did not produce very much and an unknown amount of slurry has been pumped into the cavern. For the single cavern a fill factor of approximately 38% would result in an extinction depth of 288m depth. The final cavern would need a fill of 58% in order to exterminate the migration at 288m depth. Slight differences in the compaction and consolidation behavior could alter the situation; however the fill values required will be within +/- 10% of these values.

Conclusion: Since the extinction depth is known for this cavern it can be concluded that no severe subsidence –belonging to phase III- can occur anymore. The maximum potential subsidence is phase II.

6.8 Cavern 8

Here the most recent indication for the roof position is at 313m depth and comes from 1959. This is almost 34m higher than the top of the salt and the migration therefore must have started. For this cavern in both the single and final case the solids fill factor from the slurry needs to be

approximately 50% in order to make the cavern safe. Again there are hints that slurry has been brought into this cavern while the numbers are not known.

Conclusion: Under the assumption that the necessary amount of slurry has been brought into this cavern the cavern cannot migrate to the BT+40 boundary. The maximum potential subsidence is phase II.

6.9 Cavern 9

This is the first cavern in line where no indications of slurry fill can be found. In fact the AkzoNobel overview from 2005 actually categorizes this cavern as production well where the first 8 were categorized as waste disposal caverns. The function of waste disposal logically comes after the cavern has produced for a substantial amount of time. For the single cavern the diameter is only a little over 60m and in that case the migration would have stopped just before the BT+40 boundary in case of the decreasing diameter. It should be noted that it this extinction is geometrical based and not volumetric. In case of a constant diameter the migration would have extinguished at 181m depth. In case of the series phase the diameter would grow to about 98m, which has a large impact on the migration behavior. The extinction depth can be found at approximately 277.5m and 241.8m depth for the constant and decreasing diameter respectively. It can be identified that lowering the bulking factor in case of the single production cavern only affects the constant diameter scenario with the cavern barely safe for BF 1.11. In case of the final cavern the opposite can be recognized; now the cavern is safe for both BF's in the case of the constant diameter and in case of the decreasing diameter only BF 1.15 results in a safe cavern. This is yet again a small indication that the BF of 1.15 fits the behavior as the cavern did not cause major subsidence, let alone a sinkhole that could have formed in case of the lower BF's.

Conclusion: No slurry has been brought into this cavern. In case of the bulking factor of 1.15 that has been adopted in this research the cavern can be declared safe for both scenarios and both the single and final production phases. The maximum subsidence potential is phase II.

6.10 Cavern 10

This is a particularly interesting cavern. No slurry has been pumped into this cavern and it can be seen that for the constant diameter the cavern would have been safe for both the single and final production cases when applying the BF of 1.15 for the BF of 1.11 as well. On the other hand the scenario of the decreasing diameter is not safe for all cases. A large subsidence bowl that can be allocated to the migration of cavern 10 is observed at the surface and has formed between 1954 and 1974. From research well ON2 it can be derived that the migration indeed reached the base of the Tertiary (ON2 is positioned approximately 25m to the Northwest of 10; with the cavern diameter of at least 90m this is can be considered as the center of the initial cavern). In the GR logs (figure 6.1) that are taken 2.5 years apart from each other, the consolidation and compaction effect of the debris column can be seen in the increasing downward shift of the latest GR log.

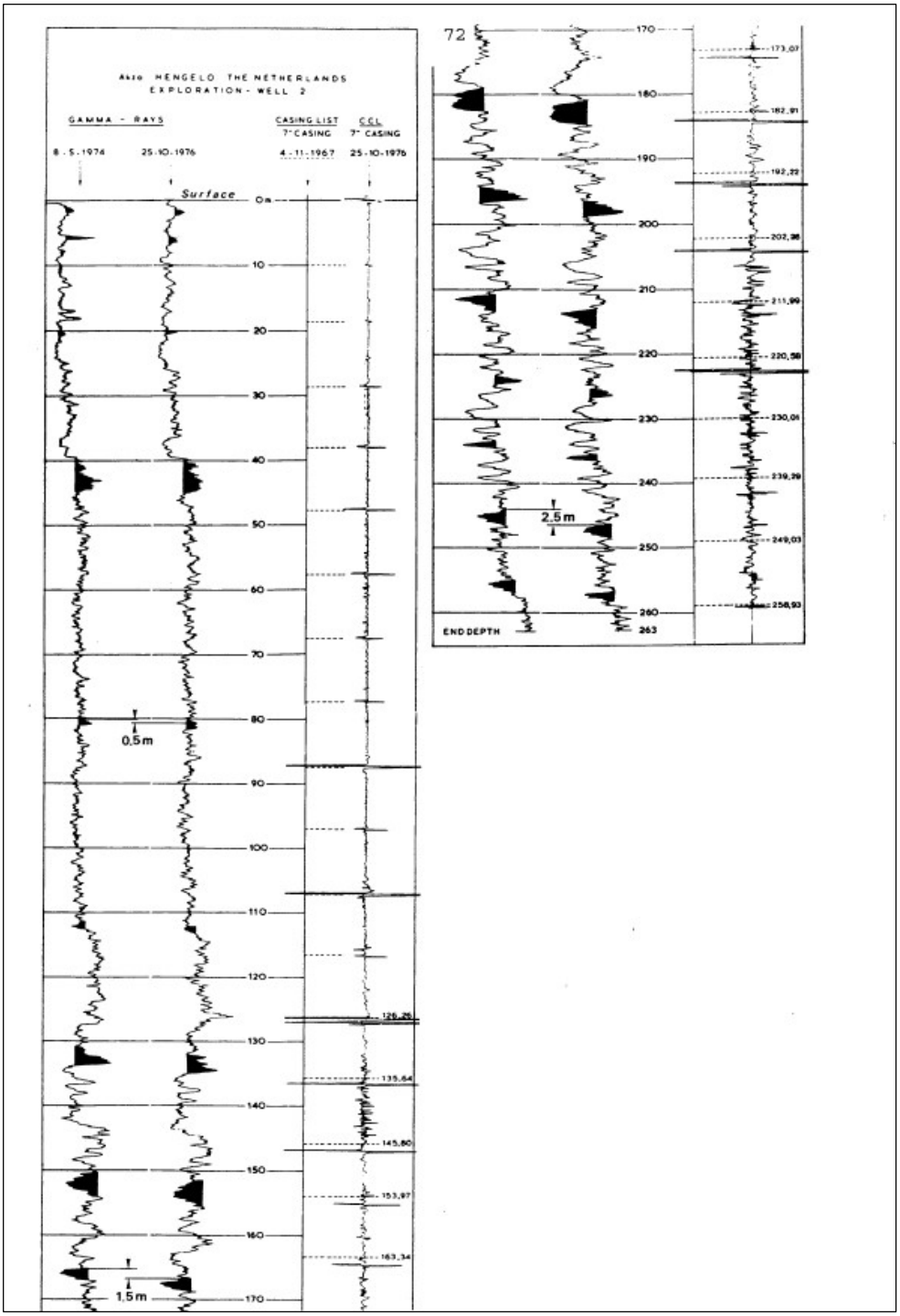

Figure 6.1 CCL logs taken at research well ON2 (source: Wassmann, 1980)

In this particular case either the overall compaction and consolidation factor should be less profound or the cavern diameter should have been larger. With the cavern diameters from the simulations and the standard migration settings the model predicts that the cavern would have migrated to 64.8m below surface. The extinction would in that case be geometrical instead of volumetric. Upon

passing the Base of the Tertiary the volume would be still approximately 7000m^3 and the diameter between 35 and 40m. The diameter corresponds to the sinkhole diameter of cavern 70 and the volume is more than double that of cavern 70. In reality a sinkhole did not occur here wile compared to 70 a much more severe one could have formed. This could also have to do with the Muschelkalk FM being present here and not at 70. Yet with the overall consolidation and compaction factor at values between 0.9 and 0.8 instead of standard 0.77, the migration could have indeed reached the base of the Tertiary without still having a large migrated residual volume. Therefore it does indeed seem that the consolidation and compaction was less severe.

The location of the subsidence bowl is however not directly above the location of well 10. Instead the center of the bowl is more or less located in the middle between wells 10,11,15,14. Due to this location and the abnormal subsidence rate Bekendam (2006) developed and adopted the theory that the subsidence bowl was largely caused by pillar deformation. Again it should be noted that with applying the old model- and using the lesser representative reconstructions of Oranjewoud (2005) - the cavern would have been safe and therefore an explanation was indeed still needed. With the model from this research the migration in case of the decreasing diameter could explain that cavern 10 would have migrated severely and due to geological structures it can have shifted during the migration as well. Therefore the subsidence bowl could have been created by cavern 10 instead of the pillar deformation as well. At least the migration model clearly suggests that cavern 10 could not have been safe (migration extinction before reaching BT+40). In case the diameter remained constant or did decrease less during the migration the cavern could not have migrated enough for causing serious subsidence.

Conclusion: In case of scenario 2 either due to an even larger diameter at the top of the salt, or due to less severe compaction and consolidation behavior (or both combined) the cavern migration did not migrate as excessively as the maximum potential from the model indicates. In case of scenario 1 the cavern would have been safe. Phase III subsidence is the maximum subsidence potential.

6.11 Cavern 11

In 1967 measurements were performed at this location and the roof was found at 307m depth. A sonar measurement (unfortunately the data is lost and only a report can be found) indicated a thin cavity at this depth. From this it can be derived that the cavern had migrated for 50m and that the migration was probably not extinguished yet. The cavern height was according to the measurements 3m. During later measurements in 1991, 1994, 1995 and in 2001 the CCL probe stumbled at approximately 250m depth. This indicates that deformed rock strata at this depth damaged the casing and it is analogous to the continued cavern migration.

The scenario 2 extinction depths are all caused by the geometrical limit instead of the volumetric reason. In order to let the extinction depth become 250m in scenario 2, the cavern diameter needs to be slightly larger and the consolidation and compaction factor slightly less severe. The same thing applies for scenario 1.

In chapter 4 it already became clear that in some cases the cavern development progressed upwards much faster than the simulations sometimes indicate. The most distinct reason is that it does occur that insoluble rock layers fail without causing noticeable damages. Therefore if the exact moment is

not known, the simulation could wrongfully be kept underneath this 'blanket' for too long. This phenomenon would suggest that the diameter at the top could indeed have been larger than the simulated diameter is at the moment. In case of scenario 1 a deflecting roof layer would help to explain the extinction at 250m depth as the extinction depths would otherwise be 206.4m and 219.6m for the single and final production phase respectively (using the 4° degree 'deflection angle').

Conclusion: If the migration indeed stopped at 250m depth either a larger diameter or less serious compaction and consolidation (or a combination of both) is needed for scenario 2. Potentially the scenario 1 with the help of a downward deflecting roof layer has occurred in reality. The strongest indication still remains that the extinction depth is around 250m. The maximum subsidence potential is phase II.

6.12 Cavern 12

The most recent roof indication is from 1951 and was at 307m depth. This indicates that the roof had already migrated for almost 30m. Due to the striking small diameter for the single production phase the cavern would need abnormal high fill ratios for scenario 2 to become safe. Even scenario 1 does need some fill in order to be safe. As the fill ratios of more than 100% are just simply not physically possible it can be out ruled that this occurred in reality (for BF 1.11 it is 105%). Yet the most likely explanation is the larger diameter that indeed can be found in the series phase. In that case a fill factor of at least 41% would already make the cavern safe.

Conclusion: Since virtually no subsidence has been observed here, it can be concluded that the migration has most likely extinguished before reaching the BT+40 boundary. Since it is very plausible that the required fill ratio of 41% has been reached with the slurry fill the cavern can be declared safe under the assumption that this sufficient slurry fill did occur. The maximum subsidence potential is phase II.

6.13 Cavern 13

Analogues to cavern 12 the roof has most recently been identified at about 307m depth indicating a migration of at least 27m in this case. Slurry fill ratios of at least 37% and 32% for the single and final production phase respectively, are needed in order to declare the most likely cases safe – scenario 2 for the single and the final production phase with BF 1.15 respectively. Additionally the logbook reports that in 1961 no more slurry fitted into the cavern as was completely filled.

Conclusion: No real subsidence has occurred here either. It can be concluded that the sufficient slurry fill did probably occur, ensuring that the extinction of the migration occurred deeper than the BT+40 boundary. The maximum potential subsidence is phase II.

6.14 Cavern 14

This cavern did not become connected to any other caverns according to the available data. Only the single cavern production therefore has to be reviewed. With a cavern diameter of 100m and the

strong indications from the logbook that only salt A has been produced the migration indeed has no extensive potential. Moreover in the last known roof indication the cavern had not started with phase II migration. If the phase II migration did eventually occur: In the most likely case of BF 1.15 both scenarios extinguish at safe depths; 286.5m and 233.1m respectively.

Conclusion: The bulking factor of 1.15 has been largely adopted in other distinct examples during this research and this is another example that can be explained on behalf of this value. The lower bulking factor of 1.11 can only explain the migration behavior if the cavern diameter would have remained constant. Yet even more cases cannot be explained by a constant diameter during the migration. However more importantly it can be said that if the cavern started migrating it has most likely stopped migrating at more than 200m depth. The maximum subsidence potential is phase II.

6.15 Cavern 15

This cavern has been extensively discussed during chapter 5 as a lot of data about the migration behavior was available. In order to avoid repetition the description will be kept short here. The migration parameters concerning the decreasing diameter and partly the slurry behavior are derived from cavern 15. Other scenario's do not fit this case and cannot fully explain what happened. Important is that the overall compaction and consolidation factor of 0.77 is derived from this case as well. The slurry fill factor was in this case approximately 73% and in this case the slurry volume was known and the solids content and porosity have been cross-correlated with other data, making the fill factor a quite reliable value.

Conclusion: The most likely scenario, of the decreasing diameter, is derived from here and is the only scenario that fully explains the migration behavior. The migration has certainly extinguished at approximately the BT+40 boundary – which also has been derived from the migration of cavern 15. The cavern therefore can be declared safe and the maximum subsidence potential is phase II.

6.16 Cavern 16

Since there is no indication that slurry has been pumped into this cavern either the diameter should have remained constant or the bulking factor should have been higher in order to let the migration extinguish at safe depths.

From an indicative roof position at 330m depth (more than 4m higher than the top of the salt) in 1960 it can be derived that the migration had started at that point. The simulated cavern has a diameter of 68m in both the single and final production cases. In both cases only the bulking factor of 1.15 and 1.11 and scenario 1 would be safe. In this case the decreasing diameter shows a potential migration that extinguishes at 161.3m depth. This extinction is in both production cases caused by the geometrical and not the volumetric option.

A combination of a less severe compaction and consolidation factor and a larger diameter would enable the safe extinction depth for scenario 2 as well. However only in case for bulking factor 1.15 this would be possible, though there is a high uncertainty here. The geometrical extinction at 161.3m is only 10m beyond the BT+40m line. If the structure is stable it would explain why the boundary is exceeded wile no subsidence has occurred.

Conclusion: Since no serious subsidence has been detected here yet it is very likely that the extinction did occur according to the above stated scenarios. It can however not be fully explained with high certainty what really happened here. While phase III subsidence should have occurred much sooner it cannot be fully out ruled. The maximum potential migration is phase II, but under the assumption that the migration did extinguish according to one of the outlined scenario's.

6.17 Cavern 17

In this case the single production would only be safe in case of scenario 1. The second scenario will only become safe if a slightly larger diameter and still a little less severe compaction and consolidation factor are needed. Both events are not unrealistic as earlier examples indicated. At least it can directly be concluded that the lower bulking factor would never have been safe in case of scenario 2, as it has been for a lot of caverns already. Additionally it became apparent in chapter 5 that it is very likely that doublet 18-24 produced much more in the series phase; perhaps even close to the full production of wells 17,18,19,20,21,22,24 in the series phase. In that case cavern 17 would not have contributed much to the series phase. Based on the migration potential of scenario 2 the cavern should however have had a larger diameter at its top in order to be safe. That would be possible if the leaching progressed in a more upwards direction from the start or if the cavern did contribute some during the series phase (where probably only at the top more leaching occurred).

Conclusion: The maximum subsidence potential of phase III cannot completely be out ruled. Still the most likely maximum subsidence potential is phase II.

6.18 Cavern 18-24

From the seismic data and the reconstruction of the subsidence bowls extent into depth it became clear that the ellipsoidal shaped cavern at the base of the Tertiary should have had a larger diameter of +/- 80 to 90m and a smaller diameter of +/-50 to 60m. This corresponds to an equivalent circular diameter range of 60 to 70m. The migration has certainly exceeded the BT+40 and from the seismic data it could be retrieved that even the base of the Tertiary was deformed. Therefore it can be concluded that the extinction did not occur before exceeding the BT and that the breach of the BT boundary by the migration is justified as potential phenomenon.

The single production phase that results into a diameter of 90m at the top of the cavern can indeed migrate too extensively for all bulking factors with scenario 2. Based on the extent of the subsidence bowl and the downward projection with the angle of draw, and the correlation with the seismic data, scenario 1 does not fit the migration behavior observed here.

Additionally it can safely be assumed that the production at this doublet did not stop after it became connected to the other caverns. So the more likely scenario of the final production phase should be investigated and additionally the scenario of the so-called maximum production should also be considered.

The resulting cavern for the final production phase has an equivalent circular diameter of 120m and is under the standard parameters actually safe. This is primarily due to the fact that the diameter did increase drastically at the upper part of the cavern enabling the fast extinction. It is important that

here the migration diameter can, according to the assumption about the so-called thin pinch outs, be chosen a bit smaller actually. This is because the simulated cavern does indeed form pinch-outs to the sides in the later stages. If for example the diameter is set at 110 or even 100m the migration would already exceed the BT.

In case of the maximum production a similar effect can be seen and the migrating diameter of 135m is justified as the cavern has at least 5m height for that diameter. The migration in this case exterminates at 128m depth, which is only 9m past the BT boundary. The migrated cavern would in this case still have a diameter of 63m and a height of more or less 1.5m. This does actually correspond to what can be observed in the seismic data.

Conclusion: The final or most maximum production scenario explains the extent of the migration. The single production does not fully. Scenario 1 can be out ruled as it does not correlate with the seismic data and size of the subsidence bowl. What is left is scenario 2 for the straight divided production during the series phase or the maximum during the series phase. Both cases can be fitted to the observed seismic and subsidence bowl data and do need a somewhat smaller diameter to account for the thin pinch-outs. The most important conclusion is that the most severe potential subsidence has already occurred.

6.19 Cavern 19-20

From the simulated cavern the migrating diameters of 120m and 130m can be derived. In this case these diameters can be assumed as the migrating diameters even though the pinch-outs at the top of the cavern are present in this cavern as well. The reason is that the leaching in the simulation most likely continued underneath the first insoluble rock layer too long again. If the insoluble rock layer were to be removed earlier during the simulation the leaching would progress upwards much faster, resulting in a thicker leached out upper section indeed.

In the case of the single production phase the diameter of 120m would correspond to an extinction depth of 156.6m for scenario 2. The final production case with the diameter of 130m would consecutively result in an extinction depth of 181.7m.

Scenario 1 would be safe for both the production cases. Additionally a downward deflecting roof layer could exterminate the migration 14m earlier, which helps scenario 1 in the single phase to become safe. This is under the 4° 'deflection angle' and the diameter of 60m at the corresponding depth.

Conclusion: Since it seems that the subsidence area that can be detected in this vicinity can be primarily or perhaps even purely attributed to 18-24, it can be said that it is likely that this cavern has indeed extinguished before reaching the BT+40 boundary. Additionally it is known that prior to the most extensive part of the migration of both 18-24 and 19-21 the caverns were already connected. Therefore it can be concluded that the most serious subsidence has occurred simultaneously to that of 18-24. The maximum subsidence potential is phase II subsidence.

6.20 Cavern 21

After cavern 14 this is the second cavern where the cavern migration cannot be observed in the most recent roof location. The roof was still at least 1m underneath the top of the salt in 1960. Although it can normally be assumed that this last meter will not hold the overlying anhydrite, in case of only the single production for this cavern that would be possible.

In fact the diameter of only 30m at the top of the cavern is so small that if migration would have commenced with this diameter all possible scenarios would have resulted in a sinkhole. This can be explained by the volume that in that case needed to be filled up through this small upward migrating channel. The best visual way to describe this is by the 'straw effect'. Yet it is extremely unlikely that this occurred since a sinkhole would definitely have formed in that case.

In the seismic data it can actually be derived that at the location of well 21 some deformation was present at the near top salt reflector. Directly above 21 at the Base of the Tertiary reflector nothing is present. While this seems as an additional indication that the migration did not commence, it cannot be out ruled. The seismic data simply does not show migration that extinguishes between the top of the salt and the Tertiary base. It only shows the deformations at the near top salt reflector and at the Base Tertiary.

In case of the final simulated cavern the production is quite more extensive and the diameter at the top increases to 90m. If the migration would have commenced with this diameter it would have extinguished at 160.6m (This is for BF 1.15) depth. As the extinction now does not exceed the Base Tertiary it helps to explain why it is not present in the seismic data. Additionally scenario 1 would with the bulking factor at 1.15 be safe for both production cases.

Conclusion: Either if according to the last example migration did occur, or if migration did not even commence at all the cavern can be declared safe. The main reason is that based on the seismic data it does indeed seem most likely that migration did not commence at all or in the case it did occur at least extinguished before reaching the Base Tertiary. The maximum subsidence potential is phase II.

6.21 Cavern 22

In 1960 the cavern had migrated at least 30m already. Under the standard parameters the cavern would migrate to 260.6m and 96m depth for the single and final production case respectively. The extinction would in final case be geometrically.

The cavern diameter of 100m for the final phase and slightly less compaction and consolidation can result in extinction depths around 189m. Yet with the indication that it is very likely that doublet 18-24 has produced substantially more during the series phase, this cavern could have produced only a small amount in the series phase. The single phase is in case of scenario 2 safe. Additionally scenario 1 is safe in both production cases.

Conclusion: The reconstructed single production phase cavern is safe for both scenario's and seems the most likely fit. In case the production during the series phase is adequately represented by production numbers from chapter 3, the cavern would only have been safe with scenario 1. The maximum subsidence potential is phase II.

6.22 Cavern 23

In 1996 the most recent roof indication was at 296m depth, this corresponds to a migration of almost 68m. The migration model also clearly suggests that extensive migration could have occurred here. In fact without slurry deposition in this cavern the migration potential would have been too excessive. On the surface level a workshop was located in the barnlike structure attached to the derrick above this well. According to multiple sources lots of waste materials from the workshop have been dumped into this cavern besides the already indicated slurry deposition. In order to terminate the migration at safe depths for the most likely scenario, the fill factors of 65% and 72% are required for the single and final production phase respectively.

Conclusion: Since no subsidence occurred here it is very likely that at least the required minimum amount of slurry (and other material) has been brought into the void. This does correlate with the statements in the logbooks. The maximum subsidence potential is phase II.

6.23 Doublet 25-26

In the most recent indication the roof has already migrated more than 32m in 1962. The simulation for this cavern has proven to be quite difficult as the repair works would imply that the insoluble rock layers either fell late or not at all. As a result the simulated cavern has leached inside salt A for a long time (perhaps too long) allowing the cavern to grow extensively there. The production that is left for the upper located salt layers is not very extensive. As a result the geometry of the cavern in the upper part has the 'morning glory' shape. The diameter that should be used in the migration model is difficult to determine. On one hand the pinch outs do suggest that a smaller diameter than the observable 90m should be taken. On the other hand the whole leaching could have taken place more upwards resulting in an even larger diameter.

This doublet was located next to 23 and the situation is very similar. Here for the most likely cases the fill factors of 61% and 66% are needed in order to ensure the extinction at safe depths.

Conclusion: Likewise to the situation of cavern 23 it is likely that the minimum required amount has at least been brought into the cavern. Therefore it can be assumed that the migration terminated at safe depths. The maximum potential migration is phase II.

6.24 Cavern 27

This cavern was difficult to simulate as well. The logbooks indicate that the cavern had been located inside salt A for its entire production life. Above this the cavern has no known hydraulic connections and still the production was respectable (187602 tons). The limiting dissolution angle at some point demanded that the cavern would grow upwards (see figure 4.7). The simulated cavern has a diameter of more than 110m at its top. The cavern does have the 'morning glory' shape in its upper section with thin pinch-outs directly underneath the anhydrite roof. From the absent known hydraulic connections and the constructed map (figure 4.15) it can be derived that this cavern cannot have been larger. Therefore either the pinch-outs are correctly simulated and are in reality not spreading more extensively, like for other caverns would be the case, or the cavern in reality has

vertical walls. A diameter of 100m as starting diameter for the migration would be justified as cavern height is at least several meters (even at the sides). With this the cavern is safe for both scenarios as the extinction depths for scenario 1 and 2 are 290m-and-230m below surface respectively.

If the simulation is not representative it can be concluded that the migration potential would have been very extensive if the diameter would be around 80m (for a cavern with a cylinder shape). No slurry fill has occurred here and no subsidence has been reported. And in that case only a constant diameter during migration would explain the migration phenomena.

Even though it is also possible that the leaching continued inside salt A instead of moving to the upper salts, it is not very likely. This is due to fact that the cavern has no hydraulic connections to other caverns while in this case the diameter would have been much larger. However A much larger cavern only located in salt A does not have a large migration potential as it is broad and flat (salt A is roughly 10m thick). Additionally if only salt A has been produced it does become much more likely that the migration did not actually occur at all.

Conclusion: The cavern migration probably extinguished at a safe depth. The maximum surface subsidence potential is phase II

6.25 Cavern 28

The most recent roof indication implies that the roof had migrated about 19m already in 1962. The production at this cavern was even more extensive than for 27. Again no known hydraulic connections occurred and no subsidence has been encountered here yet. The pinch-outs at the top of the cavern do justify a somewhat smaller diameter for the migration. The diameter at the top of the cavern is almost 140m and the chosen migration diameter is set at 110m. This diameter can be justified as the cavern height at this diameter is more than 5m. In case of scenario 2 the migration extinguishes at 191.3m depth and in case of scenario 1 the extinction would also be at a safe depth. A slightly larger diameter – which can also still be justified up to 120m-, would result in an even deeper extinction depth.

Conclusion: Based on the production and simulation it is highly likely that the diameter would have had at least these extents. Therefore the migration should have extinguished at safe depths. The maximum subsidence potential is phase II.

6.26 Cavern 29

Both the simulation results for the single and final cavern show that the leaching out resulted in a large lower section and upper section with a small diameter. The most recent roof indication leads to believe that in 1960 the roof had migrated for 2.6m already. Still it cannot be determined with high certainty that the migration did in fact commence. The ambiguity here lies in the lack of surface subsidence as no serious subsidence has occurred here.

If the cavern would have migrated with a diameter of 30m –the smaller upper part of the single production cavern- the straw effect would have resulted in a sinkhole for scenario 1. For scenario 2 the extinction by geometrical limit would occur at 288.45m depth. Therefor it can be said that in

case the migration started with this small diameter only scenario 2 would explain why no detectible deformation at the surface level occurred.

For the series phase the same applies to a diameter of 40m and scenario 2 would in that case extinct at 259.45m depth.

If however the cavern shape is different (e.g. more upwards leaching) and the diameter at the top of the salt is much larger, the migration behavior would be completely different. In that case both the scenario 1 migrations would be safe and the scenario 2 cases would require a slightly larger diameter (105 instead of 100 for the single for example) diameter to start migrating with.

Conclusion: Perhaps due to a much larger production in the series phase the cavern extended much more underneath the top of the salt allowing the diameter to be much larger. If no such thing occurred and the simulations do represent the real cavern accurately, only scenario 2 helps to explain why no sinkhole has formed if migration commenced. Since it is not likely that a sinkhole will still form after almost 70 years have passed without any noticeable effects it can be said that probably either scenario 2 did extinct the migration at a safe depth or that the migration did not start. The maximum migration potential is phase II.

6.27 Doublet 30-31

This has caused a subsidence bowl at the surface. The subsidence was much less severe as the examples of 4, 18-24 and 35-36, however still it was noticeable. From the logbooks and especially the repair works it can be derived that production continued here for a long time. No repair works are mentioned at cavern 29 after 1960, indicating that either that no production occurred at 29 after it became connected or that indeed no roof failure occurred. While at this cavern a lot happened in the years after the connection occurred.

Therefore the single production case can actually be discarded as it can be concluded that the production was at least more than that. In case of the final production the cavern would just be safe with the standard parameters and a cavern diameter of 128m. It should be noted that this diameter is larger than the simulation shows. The diameter has primarily been based on doublet 33-34. At 33-34 this equivalent circular diameter could be derived from the sonar measurement and the production was quite similar. Choosing the diameter of 110m a sinkhole should have formed. The cavern dimensions are quite sensitive when it comes to the migration.

Based on the extensive repair works for several years within the series phase it is likely that the production was even more than the equally divided tonnages distributed in chapter 3. In that case it could indeed have occurred that the cavern grew to the extents of about 135m and have a larger volume.

In that case the migration would extinct at 152m depth, which corresponds with the formation of a subsidence bowl due to the compaction of the debris column.

Conclusion: Phase III subsidence (maximum) has already occurred.

6.28 Cavern 32

In 1979 the cavern had migrated for at least 31m according to the roof indication. This cavern has no known hydraulic connections and therefore the single production phase immediately results into the final cavern. From the simulation it can be derived that the diameter at the top is a little over 100m. However the morning glory effect again demands a somewhat smaller migration diameter at the start of the migration trajectory.

For scenario 2 even with the diameter of 90m the cavern migration terminates at 182.7m depth which is just safe. In case of scenario 1 the cavern would surely be safe.

Conclusion: The cavern has likely stopped migrating at a safe depth. The maximum surface subsidence is phase II.

6.29 Doublet 33-34

In chapter 4 it is outlined that at this doublet a sonar measurement has been made at the end of its production life. Moreover this sonar measurement has been analyzed and the approach of the equivalent cylindrical shape in order to simulate the doublets actually was derived from and correlated with this sonar measurement. The equivalent circular diameter is 128m for this doublet and the migration can continue to 166.6m depth. This is only 2.7m beyond the BT+40 boundary and does not exceed the Base Tertiary. The expected result would be a subsidence bowl belonging to the phase III category and this exactly what has occurred at the surface. Though it should be noted that the subsidence bowl is quite extensive and is located between 33-34 and 35-36. It can hereby be concluded that 33-34 could have contributed to the subsidence bowl as it would have caused its own small bowl if no connection occurred. Still doublet 35-36 remains the main cause of the subsidence bowl even if 33-34 contributed.

Conclusion: phase III subsidence has already occurred and no more serious deformation can occur.

6.30 Doublet 35-36

This doublet has caused the extensively reported subsidence bowl near the surface measuring points B and K. In 6.29 it became clear that doublet 33-34 could have contributed to this bowl as well. This was already assumed in multiple previous reports. Still the migration potential for doublet 35-36 is much more extensive. The main reasons are that the production has been larger and the second and most important reason is that the total thickness of the salt is almost twice as large. For doublet 35-36 the total thickness is approximately 60m while at doublet 33-34 the total thickness is approximately 36m.

As a result the leaching of the cavern could progress much more in the upward direction. Due to the core analysis that indicated a vertical leaching coefficient that more than doubles the horizontal coefficient, and the expected upwards thrusted behavior of the much lighter water compared to the in situ strata, it can be explained that indeed the leaching desires to progress upwards much faster than horizontally.

This effect can be observed in the simulation that results into an upper cavern diameter of approximately 100m for the single phase cavern and 140m for the final cavern. On top of this the seismic data in 5.6.2 suggests that the cavern at its top would have had an even larger diameter (194m equivalent circular diameter). If the extent of the cavern would indeed be of that size at the top of the cavern, the volume should have been much larger in order to cause a large subsidence bowl. Choosing 140m is more justified and in both cases the cavern would exceed the BT+40m boundary in case of scenario 2. For scenario 1 the cavern would actually be safe for BF 1.15 and even for BF 1.11. This indicates that the lower bulking factors as well as scenario 1 cannot explain the observed migration related subsidence.

Conclusion: phase III subsidence resulted in an extensive subsidence bowl.

6.31 Cavern 37

This cavern has extensively been described in chapters 4 and 5. The cavern was re-opened in 2003 and therefore the extinction depth is known. Based on this the model could be fitted and cross-correlated when it was still in the construction phase.

The only important ambiguity here is the question if slurry has been deposited into the cavern or not. In the logbook it is stated that no slurry has ever been deposited into this cavern. This was written in 1972 and the AkzoNobel overview from 2005 does actually mention that slurry had been pumped into the cavern.

According to the migration model the cavern should have migrated much further than the observed extinction depth of 308m if no slurry has been pumped into the cavern. In fact because the sonar measurement of this cavern was taken during the final stage of its production life it can be assumed that the final cavern dimensions are quite well represented by the sonar measurement. Therefore the residual cavern volume and diameter cannot have been any different. Additionally the downward deflected roof layers of 2.86m that Bekendam (2017) reports, can solely also not explain why the migration terminated at this depth for neither of the scenarios.

As a result only 2 reasons would help to explain the early extinction.

1. Is that the bulking factor of 1.15 is still too low, and the phase II bulking factor should even be larger.
2. Is that the right amount of slurry has been deposited into the cavern.

From the old method to derive the bulking factor (again assuming constant diameter) the bulking factor can also be determined if both the roof and bottom depths at different times are known. In this case the roof and bottom depth at the time of the sonar are known and they are known at the extinction as well. Additionally one intermediate point delivers the two required depths. When determining the overall bulking factor over the whole range the value is 1.4 which is remarkably high. When the intermediate roof and bottom from a GR measurement of 1977 are inserted the BF for the first section is 1.5 and the last section 1.3. The bulking factor over this last section could be explained that probably no compaction has occurred yet. The bulking factor of 1.5 over the first

section cannot be explained and even though the derivation method is not completely correct it can be concluded that it is very likely that some fill at the bottom of the cavern has occurred.

A slurry fill factor of 50% in case of scenario 2 and 27% in case of scenario 1 would result in approximately the right extinction depth with all the parameters still at the normal values and the2.86m downward deflected roof layer incorporated.

Conclusion: The cavern stopped migrating at 308m depth and the maximum subsidence potential is phase II.

6.32 Cavern 38

This cavern requires a fill factor of at least 34% in case of the single phase production and 44% in case of the final production in order to let the scenario 2 extinctions be at safe depths.

The cavern had migrated over 72m already in 1974 and no serious subsidence deformations have occurred so far.

Conclusion: It is very likely that the cavern has been filled with at least the sufficient amount of slurry in order to let the extinction depth be at a deeper depth than the BT+40 boundary. The maximum subsidence potential therefore is phase II.

6.33 Cavern 39

Similarly to cavern 38 this cavern can only be declared safe if sufficient amount of slurry has been brought into the cavern. Fortunately this is one of the few caverns where the volume of slurry is known. The actual amount is 395640m^3 with the solids content of 16.9wt% this corresponds to a fill factor of 125% (in case of 35% porosity), hence it can be concluded that the production must have been more. The total production phase cavern would be filled with a fill factor of roughly 71%. This is very much possible and correlates perfectly to the fill factor of 73% in cavern 15.

Conclusion: The cavern has been filled more than sufficiently and the maximum potential migration depth in that case is 307.6m. The cavern can be considered safe and the maximum subsidence potential is phase II.

6.34 Doublet 40-41

In this case the minimum fill factors of 28% and 42% are needed to declare the single and final phase safe respectively. Again these values are within the range (up to 75%) that is very plausible based on the slurry volumes that are known.

Conclusion: The cavern is most likely filled sufficiently with slurry in order to extinct the migration at safe depths. The maximum subsidence potential is phase II.

6.34 Doublet 42-43

No slurry fill has been reported here. While the logbook of 42 indicates no damages corresponding to migration, the logbook of 43 indicates that the cavern had migrated 58m in 1973. The production of this doublet was a lot lower than the production of the nearby located doublets 33-34 and 35-36. The salt thickness however is similar to that of 35-36. A likewise scenario can be expected for the leaching, with the only difference that this cavern produced around 30000 tons instead of over 500000 tons. Therefore the simulations show that the extent of the cavern is indeed much smaller. Due to the extensive salt thickness the simulated caverns are quite elongated, with a relatively small diameter. Caverns that do have a large volume – as is the case here- can migrate extremely far if the migrating diameter is indeed low. In fact the potential is so extensive that a sinkhole should have formed.

No subsidence has been detected at the surface above this cavern however. Therefore it is likely that the cavern leached out in the upward direction much earlier, resulting in a larger extent in the upper region. By taking a starting diameter of 120m for the final production case, the migration would extinguish at 167.7m depth. This is one meter deeper than the BT+40 boundary and would therefore just be safe. The diameter at this depth would have decreased to 50m and the potential of a downward deflecting roof layer could decrease the migration potential with several meters as well.

Conclusion: If the simulations are representative for the cavern shape and dimensions the migration potential is extremely high. In that case however a sinkhole should have formed already. Therefore it is likely that the geometry is slightly different. Also with scenario 1 the cavern would be safe. The maximum subsidence potential is phase II.

6.35 Cavern 44

Due to the limited thickness of the salt (about 30m) the cavern should have extended in the horizontal direction much more. Yet the production has not been very much over here and the cavern is safe for both scenarios in both production cases.

Conclusion: no subsidence has occurred over here and probably the diameter has indeed been just large enough to let the migration exterminate prior to reaching the BT+40 boundary. If not the boundary would not have been exceed very far and a relatively shallow subsidence bowl could have resulted. The maximum subsidence potential is phase II.

6.36 Cavern 45

This cavern would readily be safe for scenario 2 in case of the final production and BF of 1.15. Therefore a minimum amount of slurry is not even needed. In case of the single production phase some slurry is needed, however a fill factor of 4% would already make the cavern safe. Again the scenario 1 cases are all safe.

Conclusion: This cavern should have stopped migrating at a safe depth already without slurry fill and the hints that some slurry went into this cavern would only make it safer. The maximum subsidence potential is phase II.

6.37 Cavern 46

Likewise to cavern 45 the cavern would already be safe for scenario 2 in both production cases if indeed the phase II bulking factor of 1.15 is applied. The hints of slurry disposal would have even made the cavern safer. It should also be noted that the migration has been modelled using a diameter of 100m while both the simulations show that the cavern diameter is over 140m. This is due to the high uncertainty of the simulations. As for this cavern it has been unknown when the insoluble rock layers have fallen (if they have at all) the result is a very extensive cavern primarily in salt A. During test simulations where the insoluble rock layers have been let go much sooner the cavern could have a diameter of 100m.

Conclusion: Even with the smaller chosen diameter of 100m the cavern is readily safe. If the diameter is larger in reality and with some additional slurry fill the cavern becomes even safer. The maximum subsidence potential is phase II as the migration definitely did already start.

6.38 Cavern 47

The simulation was difficult to the same reasons as for 46. Now the cavern has a small new cavern on top to account for the last production after the insoluble rock layer fell; which is in accordance to the logbook. The diameter of the lower cavern (80m) has been chosen to migrate with. Both scenarios are safe for both production cases if BF 1.15 is applied.

Conclusion: The cavern did start migrating and the small amount of slurry that is necessary to exterminate the migration at a safe depth is very plausible to be deposited in the cavern in reality. The maximum potential subsidence is phase II.

6.39 Cavern 48

The logbook clearly suggests that only salt A has been produced here. Strangely in 1991 the indication is that the roof had migrated for at least 70m. This is however indicative and not certain. The diameter has been set at 100m for the migration modelling – same as the case was for cavern 46- and the cavern is readily safe for both the single and final production cases with scenario 2. Only for the lower – and less likely- bulking factor some slurry fill is needed.

Conclusion: This cavern could, according to the most likely scenario, not have migrated beyond the BT+40 boundary. The cavern should be safe. The maximum subsidence potential is still phase II as the indications are that the migration did commence.

6.40 Cavern 49

In chapter 4 it is extensively reported that the diameter of the simulation does correspond well to the sonar measurement. The position of the cavern was not exactly correct. In case of the single production the cavern would be safe for both scenarios. The cavern would in case of the final production phase be safe for scenario 2. This is however due to the geometrical extinction and not the volumetric. The amount of slurry needed is still quite substantial if the volumetric extinction

needs to occur before exceeding the BT+40 boundary. The slurry fill factor for the single case needs to be at least 84% and 89% for the final production case.

Conclusion: The required slurry fill in this case is quite high, however with some lesser compaction and consolidation or even potentially a larger diameter the volumetric extinction depth could be safe with lower slurry fill factors. Still based on the geometrical extinction the cavern should also be safe. The maximum surface subsidence is phase II.

6.41 Cavern 50

The exact amount of slurry that has been brought into this cavern is 380489m^3 which would correspond to a fill factor of 97% in case of the single production. This clearly suggests that the production should indeed be more allowing the cavern volume to become larger. In case of the final production simulated cavern the fill factor would be 81%. This already more likely, although it is still higher than the around 73% we have seen previously.

Based on this fill the extinction depths are sufficiently safe in all the cases. It should also be noted that without the fill the cavern would not have been that safe. The most likely extinction depth is around 304.2m depth, which is for scenario 2 in the final production case (BF at 1.15).

Conclusion: Due to the certain sufficient fill the cavern cannot migrate through the BT+40 boundary. Since the migration did start already the maximum subsidence potential is phase II.

7. Additional correlations

In contemplation of obtaining a higher reliability more data is gathered and analyzed. The additional data sometimes has been derived from caverns or researches that do not belong to the scope of this study. They do however often provide valuable correlation data and therefore these 'additional' correlation cases have been analyzed. In this chapter all the data that comes from these additional cases are depicted.

7.1 Additional data regarding the insoluble content

In chapters 4 and 5 it has already been noted that the data regarding the insoluble content is not very robust. The derived means and standard deviations for the corresponding salt layers are based on the core analysis of only 5 different locations. It is strongly recommended that more cores will be analyzed in the future in order to get more robust mean values and a smaller spread.

Besides the percentage of the insoluble content the behavior of this material is also taken into the migration model. First the bulking is considered, regarding the porosity of the material, and subsequently the consolidation and compaction is accounted for. The corresponding values that have been implemented into the model have been derived from multiple sources.

Firstly they have been obtained from literature such as Berést et al. (2006) and Schootstra (2015). This resulted in the assumption that a porosity of 35% and its corresponding bulking factor of 1.55 should be representative for this material.

Then multiple caverns outside of the phase I scope have been analyzed. In these caverns either only salt A had been produced without any roof failure yet or salt A had been produced and only insoluble rock layer AB had failed. In the former case the volume that the deposited insoluble content takes could be derived and in the latter case the volume of both the insoluble content and insoluble rock layer. After comparison with the in situ volumes from the percentage of the insoluble content in salt A and the thickness of insoluble rock layer AB this results into two bulking factors. One is the bulking factor purely based on deposition of the insoluble content of salt A and the second is based on the deposition of the insoluble content of salt A and the failed insoluble rock layer AB.

Unfortunately only one cavern provided adequate data for determining the bulking factor of only the deposition of the insoluble content from salt A. This was cavern 488 and the corresponding bulking factor is 1.68. Some more caverns seemed to fit the requirements of multiple sonars only inside salt A, however the due to the inaccuracy of the sonar measurements the bulking factor that could be derived was unrealistically high.

For the bulking factor in case of the deposition of the insoluble content of salt A and insoluble rock layer AB 5 caverns fitted to the requirements. Unfortunately in all cases the bulking factor as described was quite high as well. Yet all these caverns did continue upwards through salt B virtually directly after the insoluble rock layer AB was not there anymore. It could therefore be very much possible that salt B including insoluble rock layers AB and BC failed. The bulking factors that correspond to this phenomenon can be found in table 7.1

well	BF
314	1,37
323	1,72
331	1,26
411	1,42
413	1,09
mu	**1,37**
sigma	**0,11**

Table 7.1 phase II bulking factors derived at several wells

It can be concluded that this additional correlation material does not contribute much to making the data more robust as it is not that reliable and robust itself. Further investigations into this topic are recommended.

7.2 Additional data regarding the decreasing diameter

Two caverns from outside the scope, that have migrated thoroughly, have been investigated. In both cases the decreasing diameter plays a role.

In the first case, of cavern 70, a sinkhole was formed in the 90's and the sinkhole was the result of the migration of a part of the Multiple Cavern Completion system 69-70-71. Cavern 69 had been filled almost completely with return stream slurry and cavern 71 did not start to migrate. Still the migrating volume and surface area that started to migrate directly above well 70 is much larger than the measured volume and surface area of the sinkhole are. It can be assumed that if the migration reaches the base of the Tertiary the formation of a sinkhole can occur and moreover that the Tertiary and quaternary soils will collapse into the void with virtually no bulking at all. Therefore the volume and surface area from the sinkhole would have been approximately the same at the base of the Tertiary. The measured sinkhole (figure 7.1) had a diameter of 35m and a depth of 4.5m in the middle. The volume was almost 3000m^3 (Wassmann, 1980a)

Figure 7.1 Photograph from the sinkhole at the surface above cavern 70 (source: AkzoNobel archive)

In the sonar measurement of 1977 it can be seen that almost the whole void of 69, which was 213710m^3 in 1970, has been filled up. Curiously no cone shape with a distinct angle of repose can be seen. Instead the sonar of 1977 is a very thin slice with a surface area of 7890m^2 but no volume due to the lack of thickness. Altogether it can be assumed that the fill was successful and that the migration occurred above well 70. In 1977 a sonar measurement was taken at 70 as well and the measured volume was 14720m^3 and the surface area was 3390m^2. The cross-section of the top can at best be approached by an ellipse with the largest diameter of 100m and smallest diameter of 40m. A circular cross-section with a diameter of 35 corresponds to a surface area of 962m^2, which is 3.5 times smaller than the surface area of the sonar measured cavern. Even with placing a circle with these dimensions in the middle of the shape of the sonar measurement, and assuming that due to the irregular shape the shape does not remain constant during migration, the difference in size is significant. Therefore it can be out ruled that that the migration started with a circular cross section and diameter of 35m. If the cavern started migrating with the cross sectional area of 3390m^2 the equivalent circular diameter can be described. This equivalent diameter is 65m and if the diameter at the base of the Tertiary would have decreased to the 35m, corresponding to the sinkhole, the angle α would be 84°.

The second case is cavern 167, where the multiple sonar measurements have been taken during the extensive migration trajectory (see figure 7.2). In the older sonar -red lines- measurements it can be seen that the MCC cavern is positioned in salt A and that the sonars overlap. Later sonars – green lines- show that at 168 the cavern has pierced through salt B, C, D, all the insoluble rock layers and the top anhydrite as well. In the green filled contours the cavity is outlined that clearly has migrated about 40m already. Additionally it can be seen that the migrating cavern seems to be ascending in the direction of 167. In the last series of sonars – black contours- the migrating cavern distinctly starts to adopt a cone shape.

After analyzing the cross sections and diameters of the migrating cavern during the migration trajectory, it became clear that for the first approximately 50m the diameter did not decrease yet. However in the most recent sonars –black contours- the diameter does rapidly decrease in the upward direction. The angle that can be derived is in those sonars approximately 60°. This angle is much blunter than the 80° that can be observed at cavern 15. If the diameter at the top of salt D is considered, the overall averaged out angle would be 80°. The delayed decrease of the diameter is an interesting phenomenon that perhaps could be linked to the occurrence of a fault.

In Bekendam (1996) a theory is outlined in order to explain the smaller widths at the base of the Tertiary compared to the top of the salt that can be observed in the seismic data. The explanation is that due to the inverted cone shape of the caverns the height of the cavern is larger in the middle than at the sides. Therefore according to his model, where the migration height can directly be calculated by 1/(BF-1), the migration locally can differ. The migration would in that case be much more extensively in the middle than at the sides. Although with this theory the upwards decreasing diameter can somewhat be explained, there are cases that show contradictions.

At several caverns where the records show that return-stream slurry has been pumped into the cavern (15, 39, 40, 50 even with known volumes) a pouring cone should be present. In case of cavern 15 and here at 167 (appendix F1) the shape of the cone can clearly be seen in the sonar measurements. In the example of 167 the cone does not comprise out of slurry, but rather of the

collapsed insoluble rock layers and roof anhydrite. The migration phenomenon would according to the same theory result in the opposite; a higher migration at the sides than in the middle. An important note here is that this comprises the migrating part which is only in the middle of the triplet (figure 7.2). This does not describe the observed cavern migration in the sonar measurements of 15 and 167. Moreover no such phenomenon has been encountered in the sonar measurements of the Hengelo Brine Field at all.

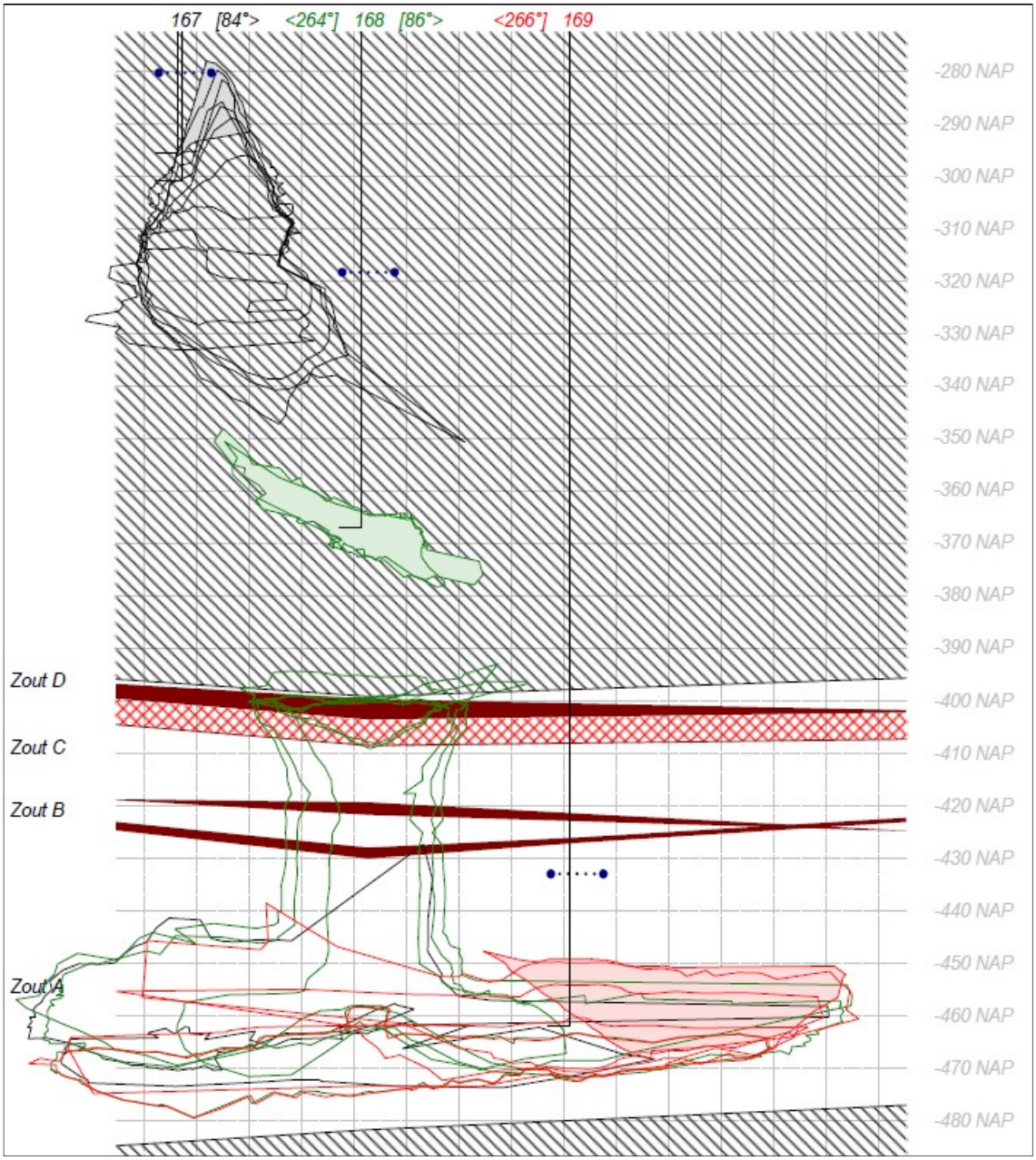

Figure 7.2 overview of all the side-views corresponding to the multiple sonar measurements taken at 167

7.3 Additional data regarding the slurry

As described in 5.4.1 Drost (2012) performed Oedometer tests on 4 samples that were taken from the return stream slurry in 2012.

Component	%	Rho (kg/m^3)
CaSO4.2H2O	62,3	2300
CaCO3	27,5	2700
Ca(OH)2	5,4	2211
Mg(OH)2	1,9	2344,6
SrCO3	0,4	1141
FeCO3	0,3	3660
insoluble content	2,2	2200

Table 7.2 slurry components and density per component (after: Drost, 2012)

Table 7.2 shows the slurry analysis and its components. The densities are taken from literature. The density of the average overall solids content is approximately 2400kg/m^3. The solids content can be between 15 and 25wt% and corresponding slurry densities are 1350 to 1450kg/m^3 (Drost, 2012).

The slurry that was described in order to fit the pouring cone, which can be observed in first sonar measurement at cavern 15, needed to consist of 28wt% solids with a porosity of 35%. The porosity directly correlates to the porosity that can be derived from the Oedometer tests from Drost (2012). The slightly higher solids content was necessary to get the right volume that the slurry actually filled up. An even higher porosity would also result in a larger fill volume, however this is extremely unlikely. After personal communication with Marinus den Hartogh it has been concluded that slightly higher solids content in the slurry would have been very much possible in those days. Table 7.3 shows the void space under the increasing load per sample from Drost (2012). In the other columns the porosity and deviations from the mean are added, and on the right-hand side the summarized sections per load show the mean and standard deviation. The maximum load of 1930kPa that Drost (2012) applied corresponds to the maximum load of a debris column up to the BT +40 boundary. Depending on the depths of the Base Tertiary and the Top Anhydrite, most caverns would have migrated between 150 and 200m. The unit weight of the debris column corresponds to 10kN/m^3. The load on caverns with a debris column height of around 150m – up to the BT+40 boundary- would therefore be smaller.

In case of cavern 15 the debris column height would be approximately 171m, corresponding to a total load of 1710kPa on the slurry. This is slightly lower than the maximum of 1930kPa and helps to explain why the compaction and consolidation at cavern was slightly less than the mean value at maximum load from Drost (2012) indicates.

The initial porosity of 35% translates to a bulking factor of 1.53 and in chapter 5 it is outlined that this correlates quite well to the value of 1.5 that Berést et al. (2006) reports.

sample 1			
load [kPa]	e [-]	n [-]	dev
0	0,49	0,3289	0,0003
10	0,5	0,3333	0,0000
130	0,24	0,1935	0,0067
550	0,07	0,0654	0,0154
1930	0	0,0000	0,0124

sample 2			
load [kPa]	e [-]	n [-]	dev
0	0,46	0,3151	0,0010
10	0,42	0,2958	0,0017
130	0,33	0,2481	0,0008
550	0,19	0,1597	0,0009
1930	0,07	0,0654	0,0021

sample 3			
load [kPa]	e [-]	n [-]	dev
0	0,56	0,3590	0,0001
10	0,52	0,3421	0,0000
130	0,45	0,3103	0,0012
550	0,32	0,2424	0,0028
1930	0,19	0,1597	0,0023

sample 4			
load [kPa]	e [-]	n [-]	dev
0	0,63	0,3865	0,0015
10	0,6	0,3750	0,0015
130	0,54	0,3506	0,0056
550	0,41	0,2908	0,0102
1930	0,283	0,2206	0,0119

start		
porosity n	[-]	[%]
mu	0,3474	34,74
std dev	0,0010	0,10

after 10 kPa		
porosity n	[-]	[%]
mu	0,3366	33,66
std dev	0,0011	0,11

after 130 kPa		
porosity n	[-]	[%]
mu	0,2757	27,57
std dev	0,0048	0,48

after 550 kPa		
porosity n	[-]	[%]
mu	0,1896	18,96
std dev	0,0098	0,98

after 1930 kPa		
porosity n	[-]	[%]
mu	0,1114	11,14
std dev	0,0096	0,96

Table 7.3 summarized results of the Oedometer tests (after Drost, 2012)

8. Evaluation & Discussion

After the implementation of the migration model it can now be said what effect the identified parameters have. Firstly this can be done by analyzing the tables with the extinction depths. At multiple caverns it became abundantly clear that the lower bulking factor (i.e. 1.11) would have resulted in a far more extensive migration of the caverns. The migration potential would be so extensive that without slurry fill, severe subsidence structures should have formed. For some caverns, where slurry fill did take place, the amount of slurry required to make the cavern safe is unrealistically large. The fill factor of solids volume to initial cavern volume would be more than 100%. Apart from this there are caverns where no slurry fill has taken place, making absence of serious surface subsidence inexplicable in relation to the migration potential. Additionally there is a distinct difference between scenario1 and 2.

Considering the single production phase, 12 out of the 42 caverns would not be safe and for the final production case still 12 out of 35 caverns would not be safe. For scenario 2 the numbers are 38 out of 42 for the single production and 33 out of 35 for the final production. Therefore this phase II bulking factor does only explain the cavern migration behavior if scenario 1 applies. Still this cannot fully be excluded yet as the slurry fill does have impact as well. Yet for some of the caverns that have indeed caused serious surface subsidence bowls, the seismic data and the extent of the subsidence bowls cannot readily be explained by the constant diameter during migration.

With the above stated the role of the slurry fill becomes quite clear as well. The scenario 2 cases do need slurry fill in most of the cases in order to become safe. Coming back on the bulking factor it can said that for cavern 15 - were the amount of slurry is known - the migration behavior cannot be explained with the bulking factor of 1.11. The extinction depths of scenario 1 and 2 are 225.5m and 55.9m respectively. This means that for scenario 1 the cavern would have stopped migrating about 50m deeper than the genuine extinction tells and that for scenario 2 the migration would have progressed an additional 120m.

So it can be shown that the decreasing diameter and larger bulking factor help to explain the observed migration behavior much better. However it should also be noted that alone they do not explain the situation for every cavern. The behavior of the sump material and the original cavern dimensions play a vital role and additionally some caverns cannot be explained without a certain amount of slurry fill. The slurry fill would in those cases enable a safe extinction depth for the cavern migration, which would help to explain why no major surface subsidence has occurred yet. This reversed argumentation is used as the amount of years that have passed by since the caverns have started migrating till present day is in most cases 60 to 80 years, and the known subsidence cases have developed much faster. This leads to the assumption that if the migration potential is extensive enough to cause serious subsidence it should have occurred by now. Therefore the combination of a high migration potential and no observed subsidence at the surface yet, requires an explanation. The most likely explanation is that the migration did not progress to its maximum potential and the slurry fill helps to explain why this did not happen. Additionally in some cases where no slurry fill has occurred the parameters: cavern diameter and the overall compaction and consolidation factor can have a positive result.

A slightly larger diameter – which is plausible considering the 'morning glory' theory and the much higher observed vertical leaching coefficient compared to the horizontal coefficient- and a less severe compaction/consolidation factor, can also help to explain why a cavern did not migrate to its maximum potential. Additionally the deformations of the Near Top Salt reflector in the seismic data (5.6.2 and appendix D4) are generally more extensive than the simulated cavern diameters suggest.

Furthermore the insoluble content can play a role as well. In the migration model the effect of having a greater or smaller insoluble content – which can be found in the sensitivity analysis- is not used extensively. The reason is that the available data regarding the insoluble content is very scarce. The spread is extremely large; in fact the standard deviations, for the insoluble content in vol% corresponding to the individual salt layers, are of the same magnitude of the averages. The result is that the content could be much higher as the standard deviation cannot be subtracted; this would result in a negative value which is not possible. The uncertainty is however so large that the insoluble content can also be greatly overestimated resulting in less reliable conclusions. For now the average values have been implemented – salt A: 2.5vol%, salt B: 6.3vol% and salt C&D: 2.4vol%- and from each a fraction of a percentage is subtracted. The fraction corresponds to 1 divided by the amount of salt layers present at the location of the well; the total will therefore be 1%. This subtracted percent accounts for the part of the insoluble content that does come up; the production plant does separate certain amounts during the purification. The 1% corresponds quite well to the actual volume of slurry that the plant produces (personal communication with M. den Hartogh 2018). The detailed realistic compaction and consolidation behavior in addition to the more detailed data gathering on the insoluble content should be further investigated.

8.1 Discussion about the decreasing diameter

In chapters 5 and 6 it became clear that a decreasing diameter can help to explain the migration behavior of the caverns and additionally it has been observed as well. In summary the following can be observed:

1. Seismic data

   The seismic data distinctly indicate that the deformations at the base of the Tertiary are of a much smaller extent than that of the deformations at the top of the salt. In fact conclusion number 5 (page 350) of the HIRES SESOM final report (1997) is: ''the horizontal extent of CTR and BTR deflections was generally less than the area of the NTS disturbances. Thus it is commonly not over its full initial extent.'' This can be explained by the decreasing migrating diameter and caverns 18-24 and 35-36 indicate an approximate angle of 80° under which the diameter decreases. On the other hand the modelled migration scenario with a constant diameter during the cavern migration cannot explain the observations from the seismic data.

2. Extent of subsidence bowls

   The extent of the observed subsidence bowls at the surface correspond to much smaller diameters at the base of the Tertiary than the initial cavern diameters. Essentially this correlates exactly with the observations with the seismic data. Based on the angle of draw of 45° the width of the subsidence bowl can be traced back to the base of the Tertiary. In the known cases these diameters were all in the order of approximately 50m, while the initial cavern diameters were in

the order of approximately 100m. Reversely the cavern diameters, initially at the start of the migration trajectory, should have caused much larger subsidence bowls if they remained constant during the migration. In 1980 Wassmann already recognized this as he literally states: ''Nevertheless the small area influenced at the surface with a diameter of only 270m could not be explained in relation to the depth of the original cavity at 340m (angle of draw)'' when he analyses the subsidence bowl above cavern 4.

3. Sonar measurements

Both cavern 15 and 167 have been measured multiple times during the migration trajectory in order to monitor the migration. As shown in chapter 5 and 7 the multiple sonar measurements in time during the migration of the cavern, do show that in both cases the extent of the migrating cavity becomes smaller. Even though this only comprises 2 examples it forms yet another case that corresponds to the decreasing diameter and needs an explanation when the diameter remains constant.

In addition to the above stated examples the migration model with the decreasing diameter implemented could explain the observed migration behavior in all cases. Subsequently most of the caverns where virtually no data is available considering the actual migration can readily be explained by this modelled scenario as well. Despite that for some caverns slightly different parameters would help to explain why the cavern did not migrate to its full potential and multiple caverns can be explained by a minimum amount of slurry fill, the model clearly fits the migration behavior. Especially compared to the old model where some very distinct examples cannot be explained and only a few parameters are implemented. Still it should be noted that in the old model the migration potential was based on the much lesser reliable volumes and initial cavern heights. Yet the implementation of the volumes and cavern heights from this research, into the old model, would still not explain the well-known cases.

Literature

In publications (Berést et al., 2016 & Ege, 1979) more examples can be found where the extent of a formed sinkhole corresponds to a decreased diameter during the migration of the cavern. Moreover the angle of break or cave angle (Laubscher, 1990 & Jeremic, 1994) help to explain a decreasing extent of deformation above a cavity. This corresponds exactly to the observed phenomena of the cavern migration of the phase I caverns. According to Laubscher (1990) the angle is between 70 and 80° for unrestrained cases and 80 to 90° for restrained cases if the rock mass is considered as very competent. In other words the best case scenario still has an angle of break that is smaller than 90°. In figure 8.1 the characterization of subsidence induced by mining activity is displayed.

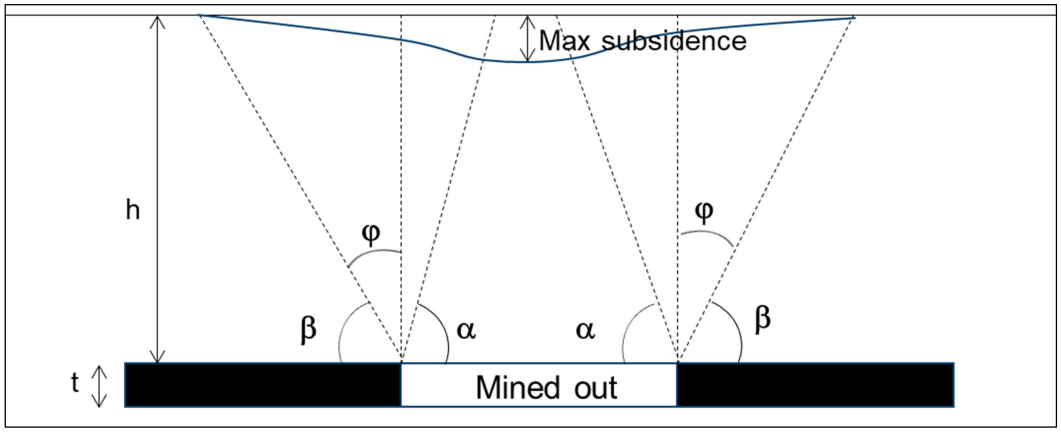

Figure 8.1 characterization of mining induced subsidence (after: Jeremic, 1994)

With:

t: Thickness of mined out section [m]
h: the depth of mined out section below surface [m]
α: Caving angle [°]
φ: The angle of draw [°]
β: Angle of subsidence limit [°]

As example Jeremic (1994) reports that the potash mines in New Mexico have a maximum caving angle of 51.5°. This correlates with the caving angle for rocks with a medium RMR in Laubscher (1990).

The characterization from Jeremic (1994) can be extended into two sections in order the display the caving behavior of the cavern upwards towards the extinction depth firstly. And secondly the subsidence bowl related to the depressed rock mass due to the compaction of the debris column (figure 8.2). An important note is that this example characterizes the subsidence related to the migrated caverns that have extinguished before reaching the base of the Tertiary. If the cavern migration exceeds the base of the Tertiary a sinkhole will form, following the lines that extend directly upwards and more material will be drawn into the void.

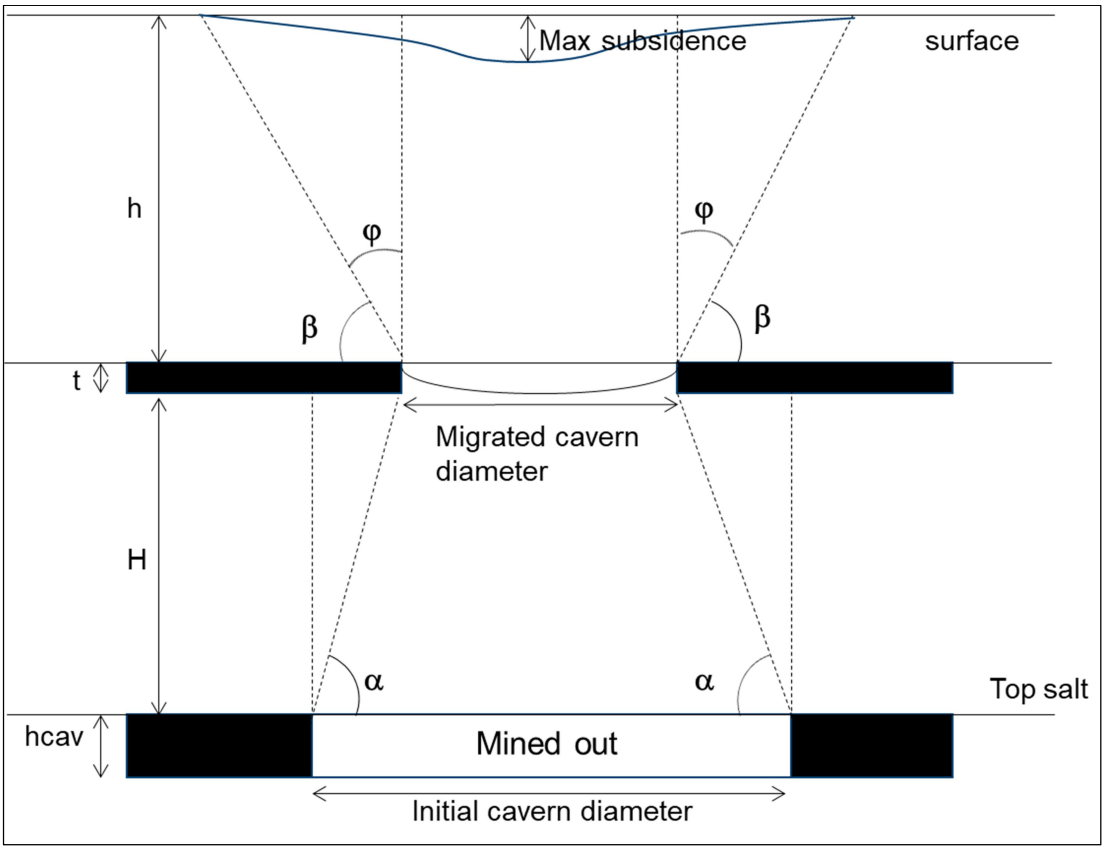

Figure 8.2 characterization of subsidence for the Hengelo Brine field phase I area.

With:

hcav: Initial cavern height [m]
H: Distance between the depth of the top of the salt and extinction depth [m]
t: depressed rock strata above debris chimney due to compaction [m]
h: extinction depth of the migrated cavern [m]
α: Caving angle [°]
φ: The angle of draw [°]
β: Angle of subsidence limit [°]

8.2 sensitivity analysis

A sensitivity analysis has been carried out on the migration model. The model was set at normal representative parameters initially. The initial parameters are the following:

1. Production is: 175000t
2. Diameter is: 100m
3. Phase I bulking factor: 1.53
4. Phase I overall compaction and consolidation factor: 0.77
5. Phase II bulking factor: 1.15
6. Insoluble contents are: salt A: 2.5vol%, salt B: 6.3vol%, salt C: 2.4vol%
7. Stratigraphical thicknesses: salt A: 25m, salt B: 5m, salt C: 20m
8. Caving angle: 80°

After this parameters have been altered individually and the resulting migration potential is displayed in graphs. The first parameter is the cavern diameter, which is the starting diameter for the migration trajectory. The results are displayed in figure 8.3.

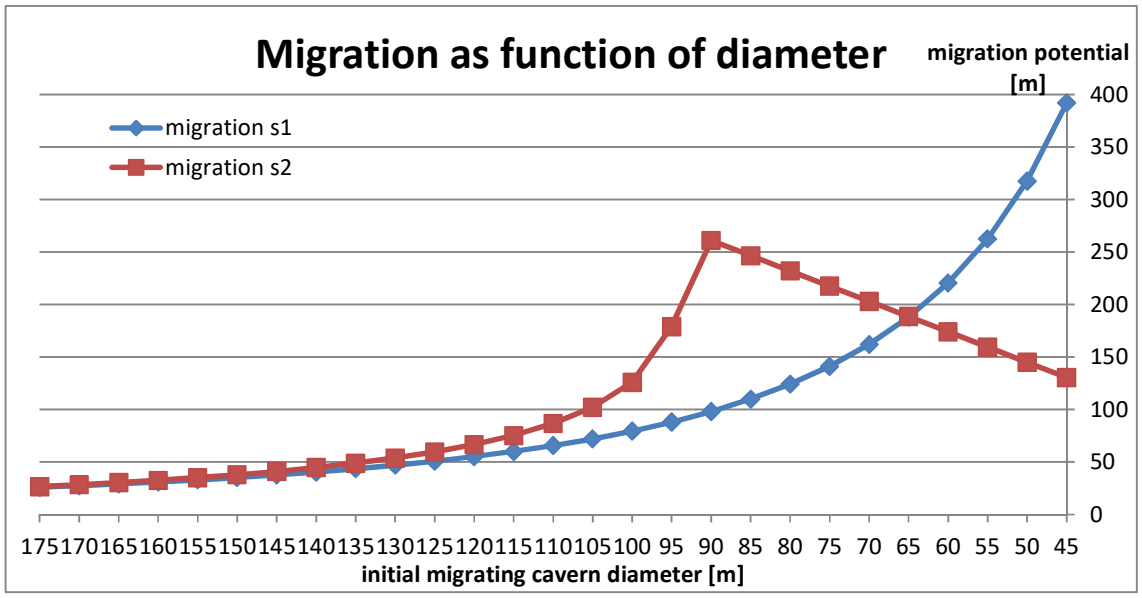

Figure 8.3 Sensitivity graph of the migration potential as function of initial migration diameter

Important in this figure is that the s2 line – scenario 2 = decreasing diameter- follows a distinct sharp linear line from the diameter of 90m and smaller. The reason is that the function has been cut-off by the geometrical limit. For the diameters of 90m and smaller the migration potential of the geometrical limit is less than the migration potential purely bases on the volumetric extinction. Yet since the diameter cannot become negative the migration by definition has to terminate. The other important phenomena are that the larger diameters –down to 125m- show similar migration potential for both scenario's and that for diameter smaller than 65m the s1 migration potential is seriously larger. In the section between 65 and 125m the s2 migration has a larger potential.

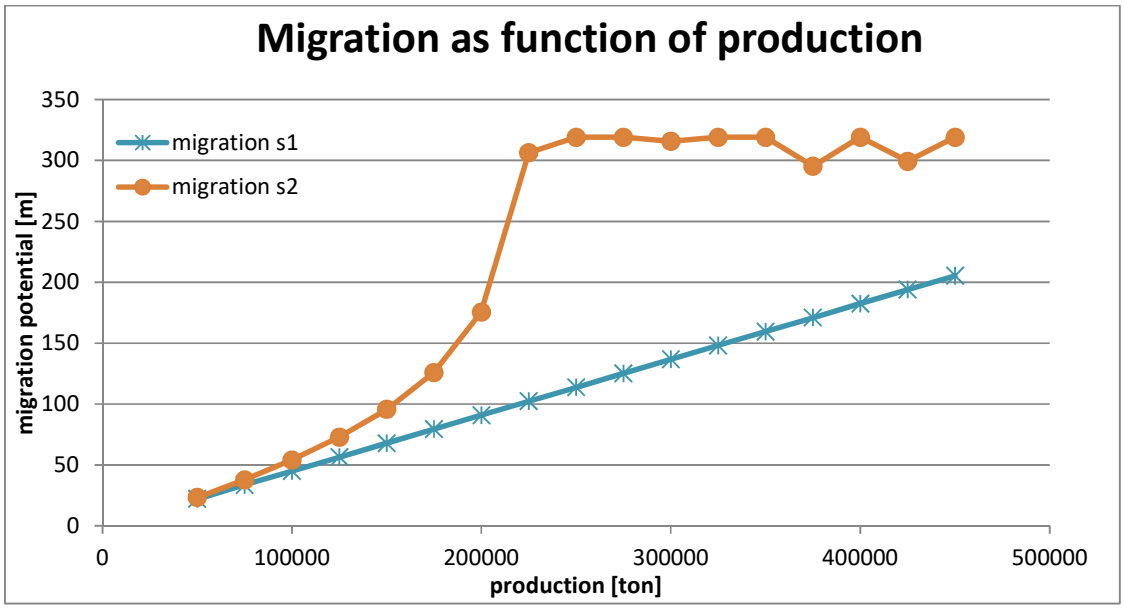

Figure 8.4 sensitivity graph of the migration potential as function of the production

In figure 8.4 the starting diameter is set back at 100m again and now the tonnages are altered. Now right from the start – minimum production set at 50000t- the two scenarios result into different migration potentials. Especially from 200000 to 225000t the scenario 2 line steeply increases. After this the scenario 2 remains quite constant, which can again be attributed to the geometrical extinction. The scenario 1 line displays a perfect linear line, which was expected.

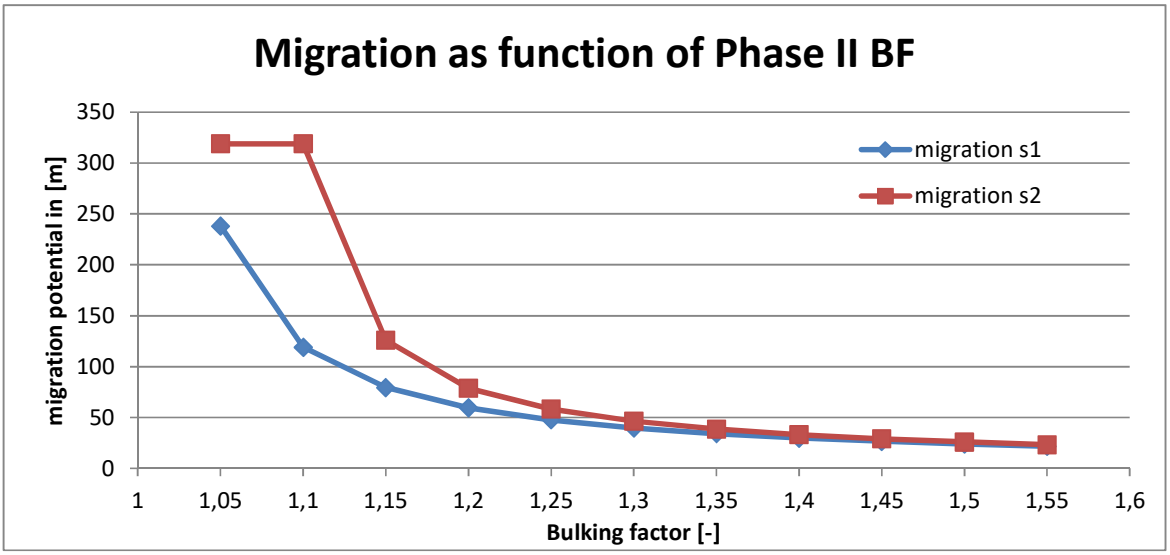

Figure 8.5 sensitivity graph of the migration potential as function of the phase II bulking factor

Figure 8.5 shows the graphs for the migration potential as function of different bulking factors for phase II (again this is by definition the migration trajectory and therefore comprises all overburden). It is clearly visible that for the discussed bulking factors the differences between the scenarios are the largest as well. For bulking factors of 1.3, and larger the difference is negligible. The most important that can be derived from the graph is that for scenario 2 the difference between the bulking factor of 1.1 and 1.15 is quite extreme. Again the scenario 2 line is cut-off for the geometrical limit (in this case exactly for bf 1.1 and smaller). The reason for this is that the decreasing diameter and marginal volume decrease of the migrating cavern (caused by the bulking effect) are so close to each other that they almost balance out. The result is a much steeper increase of migration potential compared to the constant diameter scenario, where the increase is also present for the diminishing bulking factor. Therefore it can be concluded that smaller values for the bulking factor have a much larger effect on scenario 2 and that the smallest factors approach the behavior of an asymptote.

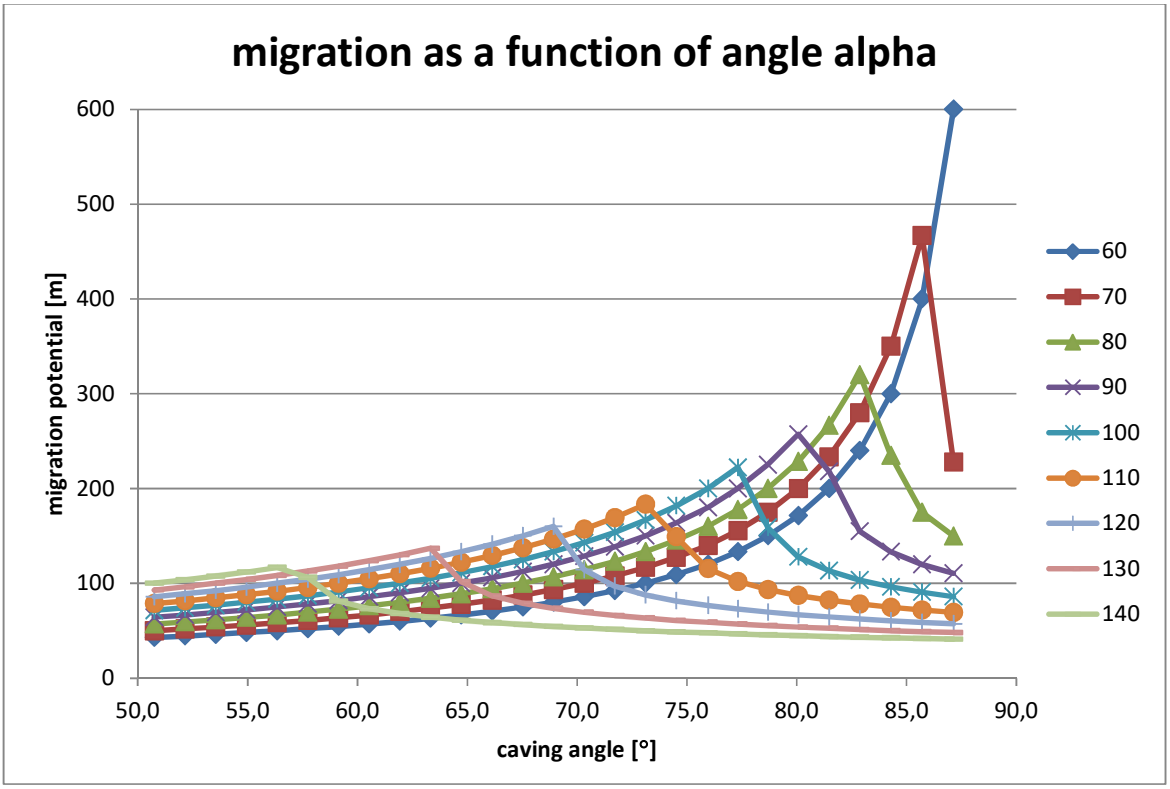

Figure 8.6 sensitivity graph of the migration potential as function of the caving angle

The caving angle that is set at standard at 80° is now changed and in figure 8.6 the migration potential are graphically displayed. As this only applies to scenario 2 the lines are not representing the different scenarios anymore. Instead the starting diameters of 60 to 140 are chosen. From this graph it can clearly be derived what the critical angle is for each starting diameter. For example for the starting diameter of 70m the critical angle is 85.7° which is distinctly visible by the steep turning point of the graph. All caving angles that are smaller show that the migration potential becomes

larger and larger as the angle becomes steeper to the critical point where it reaches its maximum. The angles that exceed this critical value result in much lower migration potentials as the bulking effect now clearly has the upper hand. It can also be derived that the effect of the migrating volume decrease by bulking is very dependent on the initial diameter. As stated in chapter 5 and 6 the migration model defines a new slice of the cone in order to fill up the previous until the extinction of the migration occurs. Due to this the height of a new slice is strongly dependent on the bulking factor –again which causes the volume decrease- and the surface area of the slice. When the diameter is large (for example 140m) the caving angle a relatively small impact on the migration potential as the surface area for the first couple of slices is very large. The resulting heights of the migrating slices now do not have to be very large as the volume is fixed. Oppositely the effect is extreme when the diameter is small.

8.3 Evaluation & discussion on the reconstructed production and simulated caverns.

In the corresponding chapters it became clear that reconstructing the produced tonnages for each cavern was quite challenging, which has a large impact on the cavern dimensions that came out of the simulations. Due to the hydraulic connections between most of the wells the production have in the end been equally divided. As a result the step from single production to the most likely final production is for most of the wells acceptable (however for some this is already quite large). Nevertheless the step towards the maximum possible production is enormous in most cases. From the migration point of view it can be derived that in most cases additional production only has a positive impact assuming that it occurred in the upper parts of the cavern, widening the cavern at its top. This assumption is highly likely as the hydraulic connections between the caverns have almost certainly been made via pinch-outs or channels directly underneath the anhydrite roof. Additionally it can be derived from the modelled migration potentials that the caverns tend to migrate much more in the single production phase compared to the final production scenario. Correlating this with the simulations it became apparent that indeed the additional production in the final phase was always in the higher regions of the cavern. Therefore it can be concluded that if the caverns have contributed to a larger extend in the series phase, the maximum potential migration would be less due to the larger initial migrating cavern diameter, making the bulking factor the dominant factor in determining the maximum migration height.

The simulations are largely affected by the uncertainty of the total production numbers. The possible correlations with existing sonar measurements proved that the simulations themselves do quite accurately approach the right cavern dimensions. The largest identified inconsistency was the position of cavern 49. The sonar indicated that the cavern dimensions and geometry were actually quite similar to the simulation, however the cavern was completely positioned a few meters higher than the simulation. This shows that the leaching progressed upwards even faster than the simulation software accounts for. The main reason is the moment the ‘blanket’ (again this is the moment of failure of an insoluble rock layer; which has proven to be difficult to determine sometimes) is moved up. Additionally the leaching coefficients also have some impact. If the simulated caverns sometimes are positioned lower than the actual cavern, the migration will not be negatively impacted. In fact if the dimensions alone are correct, the migration potential will be exactly the same as the migration model starts at the top of the salt (except for cavern 14 where

only salt A is mined). If the dimensions are in addition to the position not exactly correct the migration potential should even be less. The reason is that in that case the extent of the cavern in the most upper part is most likely larger than the simulated indicate and the earlier outlined phenomena results in less migration height.

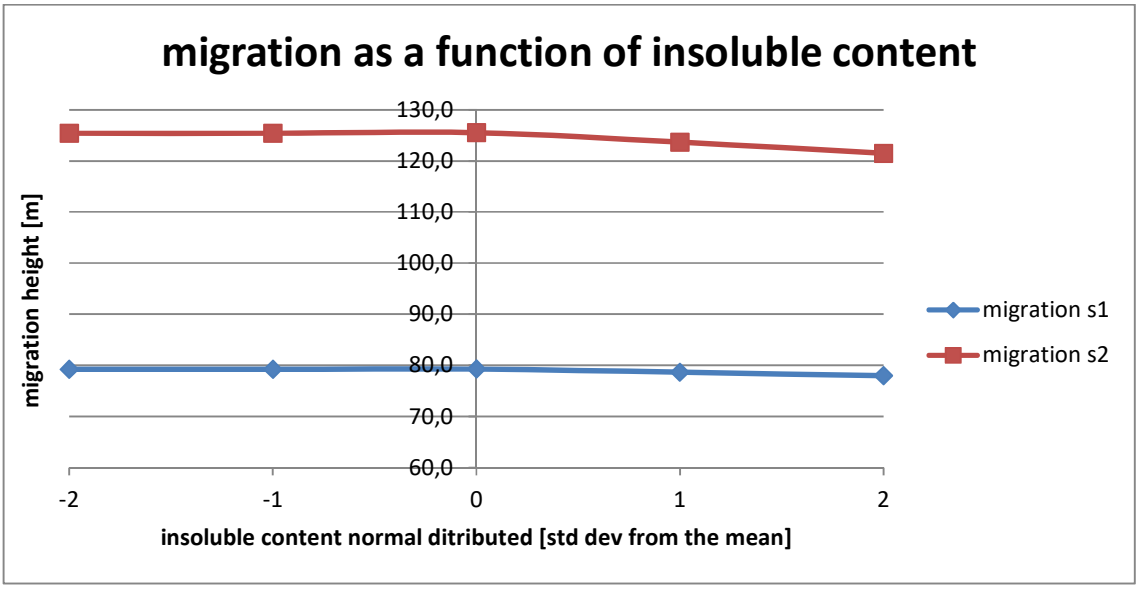

Figure 8.7 sensitivity graph of the migration potential as function of insoluble content inside the rock salt

In figure 8.7 the migration potential for both scenarios is displayed when the insoluble content is different. On the horizontal axis the insoluble content is represented by a normal distribution. The zero value depicts the mean value and the 1 and 2 on the right-hand side depict the percentage of the standard deviation once or twice added to the mean value. On the left-hand side the same applies for the minus 1 and 2. The values for the individual salt layers corresponding to this distribution can be found in table 8.1. The negative values have been set at 0 as a negative value is in reality not possible.

	2* std dev -	std dev -	mean	std dev +	2* std dev+
salt A	-2,3	0,1	2,5	4,9	7,3
salt B	-6,5	-0,1	6,3	12,7	19,1
salt C	-4,19	-1,39	1,41	4,21	7,01

Table 8.1 normal distribution of insoluble contents inside salt, per salt layer in vol%

Even though the spread of the data regarding the insoluble content is large, the effects on the potential migration are small. The main reason is that the mean values are low. Only the higher values of adding the standard deviation, once or twice, result several meters less migration potential. The effects are larger for scenario 2 than they are for scenario 1.

In summary it can be concluded that some uncertainty is present in the simulations and moreover in the reconstructed final production. However the modelled migration would only become less severe if the caverns in reality reach the maximum production scenarios. The simulations can therefore be described as worst case scenarios in reconstructing the caverns.

9. Conclusions

The main objective of this study was to reconstruct the phase I area of the Hengelo brinefield. Chronologically the following components have been reconstructed:

1. The reconstruction of the production of the caverns of the phase 1 area. This was done by an extensive analysis of the old production binders combined with the logbook interpretations. The most challenging part was the allocation of the production when the caverns became interconnected.
2. The reconstruction of the cavern dimensions and geometry. This was performed by 3D leaching simulations with WinUbro. The simulations are based on the production and available data on: insoluble content, leaching coefficients, production methodology, production rate, casing and tubing depths and geology. Before the simulations could be performed the logbooks and geological profile needed to be analyzed and cross-correlated. The resulting interpretations contained the valuable information regarding how long the leaching continued in the particular salt layers and when the interbedded anhydrite layers collapsed enabling the mining of the next salt layer.
3. The reconstruction of the cavern migration behavior based on well-known cases and subsequently the migration potential and most likely status for all the phase I caverns. The migration potential has been modelled with a model that had been fitted to well known cases and implemented to calculate the migration potential for all caverns. The model is based on multiple parameters that had been identified, narrowed down to certain ranges or values and cross-correlated with other relevant data.

Ultimately these three components add up to a comprehensive reconstruction of all the caverns of phase I and the deformations at the surface in the area. Even though a large uncertainty regarding the final production numbers per well is still present, the effect on the migration potential would not be negative. On the contrary from the above stated it can be concluded that a larger total production, especially with more production in the upper part of the cavern, would only result in a smaller potential migration height. Therefore it would actually help to explain why some of the caverns have not migrated to its full potential as the maximum potential should have caused serious subsidence.

The final conclusion with regards to the main objective is that a more accurate model has successfully been constructed. Therefore the reconstruction of the phase I area has been performed in the best possible way and the model can be considered as the best technical solution.

9.1 Answers to the research questions

The five intermediate questions have been answered extensively during the components of this report. In summary the questions and the locations of their answers are:

1. How have the phase 1 salt reserves formed in terms of geology and how are they accessed in terms of drilling technology and production configuration?
   Answer: in chapters 2 and 3.

2. How are the phase 1 salt reserves extracted in the initial setup in terms of inflow / outflow and cavern shape prior to any connection?
   Answer: in chapter 3.
3. How are the phase 1 caverns operated after connections with other caverns have been established in terms of inflow / outflow, return stream processing and final cavern shape?
   Answer: in chapters 3, 4 and 6.
4. How did the vertical position of the caverns develop during and after production in terms of migration in the main Röt Evaporite and through the overburden and surface subsidence?
   Answer: in chapters 5, 6, 7 and 8.
5. What is the current and most likely future state of the caverns in terms of the production and migration relationship and the long term safety assessment?
   Answer: in chapters 6 and 8.

Main research question:

How does the measured amount of cavern migration and subsidence in the phase 1 area of the Hengelo Brine Field relate to the production history and what does this mean for the long term safety of the area?

The cavern migration and subsidence have been measured in a few very distinct cases within the phase I area. In summary: at well 4 a large subsidence bowl is present at the surface, well 7 has been reopened (well 7A) and therefore the extinction depth is known, at well 15 the volume of return stream is known and multiple sonar measurements have been taken during the migration trajectory and finally the extinction depth is known as well, at doublet 18-24 a large subsidence bowl has been reported, between doublets 33-34 and 35-36 a large subsidence bowl is present, and at cavern 37 a sonar measurement has been taken and the extinction depth is known.

From the reconstruction of the production numbers it can be derived that the caverns that have caused subsidence have indeed produced large amounts compared to the others. Nonetheless a clear connection cannot readily be drawn as some other caverns have produced similar amounts and have not induced serious subsidence.

In order to explain this much more detailed research into the parameters affecting the migration was needed. After identifying, determining and implementing all the parameters a complex model came to life. From this model it can be derived that the maximum migration potential would actually be less if the production was large in the upper part of the cavern. This only tells something about the latest stage of the production life (i.e. the production within the series of wells) and has a high inaccuracy for most of the wells. The wells that have produced much can readily be identified in the single cavern production numbers. These numbers are pretty accurate and from this it can be said that indeed the caverns that caused severe subsidence have produced much. The caverns that stand out in case of the single production as they produced a large amount and have not caused any subsidence are: 6, 15, 28 and 38.

For cavern 6, which has a similar production and also cavern geometry compared the cavern 4, it can be concluded that this cavern did not migrate to its full potential due to the slurry fill in this cavern. In chapter 6 it becomes clear that the volume of slurry is not known while distinct hints of slurry

disposal are present. In case of the single production a fill factor of 59% (and 63% for the final) would already make the cavern stop migrating at a safe depth. In case of cavern 4 the fill factor of 58.4% leads to the migration that corresponds to the observed subsidence bowl. Additionally it can be found that although the logbook indicates that slurry has been brought into cavern 4, it also indicates the total time span of the slurry deposition was shorter compared to caverns 2,3,5,6. So in case of caverns 6 and 4 the difference in the cavern migration can be attributed to the slurry fill. In case of cavern 6 the cavern did not migrate to its full potential on behalf of sufficient slurry fill while cavern 4 migrated further on behalf of insufficient slurry fill.

In case of cavern 15 virtually all the important information is present and it can definitely be concluded that the migration extinction occurred much sooner due to the sufficient slurry fill.

In case of cavern 38 the slurry numbers are not known, yet again it can be assumed that sufficient slurry has reduced the migration height sufficiently.

Cavern 28 however is interesting as no slurry fill has been reported here and the cavern did not have any reported hydraulic connections. Therefore the explanation why the cavern did not cause subsidence while the production is large must come from the geometry. Upon analyzing the simulation result it can indeed directly be derived that the cavern height is not that much and that the cavern is actually mainly wide. The reason is that the total salt thickness at this location is only 26.5m. The phenomenon of the fixed volume and large starting diameter for the migration (as described in chapter 8) applies here. The result is the maximum migration potential is not large and that the extinction is at a safe depth.

In summary it can be said that the migration potential of the caverns is largely dominated by the cavern dimensions – which is a result of the production and geology- but is also affected by additional parameters such as the amount and behavior of the return stream. With all of that being said the answer to the question would be: as the migration potential of a cavern is dominated by the residual cavern volume and the cavern geometry the production and salt thickness play a large role in the maximum migration potential. If the production in the single phase has been very extensive and the resulting cavern shape is extensive in height (dependent on salt thickness) the migration potential is severe. In case of a maximum migration potential that is extensive enough to induce serious subsidence, either sufficient slurry fill or a larger cavern diameter in the upper part of the cavern due to the contribution in the series phase can lead to an earlier extinction of the migration.

10. Recommendations

The recommendations that can be distilled from this research could include some very logical recommendations that are not relevant for either field implementations or further research. An example is that the monitoring of the caverns will result in more data and certainty when it comes to predicting the migration potential. As mentioned a lot of improvements have been implemented during the years and recommendations regarding improvements that have already been implemented are not relevant to report here. Instead recommendations that are relevant and recommendations regarding follow up studies will be stated.

10.1 recommendations regarding the production

1. Firstly the most important recommendation is to report everything thoroughly. The production methodology, brine quality, flow rate in the production archive and as much details as possible in the logbooks regarding the repair works during the production life. In case of the phase I area the production methodology has been challenging to retrieve; especially for the series phase. However it should be noted that the logbooks have proven to contain very valuable information. This research proves how valuable the extensive reporting in the logbooks can be.

10.2 recommendations regarding the simulations

2. In contemplation of reconstructing the cavern geometry and residual cavern volume more precisely the insoluble content should be investigated more thoroughly. Especially much more data from analyzed core sections are needed to obtain a robust data set. Furthermore tests with data regarding the porosity, in situ-density and strength are desirable. **this recommendation is relevant to the migration model as well*
3. More data on the leaching coefficients will help to simulate the leaching, and therefore the constructed geometry, more precisely. In addition to the first recommendation the core analysis can be tested on the leaching coefficients as well.
4. Multiple Cavern Completion systems can be addressed by equivalent cylindrical single completion simulations. The result however needs to be converted to the right geometry and it is highly recommended that in order to do so additional correlation material is present. The best available data regarding this correlation can possibly come from a sonar measurement. An improvement however will be the possibility to simulate MCC's directly in WinuBro.

10.3 recommendations regarding the migration model

5. More data on regarding the bulking factor will certainly make the model more robust. The bulking factor that has been reported throughout several documents ranges from 1.07 to 1.3. In the current adopted model it has been set at 1.11 primarily due to conservative predictions it enables. This bulking factor however does not fit the migration behavior that has been observed in the phase I area perfectly. Moreover the density measurement of well 7A is much more reliable. Therefore an important recommendation is to perform more density measurements. First of all the in situ rock masses of the over burden need to be known accurately and secondly more robust data regarding the density of the debris column is important.
6. More extensive research into the mechanisms behind the caving angle is vital. In this thesis it became clear that the caving angle – which results into a decreasing cavern diameter during the migration- helps to explain the migration behavior. Moreover the constant diameter during migration could in several cases not explain the migration behavior and especially not the

extents of the subsidence bowls and the observations in the seismic data. Yet the theory of the constant diameter cannot completely be ruled out yet as there are also caverns were it does fit the observed so far. It could be that the diameter may not decrease sometimes and does very rapidly decrease in other cases. Therefore the mechanism behind this and the possibilities in reality need to be further investigated.

7. The subsidence potential is not precisely indicated. This should be further investigated. From this research the most likely maximum subsidence potential in terms of phase I, II or III are stated. While most caverns are in the phase II category the maximum potential within that phase is not determined accurately yet.
8. Regarding the second recommendation concerning the production it can be further investigated under which conditions the insoluble rock layers and roof anhydrite does collapse. Or more importantly under which span it remains stable. In previous reports this is briefly mentioned theoretically; however no real tests have been carried yet. The assumption that the insoluble rock layers and anhydrite roof layer will definitely fail when exposed is justifiable. The caverns tend to have small diameters in the lower regions ('morning glory') and yet the insoluble rock layers do fail. Even though the simulations show that the leaching probably continued sufficiently underneath an insoluble rock layer, to expose it enough enabling the failure conditions, it does not explain the failure in all cases. Especially the caverns where the diameter is small for the whole cavern it is remarkable that both the insoluble rock layers and the roof anhydrite still fail. This could possibly be explained by the geological faults. Bekendam (2014) reports that there is a statistical relation between the densely faulted areas and the cavern migration.
9. More research into the connections between the caverns can provide valuable new insights for the cavern geometry and therefore the migration potential. As outlined in chapter 3 the previous adopted cavern reconstructions of phase I caverns are extremely large in the upper region. This was based on the 'morning glory' theory and moreover helped to explain that the caverns had established connections. In this research it became quite clear that the caverns did generally not have those geometries and moreover not those extensive upper diameters. Additionally the hydraulic connections generally cannot be identified during the sonar measurements that also indicate that the cavern is much smaller than the connection demands. Based on this and the assumption that thin 'pinch-outs' or channels are most likely the cause of the connections the assumption emerged that this can be neglected in the migration model. Again the main reason is that these thin pinch-outs and/or channels will have small volumes and therefore will be filled up very quickly during the migration. The real migrating dimension can therefore be approached by the corresponding simulation results that do not indicate the connections. Yet it also became clear in this report that a wider diameter at the top of the cavern would actually result in a smaller migration potential. In light of finding the maximum migration potential it could be said that the caverns would only become safer. However in light of more accurately reconstructing the caverns dimensions and real extinction depth it can provide valuable information.
10. The downward deflecting roof layer (roof bed separation) phenomena should be further investigated. It would help to explain why the migration did not progress to its full potential for some of the caverns. However it should be further investigated what the limitations are.
11. The characteristics and mechanisms behind the hydraulic connections should intensively be investigated. As the simulations, in this thesis, and often the sonar measurements do not

illustrate caverns that are large enough to explain the hydraulic connections, the described small pathways are very likely. Specialized research from a fluid flow and geology perspective could provide vital information to the migration model. From the phase 1 area none of the single caverns have caused serious subsidence; the 6 subsidence bowls can all be related to connected caverns. The role of this can become clear if the mechanisms behind the pathways is investigated.

12. Reference list

AkzoNobel (2018): Hengelo Uitloogtechniek. Internal document. p.4-30

Bekendam, R. F. & Van Vliet, A.J.J. (1995): Delineation of solution cavities and subsidence evaluation by means of high resolution 3D seismic reflection in Twenthe, East Netherlands. In: Barends FBJ, Brouwer FJJ, Schroder FH (eds) Land subsidence. Proc Fifth Int Symp Land Subsidence, The Hague. Balkema, Rotterdam, pp. 247–258

Bekendam, R. F. (1996): Subsidence over solution cavities in salt in the Twente-Rijn concession area, Memoirs Centre of Engineering geology in the Netherlands. Internal report. AkzoNobel.

Bekendam, R. F. (2002): Induction of subsidence by brine removal. Internal report. AkzoNobel.

Bekendam, R. F. (2009): Subsidence over upwards migrated salt solution cavities in the Hengelo brine field - a follow up study- Revised version. File number S2001_R2009. Internal report. AkzoNobel.

Bekendam, R.F. (2014): Invloed van tektonische breuken en cavernedimensies op cavernemigratie voor het twenthe-rijn zoutwinningsgebied. Internal report AkzoNobel. p. 17-19.

Bekendam, R. F.; Urai, J. L. (2006): Pillar deformation-induced subsidence. File number S00605. Internal report. AkzoNobel.

Berést, P. (Ed.) (2006): In situ mechanical tests in salt caverns. With assistance of M. Karimi-Jafari, B. Brouard, B. Bazargan. SMRI Spring 2006 Technical Meeting. Brussels.

Den Hartogh, A. M.; Leusink, H.; van Steveninck, R.; Schicht, T.; Pinkse, T. (Eds.) (2017): Preventing subsidence caused by cavern migration in Hengelo and Enschede, The Netherlands. A risk based approach to monitoring and backfilling potentially instable caverns in the Hengelo brinfield, The Netherlands. SMRI fall conference 2017. Munster, 25-26 September.

Doornenbal, J. C.& Stevenson, A.G. (2010): Petroleum Geological Atlas of the Southern Permian Basin Area: TNO. p. 2.

Drost, G.I.A. (2012): Geomechanical properties of a backfill material suitable for stabilising salt caverns in Twente. MSc thesis, TUDelft. p.15-17, 74-96.

Durie, R. W. & Jessen, F. W. (1964a): Mechanism of the dissolution of salt in the formation of underground salt cavities. In *Society of Petroleum Engineers Journal* 4 (2). pp.183-199.

Durie, R. W. & Jessen, F. W. (1964b): The influence of surface features in the salt dissolution process. In *Society of Petroleum Engineers Journal* 4 (3), pp. 275–281.

Ege, J. R. (1979): Surface subsidence and collapse in relation to the extraction of salt and other soluble evaporites. open-file report 79-1666, US department of the interior geological survey.

Geluk, G. (2005): Stratigraphy and tectonics of Permo-Triassic basins in the Netherlands and surrounding areas. Doctoral dissertation, University of Utrecht. p. 49-136.

Geowulf (2010): Detailed geology of the Hengelo solution mining area part 1. File number GL10.101. Report. AkzoNobel.

Harteveld, R.B. (1961): Exploratie en exploitatie van zoutlagen in Oost-Nederland. In Geologie van Twente, Zutphen. pp. 113-114

HIRES SESOM (1995). confidential internal report.

Jeremic, M. L. (1994): Rock mechanics in salt mining. Balkema, Rotterdam.

Karimi-Jafari, M.; Berést, P.; Brouard, B. (Eds.) (2006): Some aspects of the transient behavior of salt caverns. SMRI fall conference 2006. Rapid City, South Dakota, 1-4 October.

Knappett, J.A. & Craig, R.F. (2012): Craig's soil mechanics. 8th ed., London: Spon Press. p.18-21.

Kombrink, H.; Doornenbal, J. C.; Duin, E.J.T.; Den Dulk, M.; van Gessel, S. F.; Veen, T. H. ten; Witmans, N. (2012): New insights into the geological structure of the Netherlands. Results of a detailed mapping project. In *Netherlands Journal of Geosiences - Geologie en Mijnbouw* 91 (4), pp. 419–446.

Kurlansky, M. (2003): Salt: A world history. Penguin putnam inc.p.3-20

Laubscher, D.H. (1990): A geomechanics classification system for the rating of rock mass in mine desgin. In *J.S. Afr. Inst. Min. Metall.* 90 (10), pp. 257–273.

Lintker, S. (1994): Data processing report of the areal reflection seismic survey Hengelo 3 in the Hires project. Hires report BRE2. CT'92.0316 94.A.06.

Meekes, J.A.C. & Van Vliet, L.J.J. (Ed.) (1994): High resolution seismic methods applied to subsidence evaluation and solution mine design. SMRI fall meeting. Hannover. SMRI.

Ofoegbu, G. I. (2006): Bulking factor of rock for underground openings. prepared for U.S. Nuclear regulatory commission. Report. With assistance of R.S. Read, F. Ferrante.

Oranjewoud (2005): Reconstructie holruimten oude boorterrein. File number 15575-64872-80. Internal report. AkzoNobel.

Roordink, R. (1993): De Koninklijke Nederlandse Zoutindustrie: Zout uit de bodem van Twente. De geschiedenis van KNZ 1918-1840. In *OHB* 108. pp 97-129.

Schonfeldt, H. A. von (1972): A computer program to simulate development dissolution cavities in massive salt formations. File number 72-0008-SMRI. A report to SMRI. p.7.

Schootstra, J. (2015): Development of a reserve reconciliation tool for the Hengelo Brine Field. MSc thesis, TUDelft. p.97-103.

Time Magazine (1982): A brief history of salt. Available online at http://time.com/3957460/a-brief-history-of-salt/.

van Berkel, J.D.D. (2014): An insight in the mass balance and reserve reconsiliation of salt caverns in the Hengelo brine field. MSc thesis, TUDelft. p.36,37.

van Lange, M.W.P. (1994): The devolopment, geology and lithology of the central-northern part of the Hengelo rock salt solution mining area and its geotechnical characterisation. MSc thesis, TUDelft. p. 5, 99-101, 190

van Wees, J.; Stephenson, D.R.A.; Ziegler, P. A.; Bayer, U.; McCann, T.; Dadlez, R. et al. (2000): On the origin of the Southern Permian Basin, central Europe. In *Marine and Petroleum geology* 17, pp. 43–49.

Visser, W.A., Zonneveld, J. I. S. & Loon, A. J. van 1987. The mining of rock salt. In: Seventy-five years of geology and mining in the Netherlands (1912 - 1987), edited by W. A. Visser, J. I. S. Zonneveld & A. J. van Loon. Royal Geological and Mining Society of the Netherlands (K.N.G.M.G.), Den Haag.

Wassmann, T. H. (1980a): Mining subsidence in Twente, East Netherlands. In *Geologie & Mijnbouw* 59 (3), pp. 225–231.

Wassmann, T. H. (1980b): Oplosmijnbouw. De winning van steenzout via boorgaten in Nederland.

Westendorp, J. (1969a): Onderzoek van boorkernen, afkomstig uit boring 151. File number 69.604. Internal document. AkzoNobel.

Westendorp, J. (1969b): Onderzoek van boorkernen, afkomstig uit boring 182. File number 69.819. Internal document. AkzoNobel.

Westendorp, J. (1969c): Onderzoek van boorkernen, afkomstig van boring 171. Internal document. AkzoNobel.

Ziegler, P.A., (1990): Geological atlas of western and central Europe. Second edition Shell Internat. Petrol. Mij, 239 pp., 56 annexes.

Personal communications

den Hartogh, A.M.
Technology Manager Brinefields
Mining Development & Compliance
AkzoNobel Specialty Chemicals

13. Bibliography

Berést, P. (Ed.) (2016): Craters above salt caverns. SMRI spring 2016 Technical Conference. Galveston, Texas, 25-26 April.

Bokhove, G. (2013): Testen pekelkwaliteit op basis van zoutkernen. File number O/BPB/2013015-1. Report. AkzoNobel.

Brouwer, M.S. & Wassmann, T.H. (1987): Chapter 13: The mining of rock salt. Seventy-five years of geology and mining. Royal Geological and Mining Society.

Esterhuizen, G. & Karacan, C. (Ed.) (2007): A methodology for determining gob permeability distributions and its applications to reservoir modeling of coal longwalls. 2007 SME Annual

meeting and exhibit. Denver, 25-26 February. Colorado: preprint (Society for Mining, Metallurgy and Exploration).

Geowulf (2011): Detailed geology of the Hengelo solution mining area part 2. File number GL11.901. Report. AkzoNobel.

Geowulf (2012): Geological framework TWR Area Compilation report. File number GL08.502. Report. AkzoNobel.

Harsveldt, H.M. (1978): Salt resources in the Netherlands as surveyed mainly by AKZO. Fifth International Symposium on Salt, Northern Ohio Geological Society, pp 65-81.

Meekes, J.A.C. & van Wijn, S.P. (1994): Acquisition, processing and interpretation of 2D high resolution seismic and checkshot data Hengelo. HIRES Report Bre2.CT92.0316-93.A.06.

Terzaghi, R. D. (Ed.) (1970): Brine field subsidence at Windsor, Ontario. Symposium on salt 3rd edition. Cleveland, 1969. 2 volumes: Northern Ohio Geological Survey.

Tsesarsky, M. (2006): Mechanical response of a jointed rock beam. Numerical study of centrifuge models. In *Int. J. Numer. Anal. Meth. Geomech.* 10.1002 (568).

van Eysinga, F.W.B. (1970): Stratigraphic terminology and nomenclature. A guide for editors and authors. In *Earth-science reviews* 6, pp. 267–288.

Wassmann, T. H. (1983): Cavity utilization in the Netherlands. Sixth international symposium on salt vol II.

Internal documentation from AkzoNobel:

- All the logbooks of the wells of the phase I area (both scrap and neat versions)
- Production binders
- BoorPuttenBeheer
- AkzoNobel digital archive
- AkzoNobel hardcopy archive
- AkzoNobel overview of well connections (overzicht boringen.pdf)
- AkzoNobel overview of wells (gegevens cavernes.pdf)

External documentation that is publicly available:

All information regarding the 53 wells on www.nlog.nl

Appendix A

salt thickness in meters					
well	salt A	salt B	salt C	salt D	Total
1	30	1,08	3,07	16,6	50,75
2	24,3	4,75	16,45	0	45,5
3	36,35	4,28	0,31	17,2	58,14
4	29,56	3,75	14,5	0	47,81
5	22,15	4,75	17,25	0	44,15
6	23,1	4,14	18,85	0	46,09
7	16,2	5	17,15	0	38,35
8	16,79	15,94	0	0	32,73
9	11,4	3,55	18,45	0	33,4
10	16,17	3,45	17,75	0	37,37
11	18,9	4,05	18,03	0	40,98
12	22,58	1,25	3,48	17,7	45,01
13	13,94	3,2	17,32	0	34,46
14	23	5,1	18,42	0	46,52
15	29,2	4,7	18,97	0	52,87
16	14,4	1,47	6,14	0	22,01
17	16,35	3,01	12,25	0	31,61
18	5,32	14,24	4,43	17,42	41,41
19	20,09	0,7	18,52	0	39,31
20	25,9	2,85	18,85	0	47,6
21	13,39	2,39	32,96	0	48,74
22	15,95	4,53	16,65	0	37,13
23	14,75	6,35	20,75	0	41,85
24	26,8	16,51	0	0	43,31
25	11,7	15,1	4,9	19,81	51,51
26	10	14,6	4,9	19,5	49
27	10,75	18,15	0	0	28,9
28	12,9	13,6	0	0	26,5
29	3,38	11,05	31,54	0	45,97
30	33,5	5,1	20,1	0	58,7
31	31,68	1,2	3,4	19,9	56,18
32	12,93	16,2	0	0	29,13
33	17,1	18,35	0	0	35,45
34	16,2	21,55	0	0	37,75
35	14,2	20,26	4,8	18,82	58,08
36	16,98	22,03	3,4	19,48	61,89
37	26,5	4,68	17,58	0	48,76
38	18,44	4,48	17,52	0	40,44
39	15,07	2,4	14,3	0	31,77
40	11,93	1,08	16,84	0	29,85
41	10,95	2,7	17,25	0	30,9
42	30,34	4,45	20,47	2,6	57,86
43	30,35	4	21,25	3,3	58,9
44	7,4	3,86	18,1	0	29,36
45	7,25	4	17,7	0	28,95
46	12,8	3,8	18,5	0	35,1
47	34,55	5,15	13,05	0	52,75

48	11,2	16,5	3,7	15,86	47,26
49	19,85	3,43	17,75	0	41,03
50	8,7	4,25	17,35	0	30,3

Appendix A1. Table with salt thickness per well

Appendix B

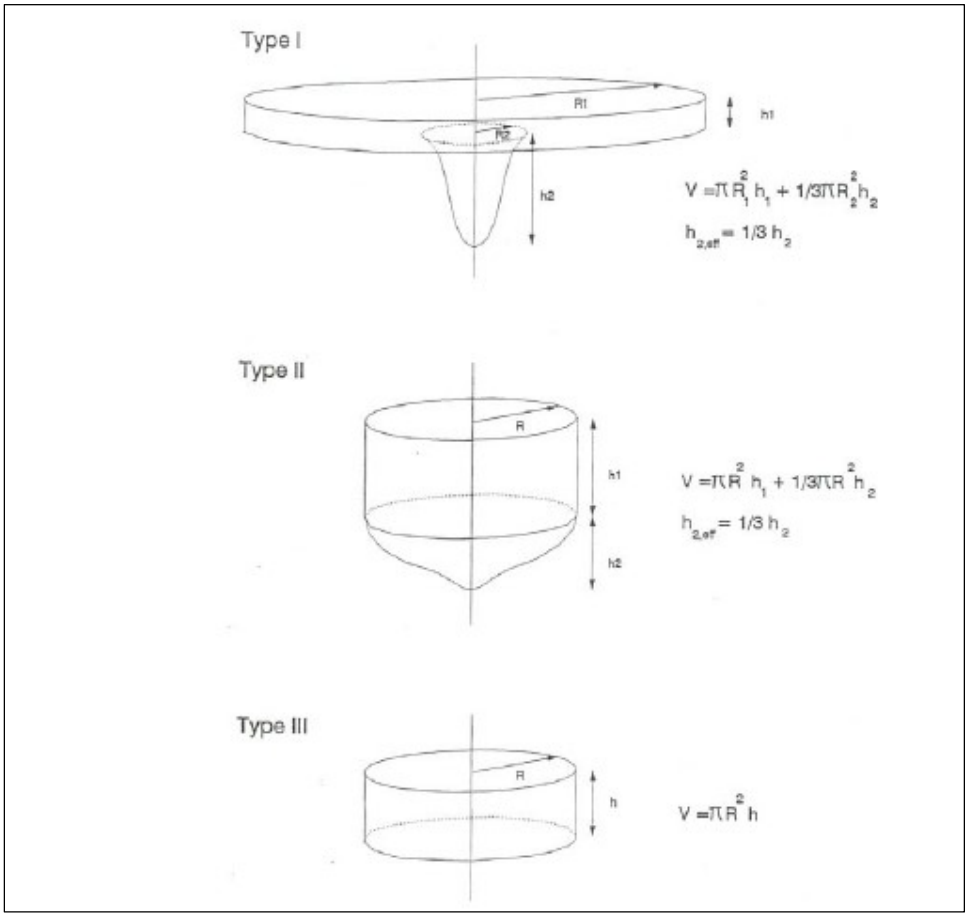

Appendix B1. Overview of the three possible shapes identified by Oranjewoud (source: Oranjewoud, 2005)

well	total	1935	1936	1936 &1937	1938	1939	1940	1941	1942	1943	1944	1945	1946	1947	1948	1949	1950	1951	1952	1953	1954	1955	1956	1957	1958	1959	1960	1961	1962	1963	1964	1965	1966	1967	average annual production during production life
1	101119	0	0	13009	11230	5620	4005	6640	30685	13500	1940	945	8725	4820																					7778
2	241240	0	0	13045	29770	37175	39410	16920	7725	20160	21880	12560	31300	11295																					18557
3	63895	0	0	9600	4295	4825	10380	13295	16945	1700	720	395	1335	405																					4915
4	344445	0	0	9185	17465	35830	28340	16140	25550	45260	22705	13130	36810	41650	28550	14550	8810	470																	20261
5	110555	0	0	23485	25420	10130	8795	6015	5660	590	365	225	970	6125	3980	6830	8280	3415	270																6142
6	322890	0	0	7515	15240	28590	32230	19080	32870	34460	21340	13795	36930	36420	24410	7660	6860	3090	1970	215	215														16145
7	129360					4870	7695	15750	2545	5180	9040	10375	3775	2400	2140	5650	26310	28080	5550																9240
8	174080					1940	11700	7300	75	21795	10280	565	26745	18695	17340	14120	32000	11525																		13391
9	120500						8320	6570	6230	8645	15210	3130	6150	11680	12620	21760	7450	12735																		10042
10	249885						5160	11820	19770	5405	355	3325	23100	32650	34930	33710	38180	39790	1690																	19222
11	172120							8410	20985	4485	535	105	7535	5175	1240	3430	1320	865	32245	52220	33570															12294
12	123750													1610	26050	43680	44360	8050																	24750
13	221840														26510	37120	47640	60390	50180																	44368
14	176610														12760	30200	19480	30775	31020	34510	8455	610				6525	2275									17661
15	413919														6120	28010	31320	36410	35935	44925	34190	25719	32250	37520	60440	34875	5780	425								29566
16	79370															8510	17790	14325	3400	15290	19205	850														11339
17	195700															9250	7480	28380	26085	30225	48620	45660														27957
18-24	215690															9745	5870	38040	46090	37565	52520	25860														30812,85714
19-20	342640															2090	54680	60810	18720	52290	57510	58760	37780													42830
21	72570																4410	5450	4480	9080	34660	14490														12095
22	119320																1920	14240	30435	17055	36800	18870														19887
23	220515																660	27910	29400	27420	14980	35285	42160	40180	2520											24502
25-26	266380																	7340	17005	34775	47480	43420	49975	64655	1730											33297,5
27	187602																		8095	5885	15055	32850	35510	35540	31160	6740	5140	3775	7852	0						15634
28	272118																		1390	15295	30655	30960	37460	30805	29395	29675	24655	25605	16223							24738
29	233865																			11965		32815	33385	43700	52835	36335	22830								33409
30-31	321720																			9585	29080	30955	27535	52000	78610	74095	19860								40215
32	154420																				27550	36900	32265	11195	9810	36265	435								22060
33-34	410783																				13750	44030	57395	19600	36920	59810	49400	37455	39615	44211	8597				37343,90909
35-36	457750																				295	29850	58600	117370	77045	78335	65095	31160								57218,75
37	125892																					4740	6485	5174	32185	37365	6965	1630	2549	3127	2848	10185	8237	4402	9684
38	278467																					2970	23055	28085	32040	31445	16975	27900	23327	28872	34705	28936	157		23206
39	150556																						7935	5030	25360	23515	30600	23780	23904	10432						18820
40-41	300933																						16990	51005	43815	42045	41015	45970	43332	16761						37616,625
42-43	292555																						1355	49005	85500	73150	28675	36830	18040							41793,57143
44	45315																							17850	9550	9040	6085	2790								9063
45	127535																							10940	59560	45615	7830	3590								25507
46	191432																							3560	16995	14780	22185	35965	37465	37986	20540	1956				21270
47	82854																								21485	25060	7625	4580	4451	4943	5524	5435	3751			9206
48	148548																								13000	8305	4915	3720	2862	18993	31767	39515	25471			16505
49	138886																								9010	10960	25115	34375	33221	13324	6293	6588				17361
50	188362																								2910	13820	27345	31625	30926	29044	27676	25016				23545

Appendix B2. Table with annual production during single production phase

boring	1935	1936	1937	1938	1939	1940	1941	1942	1943	1944	1945	1946	1947	1948	1949	1950	1951	1952	1953	1954	1955	1956	1957	1958	1959	1960	1961	1962	1963	1964	1965	1966	1967	1968	1969	1970	1971	1972	1973	1974	1975	1976	1977	1978	1979	1980
1	287	365	335	362	365	365	351	349	365	365	365	365	365	365	365	365	365	365	365	365	365	365	365	365	365	201	0	0	0	0	0	0	0	0	0	0	0	0	0	0	0	0	0	0	0	0
2	207	365	364	365	365	365	365	364	334	365	365	365	365	365	365	365	365	365	365	365	365	365	365	365	365	234	0	0	0	0	0	0	0	0	0	0	0	0	0	0	0	0	0	0	0	0
3	127	365	365	351	365	365	348	365	365	365	365	365	358	365	365	365	364	365	365	365	365	365	365	365	365	214	0	0	0	0	0	0	0	0	0	0	0	0	0	0	0	0	0	0	0	0
4	365	365	365	365	361	347	342	358	365	365	365	365	364	262	340	365	365	365	365	365	365	365	365	365	365	302	304	0	0	0	0	0	0	0	0	0	0	0	0	0	0	0	0	0	0	0
5	0	365	365	344	365	365	365	365	365	365	365	365	358	365	365	365	365	365	364	365	365	365	365	365	365	0	0	0	0	0	0	0	0	0	0	0	0	0	0	0	0	0	0	0	0	0
6	0	365	365	365	365	365	365	352	365	365	365	365	316	365	365	365	365	365	365	365	365	365	365	365	365	129	0	0	0	0	0	0	0	0	0	0	0	0	0	0	0	0	0	0	0	0
7	0	0	0	0	139	365	364	365	365	365	365	365	365	365	352	362	365	365	365	365	365	365	365	365	365	244	0	0	0	0	0	0	0	0	0	0	0	0	0	0	0	0	0	0	0	0
8	0	0	0	0	59	352	365	365	365	365	365	365	361	365	326	364	365	365	365	365	365	365	365	365	365	241	0	0	0	0	0	0	0	0	0	0	0	0	0	0	0	0	0	0	0	0
9	0	0	0	0	0	188	365	365	365	365	365	365	365	365	332	323	365	365	365	365	365	365	365	365	355	244	0	0	0	0	0	0	0	0	0	0	0	0	0	0	0	0	0	0	0	0
10	0	0	0	0	89	356	356	365	357	365	365	365	365	365	365	365	365	365	365	365	365	365	365	365	365	244	0	0	0	0	0	0	0	0	0	0	0	0	0	0	0	0	0	0	0	0
11	0	0	0	0	0	234	364	342	365	365	365	365	365	365	365	365	365	356	365	365	365	365	365	365	365	0	0	0	0	0	0	0	0	0	0	0	0	0	0	0	0	0	0	0	0	0
12	0	0	0	0	0	0	0	0	0	0	0	0	34	365	361	353	351	365	365	365	365	365	365	365	365	172	0	0	0	0	0	0	0	0	0	0	0	0	0	0	0	0	0	0	0	0
13	0	0	0	0	0	0	0	0	0	0	0	0	0	262	337	365	365	364	365	365	364	365	365	365	365	311	0	0	0	0	0	0	0	0	0	0	0	0	0	0	0	0	0	0	0	0
14	0	0	0	0	0	0	0	0	0	0	0	0	0	178	365	365	365	365	365	365	288	0	0	0	91	145	0	0	0	0	0	0	0	0	0	0	0	0	0	0	0	0	0	0	0	0
15	0	0	0	0	0	0	0	0	0	0	0	0	0	78	365	365	365	365	365	365	365	365	365	345	365	279	0	0	0	0	0	0	0	0	0	0	0	0	0	0	0	0	0	0	0	0
16	0	0	0	0	0	0	0	0	0	0	0	0	0	0	330	365	365	365	365	365	365	365	365	257	365	69	0	0	0	0	0	0	0	0	0	0	0	0	0	0	0	0	0	0	0	0
17	0	0	0	0	0	0	0	0	0	0	0	0	0	0	226	306	365	365	347	364	352	365	365	257	365	0	0	0	0	0	0	0	0	0	0	0	0	0	0	0	0	0	0	0	0	0
18-24	0	0	0	0	0	0	0	0	0	0	0	0	0	0	248	246	330,5	365	364	364	365	365	365	73	315	261,5	0	0	0	0	0	0	0	0	0	0	0	0	0	0	0	0	0	0	0	0
19-20	0	0	0	0	0	0	0	0	0	0	0	0	0	0	35	338,5	301	365	341	361	365	365	365	311	365	104	0	0	0	0	0	0	0	0	0	0	0	0	0	0	0	0	0	0	0	0
21	0	0	0	0	0	0	0	0	0	0	0	0	0	0	0	203	365	365	365	365	365	365	365	257	365	116	0	0	0	0	0	0	0	0	0	0	0	0	0	0	0	0	0	0	0	0
22	0	0	0	0	0	0	0	0	0	0	0	0	0	0	0	91	365	355	364	365	365	365	365	257	90	0	0	0	0	0	0	0	0	0	0	0	0	0	0	0	0	0	0	0	0	0
23	0	0	0	0	0	0	0	0	0	0	0	0	0	0	0	24	300	365	364	365	365	365	322	350	119	0	0	0	0	0	0	0	0	0	0	0	0	0	0	0	0	0	0	0	0	0
25-26	0	0	0	0	0	0	0	0	0	0	0	0	0	0	0	0	192	300	349	365	365	359	365	352	119	0	0	0	0	0	0	0	0	0	0	0	0	0	0	0	0	0	0	0	0	0
27	0	0	0	0	0	0	0	0	0	0	0	0	0	0	0	0	0	130	342	365	365	365	365	365	365	334	365	365	365	365	365	332	0	0	0	0	0	0	0	0	0	0	0	0	0	0
28	0	0	0	0	0	0	0	0	0	0	0	0	0	0	0	0	0	36	364	365	365	365	363	365	365	343	355	327	363	365	365	322	0	0	0	0	0	0	0	0	0	0	0	0	0	0
29	0	0	0	0	0	0	0	0	0	0	0	0	0	0	0	0	0	0	172	0	344	365	365	365	365	323	365	365	365	365	365	63	0	0	0	0	0	0	0	0	0	0	0	0	0	0
30-31	0	0	0	0	0	0	0	0	0	0	0	0	0	0	0	0	0	0	217	365	365	345,5	365	365	365	330	328	365	365	365	365	61	0	0	0	0	0	0	0	0	0	0	0	0	0	0
32	0	0	0	0	0	0	0	0	0	0	0	0	0	0	0	0	0	0	0	306	365	307	319	321	338	337	322	365	350	0	0	0	0	0	0	0	0	0	0	0	0	0	0	0	0	0
33-34	0	0	0	0	0	0	0	0	0	0	0	0	0	0	0	0	0	0	0	305	363	365	365	312	343	365	349	348	365	348	0	0	0	0	0	0	0	0	0	0	0	0	0	0	0	0
35-36	0	0	0	0	0	0	0	0	0	0	0	0	0	0	0	0	0	11	310	363	365	359	362	365	365	365	365	365	365	365	365	112	0	0	0	0	0	0	0	0	0	0	0	0	0	0
37	0	0	0	0	0	0	0	0	0	0	0	0	0	0	0	0	0	0	138	365	365	341	356	365	365	345	365	365	365	365	230	365	365	365	365	337	365	365	365	365	365	365	136	0	0	0
38	0	0	0	0	0	0	0	0	0	0	0	0	0	0	0	0	0	0	78	365	365	365	359	282	365	365	365	365	365	356	365	365	365	365	365	365	365	365	365	365	83	0	0	0	0	0
39	0	0	0	0	0	0	0	0	0	0	0	0	0	0	0	0	0	0	0	327	355	363	227	365	344	365	365	289	365	361	365	365	365	365	365	365	365	365	304	365	365	365	136	0	0	0
40-41	0	0	0	0	0	0	0	0	0	0	0	0	0	0	0	0	0	0	0	350	362	365	343	337	365	365	365	365	365	361	365	365	365	365	365	365	365	365	365	333	365	355	136	0	0	0
42-43	0	0	0	0	0	0	0	0	0	0	0	0	0	0	0	0	0	0	0	23	325,5	354	341	317	365	365	362	365	365	365	365	0	0	0	0	0	0	0	0	0	0	0	0	0	0	0
44	0	0	0	0	0	0	0	0	0	0	0	0	0	0	0	0	0	0	0	0	202	365	365	348	365	365	365	365	356	356	351	6	0	0	0	0	0	0	0	0	0	0	0	0	0	0
45	0	0	0	0	0	0	0	0	0	0	0	0	0	0	0	0	0	0	0	0	112	365	309	365	365	365	365	365	365	365	365	359	365	365	365	365	365	151	0	0	0	0	0	0	0	0
46	0	0	0	0	0	0	0	0	0	0	0	0	0	0	0	0	0	0	0	0	51	365	365	365	365	365	365	365	348	361	365	365	365	365	365	365	181	0	0	0	0	0	0	0	0	0
47	0	0	0	0	0	0	0	0	0	0	0	0	0	0	0	0	0	0	0	0	0	324	328	334	365	365	365	365	365	365	365	365	365	365	365	365	365	365	365	365	365	365	365	365	365	365
48	0	0	0	0	0	0	0	0	0	0	0	0	0	0	0	0	0	0	0	0	0	248	365	343	362	365	365	360	365	365	365	336	365	356	365	365	357	365	365	365	365	365	365	365	365	365
49	0	0	0	0	0	0	0	0	0	0	0	0	0	0	0	0	0	0	0	0	0	152	365	365	365	351	365	365	332	354	365	351	360	365	363	361	365	365	365	365	365	365	365	365	365	365
50	0	0	0	0	0	0	0	0	0	0	0	0	0	0	0	0	0	0	0	0	0	77	365	364	362	361	294	365	357	359	365	365	365	365	365	353	365	365	314	0	0	0	0	0	0	0

Appendix B3. Table with overview of productive days per well

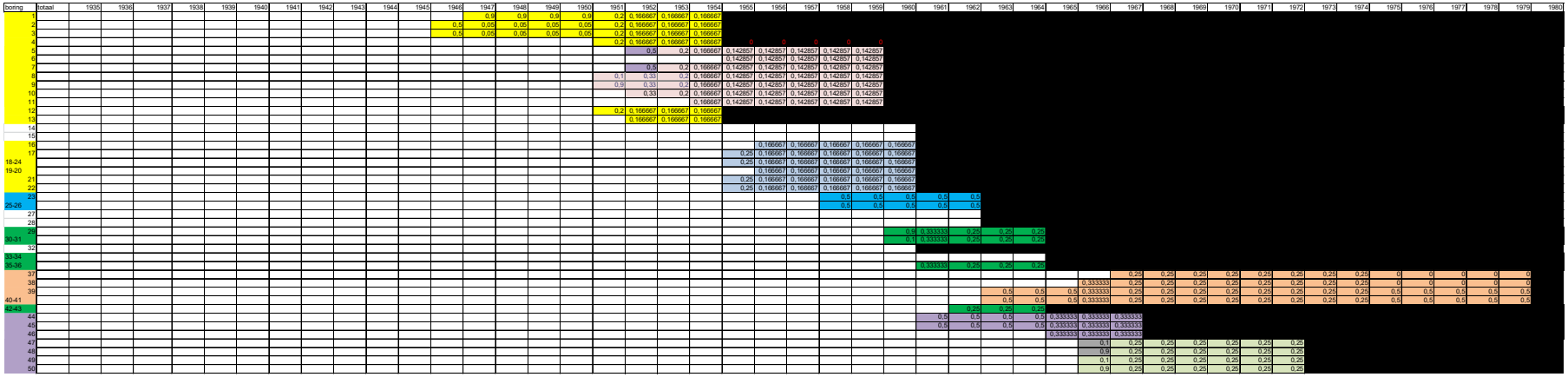

Appendix B4. Table with overview of production allocation in series phase

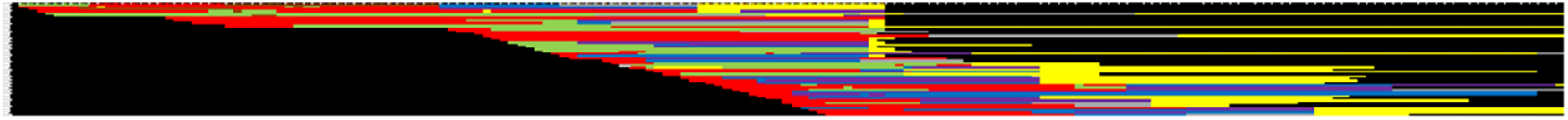

Appendix B5. Table with overview of production setup; red=TOP, green=BOT, blue=only water in, grey=only slurry in, yellow=out of production, brown=slurry in and brine out and purple=only brine out.

Appendix C

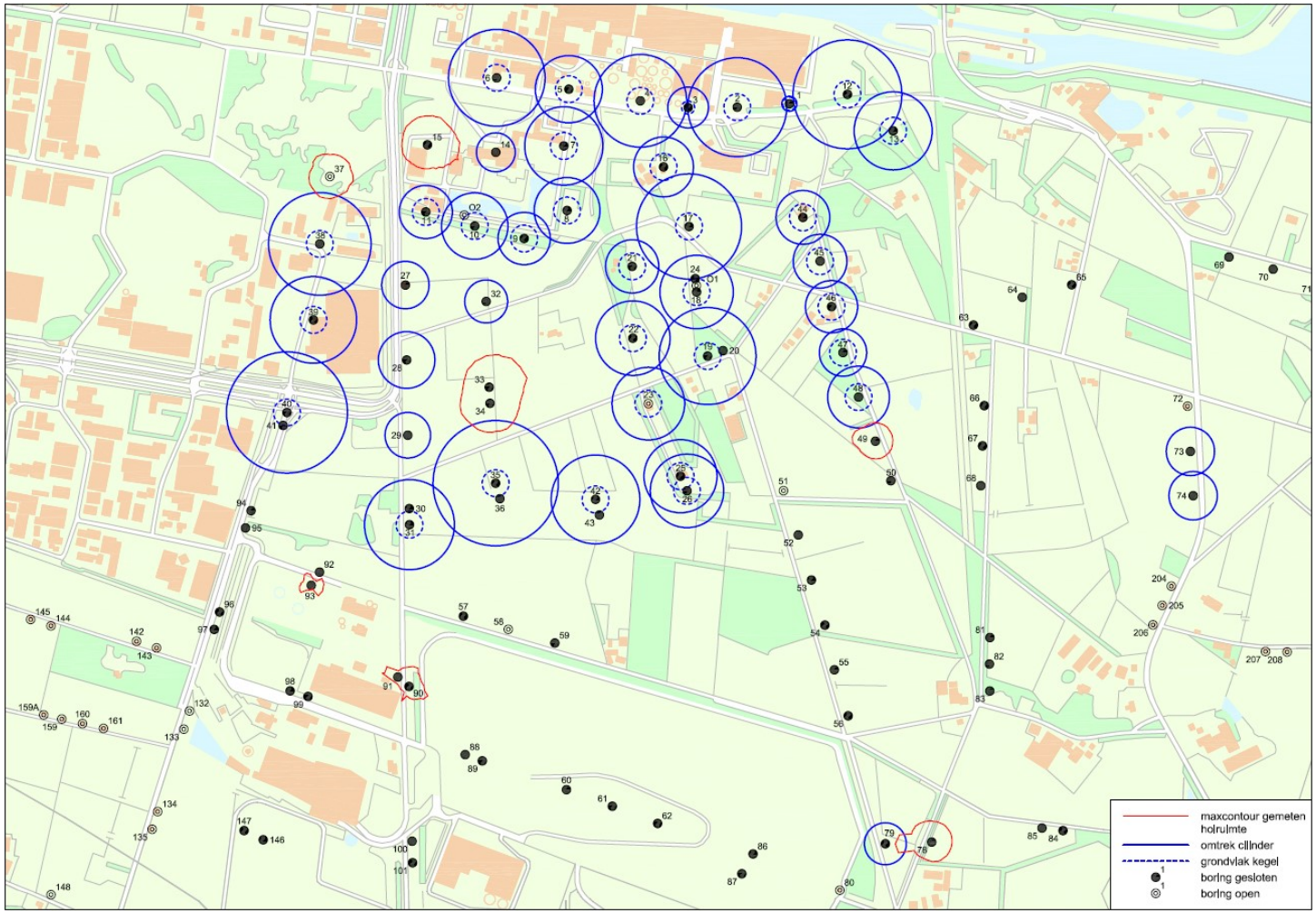

Appendix C1. Map with reconstructed caverns by Oranjewoud (source: Oranjewoud, 2005)

Appendix C2

Production volumes, mass balance and recovery of rock salt calculations and factors (after: Van Lange, 1994).

With Halite, dissolved in pure H_2O, strongly saturated brine with the concentration of 0.26kg/kg – at atmospheric pressure and room temperature- the following relations apply:

1. In situ density of Halite is: 2165 kg/m
2. The water density is: 998 kg/m^3
3. The density of saturated brine is: 1201 kg/m^3
4. 1m^3 of saturated brine contains 312kg of NaCl and 889kg of H_2O
5. In order to dissolve 1m^3 (e.g. 2165kg) of rock salt the following amount of water is required: 2165 * 889 / 312 = 6.169m^3 water.
6. For every leached out m^3 of void, 1 m^3 of brine will remain in-situ and 5.939m^3 brine is liberated for extraction.
7. The brine to water yield is: 5.939 / 6.181 = 0.96
8. For every m^3 of void 312kg of salt remains in-situ, from the original 2156 kg that has been leached out for 1m^3 of cavity this means: 312 / 2165 * 100 = 14.4%
9. Therefore the recovery of the leached rock salt is: 85.6%
10. Water recovery is: ((5.939*0.889)/(6.181*0.998))*100% = 85.6%

Appendix C3

analyzed core sections with corresponding depths and insoluble content [wt%] for well 151											
salt C			salt A						salt B		
from	to	wt % ins	from	to	wt % ins	from	to	wt % ins	from	to	wt % ins
448,17	448,5	3,9	472,12	472,5	0,7	486	486,51	0,7	465,5	466,15	2,6
448,5	449	8,9	472,5	473,01	1,7	486,51	487	1,4	466,15	466,65	1,7
449	449,5	8,2	473,01	473,99	0,4	487	487,52	0,7	466,65	467,15	4,2
449,5	450	3,7	473,5	473,99	10,5	487,52	488,01	7,3	467,15	467,65	2,9
450	450,5	2,3	473,99	474,5	6,5	488,01	488,5	2	467,65	468,15	4
450,5	451	1,1	474,5	475	4,3	488,5	489	9,4	468,15	468,65	1,8
451	451,5	2,2	475	475,5	6,8	489	489,5	6,1	468,65	469,15	12,1
451,5	452	2,2	475,5	476	3,2	489,5	490	4,2	469,15	469,65	34
452	452,5	1,1	476	476,5	4,9	490	492,27	3,1	469,65	470,15	38,2
452,5	453	1,6	476,5	477	5,4	492,27	492,48	6,7	470,15	470,65	15
453	453,5	2	477	477,48	6,8	492,48	493	2,1	470,65	471,15	28,4
453,5	454	2,9	477,48	478	10,1	493	493,5	5			
454	454,5	8,2	478	478,5	11,5	493,5	494	3,4			
454,5	455	2,3	478,5	479	7,8	494	494,5	9,9			
455	455,5	3,6	479	479,5	4,2	494,5	495	8,8			
455,5	455,98	4,4	479,5	480	4,2	495	495,5	6,1			
455,98	456,5	2,7	480	480,5	7,1	495,5	496	4,9			
456,5	457	2,1	480,5	481	6,8	496	496,65	10,3			
457	457,5	3,2	481	481,19	7,9						
457,5	458	2,1	482,17	482,5	1,3						
458	458,5	3	482,5	483	4						
458,5	458,96	2,4	483	483,5	11,1						
458,96	459,5	1,3	483,5	484	1,8						
459,5	460	1,9	484	484,49	36,1						
460	460,5	1,5	484,49	485	18,7						
460,5	461	2,9	485	485,5	4,5						
461	461,5	3,1	485,5	486	1,2						
461,5	461,98	13,4									
461,98	462,48	19,8									
462,48	463	29,1									
463	463,48	8,9									
463,48	464,04	11									
464,04	464,54	0,2									

Appendix C3, Table 1. Table with insoluble content in wt% per core section for well 151 (digitalized after: Westendorp, 1969a; tabel 1)

additionally tested (dissolving in HCl) core sections from well 151					
salt C			salt A		
from	to	wt % ins	from	to	wt % ins
454	454,5	8,2	475	475,5	6,8
458	458,5	3	478	478,5	11,5
462,48	463	29,1	481	481,19	7,9
			484	484,49	36,1
			488,5	489	9,4
			496	496,65	10,3

Appendix C3, Table 2. Table with additionally tested insoluble content in wt% per core section for well 151 (digitalized after: Westendorp, 1969a; tabel 2). These samples have been dissolved in HCl after the first test with water.

analyzed core sections with corresponding depths and insoluble content [wt%] for well 181								
salt A								
from	to	wt % ins	from	to	wt % ins	from	to	wt % ins
500,23	500,73	22,4	512,31	512,81	1,3	524,3	524,8	7,5
500,73	501,23	1,5	512,81	513,3	1,8	524,8	525,3	9,3
501,23	501,73	2	513,3	513,81	0,9	525,3	525,8	1,1
501,73	502,23	13,8	513,81	514,3	5,1	525,8	526,3	6,8
502,23	502,73	7	514,3	514,8	0,8	526,3	526,8	7,3
502,73	503,23	10,3	514,8	515,3	2,9	526,8	527,3	5,4
503,23	503,73	6,6	515,3	515,8	5,7	527,3	527,8	9,2
503,73	504,23	5,5	515,8	516,3	8,8	527,8	528,3	3,7
504,23	504,73	8,9	516,3	516,8	0,2	528,3	528,8	2,2
504,73	505,23	7,8	516,8	517,3	3	528,8	529,28	0,5
505,23	505,73	5,7	517,3	517,8	1,6	529,28	529,8	1,2
505,73	506,23	6,1	517,8	518,3	3,4	529,8	530,3	1,3
506,23	506,73	7,7	518,3	518,8	1,6	530,3	530,8	0,6
506,73	507,23	5,2	518,8	519,3	0,7	530,8	531,3	0,3
507,23	507,73	9,6	519,3	519,8	35,1	531,3	531,8	0,7
507,73	508,23	21,4	519,8	520,3	6	531,8	532,3	0,6
508,23	508,81	9,1	520,3	520,8	2,5	532,3	532,8	0,4
508,81	509,31	7,2	520,8	521,3	8,4	532,8	533,3	0,8
509,31	509,82	7	521,3	521,8	7,4	533,3	533,8	0,4
509,82	510,31	8,6	521,8	522,3	12,6	533,8	534,29	11,2
510,31	510,81	6,5	522,3	522,8	5,2	534,29	534,8	3,2
510,81	511,31	6	522,8	523,3	3,9	534,8	535,3	1,2
511,31	511,81	26,2	523,3	523,8	3,5	535,3	535,8	2,3
511,81	512,31	0,5	523,8	524,3	4,7	535,8	536,35	5,6

Appendix C3, Table 3. Table with insoluble content in wt% per core section for well 181 (digitalized after: Westendorp, 1969b; tabel 1)

analyzed core sections with corresponding depths and insoluble content [wt%] for well 171								
salt A								
from	to	wt % ins	from	to	wt % ins	from	to	wt % ins
494,44	494,94	2,3	503,24	503,74	1,1	511,31	511,81	6
494,94	495,43	2	503,74	504,24	1,1	511,81	512,31	4,3
495,43	495,94	0,6	504,24	504,74	2,3	512,31	512,83	10,5
495,94	496,44	9,2	504,74	505,24	3	512,83	513,35	4,4
496,44	496,94	7,5	505,24	505,75	5,1	513,35	513,85	2,6
496,94	497,44	1,6	505,75	506,32	0,6	513,85	514,35	3,2
497,44	497,94	7,7	506,32	506,82	0,3	514,35	514,85	0,6
497,94	498,44	2,9	506,82	507,32	14,1	514,85	515,35	0,5
498,44	498,94	1,1	507,32	507,82	8,7	515,35	515,85	1
498,94	499,44	1,3	507,82	508,32	10,4	515,85	516,35	0,5
499,44	499,94	0,9	508,32	508,82	6,9	516,35	516,9	0,7
499,94	500,44	1,5	508,82	508,84	2,5	516,9	517,46	0,5
500,44	500,93	0,4	508,84	509,34	1,3	517,46	517,96	12,8
500,93	501,42	3,3	509,34	509,84	2,6	517,96	518,46	1,5
501,42	501,76	1,6	509,84	510,34	2,5	518,46	519,17	0,6
501,76	502,26	1,4	510,34	510,81	9			
502,26	503,24	12	510,81	511,31	10,7			

Appendix C3, Table 4. Table with insoluble content in wt% per core section for well 171 (digitalized after: Westendorp, 1969c; tabel 1)

analyzed core sections with leaching coefficients and insoluble content for well 534					
	vertical leaching	horizontal leaching	insoluble content	color	insoluble content
sample	[mm/hr]	[mm/hr]	[wt%]	[-]	[vol%]
1	29,5	9,3	6,08	brown	2,49
2	20,2	8,5	9,96	grey	4,86
3	11,5	9,8	6,17	grey	3,01
4	18,2	8,3	17,53	grey	8,55
5	17,8	7,6	0,93	grey	0,45
6	13,2	8,1	6,77	brown	2,77
7	22,5	9,6	7,31	grey	3,56
8	21,4	8,65	1,77	grey	0,86
9	18,8	8,5	0,80	grey	0,39
10	17	8,5	3,50	grey	1,71

Appendix C3, Table 5. Table with leaching coefficients and insoluble content per cored section (only salt A) for well 534 (directly after an internal file from AkzoNobel)

analyzed core sections with leaching coefficients and insoluble content for well Beckum 2					
	vertical leaching	horizontal leaching	insoluble content	color	insoluble content
sample	[mm/hr]	[mm/hr]	[wt%]	[-]	[vol%]
1	13,6	13,28	7,87	grey	3
2	15,7	12,88	1	grey/brown	0,4

Appendix C3, Table 5. Table with leaching coefficients and insoluble content per cored section (only salt A) for well 534 (directly after an internal file from AkzoNobel)

Appendix D

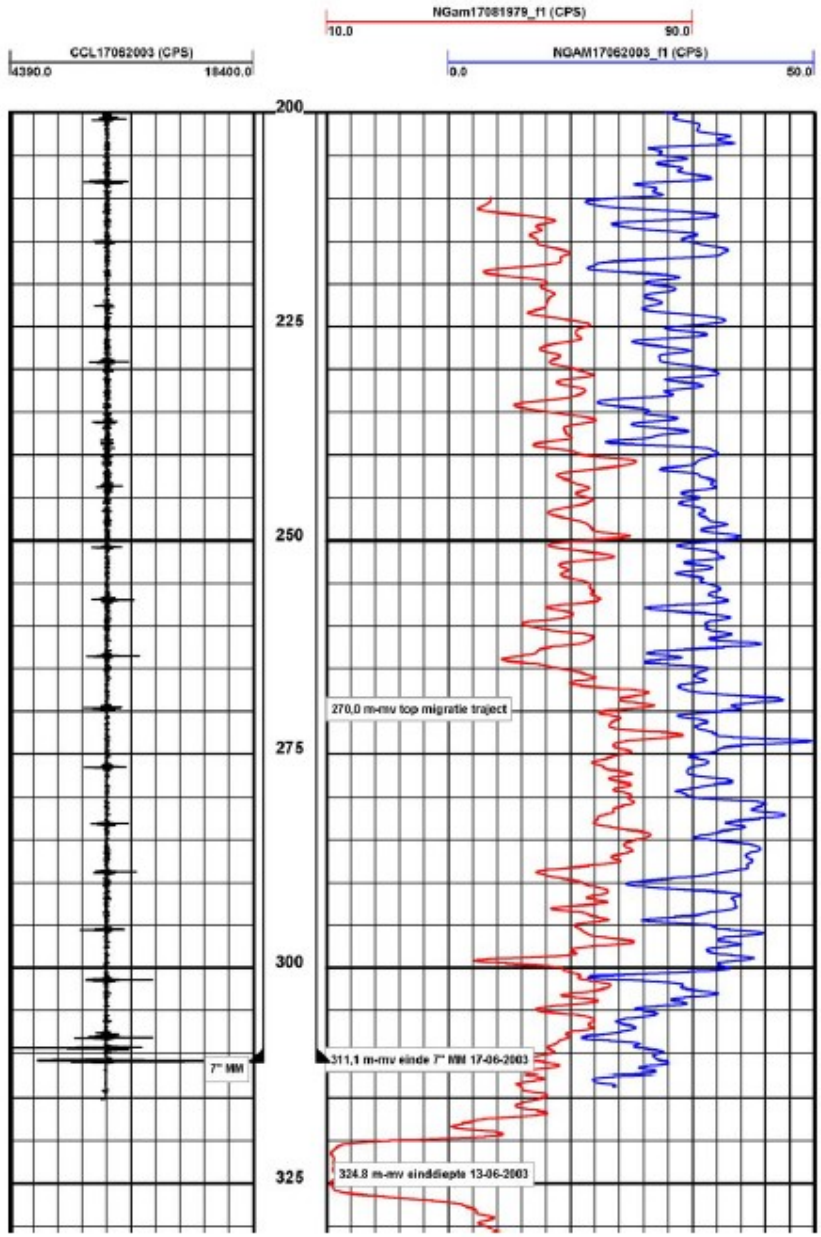

Appendix D1. Gamma Ray logs of well 37 from 1979 and 2003 (source: eindrapport put reparatie boring 37)

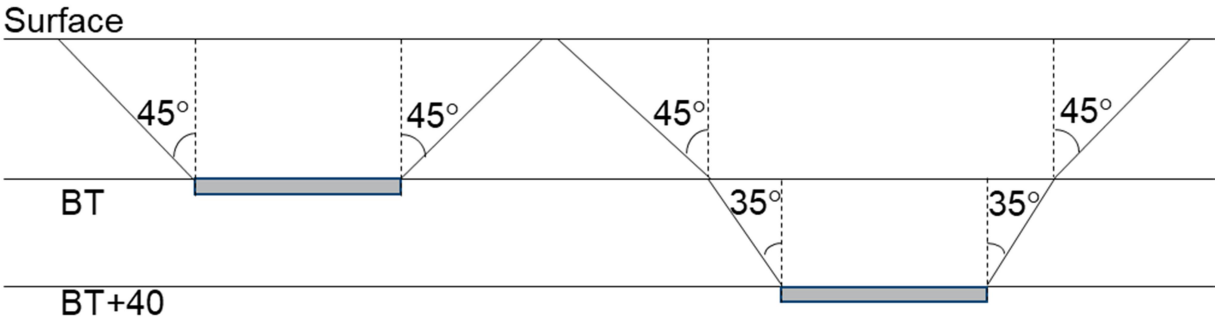

Appendix D2. Illustration of subsidence bowl extends in relation to the angle of draw and depth.

Source type	125g seismogelite
Source depth	Approx. 6m
Source interval	20m
Sample rate	0.5ms
Record length	2048 samples (1024ms)
Number of channels	64
Spread type	4 lines of 16 channels each
Receiver type	Sensor 10Hz
Receiver array	6 geophones on a 16m base
Receiver interval	20m
Shooting type	Swatch shooting, traversal shooting
Longest offset	260m
Low cut filter	20Hz
High cut filter	Ati alias 750Hz
Recording instrument	Summit V1.0 and V1.1
Format	SEG-Y

Appendix D3. List of field parameters belonging to the seismic survey, after Lintker (1994)

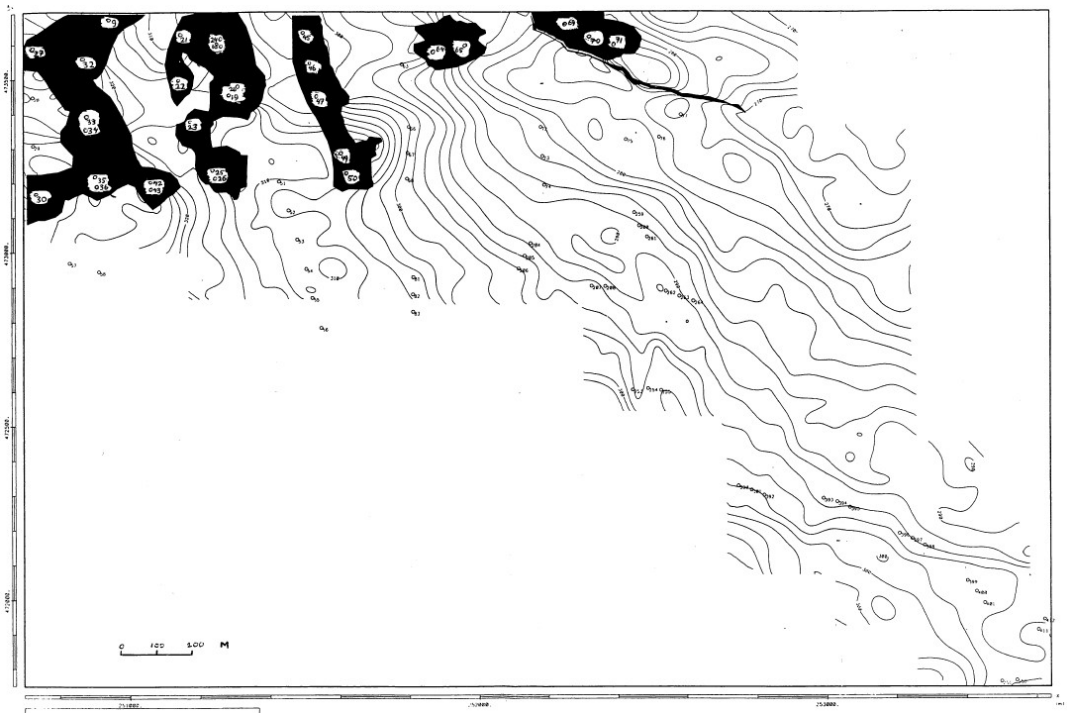

Appendix D4. Contour map of the deformations at the NTS reflector (source: Bekendam, 1996)

Appendix E

well	migration has commenced?	amount of migration into anhydrite roof [m]	Roof depth at time of abandonment [m-MV]	depth of the top of the salt [m-MV]	Most recent roof depth indication		
					year	roof depth [m-MV]	comment
1	Yes	34	281,8	315,8	1960	282	indication
2	Yes	40,3	279	319,3	1951	279	indication
3	Yes	34,95	288,3	323,25	1960	288	indication
4	Yes	28	302	330	present day	BT	max. mig.
5	Yes	30,26	303,14	333,4	1985	281	measured
6	Yes	31,73	304,87	336,6	1953	305	indication
7	Yes	30,6	308	338,6	2017	289	measured
8	Yes	33,8	313	346,8	1959	313	indication
9	Yes	26,57	323,43	350	1960	325	indication
10	Yes	26,53	328,27	354,8	1967	289	indication
11	Yes	26,76	330,12	356,88	1967	305	indication
12	Yes	29,5	278	307,5	1951	278	indication
13	Yes	27,73	281,55	309,28	1952	282	indication
14	FALSE	-34,27	372,5	338,23	1960	369	indication
15	Yes	3,5	342,35	345,85	1996	176	measured
16	Yes	4,67	330,63	335,3	1960	331	indication
17	Yes	28,03	309,42	337,45	1960	309	indication
18	Yes	14,2	322,8	337	present day	BT	max. mig.
19	Yes	20,13	327,85	347,98	1959	317	indication
20	Yes	34,13	311,67	345,8	1960	312	indication
21	FALSE	-1,2	329	327,8	1958	329	indication
22	Yes	31,37	322,13	353,5	1960	319	indication
23	Yes	24,37	332,58	356,95	1996	289	indication
24	Yes	48,3	287,5	335,8	present day	BT	max. mig.
25	Yes	17,96	336,38	354,34	1958	338	indication
26	Yes	32,7	321,2	353,9	1962	321	indication
27	Yes	164,73	211	375,73	1961	211	indication
28	Yes	18,83	364,27	383,1	1962	364	indication
29	Yes	2,6	372,65	375,25	1961	372	indication
30	Yes	5,9	378,1	384	1960	378	indication
31	Yes	235,6	150	385,6	1978	150	indication
32	Yes	31,06	340,24	371,3	1961	340	indication
33	Yes	10,78	364,07	374,85	present day	BT	max. mig.
34	Yes	71,95	300	371,95	present day	BT	max. mig.
35	Yes	72,28	300	372,28	present day	BT	max. mig.
36	Yes	66	307,5	373,5	present day	BT	max. mig.
37	Yes	40,42	319,8	360,22	2003	270	measured
38	Yes	87,65	280	367,65	1966	280	indication
39	Yes	66,2	317,2	383,4	1986	317	indication
40	Yes	31,42	366,28	397,7	1978	366	indication
41	Yes	30,4	367,9	398,3	1978	368	indication
42	FALSE	-0,4	362,9	362,5	1960	363	indication
43	Yes	58,2	305	363,2	1959	364	indication
44	Yes	51,64	278,91	330,55	1977	279	indication
45	Yes	3,88	332,72	336,6	1959	333	indication
46	Yes	8,2	331,4	339,6	1965	342	indication
47	Yes	64,85	273,4	338,25	1991	273	indication
48	Yes	71,04	267,85	338,89	1991	268	indication
49	Yes	54,66	288,84	343,5	1991	289	indication
50	Yes	23,75	319,15	342,9	1975	319	indication

Appendix E1. Table with roof depth indications at time of abandonment and most recent roof depth indications

BF 1,11				Extinction depths [m-MV]							
	[m]	[m-MV]	[m-MV]	single direct		single with fill		[m3]	[m3]	[m3]	[-]
cavern	Dmig	top salt	BT+40	scenario 1	scenario 2	scenario 1	scenario 2	V_slurry needed	V_solids	V_cav_leach	fill factor
1	60	315,8	166,8	124,0	141,8	259,0	190,0	210000	54300	59428	0,91
2	90	319,3	180,3	133,0	58,3	241,0	181,0	380000	98257	245345	0,40
3	40	323,5	170,5	76,8	207,5	177,8	207,5	70000	18100	34483	0,52
4	100	330,0	173,2	118,0	40,0	238,2	148,7	520000	134456	185891	0,72
5	80	333,4	174,4	228,0	118	261,0	211,0	100000	25857	59664	0,43
6	100	336,6	175,3	137,8	46,6	248,6	177,0	480000	124114	174256	0,71
7	90	348,5	172,4	254,0	116,5	299,7	286,7	160000	41371	67346	0,61
8	80	346,8	169,2	179,0	114,8	272,7	196,6	260000	67228	93947	0,72
9	65	350,0	171,4	204,5	176,0			no fill at this cavern			
10	90	354,8	172,3	190,0	64,8			no fill at this cavern			
11	72	356,9	173,8	151,6	153,9			no fill at this cavern			
12	60	307,5	167,9	95,0	133,5	250,0	170,5	270000	69814	66785	1,05
13	95	309,3	166,0	159,0	48,3	230,6	179,0	280000	72400	119721	0,60
14	100	368,9	170,9	256,6	78,9			no fill at this cavern			
15	96	345,9	174,8	64,9	55,9	225,5	55,9	**634347**	164023	223382	0,73
16	68	335,3	171,8	195,3	132,3			no fill at this cavern			
17	92	337,5	167,7	198,5	76,5			no fill at this cavern			
18-24	90	337,0	166,5	178,5	76,0			no fill at this cavern			
19-20	120	332,1	165,6	193,0	0,0			no fill at this cavern			
21	30	327,8	167,0	0,0	0,0			no fill at this cavern			
22	90	357,0	166,4	267,7	154,0			no fill at this cavern			
23	80	357,0	166,4	146,5	96,0	279,8	166,0	370000	95671	119006	0,80
25-26	90	354,3	164,9	148,3	93,3	269,0	165,6	450000	116357	143759	0,81
27	100	375,7	172,0	260,0	143,7			no fill at this cavern			
28	110	383,1	169,9	265,9	35,1			no fill at this cavern			
29	30	375,3	169,8	0,0	288,5			no fill at this cavern			
30-31	72	384,0	169,9	67,9	152,0			no fill at this cavern			
32	90	371,3	171,0	255,0	110,3			no fill at this cavern			
33-34	128	374,9	169,3	220,2	0,0			no fill at this cavern			
35-36	100	372,3	167,9	85,9	82,3			no fill at this cavern			
37	84	360,2	176,0	239,7	128,2	239,7	312,6	280000	72400	71800	1,01
38	100	367,7	173,5	192,5	77,7	277,6	197,7	350000	90500	150282	0,60
39	100	383,4	172,3	122,3	209,4	333,5	300,7	**395640**	102301	81251	1,26
40-41	100	397,7	171,5	213,0	107,7	309,0	239,7	420000	108599	162406	0,67
42-43	110	367,5	166,8	220,0	77,5			no fill at this cavern			
44	60	330,6	165,7	253,3	156,6			no fill at this cavern			
45	84	336,6	164,8	226,8	144,2	266,5	219,3	140000	36200	68827	0,53
46	100	339,6	165,2	223,0	49,6	255,6	184,6	100000	25857	103311	0,25
47	80	338,3	165,0	255,7	106,3	262,5	172,1	20000	5171	44714	0,12
48	100	338,9	165,9	248,0	163,3	250,0	175,1	20000	5171	80168	0,06
49	60	343,5	167,3	106,7	169,5	286,0	211,3	280000	72400	74953	0,97
50	90	342,9	165,6	197,2	81,9	299,3	289,0	**380489**	98383	101654	0,97

Appendix E2. Table with cavern migration extinction depths [m below surface] for the single production phase in case of BF 1.11

BF 1,11				Extinction depths [m-MV]							
	[m]	[m-MV]	[m-MV]	final direct		final with fill		[m3]	[m3]	[m3]	[-]
cavern	Dmig	top salt	BT+40	scenario 1	scenario 2	scenario 1	scenario 2	V_slurry needed	V_solids	V_cav_leach	fill factor
1	80	315,8	166,8	136,4	83,8	243,0	175,0	290000	74985	182111	0,41
2	100	319,3	180,3	150,7	29,3	236,4	181,4	360000	93085	269425	0,35
3	40	323,5	170,5	0,0	178,5	183,0	178,5	150000	38786	49693	0,78
4	110	330,0	173,2	144,3	11,0	235,0	168,0	480000	124114	197078	0,63
5	80	333,4	174,4	199,0	101,4	264,0	211,0	180000	46543	75540	0,62
6	100	336,6	175,3	125,5	46,6	252,4	194,0	550000	142214	184921	0,77
7	90	348,5	172,4	244,0	116,5	300,0	287,6	370000	95671	137761	0,69
8	84	346,8	169,2	164,0	114,8	268,6	185,9	320000	82742	113112	0,73
9	98	350,0	171,4	169,5	60,0			no fill at this cavern			
10	100	354,8	172,3	177,0	64,8			no fill at this cavern			
11	80	356,9	173,8	179,7	124,9			no fill at this cavern			
12	80	307,5	167,9	170,2	75,5	235,0	169,0	180000	46543	76603	0,61
13	100	309,3	166,0	163,7	19,3	228,4	178,6	280000	72400	128318	0,56
14	0	368,9	170,9								
15	0	345,9	174,8								
16	68	335,3	171,8	204,4	161,3			no fill at this cavern			
17	104	337,5	167,7	191,2	18,5			no fill at this cavern			
18-24	120	337,0	166,5	312,6	0,0			no fill at this cavern			
19-20	120	332,1	165,6	197,6	0,0			no fill at this cavern			
21	90	327,8	167,0	179,8	95,8			no fill at this cavern			
22	90	357,0	166,4	206,0	96,0			no fill at this cavern			
23	80	357,0	166,4	115,6	96,0	281,5	193,9	480000	124114	136061	0,91
25-26	90	354,3	164,9	135,7	93,3	269,9	175,4	500000	129285	152442	0,85
27	0	375,7	172,0					no fill at this cavern			
28	0	383,1	169,9					no fill at this cavern			
29	30	375,3	169,8	0,0	259,5			no fill at this cavern			
30-31	135	384,0	169,9	216,2	0,0			no fill at this cavern			
32	0	371,3	171,0					no fill at this cavern			
33-34	0	374,9	169,3					no fill at this cavern			
35-36	140	372,3	167,9	205,7	0,0			no fill at this cavern			
37	0	360,2	176,0								
38	100	367,7	173,5	170,7	77,7	276,6	191,5	440000	113771	169095	0,67
39	100	383,4	172,3	221,5	93,4	290,0	188,6	**395640**	102301	142715	0,72
40-41	120	397,7	171,5	221,0	49,7	288,4	185,5	420000	108599	223870	0,49
42-43	120	367,5	166,8	221,0	0,0			no fill at this cavern			
44	68	330,6	165,7	246,5	127,6			no fill at this cavern			
45	90	336,6	164,8	225,8	61,1	254,9	179,6	120000	31028	68827	0,45
46	100	339,6	165,2	216,6	49,6	249,2	167,3	150000	38786	108801	0,36
47	80	338,3	165,0	234,9	170,0	263,1	178,7	100000	25857	120817	0,21
48	100	338,9	165,9	162,3	48,9	205,6	191,1	120000	31028	80168	0,39
49	60	343,5	167,3	70,0	169,5	288,5	235,2	340000	87914	86201	1,02
50	102	342,9	165,6	202,6	52,9	296,0	286,6	**380489**	98383	120802	0,81

Appendix E3. Table with cavern migration extinction depths [m below surface] for the final production in case of BF 1.11

			single direct		single with fill			[m3]	[m3]	
cavern	top salt	BT+40	scenario 1	scenario 2	scenario 1	scenario 2	m3 slurry needed	solids V	leached Vcav	fill factor
1	315,8	166,8	173,6	141,8	262,1	215,8	200000,0	51714,0	59428,4	0,87
2	319,3	180,3	168,3	58,3	239,3	171,6	300000,0	77571,0	245345,0	0,32
3	323,5	170,5	140,1	207,5	189,9	207,5	50000,0	12928,5	34482,5	0,37
4	330,0	173,2	172,8	40,0	238,6	150,4	420000,0	108599,4	185891,0	0,58
5	333,4	174,4	253,5	101,4	278,4	255,5	100000,0	25857,0	59663,7	0,43
6	336,6	175,3	187,8	46,6	251,5	190,4	400000,0	103428,0	174255,6	0,59
7	348,5	172,4	264,9	116,5	302,8	288,5	130000,0	33614,1	67345,8	0,50
8	346,8	169,2	204,6	114,8	275,4	183,8	250000,0	64642,5	93946,6	0,69
9	350,0	171,4	220,5	176,0			no fill at this cavern			
10	354,8	172,3	230,8	64,8			no fill at this cavern			
11	356,9	173,8	203,7	153,9			no fill at this cavern			
12	307,5	167,9	149,4	133,5	252,5	199,0	260000,0	67228,2	66784,7	1,01
13	309,3	166,0	196,6	48,3	228,4	170,0	180000,0	46542,6	119721,4	0,39
14	368,9	170,9	286,5	233,1			no fill at this cavern			
15	345,9	174,8	87,3	55,9	257,4	175,2	**634347,0**	164023,1	223381,6	0,73
16	335,3	171,8	232,6	161,3			no fill at this cavern			
17	337,5	167,7	232,4	76,5			no fill at this cavern			
18-24	337,0	166,5	220,8	76,0			no fill at this cavern			
19-20	332,1	165,6	225,8	136,6			no fill at this cavern			
21	327,8	167,0	0,0	0,0			no fill at this cavern			
22	357,0	166,4	245,9	154,0			no fill at this cavern			
23	357,0	166,4	226,3	96,0	273,6	172,1	230000,0	59471,1	119006,4	0,50
25-26	354,3	164,9	203,2	93,3	270,1	177,0	340000,0	87913,8	143758,6	0,61
27	375,7	172,0	280,1	143,7			no fill at this cavern			
28	383,1	169,9	297,1	257,6			no fill at this cavern			
29	375,3	169,8	0,0	288,5			no fill at this cavern			
30-31	384,0	169,9	152,2	152,0			no fill at this cavern			
32	371,3	171,0	283,2	180,2			no fill at this cavern			
33-34	374,9	169,3	259,6	156,5			no fill at this cavern			
35-36	372,3	167,9	162,3	82,3			no fill at this cavern			
37	360,2	176,0	271,1	98,2	271,1	307,0	200000,0	51714,0	71800,0	0,72
38	367,7	173,5	239,2	77,7	275,8	185,3	230000,0	59471,1	150281,6	0,40
39	383,4	172,3	191,9	209,4	327,0	262,4	**395640,0**	102300,6	81251,3	1,26
40-41	397,7	171,5	259,6	107,7	302,6	182,4	280000,0	72399,6	162405,9	0,45
42-43	367,5	166,8	255,5	77,5			no fill at this cavern			
44	330,6	165,7	272,2	154,2			no fill at this cavern			
45	336,6	164,8	253,5	104,6	262,6	202,2	40000,0	10342,8	68827,4	0,15
46	339,6	165,2	254,1	191,5			not needed			
47	338,3	165,0	277,7	246,5			not needed			
48	338,9	165,9	270,5	242,2			not needed			
49	343,5	167,3	166,5	169,5	281,6	162,8	260000,0	67228,2	74953,3	0,90
50	342,9	165,6	236,1	81,9	310,9	306,6	**380489,0**	98383,0	101654,2	0,97

Appendix E4. Table with cavern migration extinction depths [m below surface] for the single production in case of BF 1.15 and overall compaction consolidation factor of 0.726

			final direct		final with fill			[m3]	[m3]	
cavern	top salt	BT+40	scenario 1	scenario 2	scenario 1	scenario 2	m3 slurry needed	solids V	leached Vcav	fill factor
1	315,8	166,8	184,3	83,8	246,5	193,7	200000,0	51714,0	182111,0	0,28
2	319,3	180,3	195,7	29,3	235,5	178,0	250000,0	64642,5	269424,8	0,24
3	323,5	170,5	155,5	178,5	250,4	173,9	100000,0	25857,0	49693,2	0,52
4	330,0	173,2	192,2	11,0	230,8	141,2	300000,0	77571,0	197078,4	0,39
5	333,4	174,4	232,4	101,4	284,7	268,8	210000,0	54299,7	75540,0	0,72
6	336,6	175,3	178,8	46,6	250,5	185,8	450000,0	116356,5	184921,1	0,63
7	348,5	172,4	263,2	159,0	300,6	288,1	190000,0	49128,3	137761,0	0,36
8	346,8	169,2	227,9	114,8	263,3	175,9	180000,0	46542,6	113112,0	0,41
9	350,0	171,4	273,9	231,9			no fill at this cavern			
10	354,8	172,3	224,4	64,8			no fill at this cavern			
11	356,9	173,8	226,9	124,9			no fill at this cavern			
12	307,5	167,9	205,5	75,5	235,4	170,5	120000,0	31028,4	76603,4	0,41
13	309,3	166,0	200,2	19,3	225,7	168,8	160000,0	41371,2	128317,6	0,32
14	368,9	170,9								
15	345,9	174,8								
16	335,3	171,8	239,3	161,3			no fill at this cavern			
17	337,5	167,7	239,0	153,4			no fill at this cavern			
18-24	337,0	166,5	319,1	117,2			no fill at this cavern			
19-20	332,1	165,6	229,8	171,1			no fill at this cavern			
21	327,8	167,0	219,2	130,6			no fill at this cavern			
22	357,0	166,4	243,8	96,0			no fill at this cavern			
23	357,0	166,4	214,1	96,0	273,2	183,6	300000,0	77571,0	136061,4	0,57
25-26	354,3	164,9	194,0	93,3	270,7	182,8	390000,0	100842,3	152441,7	0,66
27	375,7	172,0					no fill at this cavern			
28	383,1	169,9					no fill at this cavern			
29	375,3	169,8	0,0	259,5			no fill at this cavern			
30-31	384,0	169,9	260,9	144,0			no fill at this cavern			
32	371,3	171,0					no fill at this cavern			
33-34	374,9	169,3					no fill at this cavern			
35-36	372,3	167,9	235,6	135,3			no fill at this cavern			
37	360,2	176,0								
38	367,7	173,5	223,2	190,3	274,2	171,7	320000,0	82742,4	169094,6	0,49
39	383,4	172,3	264,7	93,4	289,4	181,5	390000,0	100842,3	142715,0	0,71
40-41	397,7	171,5	265,5	49,7	289,8	194,1	220000,0	56885,4	223869,7	0,25
42-43	367,5	166,8	258,7	157,9			no fill at this cavern			
44	330,6	165,7	268,9	218,8			no fill at this cavern			
45	336,6	164,8	253,1	165,8			not needed		68827,4	0,00
46	339,6	165,2	249,4	168,2			not needed		108801,1	0,00
47	338,3	165,0	258,2	106,3	263,2	179,0	20000,0	5171,4	59408,4	0,09
48	338,9	165,9	205,5	191,6			not needed			
49	343,5	167,3	177,3	169,5	279,7	169,0	280000,0	72399,6	86201,3	0,84
50	342,9	165,6	240,0	52,9	300,7	293,0	380489,0	98383,0	120801,8	0,81

Appendix E5. Table with cavern migration extinction depths [m below surface] for the final production in case of BF 1.15 and overall compaction consolidation factor of 0.726

Appendix E5: Figures of the simulated caverns.

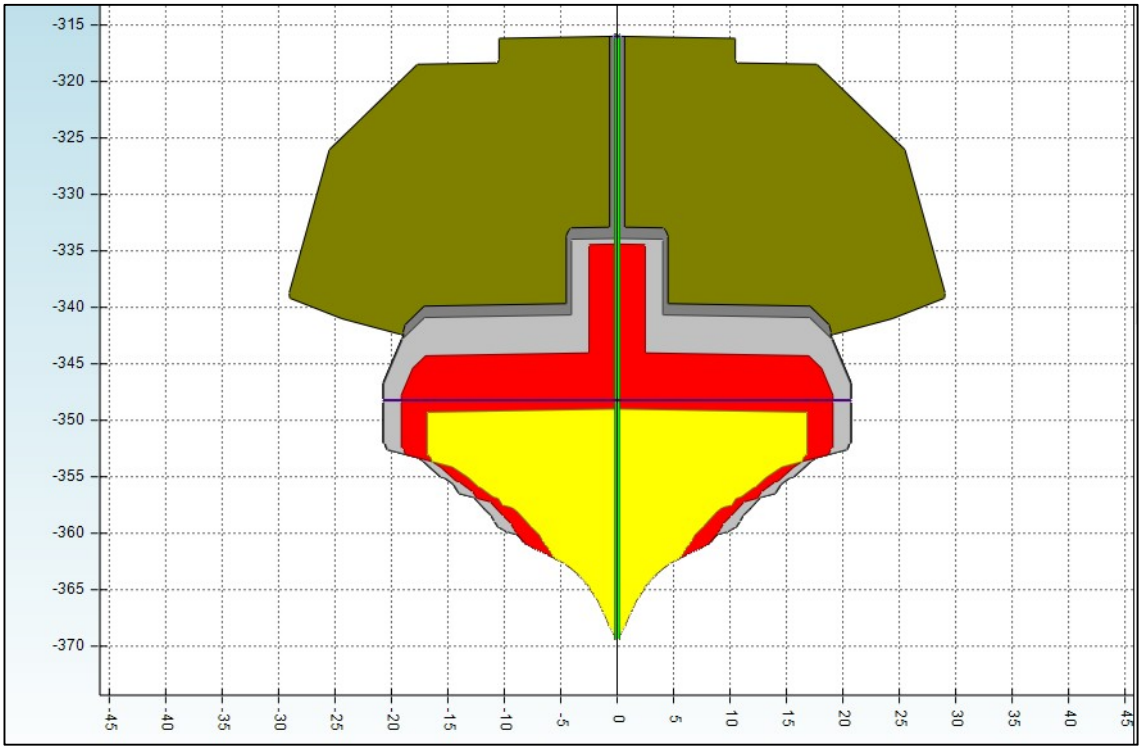

Figure 1. Side view of simulation result of single production phase for cavern 1

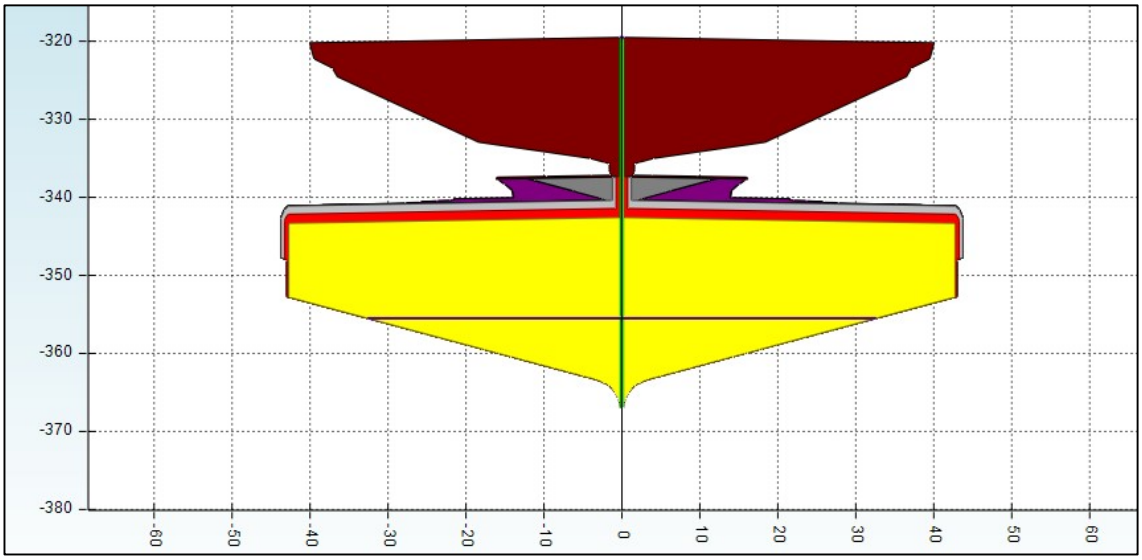

Figure 2. Side view of simulation result of single production phase for cavern 2

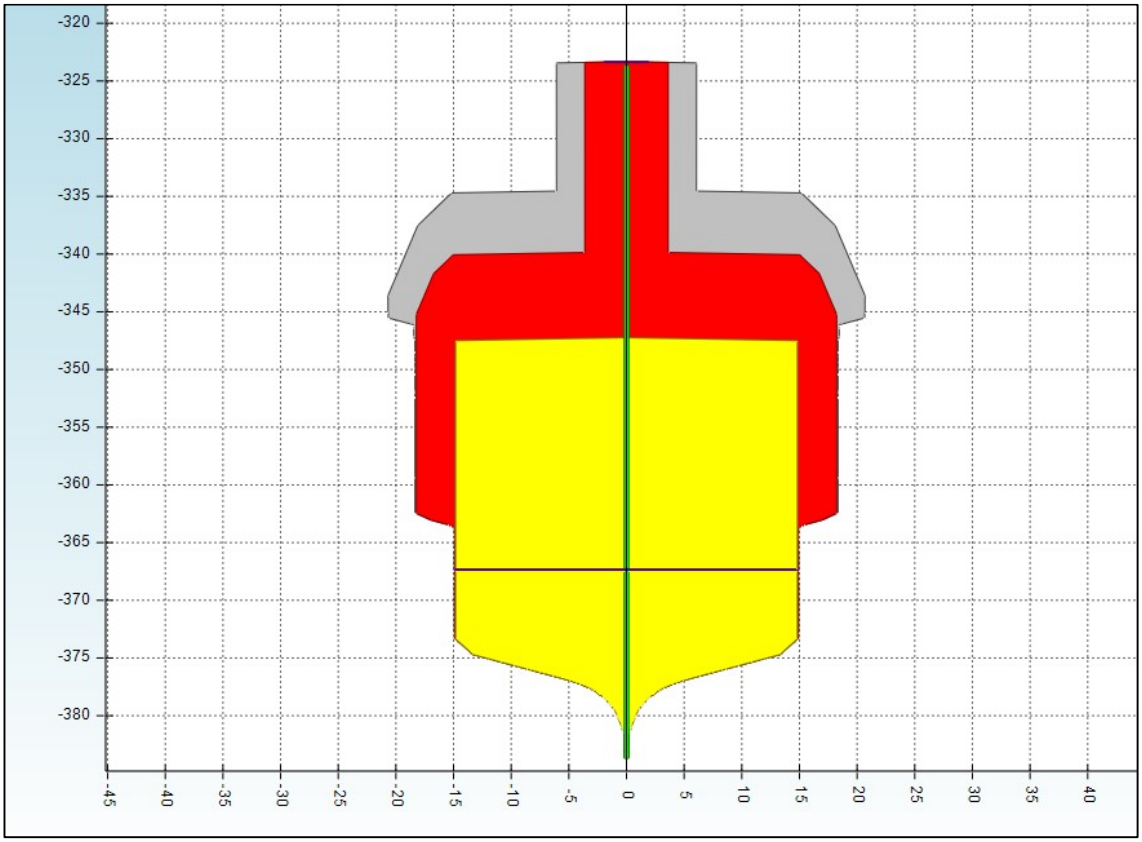

Figure 3. Side view of simulation result of single production phase for cavern 3

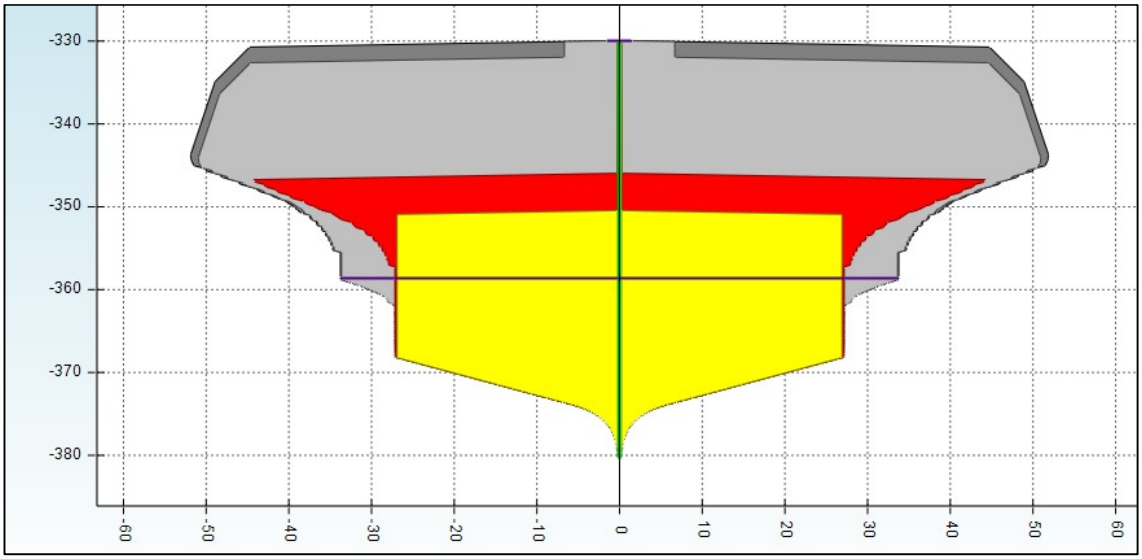

Figure 4. Side view of simulation result of single production phase for cavern 4

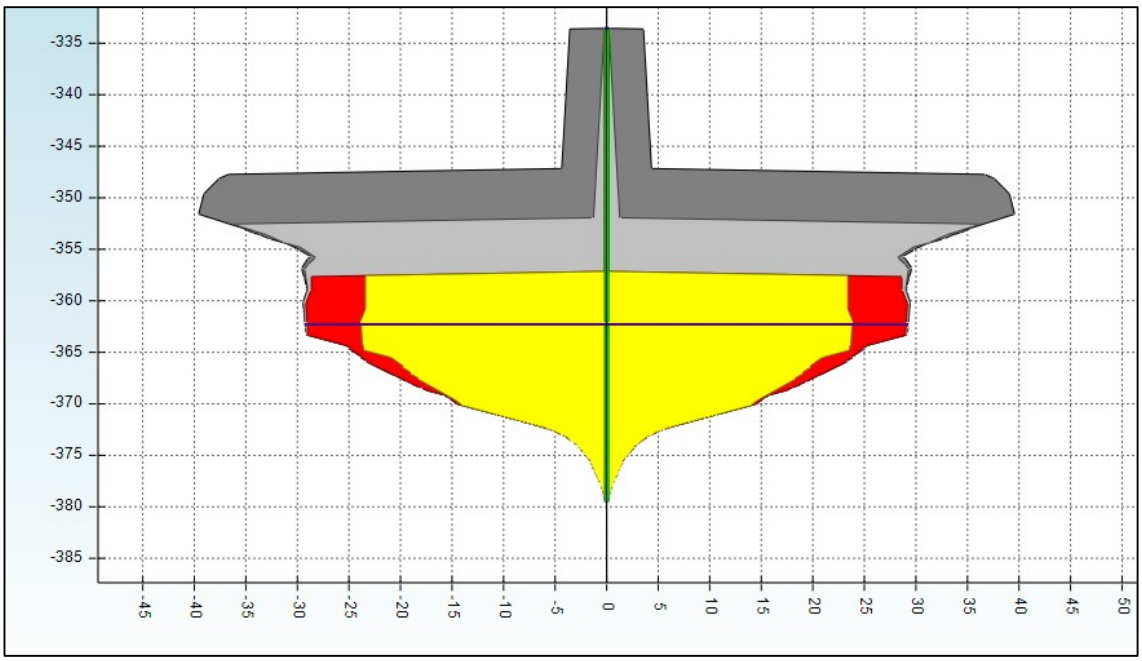

Figure 5. Side view of simulation result of single production phase for cavern 5

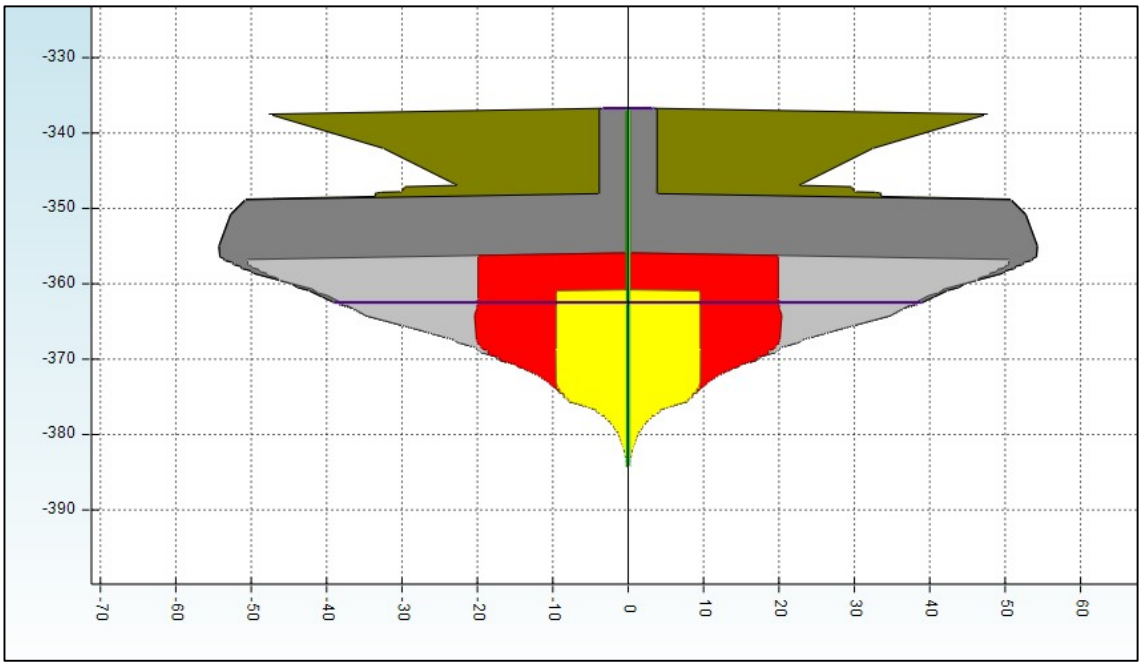

Figure 6. Side view of simulation result of single production phase for cavern 6

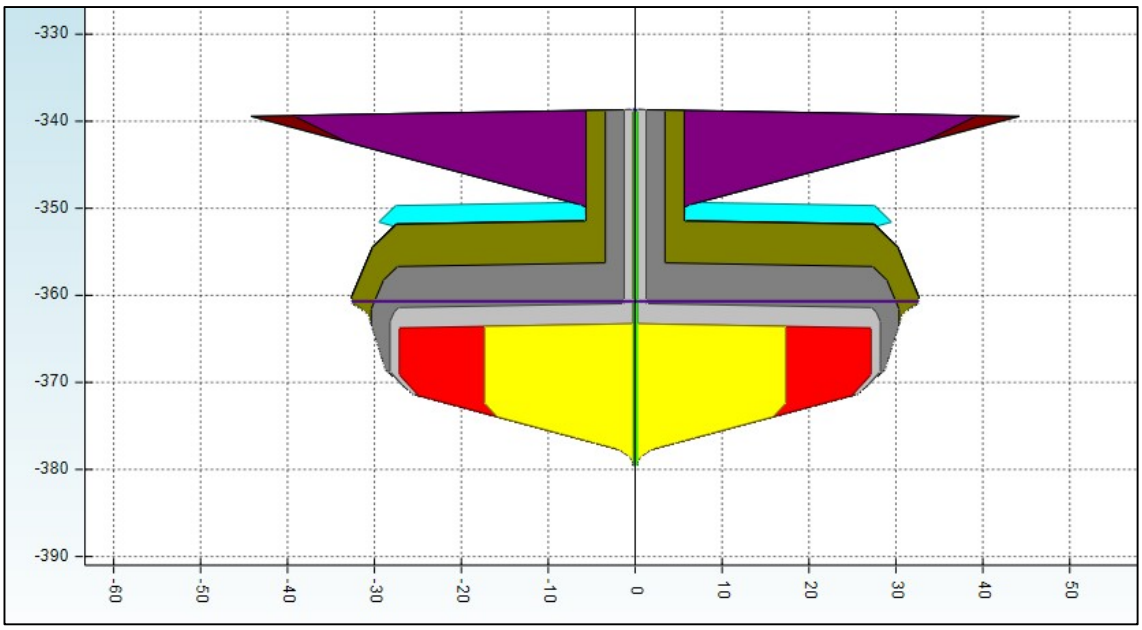

Figure 7. Side view of simulation result of single production phase cavern 7

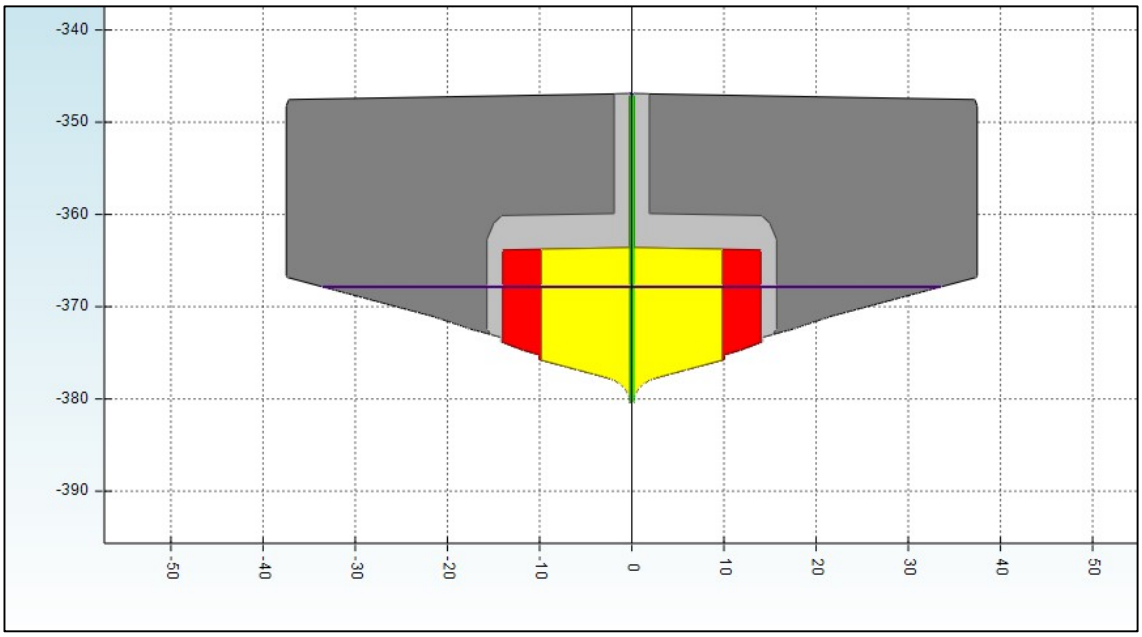

Figure 8. Side view of simulation result of single production phase cavern 8

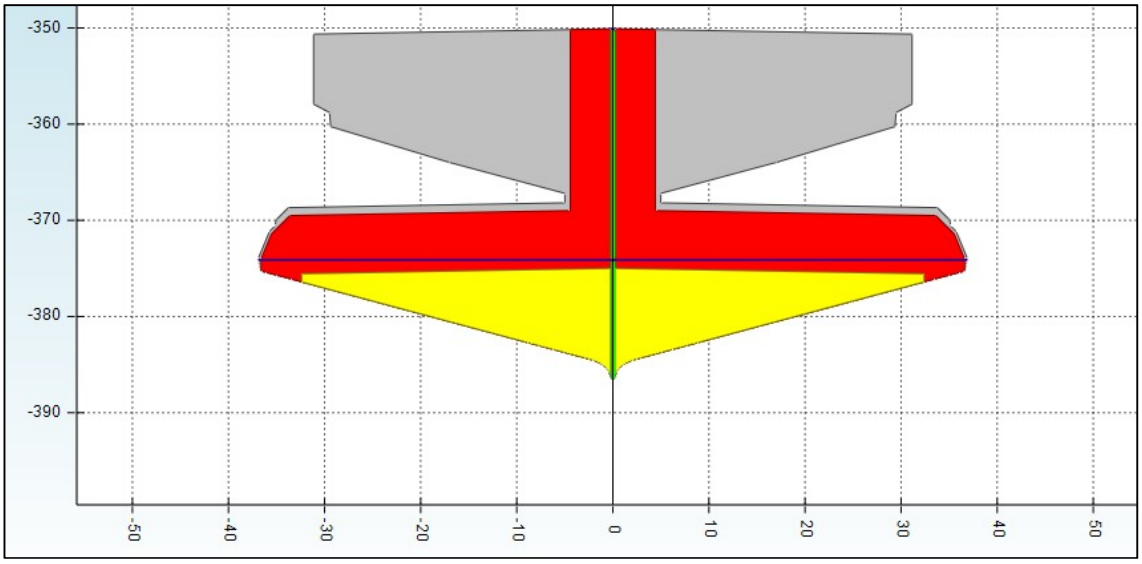

Figure 9. Side view of simulation result of single production phase for cavern 9

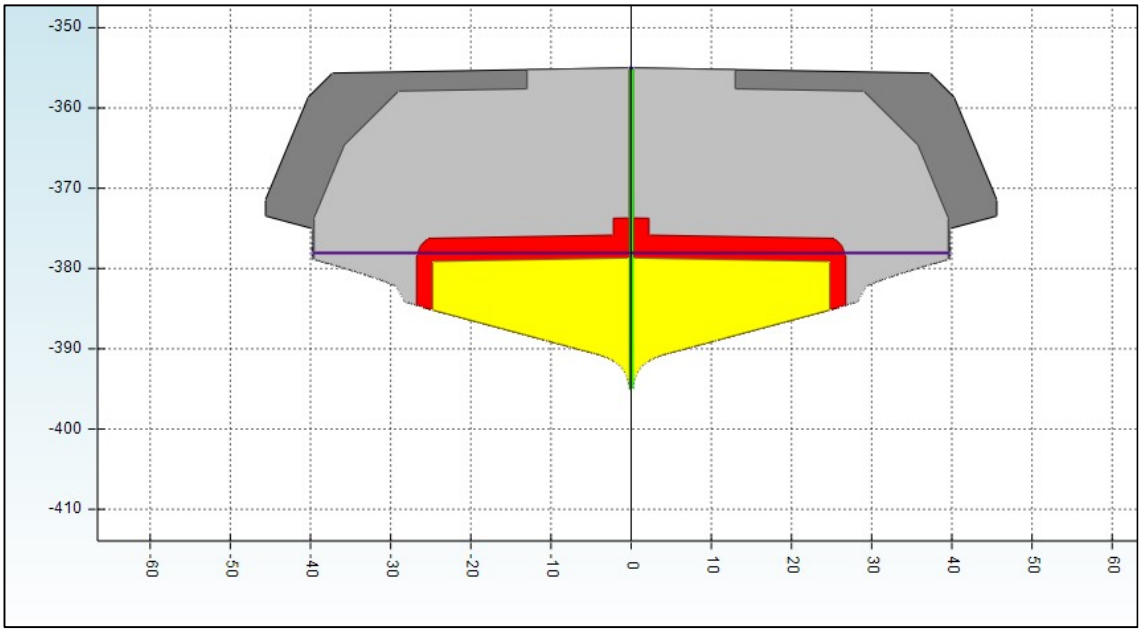

Figure 10. Side view of simulation result of single production phase for cavern 10

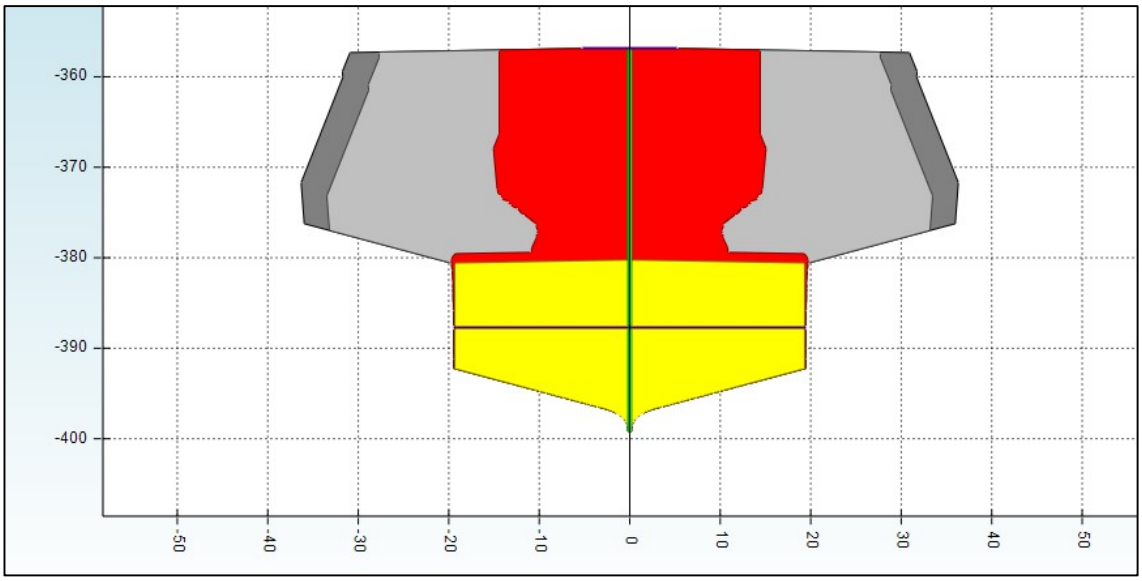

Figure 11. Side view of simulation result of single production phase for cavern 11

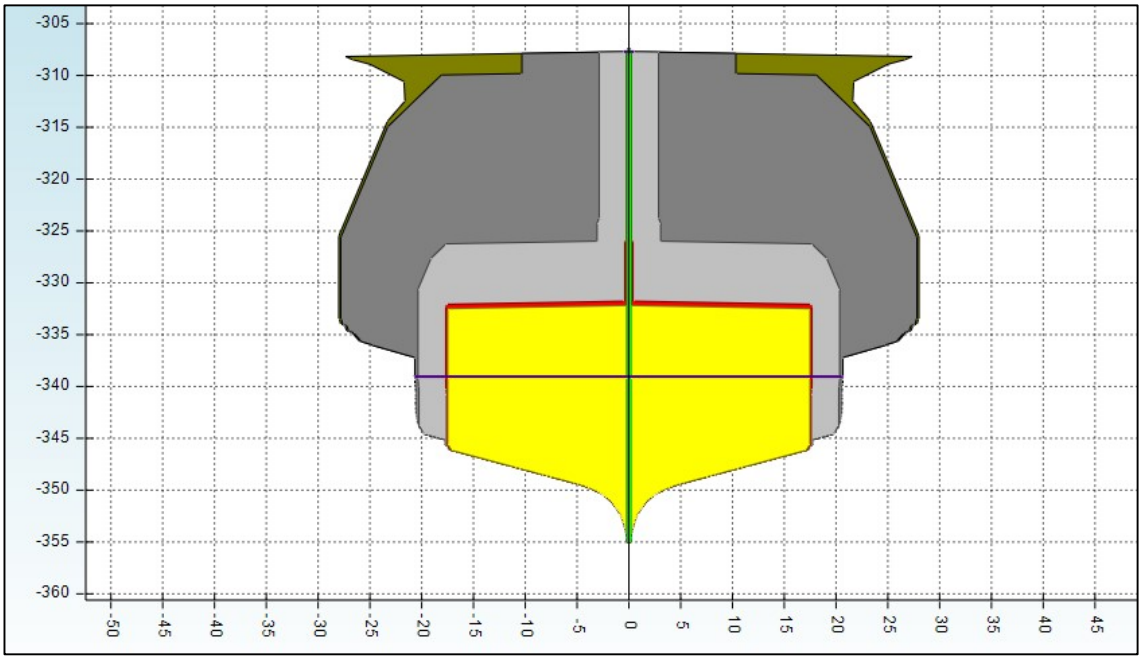

Figure 12. Side view of simulation result of single production phase cavern 12

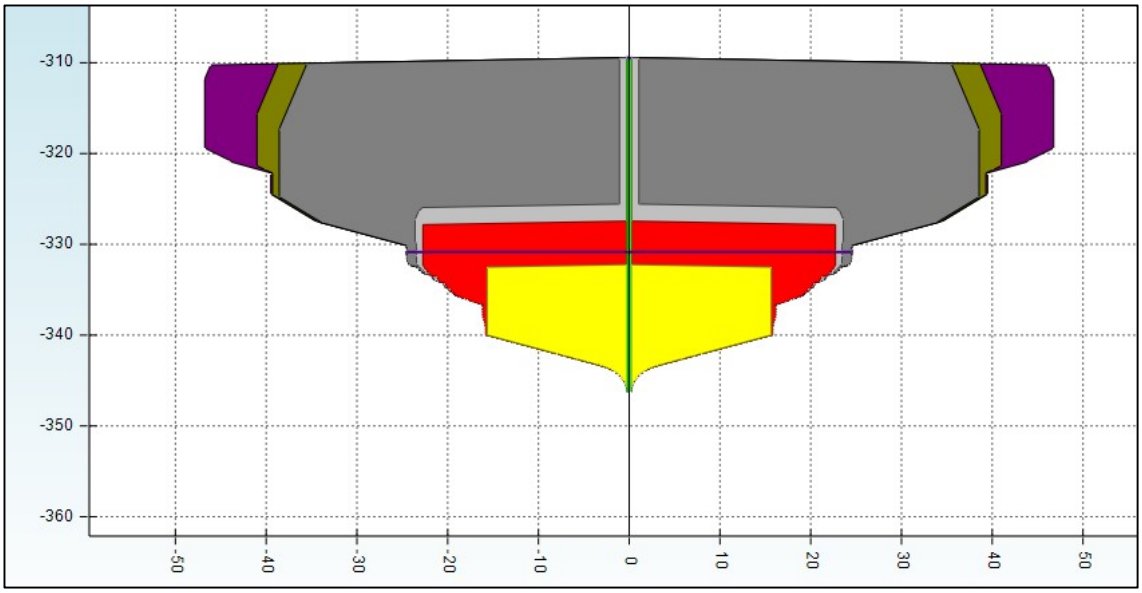

Figure 13. Side view of simulation result of single production phase for cavern 13

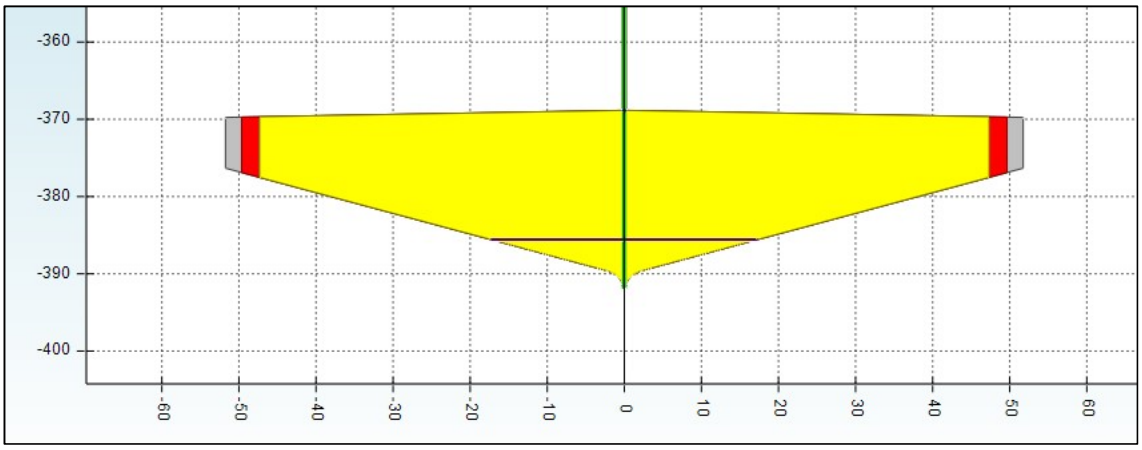

Figure 14. Side view of simulation result of cavern 14

Figure 15. Side view of simulation result of cavern 15

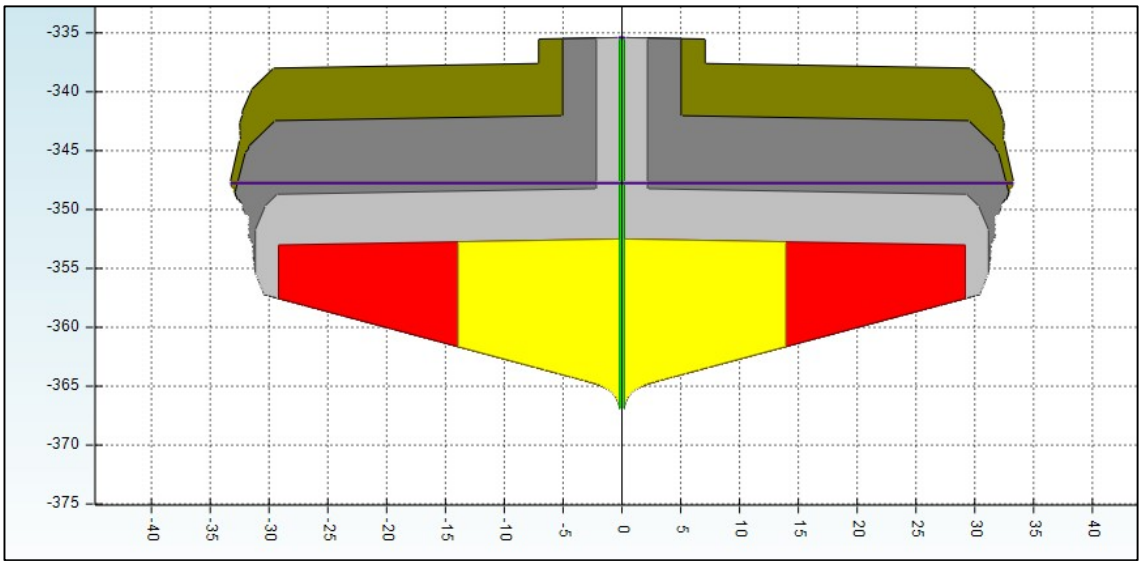

Figure 16. Side view of simulation result of single production phase for cavern 16

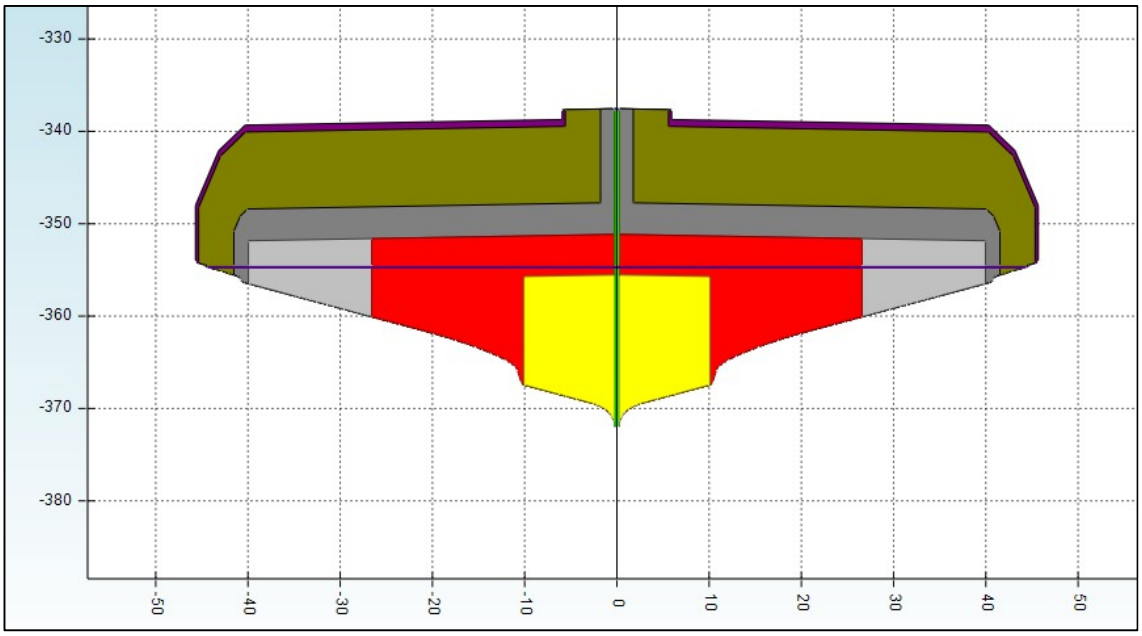

Figure 17. Side view of simulation result of single production phase for cavern 17

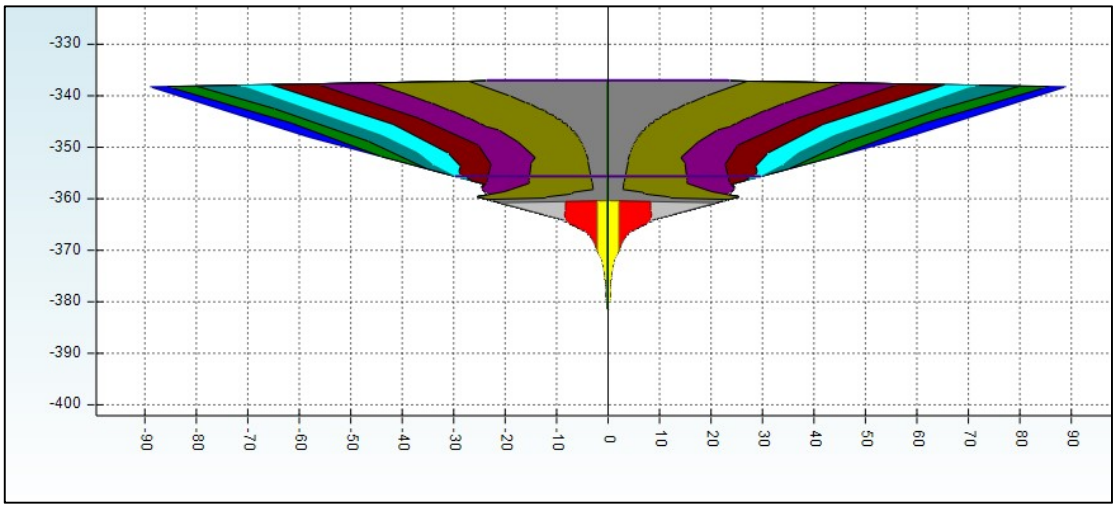

Figure 18. Side view of simulation result of doublet 18-24 considered as one cavern

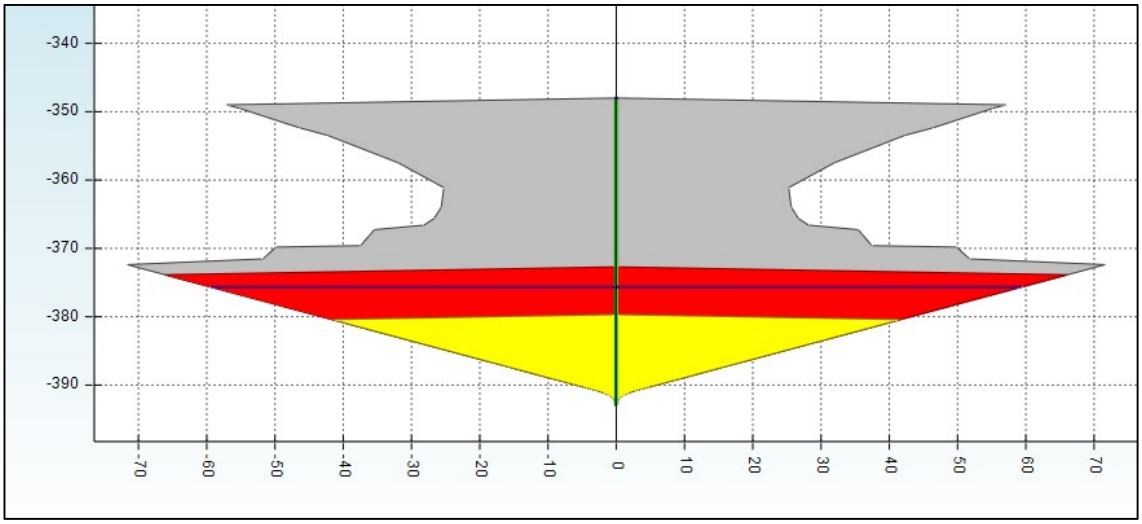

Figure 19. Side view of simulation result of doublet 19-20 considered as one cavern.

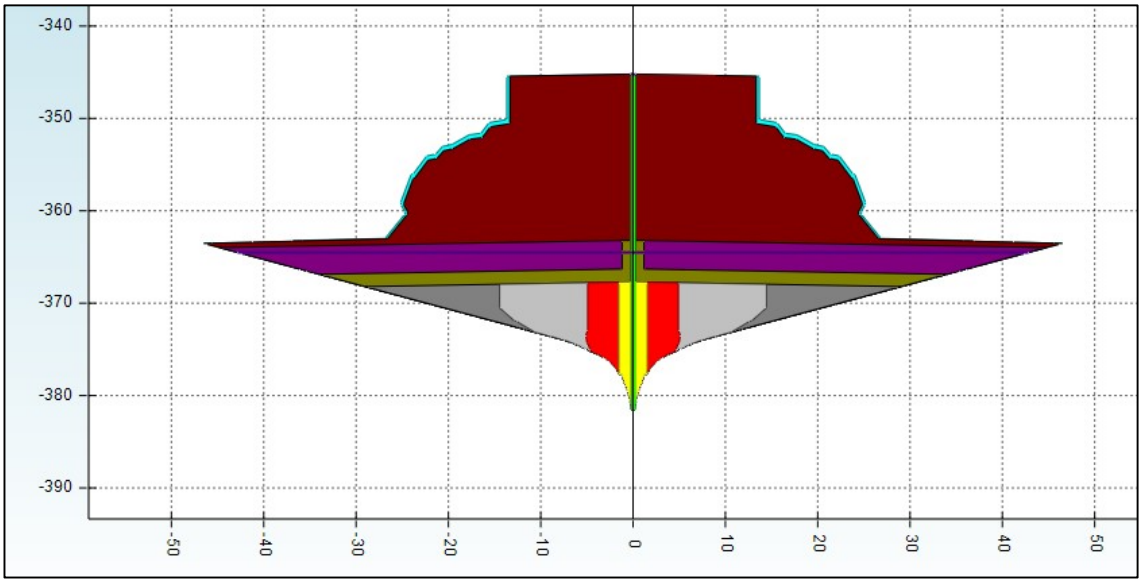

Figure 20. Side view of simulation result of single production phase for cavern 21

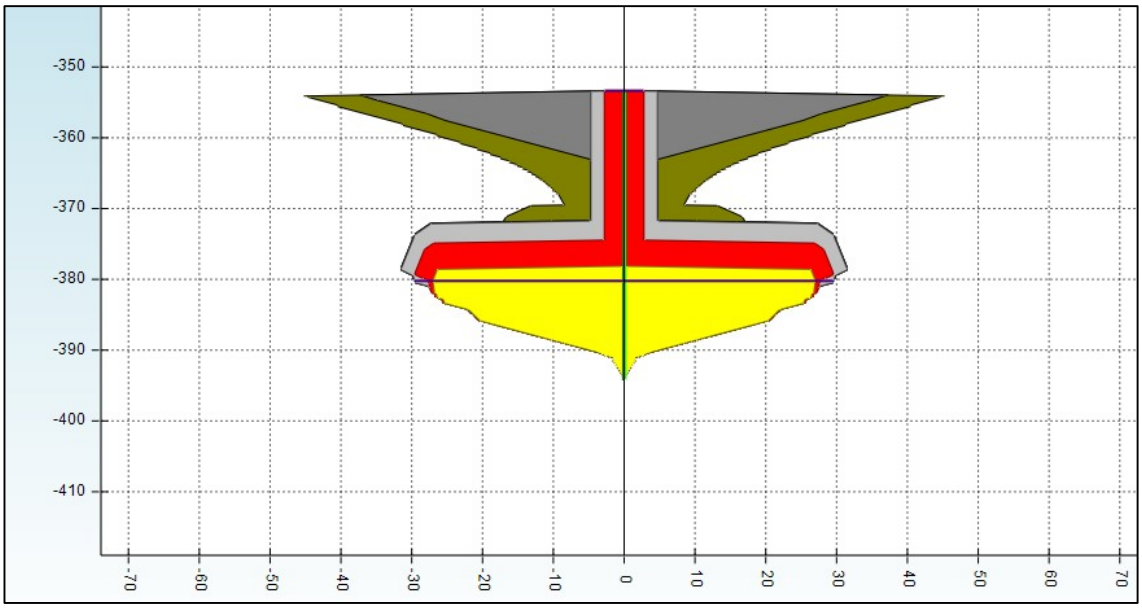

Figure 21. Side view of simulation result of single production phase for cavern 22

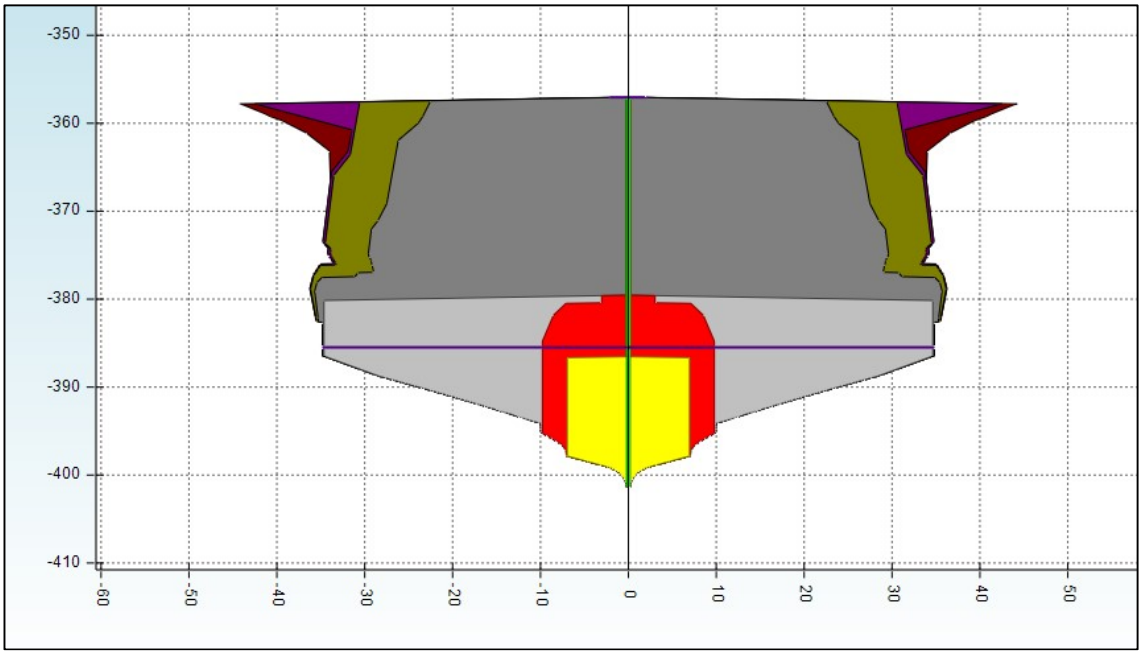

Figure 22. Side view of simulation result of single production phase for cavern 23

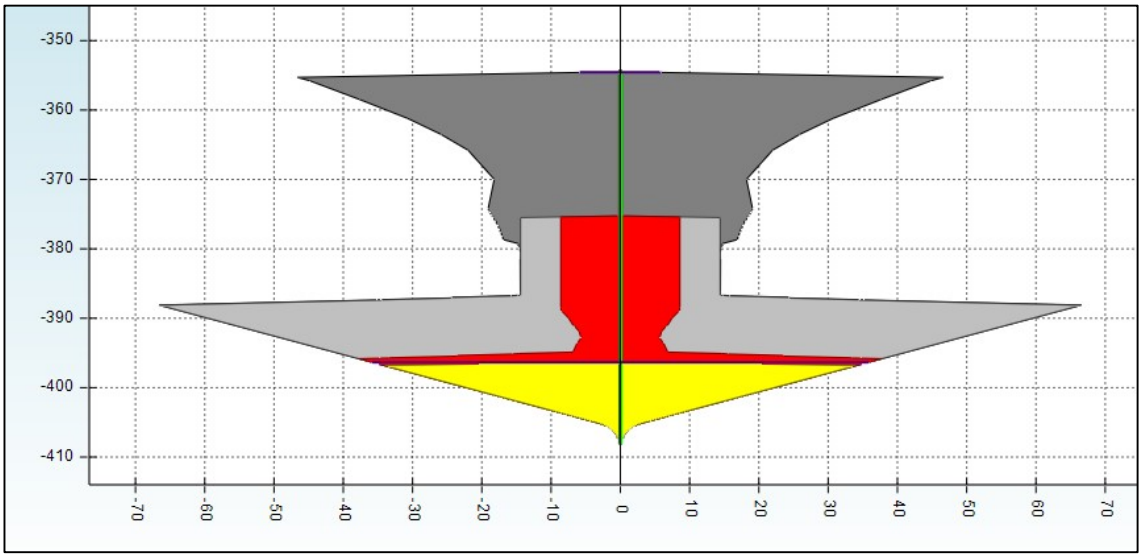

Figure 23. Side view of simulation result of single production phase of doublet 25-26

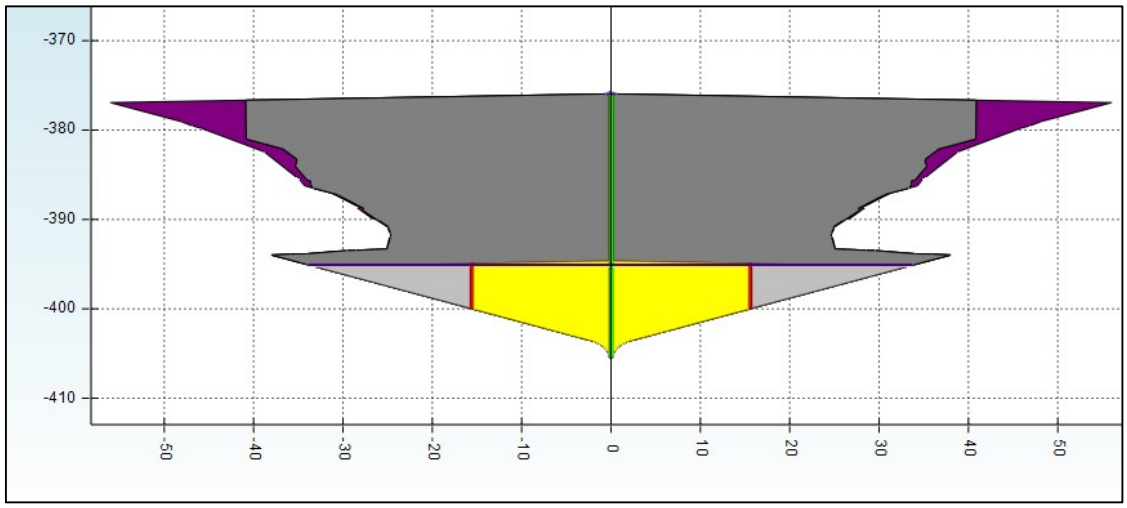

Figure 24. Side view of simulation result of single production phase for cavern 27

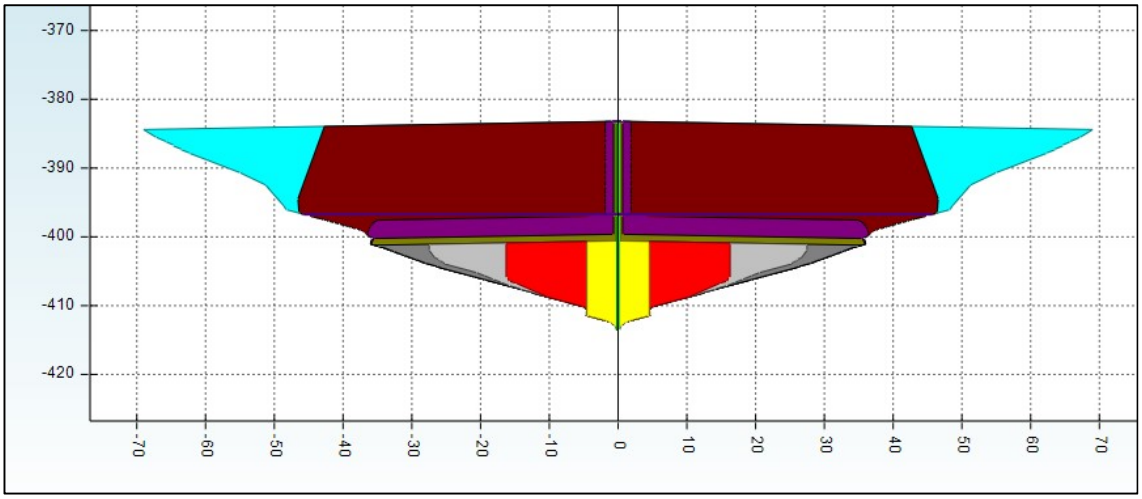

Figure 25. Side view of simulation result of single production phase for cavern 28

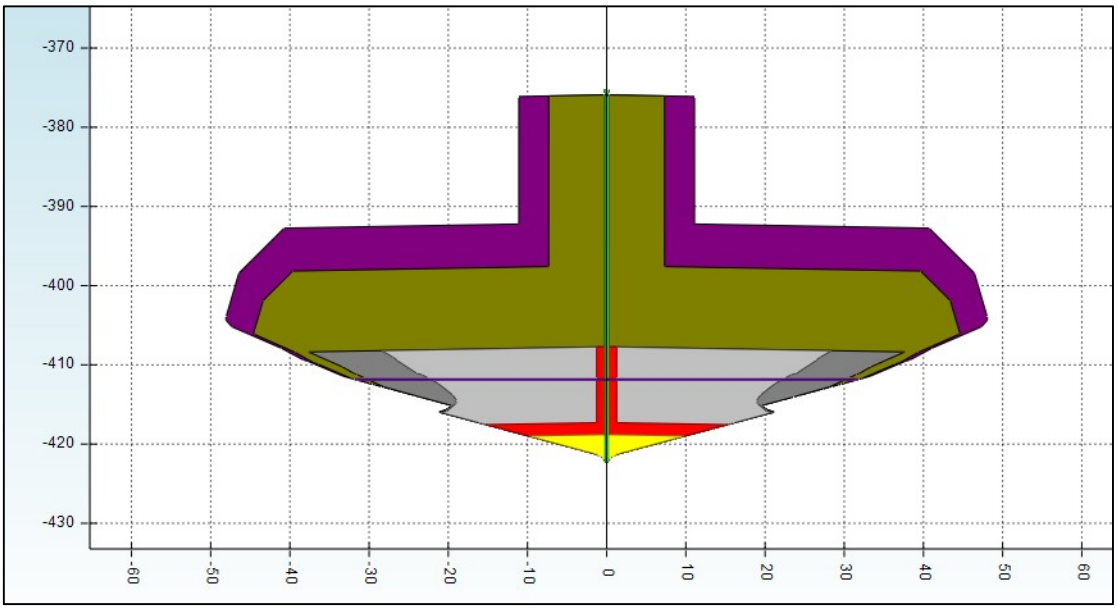

Figure 26. Side view of simulation result of single production phase for cavern 29

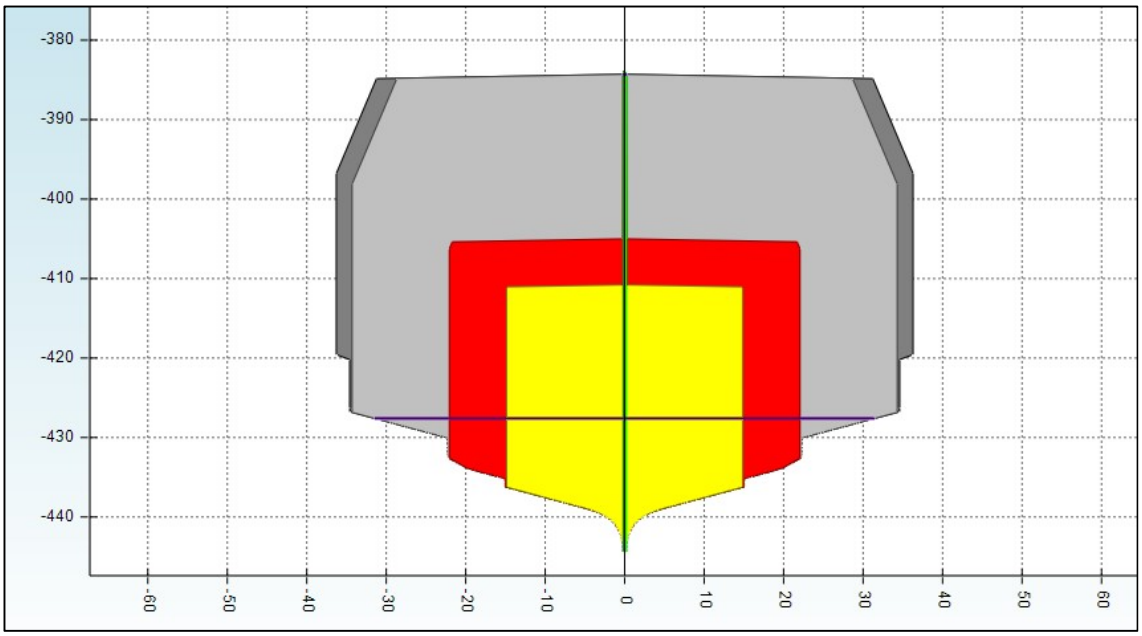

Figure 27. Side view of simulation result of single production phase for doublet 30-31

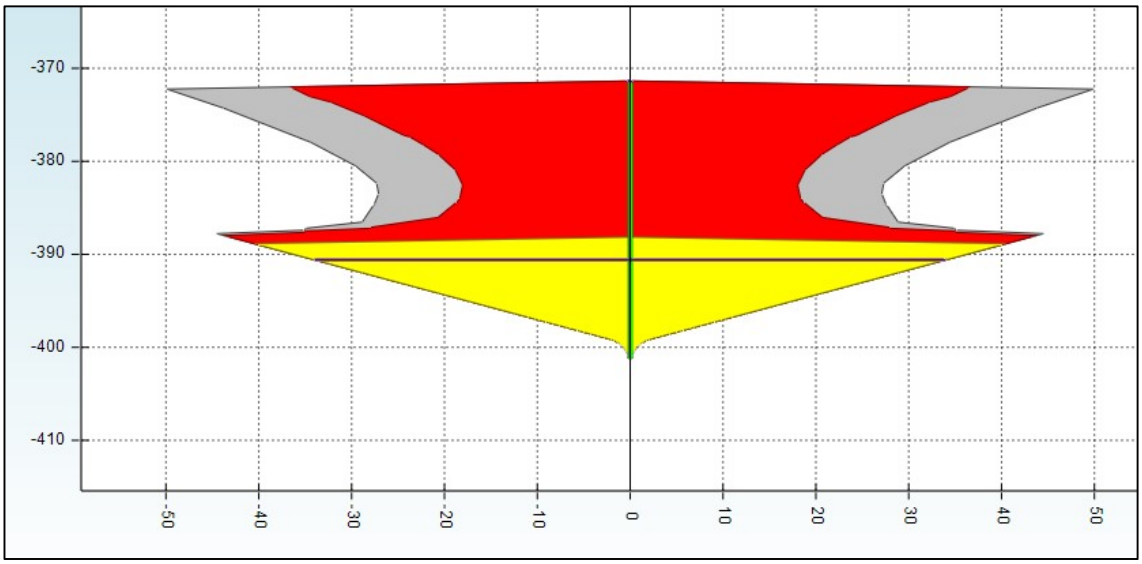

Figure 28. Side view of simulation result of cavern 32

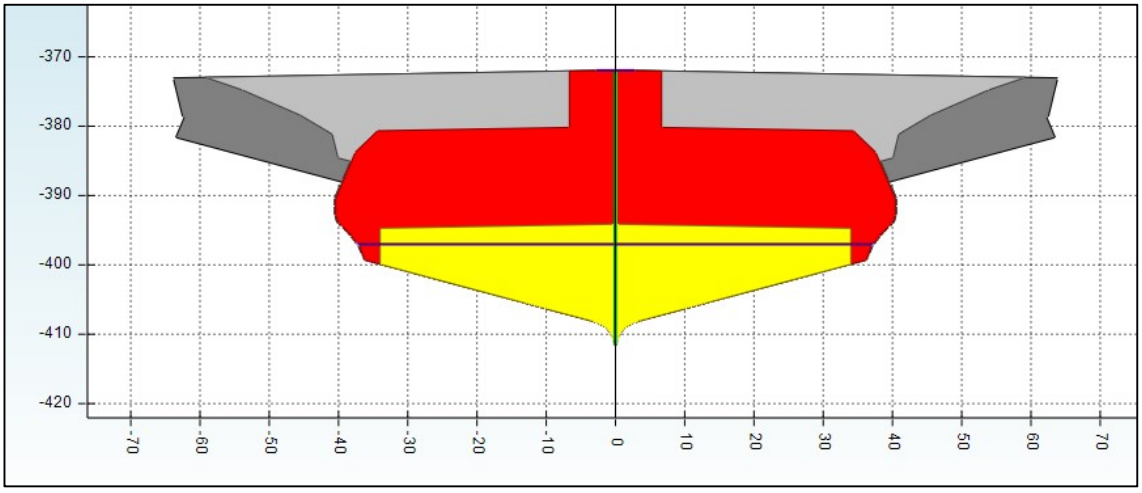

Figure 29. Side view of simulation result of doublet 33-34

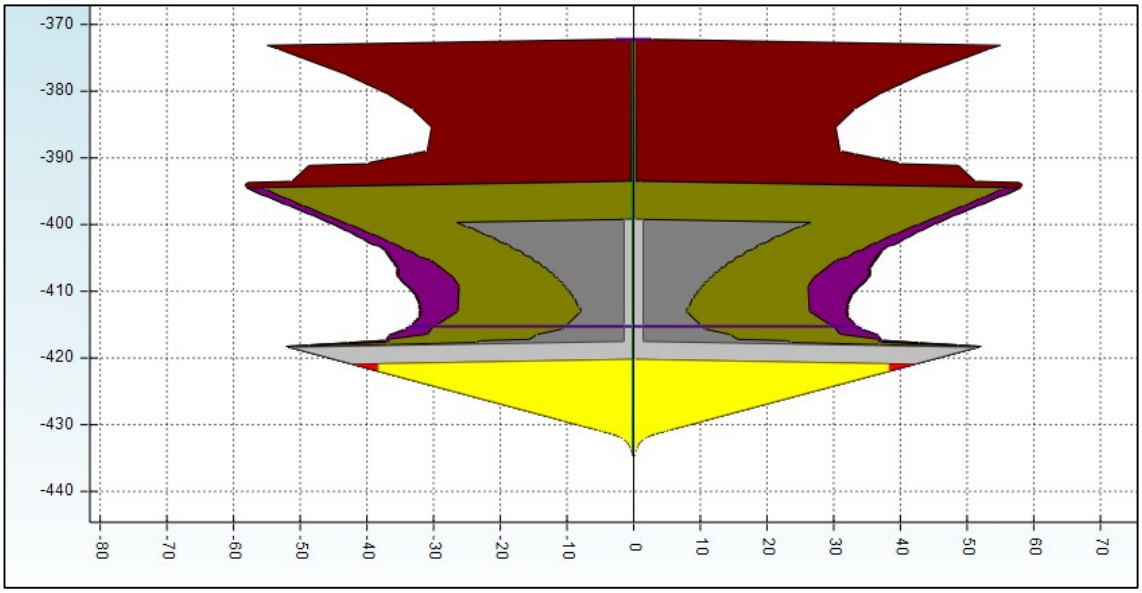

Figure 30. Side view of simulation result of single phase production for doublet 35-36

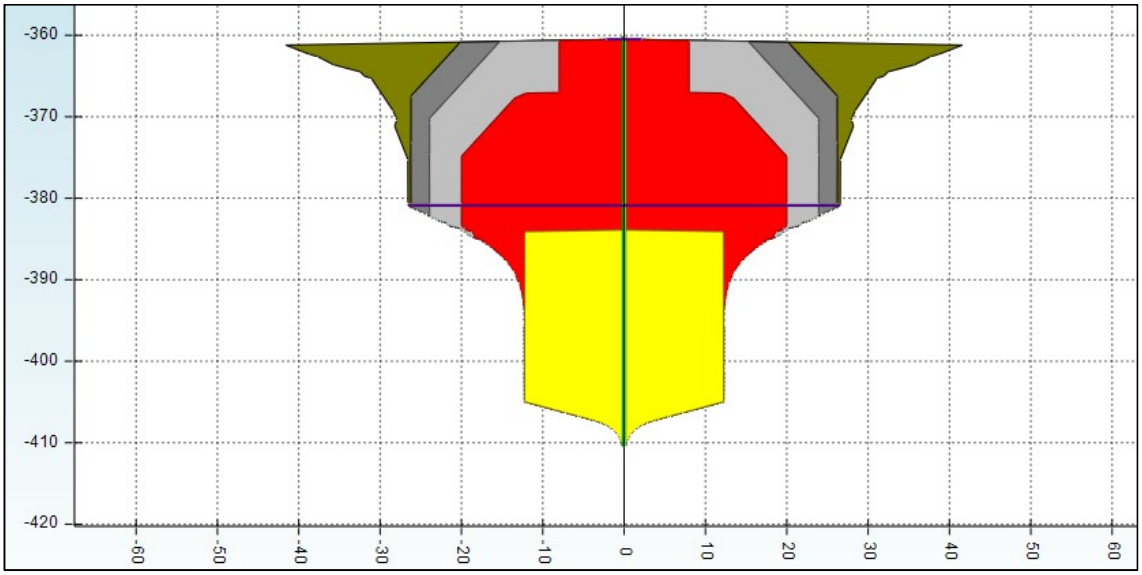

Figure 31. Side view of simulation result of single phase production of cavern 37

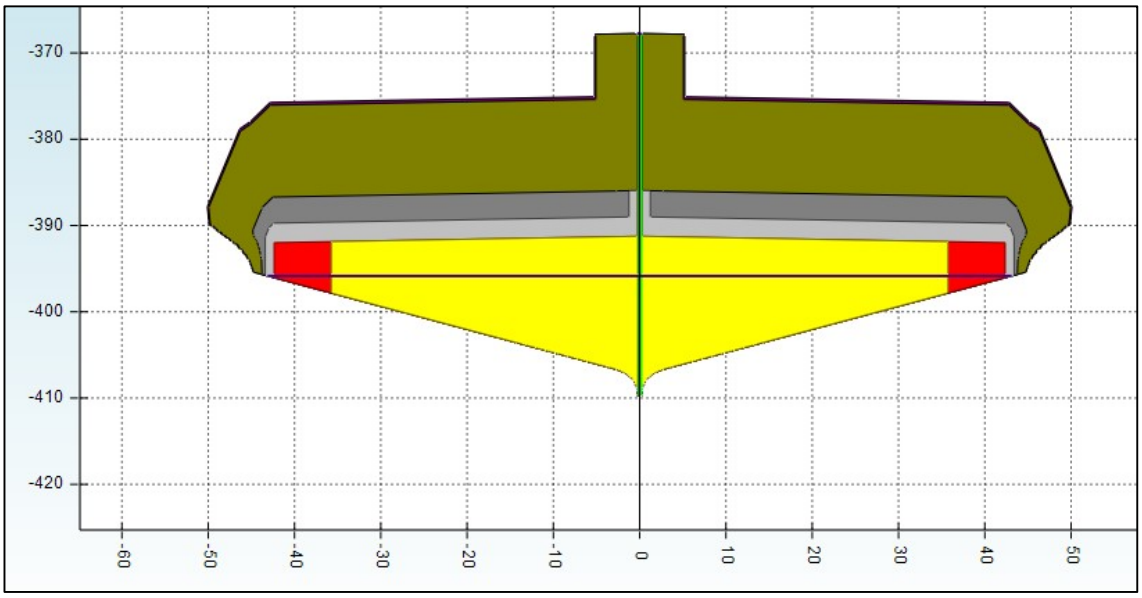

Figure 32. Side view of simulation result of single phase production of cavern 38

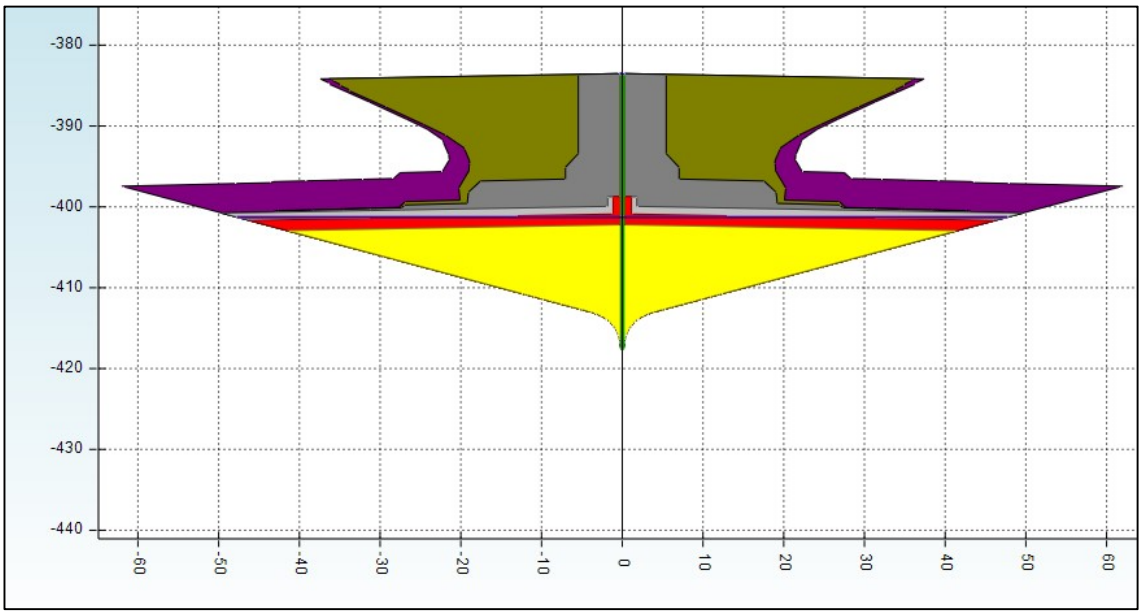

Figure 33. Side view of simulation result of single phase production of cavern 39

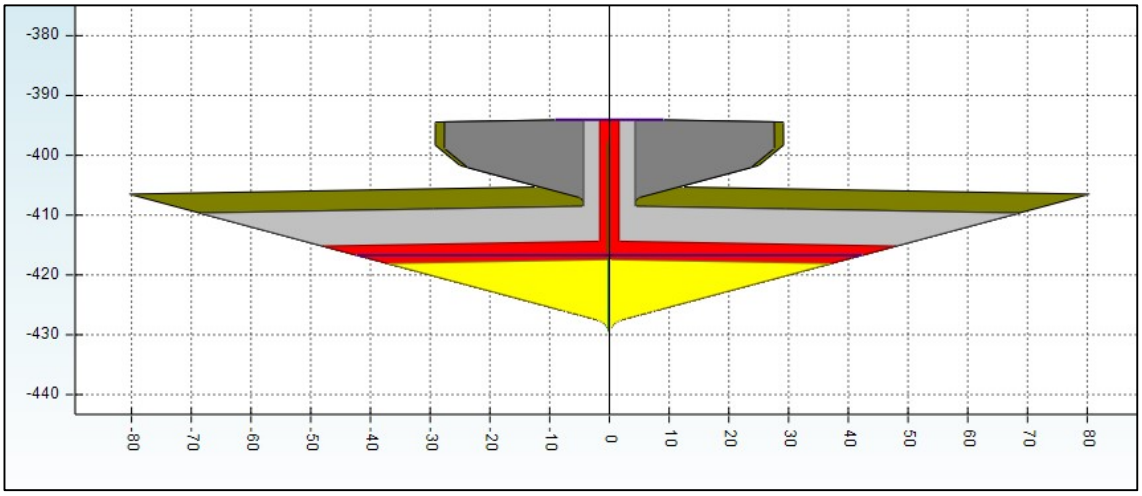

Figure 34. Side view of simulation result of single phase production for doublet 40-41

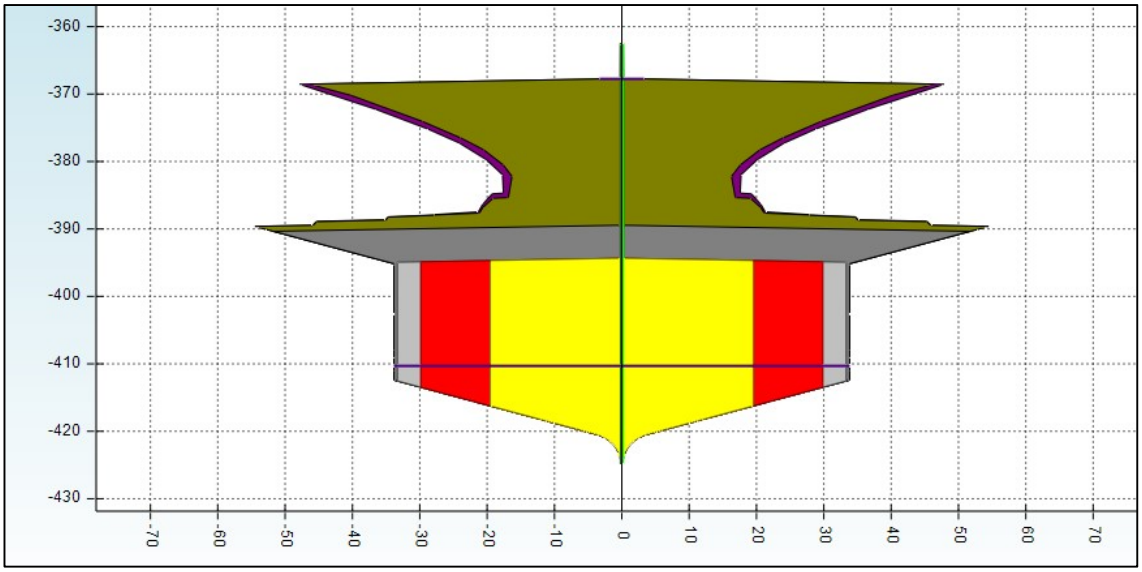

Figure 35. Side view of simulation result of single phase production for doublet 42-43

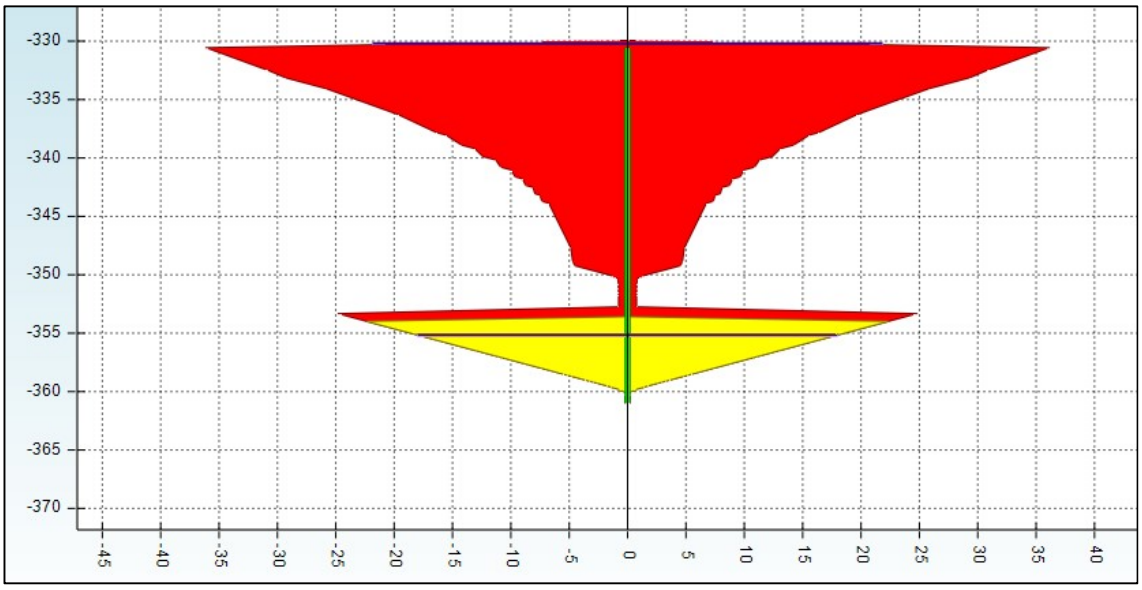

Figure 36. Side view of simulation result of single phase production of cavern 44

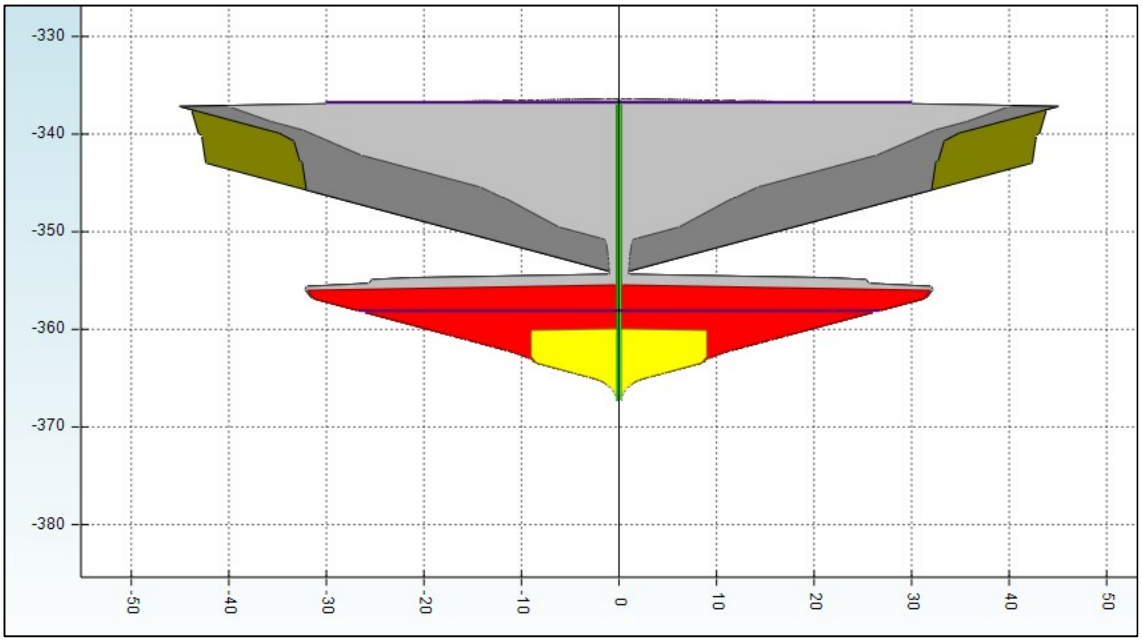

Figure 37. Side view of simulation result of single phase production for cavern 45

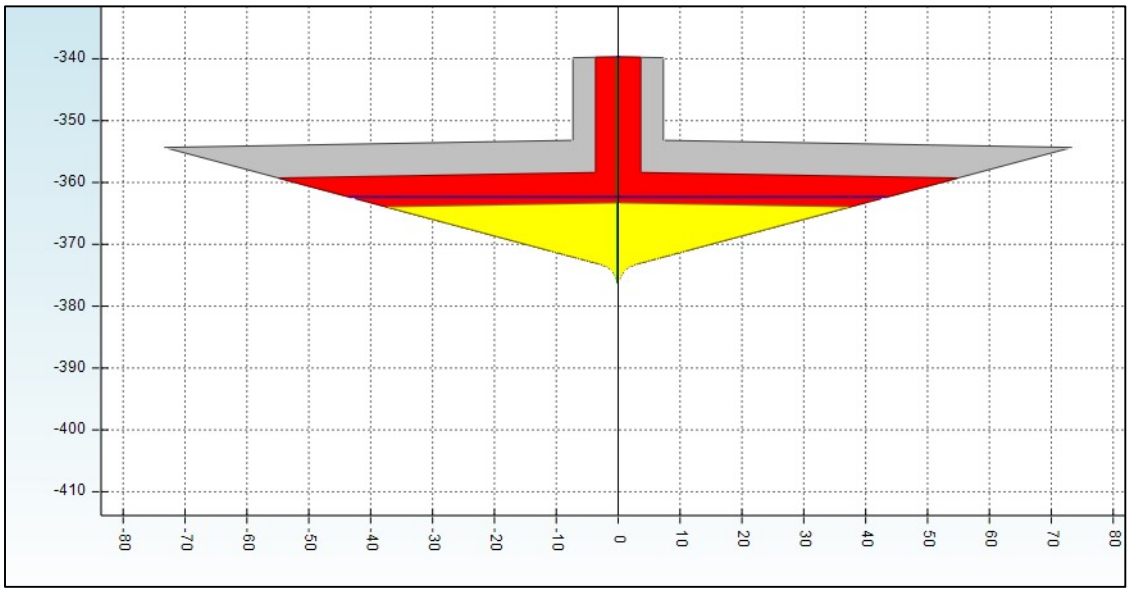

Figure 38. Side view of simulation result of single phase production of cavern 46

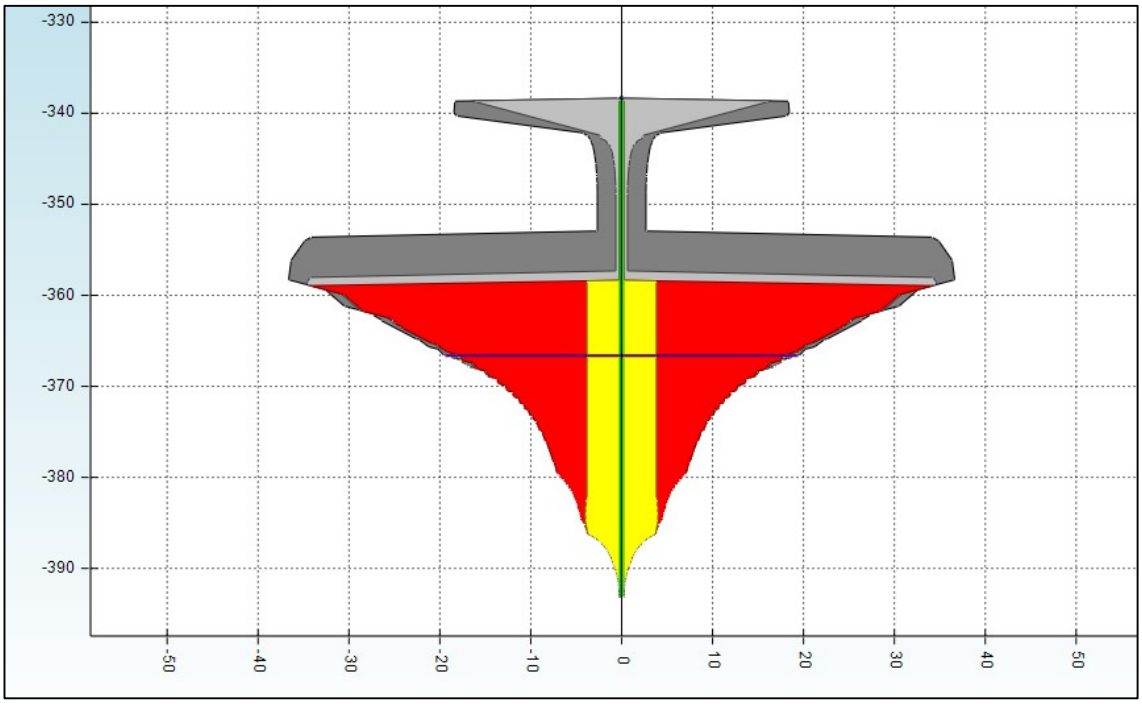

Figure 39. Side view of simulation result of single phase production of cavern 47

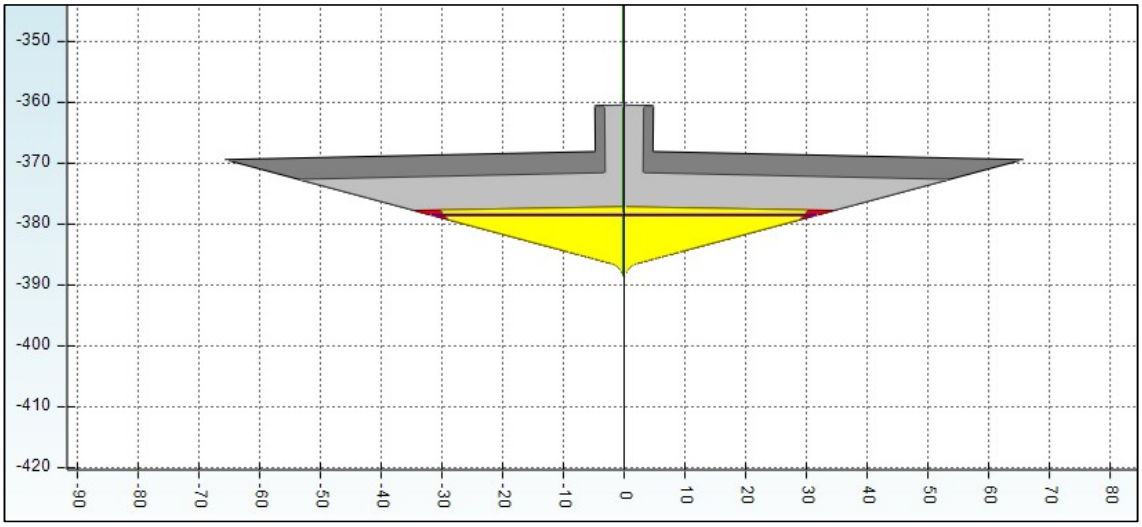

Figure 40. Side view of simulation result of single phase production of cavern 48

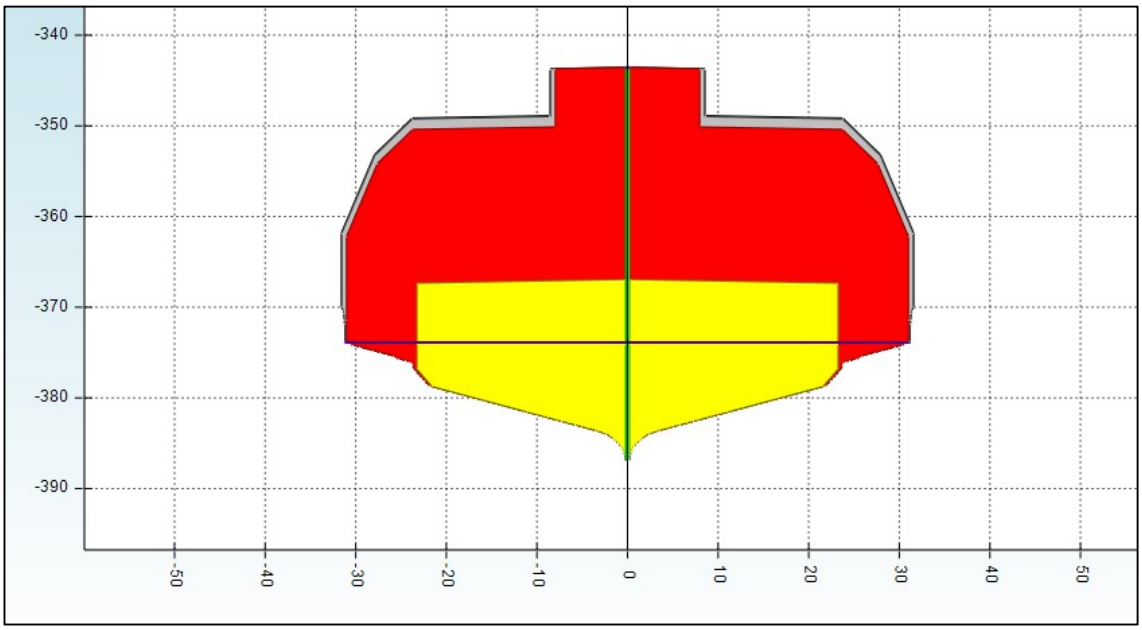

Figure 41. Side view of simulation result of single phase production of cavern 49

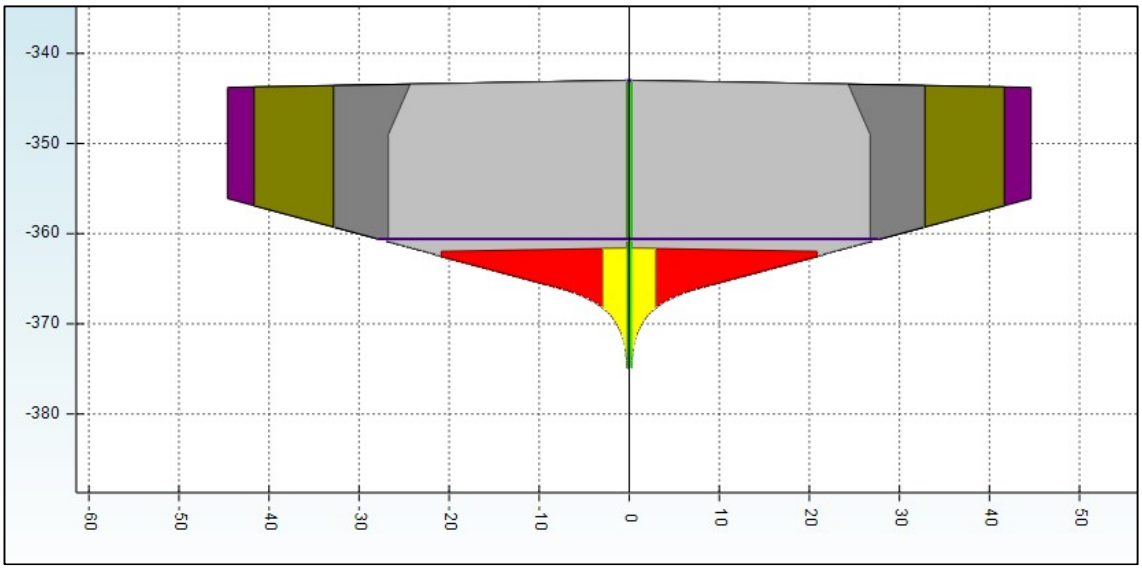

Figure 42. Side view of simulation result of single phase production of cavern 50

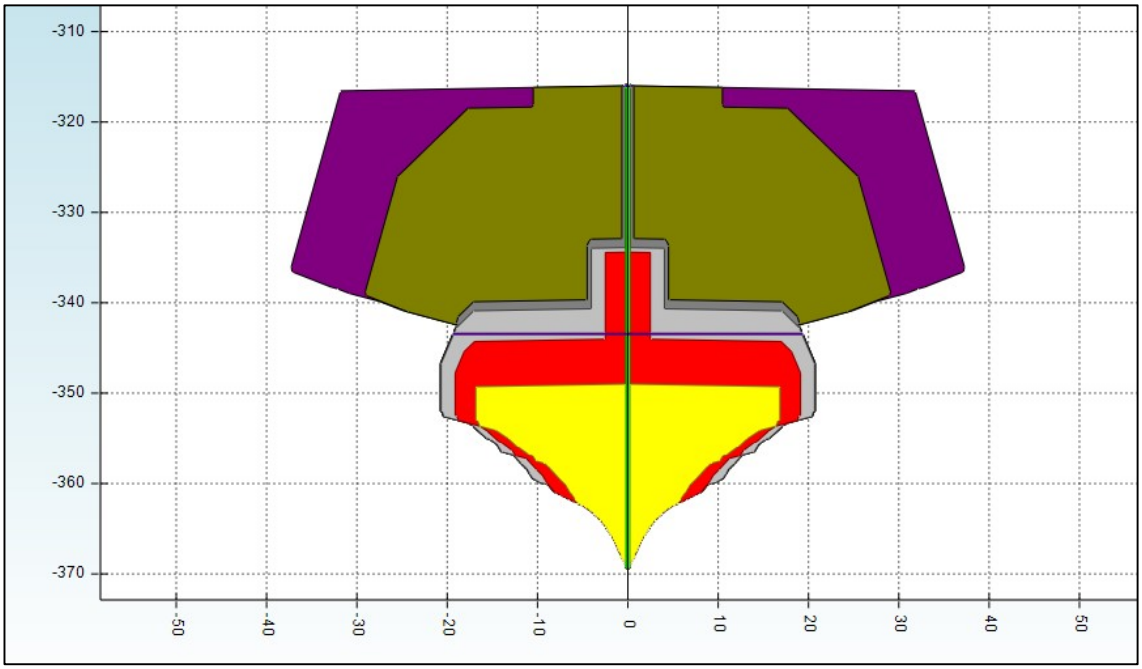

Figure 43. Side view of simulated final cavern 1.

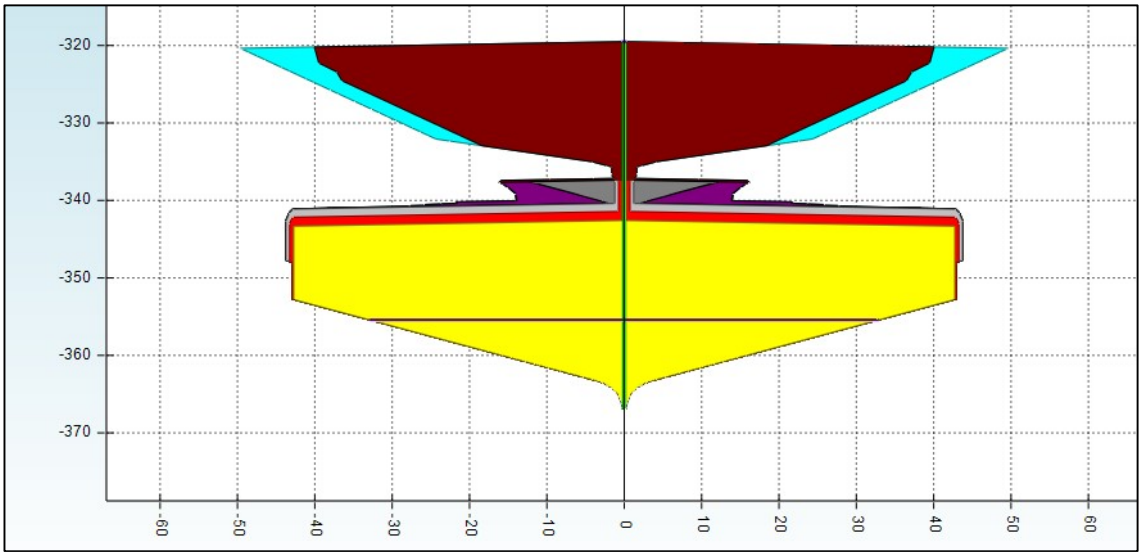

Figure 44. Side view of simulated final cavern 2.

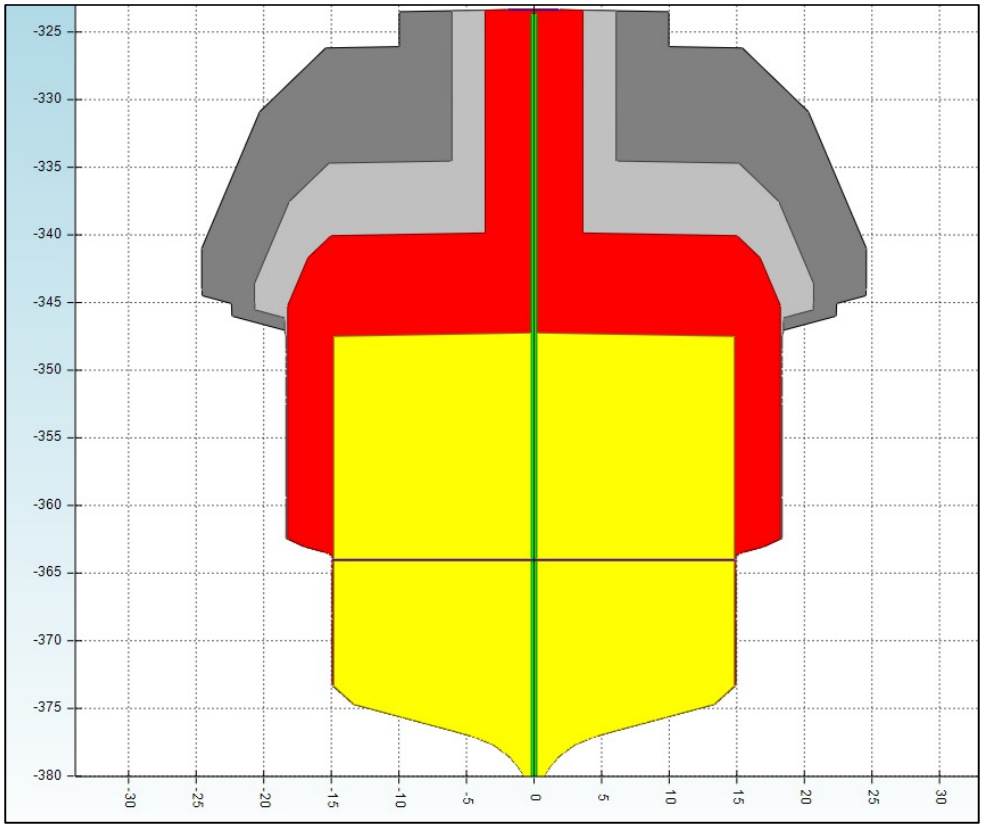

Figure 45. Side view of simulated final cavern 3

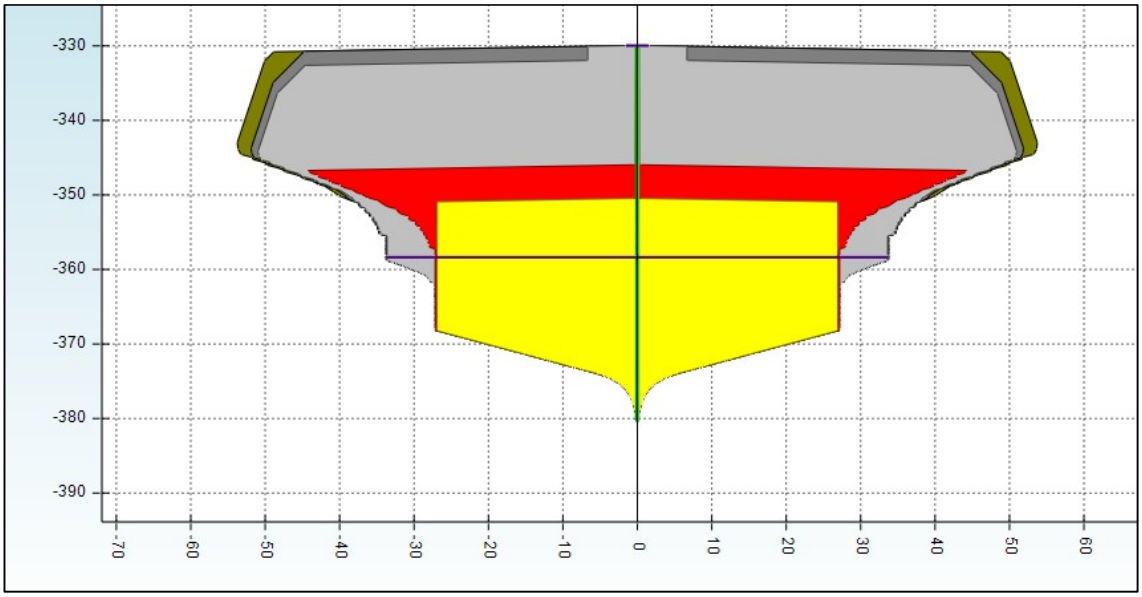

Figure 46. Side view of simulated final cavern 4

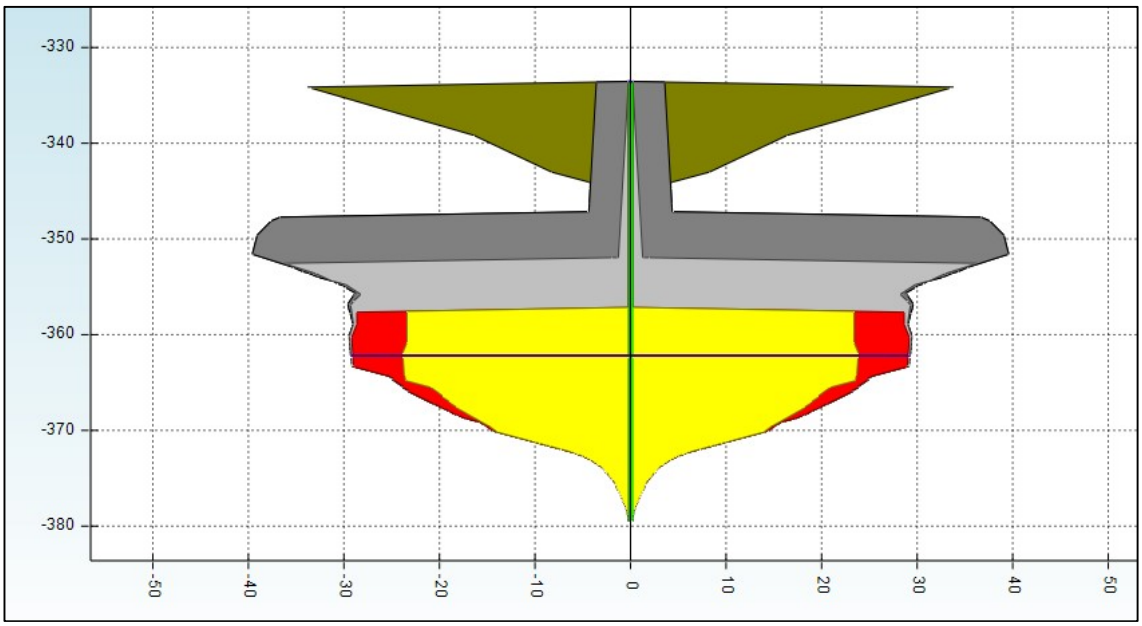

Figure 47. Side view of simulated final cavern 5

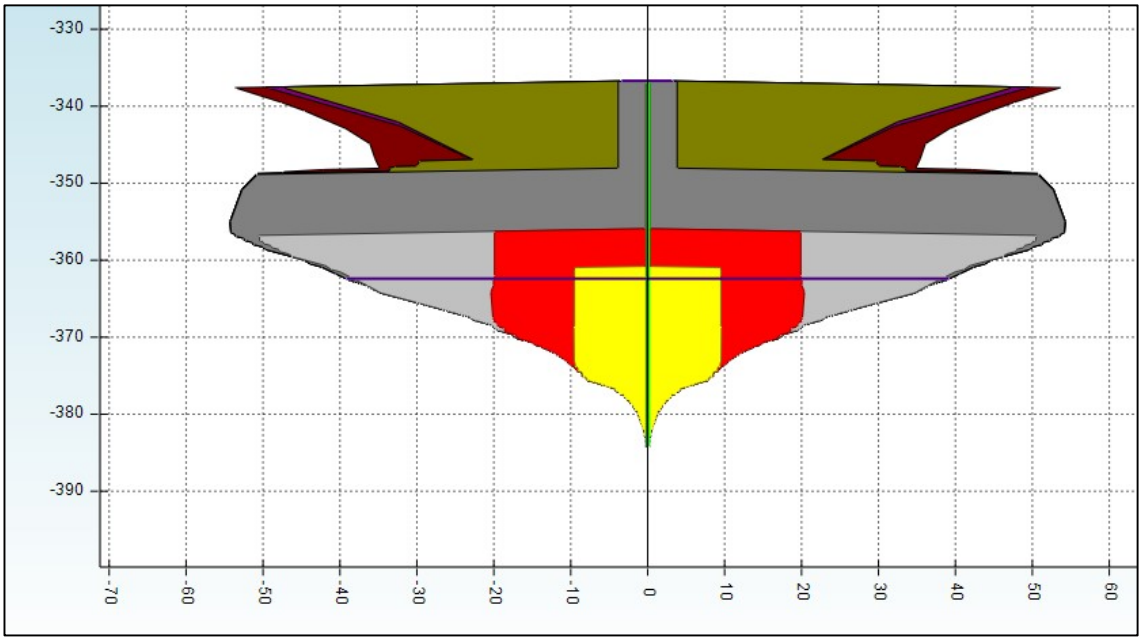

Figure 48. Side view of simulated final cavern 6

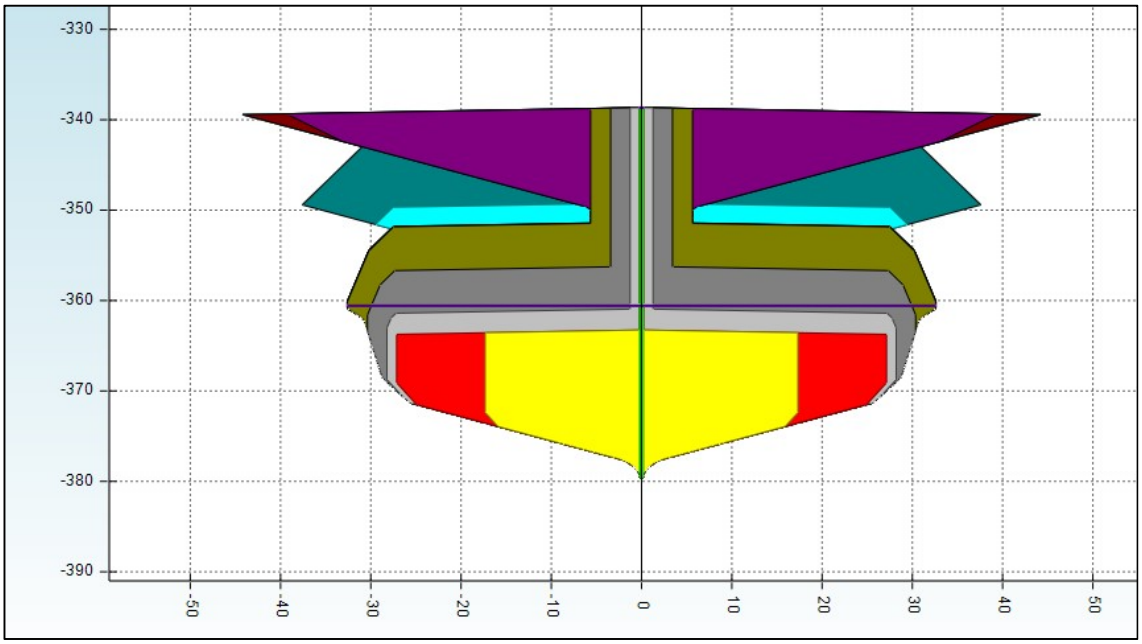

Figure 49. Side view of simulated final cavern 7

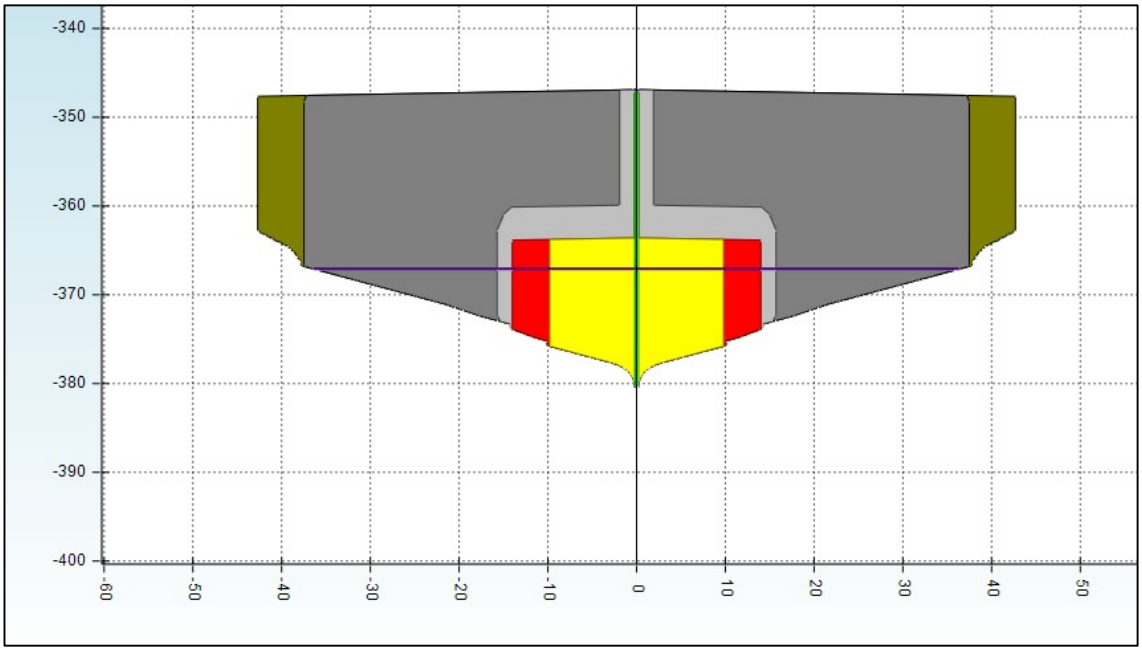

Figure 50. Side view of simulated final cavern 8

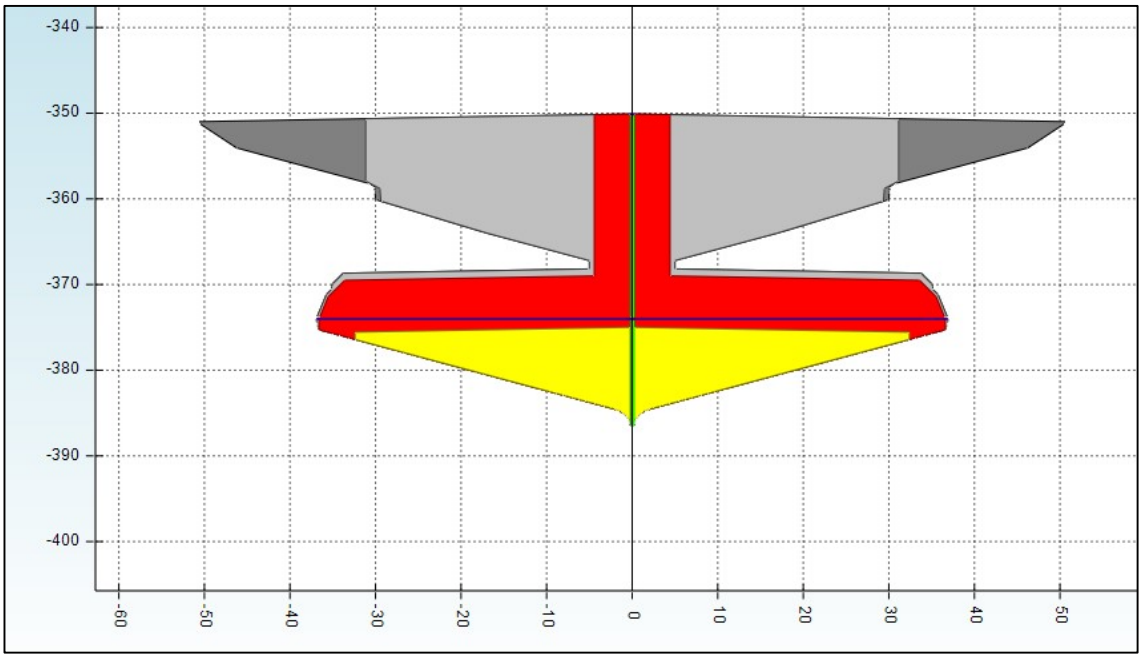

Figure 51. Side view of simulated final cavern 9

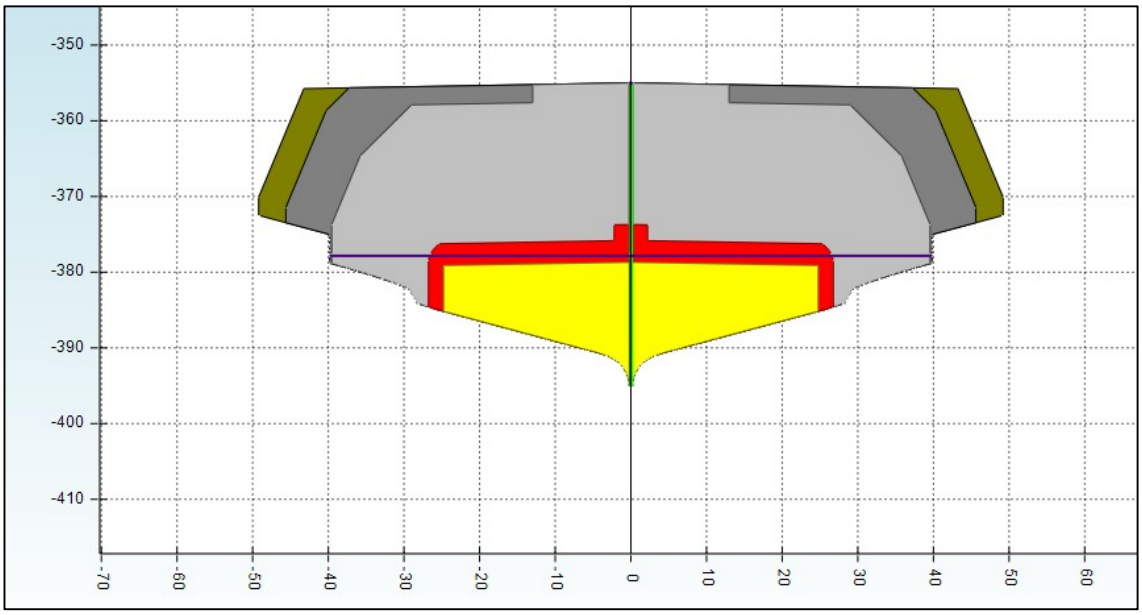

Figure 52. Side view of simulated final cavern 10

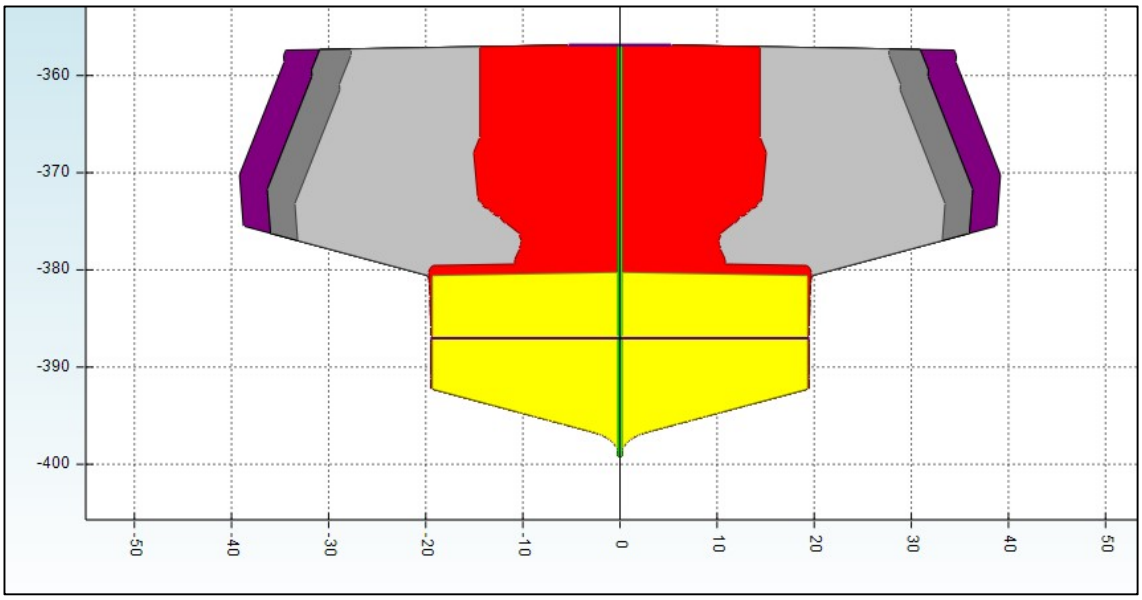

Figure 53. Side view of simulated final cavern 11

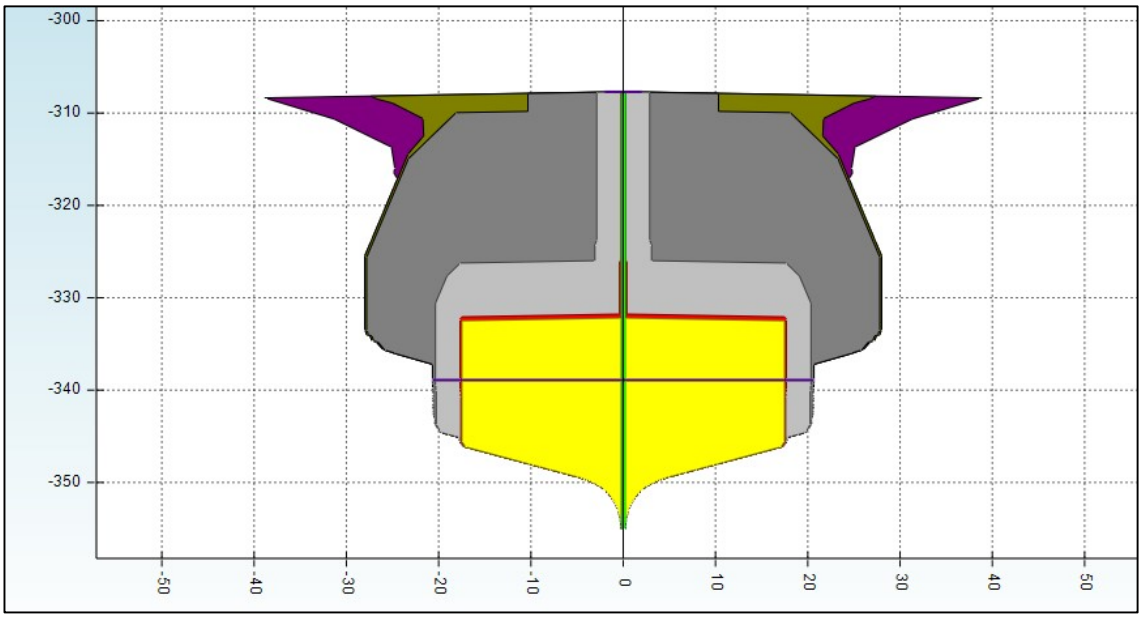

Figure 54. Side view of simulated final cavern 12

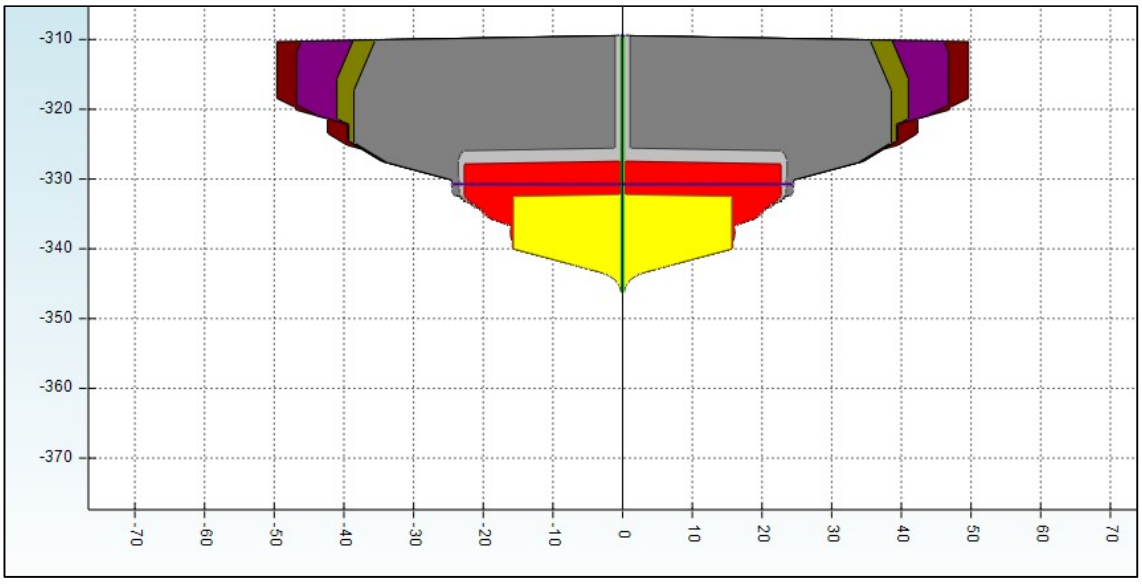

Figure 55. Side view of simulated final cavern 13

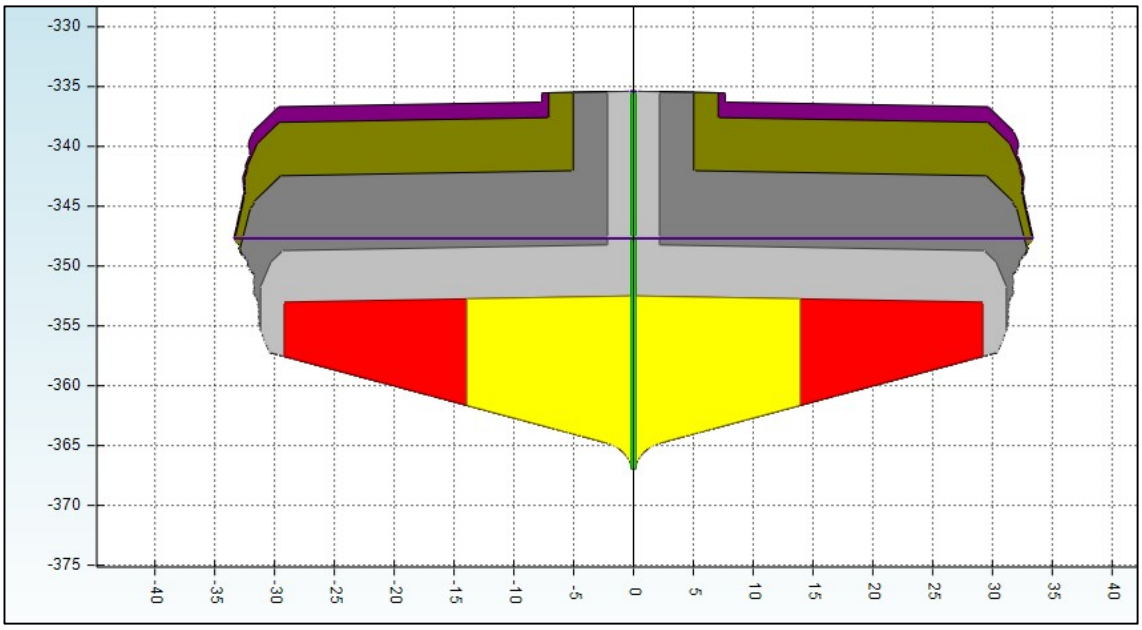

Figure 56. Side view of simulated final cavern 16

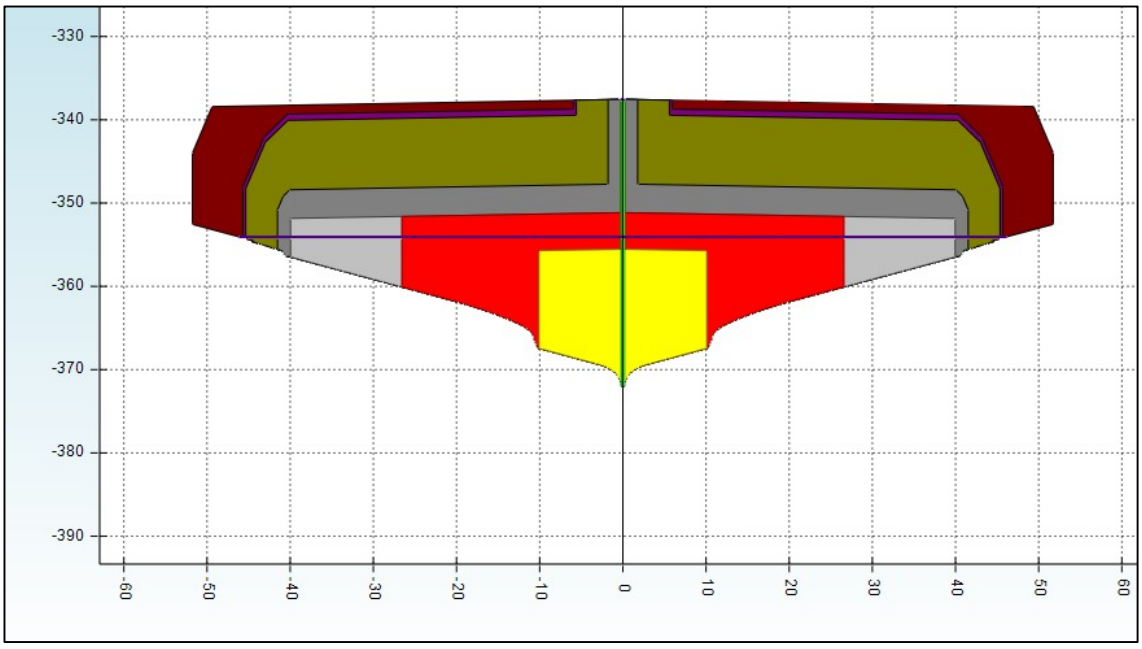

Figure 57. Side view of simulated final cavern 17

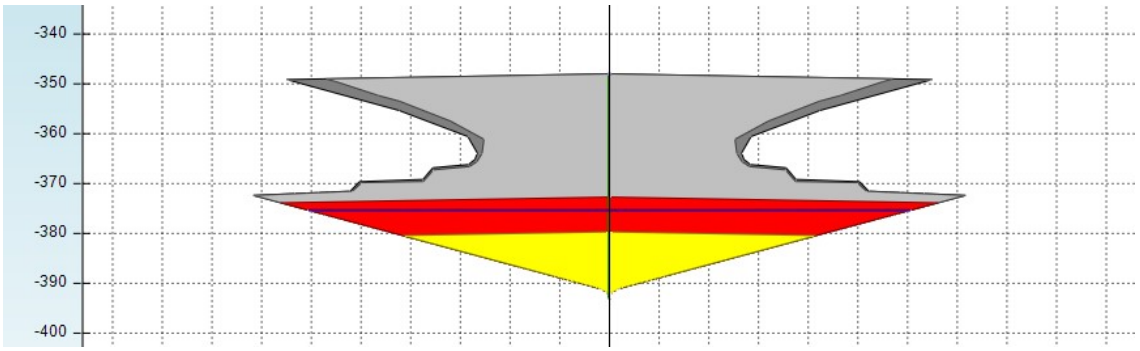

Figure 58. Side view of simulated doublet 19-20 as one cavern final

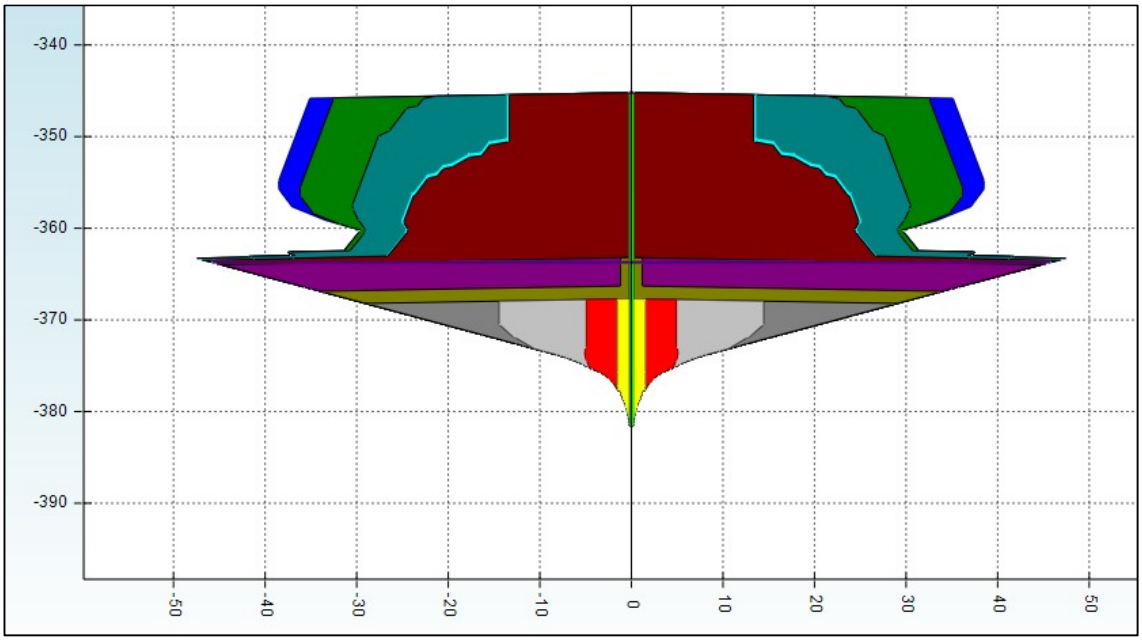

Figure 59. Side view of simulated final cavern 21

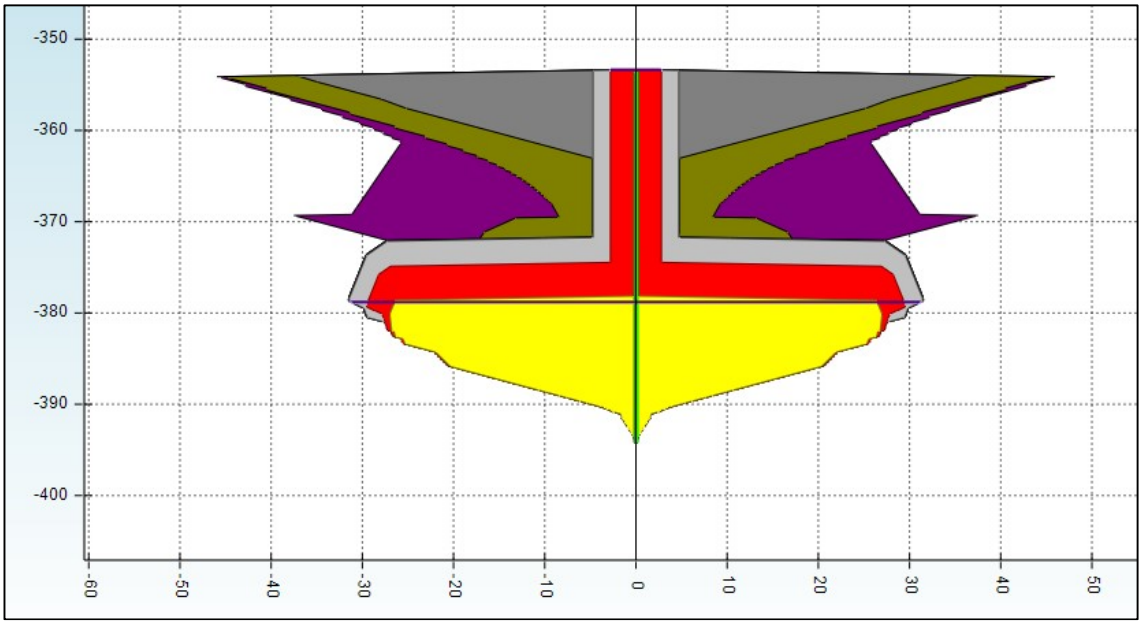

Figure 60. Side view of simulated final cavern 22

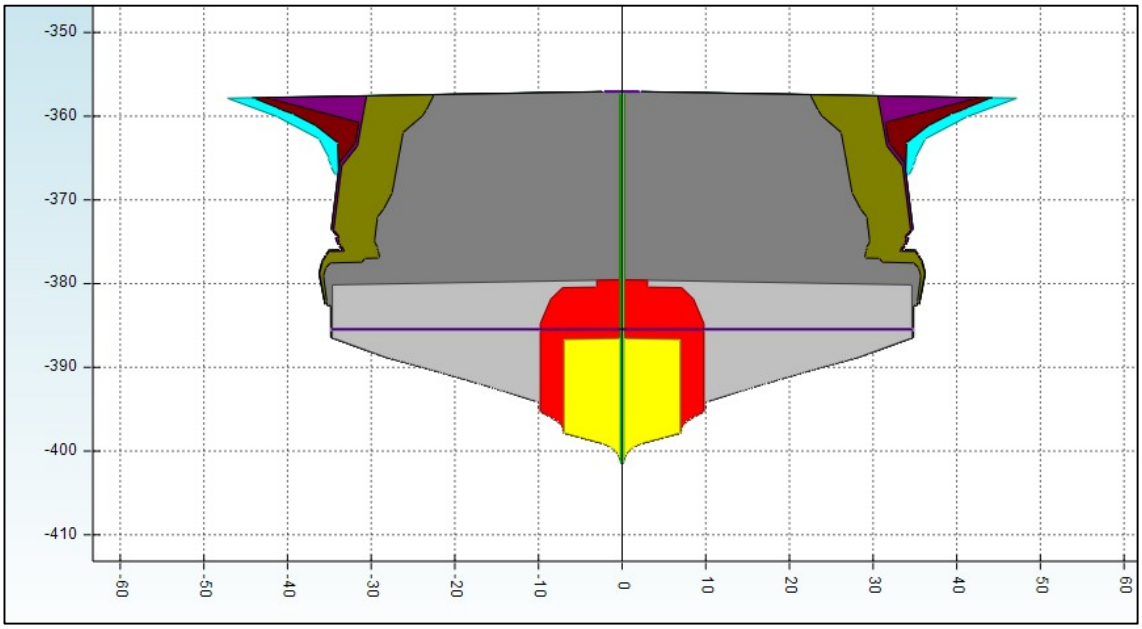

Figure 61. Side view of simulated final cavern 23

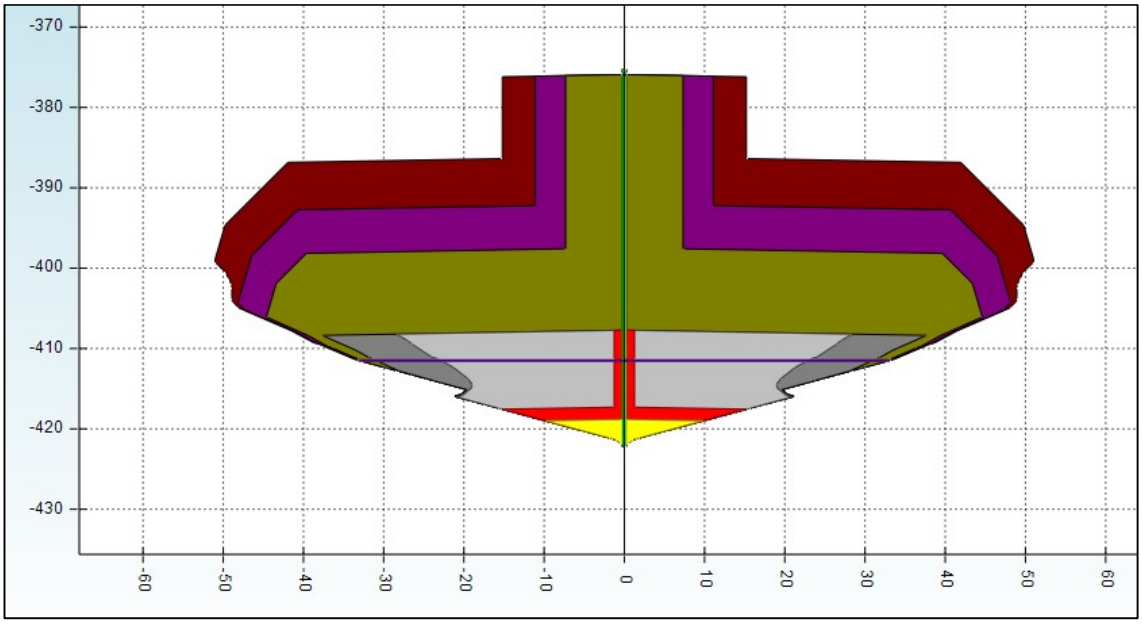

Figure 62. Side view of simulated final cavern 29

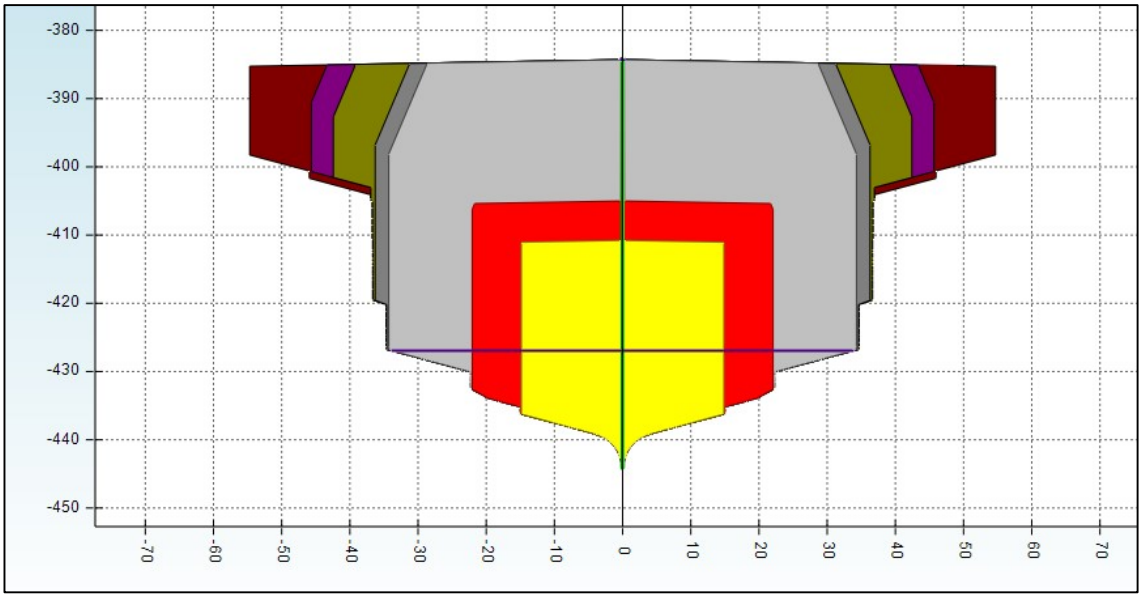

Figure 63. Side view of simulated final doublet 30-31

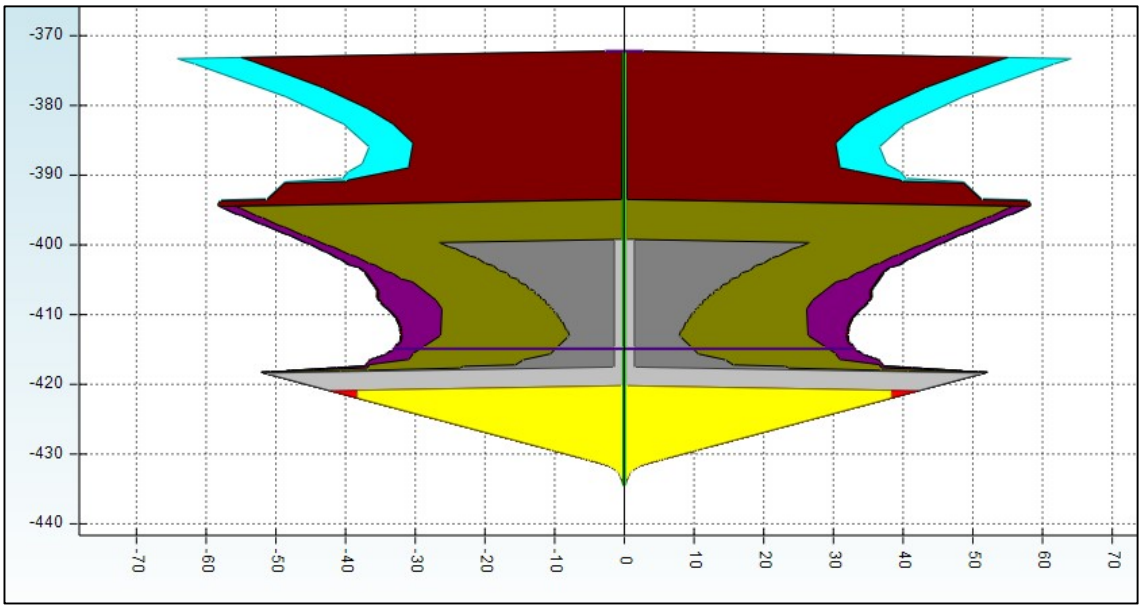

Figure 64. Side view of simulated final doublet 35-36

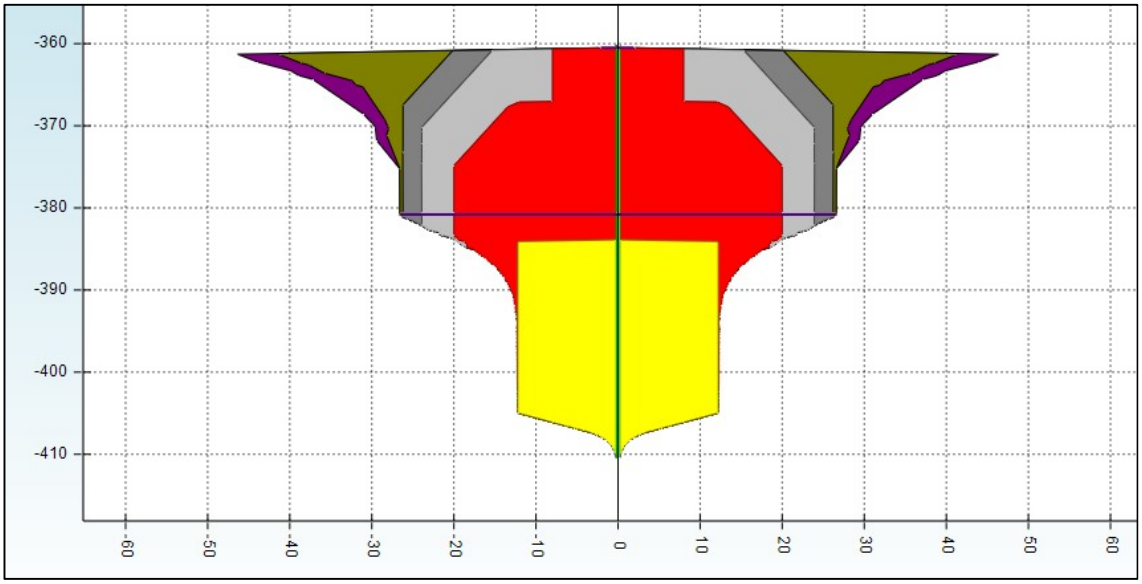

Figure 65. Side view of simulated final cavern 37

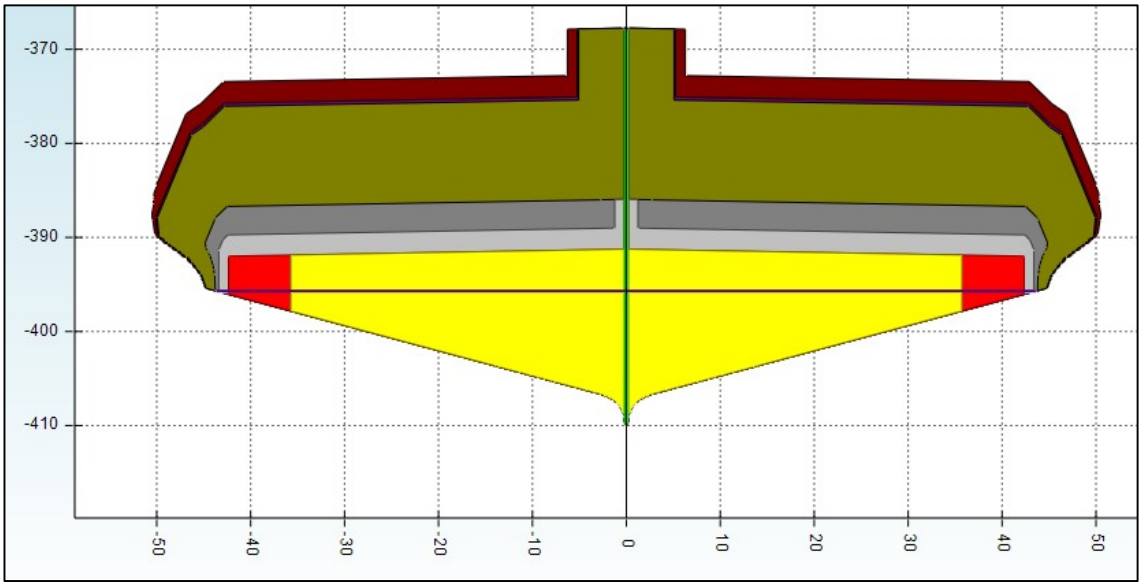

Figure 66. Side view of simulated final cavern 38

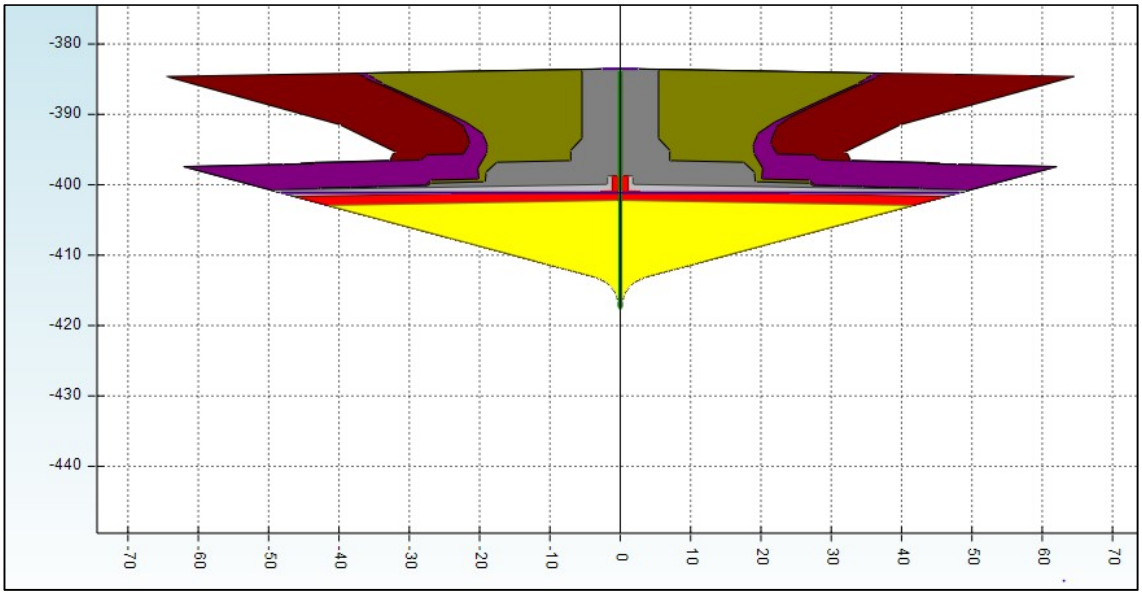

Figure 67. Side view of simulated final cavern 39

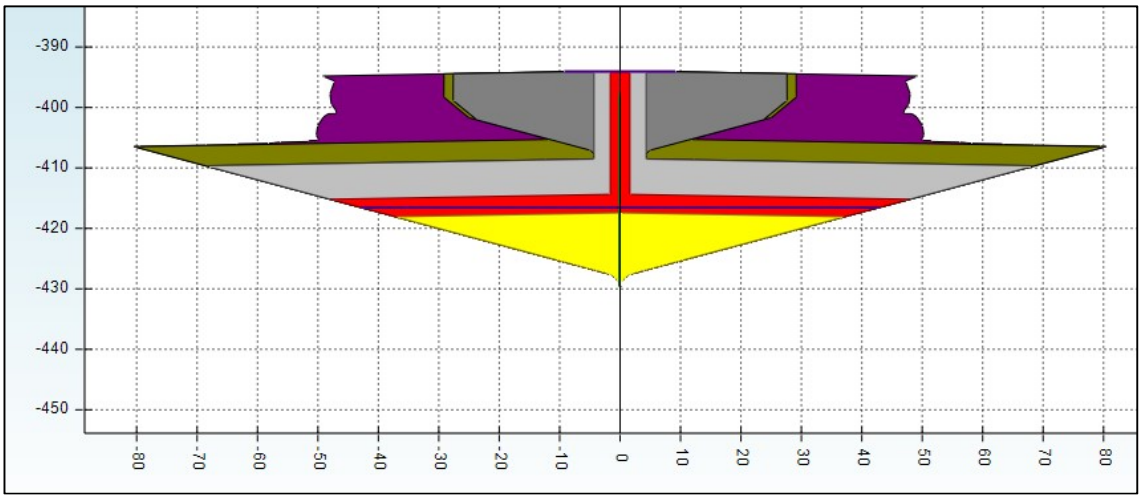

Figure 68. Side view of simulated final doublet 40-41

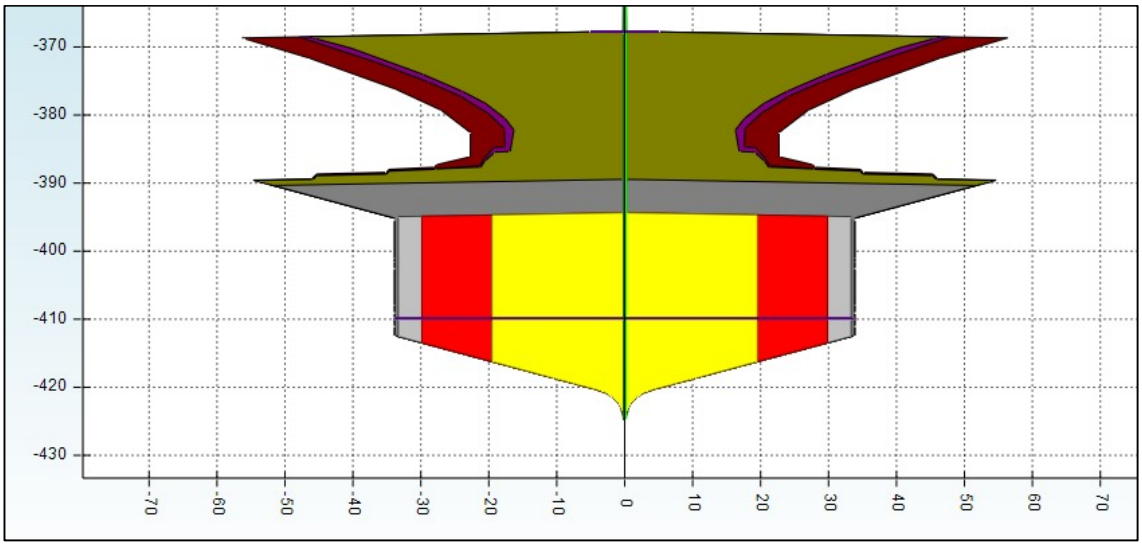

Figure 69. Side view of simulated final doublet 42-43

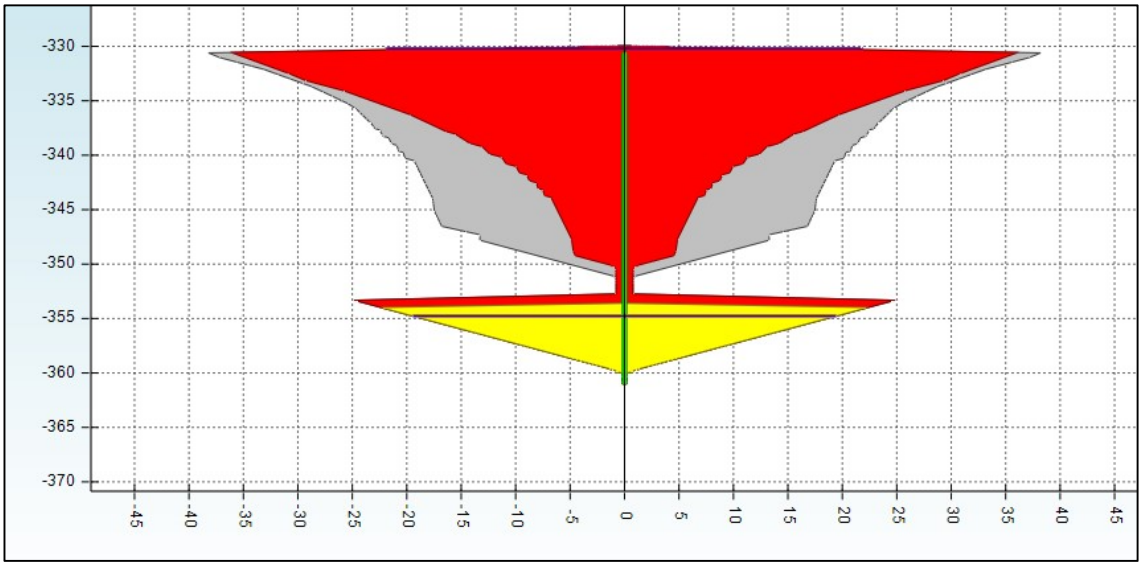

Figure 70. Side view of simulated final cavern 44

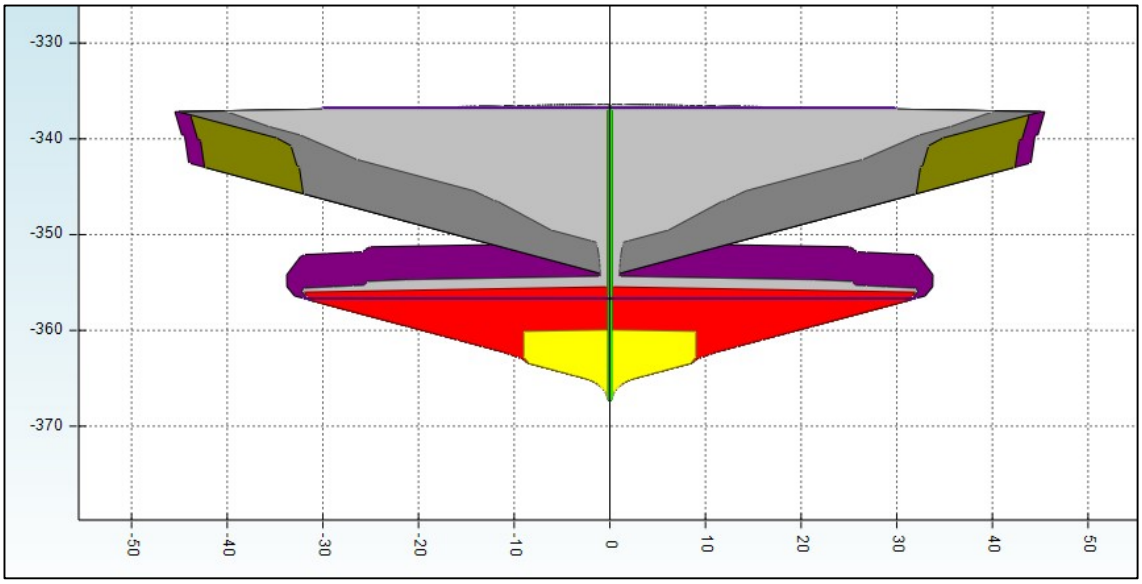

Figure 71. Side view of simulated final cavern 45

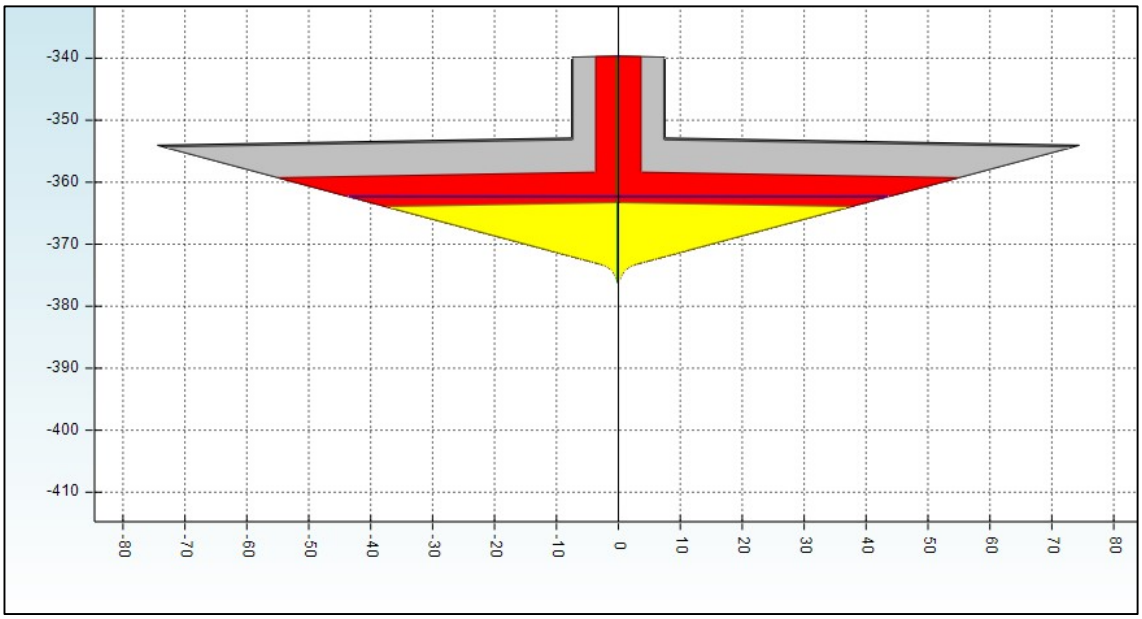

Figure 72. Side view of simulated final cavern 46

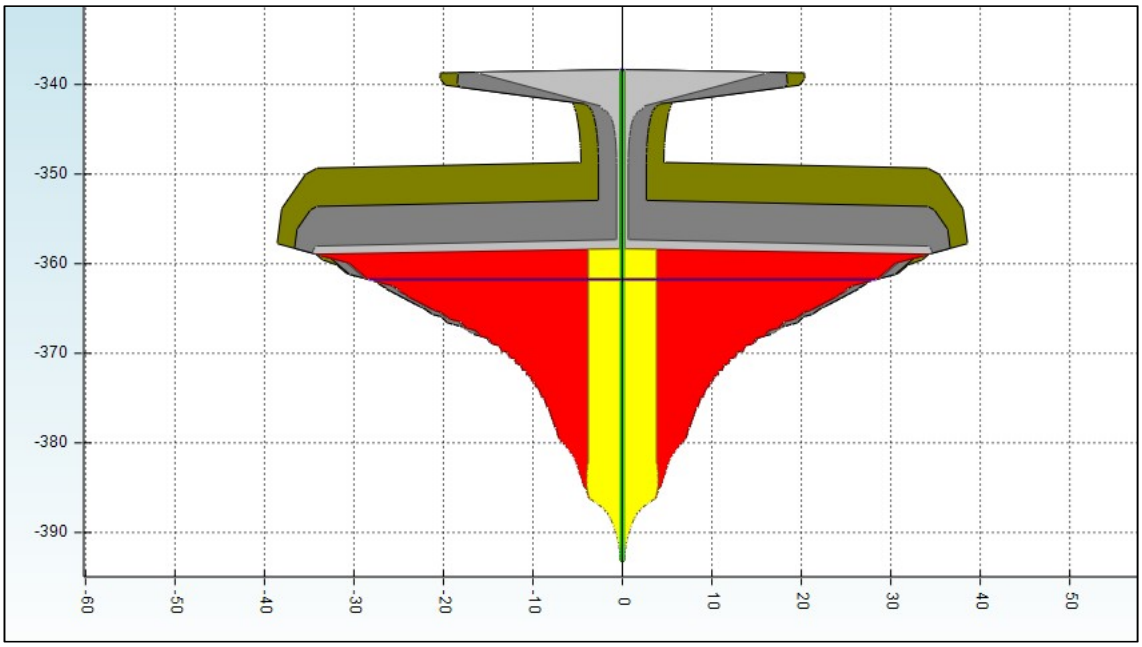

Figure 73. Side view of simulated final cavern 47

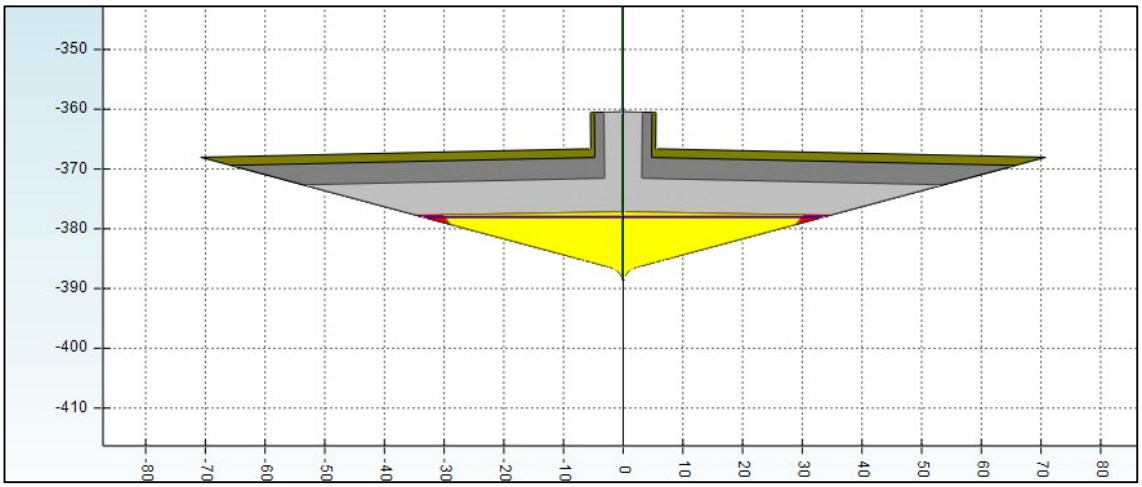

Figure 74. Side view of simulated final cavern 48

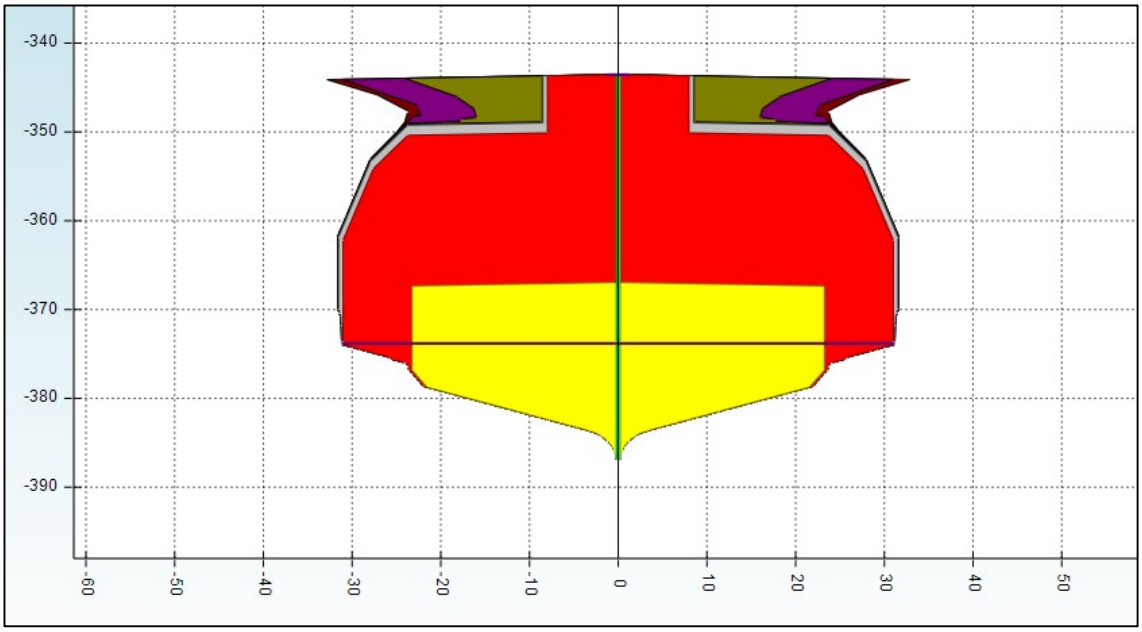

Figure 75. Side view of simulated final cavern 49

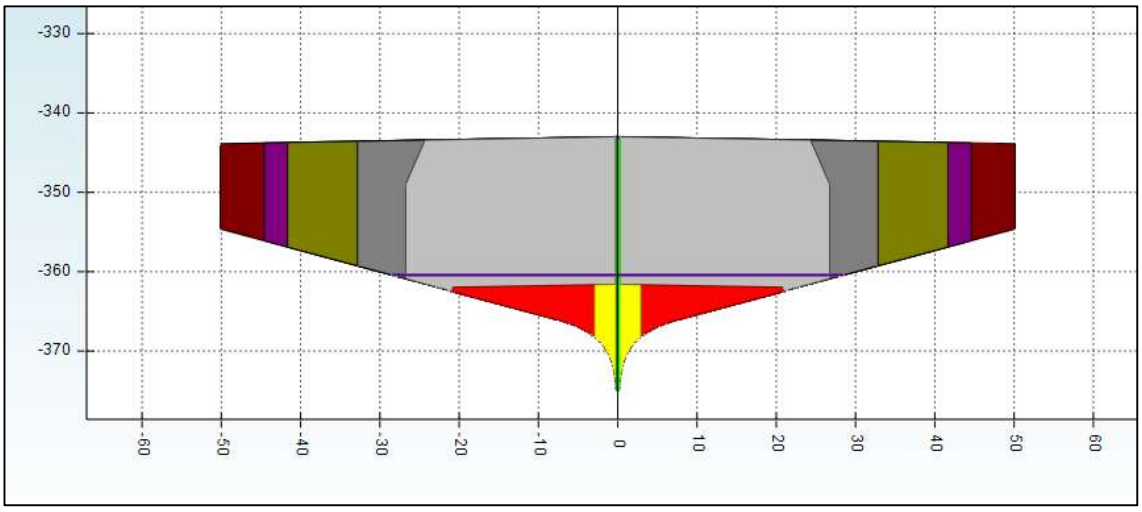

Figure 76. Side view of simulated final cavern 50

Appendix F

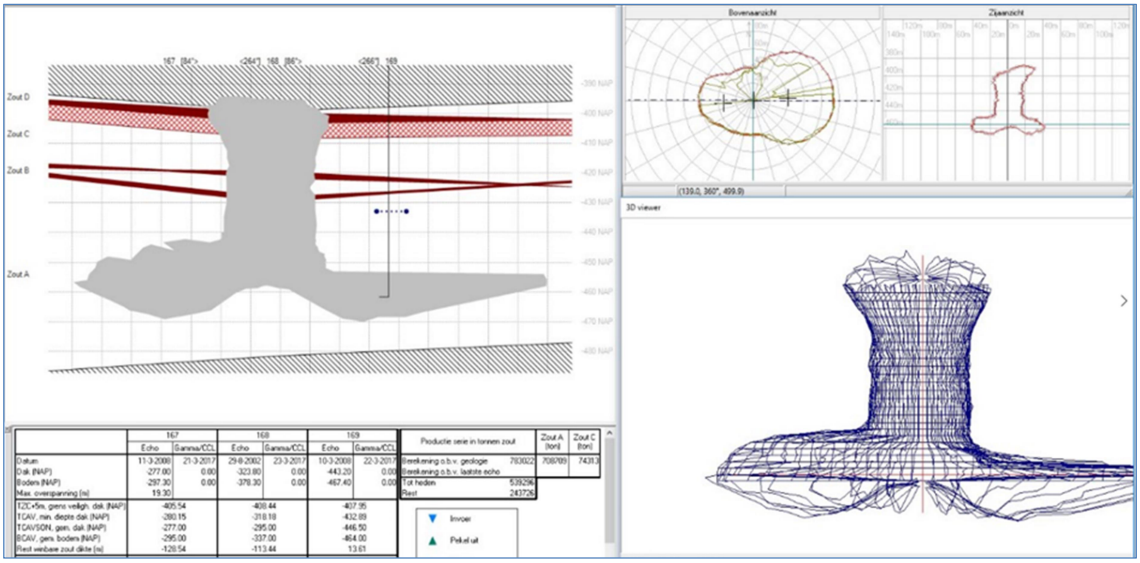

Appendix F1. Figure of sonar measurements at 167 clearly showing the slurry cone in the middle at the bottom.